

*Vasco Sérgio Correia Freitas Silva*

**Direct methanol fuel cell:  
Analysis based on experimentation and  
modeling**

Dissertation presented for the degree of  
**DOCTOR IN CHEMICAL ENGINEERING**  
by  
**PORTO UNIVERSITY**

**Supervisors**  
Adélio Miguel Magalhães Mendes  
Luis Miguel Palma Madeira



**LEPAE - Chemical Engineering Department**  
**Faculty of Engineering**  
**Porto University**  
Porto, May 2005



*to Célia, my parents and Diogo*



## Acknowledgements

This work represents the accomplishment of a dream. Reached the end of this long and hard journey, I would like to express my gratitude to my thesis supervisors, Doctor Adélio Mendes and Doctor Miguel Madeira, for their vision in proposing such an interesting PhD theme. During the present study we made many challenging discussions, leading to a fruitful strategic conduction of the thesis. In all aspects, I learned much from both and I will thank them for all my lifetime.

I want to specially thank Doctor Suzana Nunes for the opportunity of working for almost fifteen months at GKSS, research institute, Geesthacht, Germany. The experimental work of this PhD was mainly developed at GKSS, where I learned all the basics about direct methanol fuel cell technology and membrane R&D. I want to thank very specially Doctor Bastian Ruffmann, Hugo Silva, Yolanda Alvarez-Gallego and Jan Michelmann for helping me in understanding the ins and outs of the DMFC and for their outstanding friendship. I am thankful to Doctor Bastian Ruffmann for preparing the  $\alpha$ -zirconium phosphate dispersion, pretreated with *n*-propylamine and polybenzimidazole. I would like also to thank Doctor Serge Vetter for sulfonating the poly(ether ether ketone) polymers and M. Schossig-Tiedemann and M. Adherhold for making the microscope analysis and helping with the gas permeation measurements.

I am thankful also to my LEPAE colleagues for their support and help regarding the DMFC numerical modeling. A special thank to João Santos, Doctor Paulo Cruz, Doctor José Sousa and Luís Carlos Matos.

Also, I would like to express my gratitude to Professor Hans Müller-Steinhagen and Mr. Erich Gülzow for the opportunity of working for three months at the German Aerospace Center (DLR), Stuttgart, Germany. In the last stages of the thesis I received invaluable help from my DLR colleagues. I would like to thank Regine Reissner and Doctor Johannes Schirmer for their DMFC measurements and interesting and rewarding suggestions.

During my PhD study, life would be much more difficult without the support and companionship of good friends that I met at Porto, Geesthacht and Stuttgart. It is not possible to name all of them, but I could try to mention some: Luquini, Ruizinho, Fabão, Mané, Nuninho, Manel, Mena, Tiago, Renato, Valter, Herney; Doctor Luisa, Professor Zhong, Doctor Valery, Doctor Serge, Suresh, Plewka, Doctor Jerusa, Ethel, Doctor Mariela, Doctor Karthik, Doctor Dominique, Doctor Sergei, Doctor Irmgard, Antonino, Fausto, Roberto (“El vividor”), Kan, Jakob, Janina, Carmen; Nassar, Ping, Stefan, Christian, Siegfried, Peter, Til, Irmborg, Mr. Saunders, Doctor Norbert...

In addition, I specially thank my family support and continuous encouragement during my PhD, specially my father, mother and brother. Last, but not least, I would like to give the most special thank to my wife, Célia, for being incredible supportive of me over all the PhD long and hard journey. Despite many thousands kilometers distance and other difficulties, she has always supported me with a cheerful love and never failing attention. I cannot thank her enough for being such a wonderful wife and friend.

This work was supported primarily by FCT, PhD grant SFRH/BD/6818/2001. I also acknowledge the partial financial support of GKSS for my stay at GKSS Forschungszentrum GmbH, Geesthacht, Germany. I would also like to acknowledge FCT and DAAD/CRUP support (A-6/05) for my stay at German Aerospace Center, Stuttgart, Germany. The present work was also partially supported by FCT/FEDER projects POCTI/EQU/38075/2001 and POCTI/EQU/45225/2002.

## Preface

The present dissertation comprises a series of articles that were written while the PhD was carried out and now published or submitted for publication. These articles describe most of the work done, which was mainly performed by the author, both conceptual and experimental. Co-authors but the supervisors contribute allowing the author to work in their labs, with important advices and tutoring and performing important analysis (e.g. DMFC tests), as mentioned previously in the acknowledgements section.

The developed work is described in four parts according to the materials that were used and studied. Part one starts with the introduction of the direct methanol fuel cell (DMFC) topic, describing generically each of its main features and potentialities as power source (chapter 1). This part focus mainly on the proton exchange membrane, performing an overview concerning its research and development. It is also outlined a critical study taking into account the main contributions of the present work regarding the R&D on proton exchange membranes for direct methanol fuel cells.

Part two is dedicated to the sulfonated poly(ether ether ketone) (sPEEK) plain polymer (chapter 2). A critical analysis of the sulfonation degree effect on the polymer barrier and mass transport properties towards direct methanol fuel cell species was performed. Impedance spectroscopy (proton conductivity), pervaporation (water and methanol permeation) and pressure rise experiments (nitrogen, oxygen and carbon dioxide permeation) were proposed. Nafion<sup>®</sup> 112 was used as reference during this study.

Part three is devoted to the incorporation of zirconium oxide via *in situ* hydrolysis on the sPEEK polymer. This part starts with chapter 3 where the zirconium oxide influence on the sPEEK barrier and electrolyte properties was analyzed. This study is expanded in chapter 4, in which the range of the sPEEK modification with zirconium oxide was extended. The investigated properties were the proton conductivity, proton transport resistance, water uptake, water, methanol, oxygen, carbon dioxide and nitrogen permeability coefficients, morphology and elemental analysis. The fact of having hybrid membranes with a wide range of properties allowed the validation of the standard characterization methods in terms of the DMFC performance qualitative prediction (chapter 5). Furthermore, in chapter 6 is presented a mathematical model that was developed based on these membranes. This approach enabled the prediction of the DMFC performance for membranes with distinct characteristics. This part ends with chapter 7, in which the developed mathematical model

was applied to study the influence of the membrane properties on the DMFC performance, in terms of proton conductivity and permeability towards methanol.

Part four focuses on the characterization and application of composite membranes based on sPEEK polymer modified inorganically with different amounts of zirconium phosphate pretreated with *n*-propylamine and polybenzimidazole. The DMFC application of these membranes was performed at temperatures up to 130°C. Chapter 8 is devoted mainly to the characterization results. On the other hand, chapter 9 explores the use of these composite membranes and presents a novel approach for evaluating the DMFC overall efficiency accounting for the permeation of carbon dioxide through the membrane.

Finally, the present dissertation ends with the main conclusions of the developed research work and suggestions for future work.

## Contents

Abstract.....	<i>i</i>
Sumário.....	<i>iii</i>
Sommaire.....	<i>v</i>

## PART ONE

Introduction.....	<i>1</i>
-------------------	----------

### *Chapter 1. Membranes for direct methanol fuel cell applications: analysis based on characterization, experimentation and modeling.....*

Abstract.....	3
1.1. Introduction.....	4
1.2. Basics of the DMFC.....	6
1.2.1. Thermodynamic background.....	7
1.2.2. Polarization behavior.....	8
1.2.3. Membrane electrode assembly.....	10
1.2.4. DMFC test system.....	12
1.3. R&D regarding the proton exchange membrane.....	13
1.3.1. Novel materials.....	14
1.3.2. Characterization methods.....	16
1.3.2.1. Swelling measurements.....	17
1.3.2.2. Conductivity measurements.....	17
1.3.2.3. Permeability measurements.....	18
1.3.3. DMFC tests.....	19
1.3.4. DMFC efficiency.....	21
1.3.5. PEM modeling.....	23
1.4. Conclusions.....	24
Acknowledgements.....	25
References.....	25

## **PART TWO**

<b>Sulfonated poly(ether ether ketone) membranes .....</b>	<b>31</b>
--	-----------

### ***Chapter 2. Mass transport of direct methanol fuel cell species in sulfonated poly(ether ether ketone) membranes .....***

Abstract .....	33
2.1. Introduction .....	34
2.2. Experimental .....	36
2.2.1. Materials and methods .....	36
2.2.2. Membrane preparation .....	36
2.2.3. Characterization methods.....	37
2.2.3.1. Proton conductivity .....	37
2.2.3.2. Liquid permeability measurements .....	37
2.2.3.3. Gas permeability measurements .....	38
2.2.4. DMFC tests .....	39
2.3. Results and discussion .....	39
2.3.1. Proton conductivity .....	39
2.3.2. Permeability towards water and methanol.....	41
2.3.3. Permeability towards nitrogen, oxygen and carbon dioxide.....	43
2.3.4. DMFC tests .....	45
2.4. Conclusions .....	48
Acknowledgements.....	49
References.....	50

## **PART THREE**

<b>sPEEK composite membranes based on zirconium oxide.....</b>	<b>53</b>
--	-----------

### ***Chapter 3. Zirconium oxide modified sulfonated poly(ether ether ketone) membranes for direct methanol fuel cell applications.....***

Abstract .....	55
3.1. Introduction.....	56
3.2. Experimental .....	57

3.2.1. Materials and methods .....	57
3.2.2. Membrane preparation .....	57
3.2.3. Methanol and water permeability measurements.....	57
3.2.4. Proton conductivity measurements .....	58
3.2.5. Water swelling and chemical stability studies .....	58
3.3. Results and discussion .....	58
3.3.1. Water uptake and chemical stability of the composite membranes .....	58
3.3.2. Proton conductivity measurements .....	60
3.3.3. Permeability measurements .....	61
3.4. Conclusions .....	62
Acknowledgements .....	63
References .....	63

***Chapter 4. Proton electrolyte membrane properties and direct methanol fuel cell performance,  
I. Characterization of hybrid sulfonated poly(ether ether ketone)/zirconium oxide membranes***

.....	65
Abstract .....	65
4.1. Introduction .....	66
4.2. Experimental .....	67
4.2.1. Materials and methods .....	68
4.2.2. Membrane preparation .....	68
4.2.3. Characterization methods.....	68
4.2.3.1. Conductivity .....	68
4.2.3.2. Water swelling .....	69
4.2.3.3. Water and methanol pervaporation measurements .....	69
4.2.3.4. Nitrogen/Oxygen/Carbon dioxide permeability coefficients measurements .....	70
4.2.3.5. Membrane morphology .....	70
4.2.3.6. Membrane elemental analysis .....	70
4.3. Results and discussion .....	70
4.3.1. Proton conductivity .....	70
4.3.2. Water uptake .....	72
4.3.3. Permeabilities towards species present in DMFC.....	73
4.3.4. Microscopy and elemental analysis .....	75
4.4. Conclusions .....	77

Acknowledgements.....	78
References.....	78

***Chapter 5. Proton electrolyte membrane properties and direct methanol fuel cell performance,***

<b><i>II. Fuel cell performance and membrane properties effects.....</i></b>	<b>81</b>
Abstract.....	81
5.1. Introduction.....	82
5.2. Experimental.....	84
5.3. Results and discussion.....	85
5.3.1. DMFC performance.....	85
5.3.2. Membranes characterization results versus DMFC performance.....	90
5.4. Conclusions.....	95
Acknowledgements.....	96
References.....	96

***Chapter 6. Direct methanol fuel cell modeling using proton exchange membrane properties evaluated by standard characterization methods.....***

<b><i>101</i></b>	<b>101</b>
Abstract.....	101
6.1. Introduction.....	102
6.2. Mathematical modeling.....	103
6.2.1. Governing equations.....	105
6.2.2. Electrochemical kinetics.....	109
6.2.3. Cell voltage.....	111
6.2.4. Cell efficiency.....	112
6.3. Experimental.....	113
6.4. Results and discussion.....	114
6.4.1. Polarization curves.....	114
6.4.2. Current density at constant voltage and open circuit voltage.....	114
6.4.3. DMFC efficiency.....	117
6.5. Conclusions.....	119
Acknowledgements.....	120
List of symbols.....	121
References.....	123

<b>Chapter 7. Proton exchange membranes for direct methanol fuel cells: Properties critical study concerning methanol crossover and proton conductivity.....</b>	<b>127</b>
Abstract .....	127
7.1. Introduction .....	128
7.2. Mathematical Model .....	130
7.3. Results and discussion .....	131
7.3.1. DMFC performance .....	131
7.3.2. DMFC efficiency .....	137
7.3.3. Case study .....	140
7.4. Conclusions .....	142
Acknowledgements .....	143
References .....	144

## **PART FOUR**

<b>sPEEK composite membranes based on zirconium phosphate .....</b>	<b>147</b>
---	------------

<b>Chapter 8. Characterization and application of composite membranes in DMFC.....</b>	<b>149</b>
Abstract .....	149
8.1. Introduction .....	150
8.2. Experimental .....	151
8.2.1. Materials and methods .....	151
8.2.2. Preparation of zirconium phosphate .....	151
8.2.3. Membrane preparation .....	152
8.2.4. Characterization methods.....	152
8.2.4.1. Proton conductivity .....	152
8.2.4.2. Swelling measurements.....	152
8.2.4.3. Water and methanol pervaporation measurements .....	153
8.2.4.4. Nitrogen/Oxygen/Carbon dioxide permeability measurements.....	153
8.2.4.5. Membrane morphology.....	153
8.2.5. DMFC tests .....	153
8.3. Results and discussion .....	154
8.3.1. Proton conductivity .....	154
8.3.2. Swelling measurements.....	156

8.3.3. Permeability towards species present in DMFC (methanol, water and gases) .....	157
8.3.4. Membrane morphology .....	159
8.3.5. Polarization curves .....	160
8.4. Conclusions .....	163
Acknowledgements .....	164
References .....	165

***Chapter 9. Performance and efficiency of a DMFC using non-fluorinated composite membranes operating at low/medium temperatures..... 169***

Abstract .....	169
9.1. Introduction .....	170
9.2. Experimental .....	171
9.2.1. Materials and methods .....	171
9.2.2. Zirconium phosphate preparation .....	172
9.2.3. Membrane preparation .....	172
9.2.4. Characterization methods.....	172
9.2.4.1. Proton conductivity .....	172
9.2.4.2. Swelling in aqueous methanol .....	173
9.2.4.3. Pervaporation measurements .....	173
9.2.5. DMFC operation .....	173
9.2.6. Efficiency of the DMFC .....	174
9.3. Results and discussion .....	178
9.3.1. Characterization results.....	178
9.3.2. DMFC temperature study.....	180
9.3.3. Polarization curves and global efficiency .....	184
9.4. Conclusions .....	187
Acknowledgements .....	187
List of symbols.....	188
References.....	189

**Conclusions and suggestions for future work .....191**

## Figure Captions

Fig. 1.1. Sketch of the DMFC illustrating the mass transport of the different species ( $H_2O$ , $CH_3OH$ , $N_2$ , $O_2$ , $CO_2$ ).....	7
Fig. 1.2. Typical current-voltage behavior of a DMFC. ....	9
Fig. 1.3. Scanning electron micrograph of a MEA. ....	10
Fig. 1.4. Simplified flow sheet of a direct methanol fuel cell test facility.....	12
Fig. 1.5. Chemical structure of Nafion <sup>®</sup> and Teflon <sup>®</sup> (PTFE).....	14
Fig. 1.6. Sulfonation reaction of the poly(ether ether ketone).....	15
Fig. 1.7. Current-voltage and power density plots of the DMFC using a sPEEK membrane with SD=42% ( $d_M = 40\mu m$ ). ....	20
Fig. 1.8. Estimated overall efficiency of the DMFC using a sPEEK membrane with SD=42% ( $d_M = 40\mu m$ ).....	23
Fig. 2.1. Chemical structure of Nafion <sup>®</sup> . ....	35
Fig. 2.2. Sulfonation reaction of poly(ether ether ketone).....	36
Fig. 2.3. Proton conductivity of the sPEEK polymer as a function of the sulfonation degree (25°C in 0.33M $H_2SO_4$ ).....	40
Fig. 2.4. Methanol and water permeability coefficients of sPEEK membranes as a function of the sulfonation degree (pervaporation experiments at 25°C).....	42
Fig. 2.5. Selectivity towards water/methanol of sPEEK membranes as a function of the sulfonation degree (pervaporation experiments at 25°C).....	42
Fig. 2.6. Permeability coefficients of nitrogen, oxygen and carbon dioxide as a function of the sPEEK membrane sulfonation degree (pressure rise experiments at 20°C). ....	44
Fig. 2.7. Selectivity towards $N_2/O_2$ and $CO_2/O_2$ of sPEEK membranes as a function of the sulfonation degree (pressure rise experiments at 20°C).....	44
Fig. 2.8. Current density-voltage and power density plots of the DMFC using sPEEK membranes with SD= 52 and 71%, at 50°C. Nafion <sup>®</sup> 112 given as reference. ....	46
Fig. 2.9. Predicted potential and Faraday DMFC efficiencies during operation using sPEEK membranes with SD= 52 and 71%, at 50°C. Nafion <sup>®</sup> 112 given as reference.....	47
Fig. 2.10. Predicted overall DMFC efficiency during operation using sPEEK membranes with SD= 52 and 71%, at 50°C. Nafion <sup>®</sup> 112 given as reference. ....	48
Fig. 3.1. Water uptake of sPEEK membranes as a function of $ZrO_2$ content (data at room temperature). Nafion <sup>®</sup> 112 given as reference.....	59

Fig. 3.2. Proton conductivity of sPEEK membranes as a function of ZrO <sub>2</sub> content (25°C in 0.33M H <sub>2</sub> SO <sub>4</sub> ). Nafion <sup>®</sup> 112 given as reference. ....	60
Fig. 3.3. Water flux through sPEEK membranes as a function of ZrO <sub>2</sub> content (pervaporation experiments at 55 °C). Nafion <sup>®</sup> 112 given as reference. ....	61
Fig. 3.4. Methanol flux through sPEEK membranes as a function of ZrO <sub>2</sub> content (pervaporation experiments at 55 °C). Nafion <sup>®</sup> 112 given as reference. ....	62
Fig. 3.5. Selectivity towards water/methanol of sPEEK membranes as a function of ZrO <sub>2</sub> content (pervaporation experiments at 55 °C). Nafion <sup>®</sup> 112 given as reference. ....	62
Fig. 4.1. Sketch of the DMFC illustrating the mass transport of the different species through the proton exchange membrane. ....	66
Fig. 4.2. Proton conductivity and impedance resistance of the sPEEK composite membranes in an acid electrolyte as a function of the ZrO <sub>2</sub> content (25°C in 0.33M H <sub>2</sub> SO <sub>4</sub> ). ....	71
Fig. 4.3. Proton conductivity (a) and impedance resistance (b) of the sPEEK composite membranes in water vapor as a function of the ZrO <sub>2</sub> content (100% r.h.). ....	72
Fig. 4.4. Water uptake of sPEEK composite membranes as a function of the ZrO <sub>2</sub> content (room temperature). ....	72
Fig. 4.5. Methanol permeability coefficients and water/methanol selectivity of the sPEEK composite membranes as a function of the ZrO <sub>2</sub> content (pervaporation experiments at 55°C, 1 Barrer = 10 <sup>-10</sup> cm <sup>3</sup> [STP] cm / (cm <sup>2</sup> s cmHg) ). ....	73
Fig. 4.6. Nitrogen, oxygen and carbon dioxide permeability coefficients of sPEEK composite membranes as a function of the ZrO <sub>2</sub> content (pressure rise experiments at 20°C). ....	74
Fig. 4.7. Oxygen/nitrogen and carbon dioxide/nitrogen selectivities of the sPEEK composite membranes as a function of the ZrO <sub>2</sub> content (pressure rise experiments at 20°C). ....	75
Fig. 4.8. Scanning electron micrograph of sPEEK composite membranes with 2.5 wt.% of ZrO <sub>2</sub> . ....	76
Fig. 4.9. Scanning electron micrograph showing the ZrO <sub>2</sub> particles finely dispersed in the sPEEK composite membrane with 5 wt.% of ZrO <sub>2</sub> . ....	76
Fig. 4.10. Ratio between zirconium and carbon content of the sPEEK composite membranes as a function of the ZrO <sub>2</sub> content (elemental analysis by X-ray microfluorescence, EDAX). ....	77
Fig. 5.1. Sketch of a DMFC illustrating proton, water and methanol permeation across the PEM and related characterization methods. ....	83
Fig. 5.2. Current density-voltage and power density plots of the DMFC using sPEEK composite membranes with: a) 5.0, b) 7.5 and c) 10wt.%ZrO <sub>2</sub> . ....	86
Fig. 5.3. Null phase angle impedance (a), current density (b) and CO <sub>2</sub> concentration at the cathode outlet (c) for constant voltage DMFC experiments (35mV) as a function of the ZrO <sub>2</sub> content. ....	88

Fig. 5.4. Null phase angle impedance (a), voltage (b) and CO <sub>2</sub> concentration at the cathode outlet (c) for open circuit DMFC experiments as a function of the ZrO <sub>2</sub> content.....	89
Fig. 5.5. DMFC current density for constant voltage experiments (35mV) as a function of proton conductivity evaluated in the acid electrolyte cell (25°C). .....	90
Fig. 5.6. DMFC null phase angle impedance for constant voltage experiments (35mV) as a function of proton transport resistance evaluated in the acid electrolyte cell (25°C).....	91
Fig. 5.7. DMFC current density for constant voltage experiments (35mV) as a function of proton conductivity evaluated in the vapor cell (50, 70 and 90°C). .....	91
Fig. 5.8. DMFC null phase angle impedance for constant voltage experiments (35mV) as a function of proton transport resistance evaluated in the vapor cell (50, 70 and 90°C). .....	92
Fig. 5.9. DMFC current density and null phase angle impedance for constant voltage experiments (35mV) as a function of water uptake evaluated by batch experiments (room temperature)....	93
Fig. 5.10. Carbon dioxide concentration (%) at the cathode outlet for constant voltage experiments (35mV) as a function of water uptake evaluated by batch experiments (room temperature)....	93
Fig. 5.11. Carbon dioxide concentration (%) at the cathode outlet for constant voltage experiments (35mV) as a function of the methanol permeability coefficient evaluated by pervaporation experiments (55°C). .....	94
Fig. 6.1. Sketch of the DMFC illustrating the mass transport of the different species through the proton exchange membrane and the characterization methods used for fuel cell modeling. ...	104
Fig. 6.2. Predicted (curves) and experimental (points: ● 50°C; ▲70°C; ■ 90°C; ◆ 100°C; * 110°C) current density-voltage and power density plots for DMFC operation using sPEEK composite membranes with: a) 5.0, b) 7.5 and c) 10wt.%ZrO <sub>2</sub> .....	115
Fig. 6.3. Predicted (curves) and experimental (points: ● 50°C; ▲70°C; ■ 90°C) current density (a) and CO <sub>2</sub> concentration at the cathode outlet (b) for DMFC operation at constant voltage (35mV) as a function of the ZrO <sub>2</sub> content.....	116
Fig. 6.4. Predicted (curves) and experimental (points: ● 50°C; ▲70°C; ■ 90°C) voltage (a) and CO <sub>2</sub> concentration at the cathode outlet (b) for open circuit DMFC operation as a function of the ZrO <sub>2</sub> content.....	117
Fig. 6.5. Predicted DMFC efficiency using sPEEK composite membranes with 5.0wt.%ZrO <sub>2</sub> : Faraday and potential efficiencies (a) and overall efficiency (b).....	118
Fig. 6.6. Predicted DMFC efficiency using sPEEK composite membranes with 7.5wt.%ZrO <sub>2</sub> : Faraday and potential efficiencies (a) and overall efficiency (b).....	119
Fig. 6.7. Predicted DMFC efficiency using sPEEK composite membranes with 10.0wt.%ZrO <sub>2</sub> : Faraday and potential efficiencies (a) and overall efficiency (b).....	119

Fig. 7.1. Sketch of a DMFC illustrating protons, methanol and water transport through the proton exchange membrane.....	128
Fig. 7.2. Predicted current density-voltage plots of the DMFC, at 70°C, as a function of the PEM: (a) proton conductivity (permeability towards methanol of $2.95 \times 10^{-6} \text{ mol s}^{-1} \text{ m}^{-1}$ ) and (b) permeability towards methanol (proton conductivity of $2.98 \text{ S m}^{-1}$ ).....	132
Fig. 7.3. Predicted open circuit voltage, at 70°C, as a function of the PEM proton conductivity and permeability towards methanol.....	133
Fig. 7.4. Predicted CO <sub>2</sub> concentration at the cathode outlet for open circuit voltage experiments, at 70°C, as a function of the PEM proton conductivity and permeability towards methanol.....	134
Fig. 7.5. Predicted current density (constant voltage experiments, 35mV), at 70°C, as a function of the PEM proton conductivity and permeability towards methanol.....	135
Fig. 7.6. Predicted CO <sub>2</sub> concentration at the cathode outlet for constant voltage experiments, 35mV, at 70°C, as a function of the PEM proton conductivity and permeability towards methanol. .	136
Fig. 7.7. Predicted maximum power density, at 70°C, as a function of the PEM proton conductivity and permeability towards methanol. ....	137
Fig. 7.8. Predicted maximum potential efficiency, at 70°C, as a function of the PEM proton conductivity and permeability towards methanol. ....	138
Fig. 7.9. Predicted maximum Faraday efficiency, at 70°C, as a function of the PEM proton conductivity and permeability towards methanol. ....	139
Fig. 7.10. Predicted maximum DMFC global efficiency, at 70°C, as a function of the PEM proton conductivity and permeability towards methanol. ....	139
Fig. 8.1. Proton conductivity of various sPEEK membranes (sPEEK / ZrPh / PBI, wt.%) in the water vapor cell as a function of temperature (at 100% r.h.).....	155
Fig. 8.2. Swelling in 20 wt.% methanol solution as a function of temperature.....	157
Fig. 8.3. Total flux from pervaporation measurements at 55°C as a function of swelling in 20 % methanol solution (batch experiments at pervaporation conditions). ....	158
Fig. 8.4. Scanning electron micrograph of sPEEK (SD=42%) membrane with 20% ZrPh and 11.2% of PBI. ....	160
Fig. 8.5. Power density plots of the DMFC using various sPEEK membranes, at 110°C and 100% r.h. in the cathode feed. ....	161
Fig. 8.6. Power density plots of the DMFC using sPEEK composite membranes, at 110°C and 138% r.h. in the cathode feed. ....	162

Fig. 8.7. Maximum power density of the DMFC (110°C and r.h. of 100 and 138%), as a function of swelling in 20wt.% methanol solution (lines are guides to the eye), evaluated through batch experiments at 70°C. ....	162
Fig. 8.8. Maximum power density of the DMFC (110°C and r.h. of 100 and 138%), as a function of the proton conductivity (lines are guides to the eye), evaluated in acid electrolyte (0.33M H <sub>2</sub> SO <sub>4</sub> , impedance spectroscopy at 25°C).....	163
Fig. 9.1. Sketch of a DMFC: water, methanol and proton transport through the proton exchange membrane.....	170
Fig. 9.2. Current density loss due to methanol crossover as a function of the DMFC current density (linear approximation).....	178
Fig. 9.3. Proton conductivity, aqueous methanol swelling and methanol permeability coefficients of the sPEEK composite membranes, using the data of sPEEK SD42 membrane as reference. .	179
Fig. 9.4. Open circuit voltage experiments: a) Open circuit voltage and b) Null phase angle impedance as a function of temperature for the DMFC using sPEEK composite membranes. ....	180
Fig. 9.5. Constant voltage experiments, 35mV: a) Current density and b) Null phase angle impedance as a function of temperature for the DMFC using sPEEK composite membranes. ....	182
Fig. 9.6. Faraday efficiency (constant voltage experiments, 35mV) as a function of temperature for the DMFC using sPEEK composite membranes. ....	184
Fig. 9.7. Polarization curves and estimated efficiency of the DMFC using sPEEK composite membranes at 110°C. ....	185
Fig. 9.8. Polarization curves and estimated efficiency of the DMFC, for several temperatures, using the composite membrane sPEEK SD=68% 20.0wt% ZrPh 11.2wt.%PBI. ....	186



## Table Captions

Table 1.1. Energy density of fuels for direct polymer electrolyte fuel cells [7].	5
Table 1.2. Thermodynamic data and overall enthalpic and reversible voltage for the direct methanol fuel cell reactions (standard conditions, $P = 1$ atm and $T = 298.15$ K; Anode: methanol oxidation reaction; Cathode: oxygen reduction reaction) [10].	8
Table 2.1. Proton conductivity, methanol and water permeability coefficients and selectivity towards water/methanol of Nafion <sup>®</sup> 112 (pervaporation experiments at 25°C).	40
Table 2.2. Carbon dioxide, nitrogen and oxygen permeability coefficients and selectivity towards N <sub>2</sub> /O <sub>2</sub> and CO <sub>2</sub> /O <sub>2</sub> of Nafion <sup>®</sup> 112 (pressure rise experiments at 20°C).	45
Table 6.1. Model parameters and constants	106
Table 7.1. Predicted and experimented (between branches, tested in set-up described in [28]) DMFC performance, at 70°C, using a selected series of PEMs.	141
Table 7.2. Predicted DMFC efficiencies, at 70°C, using a selected series of PEMs.	142
Table 8.1. Proton conductivity of various sPEEK membranes in an acid electrolyte (25°C in 0.33M H <sub>2</sub> SO <sub>4</sub> ).	154
Table 8.2. Pre-exponential factors, $A$ , and activation energy, $E_a$ , of various sPEEK membranes in the water vapor cell.	155
Table 8.3. Swelling of membranes based on sPEEK composites when immersed in water and aqueous methanol (20wt.%) (batch experiments at room temperature).	156
Table 8.4. Methanol and water permeability coefficients and water/methanol selectivity of the sPEEK composite membranes (pervaporation experiments at 55°C with 20wt.% aqueous methanol solution used as feed, 1 Barrer = $10^{-10}$ cm <sup>3</sup> [STP] cm / (cm <sup>2</sup> s cmHg)).	158
Table 8.5. Nitrogen, oxygen and carbon dioxide permeability coefficients and oxygen/nitrogen and carbon dioxide/nitrogen selectivities of the various sPEEK membranes (pressure rise method at 20°C with swollen membranes).	159
Table 9.1. Carbon dioxide concentration (vol.%) at the cathode outlet for open circuit experiments as a function of the DMFC operation temperature.	181
Table 9.2. Carbon dioxide concentration (vol.%) at the cathode outlet for constant voltage experiments (35mV) as a function of the DMFC operation temperature.	183
Table 9.3. Peak power density and corresponding potential evaluated for DMFC using sPEEK composite membranes at 110°C.	185

Table 9.4. Peak power density at 250mV evaluated for the DMFC, at several temperatures, using the sPEEK composite membrane SD=68% 20.0wt% ZrPh 11.2wt.%PBI. .... 187

## Abstract

In the present work, a critical study of novel proton exchange membranes (PEM) for direct methanol fuel cell (DMFC) applications was performed. This study involved the preparation of plain and inorganically modified membranes, and subsequent characterization, DMFC test and mathematical modeling.

The selected polymer was the sulfonated poly(ether ether ketone) (sPEEK). Nafion<sup>®</sup> was used as reference material. The selected materials for performing the inorganic modifications were zirconium oxide ( $ZrO_2$ ) and  $\alpha$ -zirconium phosphate pre-treated with *n*-propylamine and polybenzimidazole. The incorporation of zirconium oxide was performed via *in situ* hydrolysis of the zirconium tetrapropylate, in the presence of acetyl acetone (chelating agent). The zirconium phosphate dispersion was synthesized treating its oxide dispersion with a solution of phosphoric acid. The  $ZrO_2$  dispersion was obtained treating an aqueous solution of  $ZrOCl_2$  with a solution of ammonia. The exfoliation of the zirconium phosphate was performed by adding *n*-propylamine. Polybenzimidazole was added to the dispersion in order to improve the compatibility between the inorganic particles and the polymer matrix and to improve the chemical/thermal stability of the composite membranes.

In order to characterize and select the proper materials for DMFC applications, the following characterization methods were implemented: impedance spectroscopy (proton conductivity), swelling (water uptake), pervaporation (permeation of the liquid DMFC species), gas permeation (permeation of the gaseous DMFC species), scanning electron microscopy (SEM, morphology) and x-ray microfluorescence (XRMF, elemental analysis). Apart from this, DMFC tests were implemented for a certain collection of membranes previously selected according to the characterization results. The membrane electrode assemblies (MEAs) prepared using these membranes were tested investigating the DMFC current-voltage polarization curves, constant voltage current (CV, 35mV), and open circuit voltage (OCV). The fuel cell ohmic resistance (null phase angle impedance, NPAI) and  $CO_2$  concentration at the cathode outlet were also measured.

Additionally, in order to improve the PEM research strategy for DMFC applications, a more fundamental research work concerning the overall PEM development chain was performed, starting with the membrane preparation and going till the DMFC application and numerical modeling. Besides, a validation of the standard characterization methods regarding the fuel cell performance prediction is also performed. We were able to prepare sPEEK composite membranes with a wide and well defined range of physical/chemical properties by changing the  $ZrO_2$  inorganic content. The

prepared set of membranes allowed a systematic study of the membrane properties effect on the DMFC performance. On the other hand, this systematic work was used to develop a steady-state mathematical model that uses these characterization results as inputs. This model proved to be very useful for predicting the DMFC performance for materials under development. Using the developed model, a critical study regarding the PEM properties for DMFC applications was also carried out, taking into account the compromise between proton conductivity and permeability towards methanol.

## Sumário

O presente trabalho estuda fundamentalmente novas membranas de permuta protónica (“proton exchange membrane”, PEM) para células de combustível com alimentação directa de metanol (“direct methanol fuel cell”, DMFC). O estudo envolveu a preparação de membranas não modificadas e modificadas inorganicamente e subsequente caracterização, teste na DMFC e modelização.

O polímero seleccionado foi a poli(éter éter cetona) sulfonada (“sulfonated poly(ether ether ketone)”, sPEEK). Nafion<sup>®</sup> foi utilizado como material referência. Os materiais seleccionados para a modificação inorgânica do polímero sPEEK foram o óxido de zircónio ( $ZrO_2$ ) e o  $\alpha$ -fosfato de zircónio tratado com *n*-propilamina e polibenzimidazole. A formação *in situ* de partículas cerâmicas de  $ZrO_2$  no seio do polímero sPEEK foi realizada por intermédio da hidrólise do tetrapropilato de zircónio, com adição de acetilacetona para prevenir a precipitação do alcóxido. Por sua vez, a incorporação de fosfato de zircónio foi feita por intermédio de uma dispersão preparada previamente, tendo o fosfato sido obtido a partir do tratamento de uma dispersão do respectivo óxido com ácido fosfórico. A dispersão de  $ZrO_2$  foi obtida a partir do tratamento de uma solução aquosa de  $ZrClO_2$  com uma solução de amónia. Depois de obtida a dispersão de fosfato de zircónio, esta foi tratada com polibenzimidazole e propilamina de forma a melhorar a compatibilidade entre as fases inorgânica e orgânica e esfoliar o fosfato, respectivamente.

Com o intuito de se caracterizarem e seleccionarem as PEMs mais promissoras para aplicação na DMFC, foram implementados os seguintes métodos de caracterização: espectroscopia de impedância (condutividade protónica), sorção de água (“uptake” de água), pervaporação (permeação das espécies líquidas da DMFC), permeação de gases (permeação das espécies gasosas da DMFC), microscopia electrónica de varrimento (SEM, morfologia) e microfluorescência de raios-x (XRMF, análise elementar). Foram também realizados testes na DMFC a um determinado conjunto de membranas seleccionadas de acordo com os resultados obtidos durante a etapa de caracterização. Os sistemas eléctrodos membrana preparados com estas membranas foram investigados na DMFC medindo as curvas de polarização, a corrente a voltagem constante (CV, 35mV) e a voltagem de circuito aberto (“open circuit voltage”, OCV). A resistência ohmica da célula de combustível (impedância para ângulo de fase nulo) e a concentração de  $CO_2$  à saída do cátodo foram igualmente investigados.

De forma a melhorar a estratégia de desenvolvimento de membranas para aplicação na DMFC, no presente trabalho foi feito um estudo fundamental envolvendo toda a cadeia de

desenvolvimento da PEM, começando pela sua preparação até à aplicação na DMFC e modelização numérica. Este estudo englobou a validação dos métodos de caracterização utilizados no que diz respeito à previsão dos desempenhos na célula de combustível para um dado material. A preparação de membranas sPEEK com uma modificação gradual do conteúdo inorgânico em  $ZrO_2$  permitiu a obtenção de membranas com uma gama alargada e bem definida de propriedades. Estas membranas possibilitaram um estudo sistemático da influência das suas propriedades no desempenho da DMFC. Para além disso, este trabalho de investigação sistemático foi utilizado no desenvolvimento de um modelo matemático da DMFC, em estado estacionário, que usa os resultados da caracterização como entradas. Este modelo provou ter bastante utilidade na previsão do desempenho da DMFC para materiais em desenvolvimento. Utilizando este modelo foi também efectuado um estudo relativo ao efeito das propriedades das membranas no desempenho da DMFC, tendo em conta o compromisso entre a condutividade protónica e a permeabilidade ao metanol.

## Sommaire

Le présent travail repose essentiellement sur l'étude de nouvelles membrane échangeuse de protons ("proton exchange membranes", PEM) pour la cellule à combustible directe méthanol ("direct methanol fuel cell", DMFC). Cette étude a impliqué la préparation de membranes plaines et inorganiquement modifiées et subséquente caractérisation, test en DMFC et modélage mathématique.

Le polymère étudié était le poly(éther éther cétone) sulfoné ("sulfonated poly(ether ether ketone)", sPEEK). Nafion<sup>®</sup> a été utilisé comme matériaux référence. Les matériaux sélectionnés pour exécuter les modifications inorganiques étaient l'oxyde de zirconium ( $ZrO_2$ ) et le  $\alpha$ -phosphate de zirconium traité avec n-propylamine et polybenzimidazole. L'incorporation d'oxyde de zirconium a été exécutée via *in situ* hydrolyse de le tetrapropylate de zirconium, dans la présence d'acétylacétone (agent du chélation). A son tour, l'incorporation de phosphate de zirconium a été faite à partir du traitement d'une dispersion préalablement préparée de l'oxyde respectif avec une solution d'acide phosphorique. La dispersion de  $ZrO_2$  a été obtenue avec une solution aqueuse de  $ZrOCl_2$  traitée avec une solution d'ammoniac. L'exfoliation du phosphate de zirconium a été exécutée avec n-propylamine. Le polybenzimidazole a été additionné à la dispersion pour améliorer la compatibilité entre les particules inorganiques et le polymère et la stabilité des membranes composées.

Pour caractériser et sélectionner les matériaux adéquates pour l'application en DMFC, les méthodes suivantes de caractérisation ont été appliquées: spectroscopie d'impédance (conductivité protonique), sorption de l'eau (eau "uptake"), pervaporation (perméation de l'espèce liquide), perméation du gaz (perméation de l'espèce gazeuse), microscopie électronique (SEM, morphologie) et microfluorescence X (XRMF, analyse élémentaire). Le test en DMFC d'une certaine collection de membranes sélectionnée a été aussi exécuté après la caractérisation. L'assemblage électrode-membrane ("membrane electrode assembly", MEA) préparé avec ces membranes a été testé en la DMFC mesurant les courbes de polarisation, le courant électrique à voltage constant (CV, 35mV), et voltage du circuit ouvert (OCV). La résistance ohmique de la cellule de combustible (impédance de l'angle de phase nulle, NPAI) et la concentration de  $CO_2$  à la sortie de la cathode a été aussi mesurée.

Au surplus, afin d'améliorer la stratégie de recherche du PEM pour l'application en DMFC, une étude fondamentale comprenant la totalité de la chaîne de développement a été exécutée, commençant dans la préparation de la membrane et allant jusqu'à l'application en DMFC et

modélage numérique. Aussi, a été effectuée une validation des méthodes de caractérisation relativement aux prévisions de la performance de la DMFC. Nous étions aussi capables de préparer des membranes sPEEK composées avec une large variation bien définie des propriétés en changeant le contenu inorganique en  $ZrO_2$ . Ces membranes ont permis une étude systématique de l'influence de leurs propriétés dans la performance de la DMFC. Également, ce travail systématique a été utilisé pour développer un modèle mathématique, en équilibre, qui utilise des résultats de la caractérisation comme entrées. Ce modèle s'est révélé très utile pour prédire la performance de la DMFC pour matériaux en développement. Avec le modèle développé, dans ce travail il a été fait une analyse relative à l'effet des propriétés critiques des membranes dans l'application en DMFC, en prenant en considération le compromis entre la conductivité protonique et la perméabilité au méthanol.

# PART ONE

---

## **Introduction**



## Chapter 1. Membranes for direct methanol fuel cell applications: analysis based on characterization, experimentation and modeling\*

### Abstract

A critical analysis is performed about fundamental aspects regarding the direct methanol fuel cell (DMFC) technology, focusing mainly on the proton exchange membrane (PEM). First, the basic DMFC operation principles, thermodynamic background and polarization characteristics are presented with a description of each of the components that comprise the membrane electrode assembly (MEA) and of the DMFC test system usually used for DMFC research. Next, the chapter focuses particularly on the PEM development chain, performing an overview of the research progress regarding this DMFC component. Specific efforts are devoted to research aspects related with the membrane preparation, characterization, DMFC tests and modeling. Apart from this, recent achievements regarding the PEM development for DMFC applications are emphasized.

---

\*V.S. Silva, A. Mendes, L.M. Madeira and S.P. Nunes, in *Advances in Fuel Cells*, Xiang-Wu Zhang (Ed.), Research Signpost, (accepted, 2005).

## 1.1. Introduction

In the last two decades, the interest in the fuel cell technology has increased dramatically. Earth environmental issues related with atmospheric pollution, green house effects and global warming are the main driving forces [1]. In contrast to the environmental and efficiency limitations associated to thermal processes that are commonly used for producing energy from fossil fuels, fuel cells have potentially higher efficiencies (non dependent on the *Carnot* cycle) with absence of local gaseous pollutants, such as sulfur dioxide and the various nitrogen oxides, along with striking simplicity and absence of moving parts [1,2].

Nowadays, after many years of research and development, there are several fuel cell systems near commercialization [3]. The possible applications of this technology range from stationary power production (megawatts), down to portable systems to supply portable electric equipments, such as notebooks, cellular phones and video cameras (watts). In between these two extremes lies the application for transportation, with almost all major car manufactures now having their own research programs [3].

While hydrogen is the best fuel in terms of energy conversion (chemical into electrical), its production, storage and distribution has several problems [4-7]. No efficient and practical method of storing hydrogen for fuel cell applications currently exists [8]. While liquefaction leads to a form of hydrogen that is potentially attractive for use in larger fuel cell systems, the energy density is low due to the ultra-low gravimetric density of the fuel (Table 1.1). Furthermore, if the energy consumed during the liquefaction process is taken into account, the energy density is lowered still further, by as much as 40% [7]. Another hydrogen storage approach is the application of metal hydrides. However, the reversible storage of hydrogen in metal hydrides has been limited to relatively low achievable specific energy (Wh/g of hydride) [8].

Although less reactive compared to hydrogen, methanol ( $\text{CH}_3\text{OH}$ ) is considered to be an alternative fuel due to its high energy density (Table 1.1), being easier to store and distribute (liquid at atmospheric temperature). Additionally, methanol can be easily produced from natural resources (wood, natural gas, coal) and is biodegradable. In comparison to other carbonaceous or alcoholic fuels, methanol is known to have the best combination between energy density and rate of electro-oxidation [4]. Methanol can be completely electro-oxidized to  $\text{CO}_2$  at temperatures well below  $100^\circ\text{C}$  and, furthermore, it has enough energy density in comparison to that of other fuels (Table 1.1).

The methanol drawbacks for widespread use in fuel cells systems are the facts of being toxic, causing blindness or even death if swallowed, and being flammable, forming explosive mixtures with air and burning without flame. In order to fulfill these health and safety issues, fuel cell developers plan to build up closed systems using diluted aqueous methanol solutions, which decrease significantly the toxic and flammability problems (typically 5wt.% in water).

Table 1.1. Energy density of fuels for direct polymer electrolyte fuel cells [7].

Fuel	Fuel cell reaction	Energy Density Wh cm <sup>-3</sup>
Hydrogen (liq. at -273°C)	$H_2 + 0.5O_2 \rightarrow H_2O$	2.7
Hydrogen (gas at 20MPa)	$H_2 + 0.5O_2 \rightarrow H_2O$	0.5
Methanol (liq.)	$CH_3OH + 1.5O_2 \rightarrow CO_2 + 2H_2O$	4.8
Ethanol (liq.)	$C_2H_5OH + 3O_2 \rightarrow 2CO_2 + 3H_2O$	6.3
Ethylene glycol (liq.)	$C_2O_2H_6 + 2.5O_2 \rightarrow 2CO_2 + 3H_2O$	5.9

Methanol can be used directly in fuel cells, the direct methanol fuel cell (DMFC), or indirectly as hydrogen source to polymer electrolyte membrane fuel cells (PEMFC), after reformation. The on-board reforming approach, which involves extensive, multi-step purification of the fuel, after which the resulting hydrogen-rich mixture is supplied to the PEMFC, seems to be quite complex and not a reliable power delivery source over long time applications and reasonably broad conditions of operation [7]. These limitations led the R&D community to the conclusion that DMFC operating at low/medium temperatures (up to 130°C) is the most favorable option for mobile and portable applications (ranging from mW to W). Furthermore, since methanol is fed directly as diluted aqueous solution (typically 5wt.%), it also avoids complex humidification and thermal management problems associated to the hydrogen fuel cells.

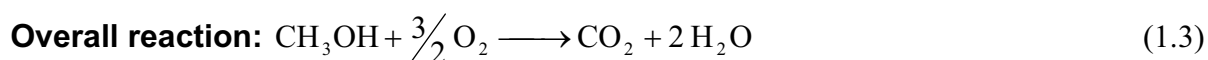
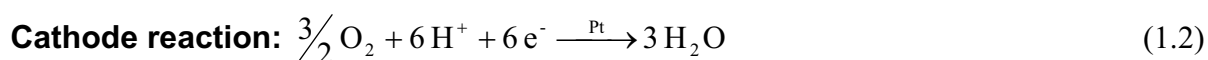
In the last years, “heavyweight players” such as Sony, Toshiba, Nokia, Siemens, Motorola and Samsung, among others, are investing serious amounts of money in the development and commercialization of the direct methanol fuel cell for portable applications [6]. They believe that the payback will be a next generation power source that will revolutionize the performance and easy-of-use of all sorts of portable electronic equipments – including notebook computers, mobile phones, video cameras and plenty more besides [7]. Furthermore, some of these companies are talking in terms of months rather than years when it comes to DMFC based products commercialization [9]. In comparison with the rechargeable battery based on lithium ion polymer,

the DMFC has theoretically 10 times more weight energy density [6]. This performance translates into larger conversation times for mobile phones, longer times for use of notebook computers between replacement of fuel cartridges and more power available on these devices to support consumer demand. Another advantage regarding consumer convenience is the instantaneous refueling of the DMFC in comparison to the rechargeable batteries that require hours for charging the depleted power.

## 1.2. Basics of the DMFC

The basic DMFC is comprised by two electrodes, anode and cathode, and a solid electrolyte in between [4]. The usually applied catalysts in the DMFC anode and cathode catalyst layers are Pt/Ru ( $\sim 2\text{mg}/\text{cm}^2$ ) and Pt ( $\sim 0.5\text{mg}/\text{cm}^2$ ), respectively. As electrolyte, the DMFC uses a proton exchange membrane (PEM) that electronically isolates the anode from the cathode and enables the transport of protons. Although the thermodynamic characteristics are similar to the hydrogen reaction, especially in terms of reversible oxidation potential, the methanol electro-oxidation reaction is a slow process, as it involves the transfer of six electrons to the electrode for complete oxidation to carbon dioxide.

The involved reactions in the DMFC are the following:



The basic operation principle of the DMFC is shown in Fig. 1.1. At the anode, methanol and water are supplied and converted to carbon dioxide, protons and electrons. Currently most of the systems described in the open literature involve a liquid methanol-water feed, although in some platforms the methanol is supplied to the DMFC anode as vapor. The produced electrons from the anode reaction are subsequently transferred via the external circuit (which includes a load), where they can perform electric work. On the other hand, protons are transported to the cathode side through the PEM. At the cathode, the protons and electrons reduce oxygen (from air) to form water.

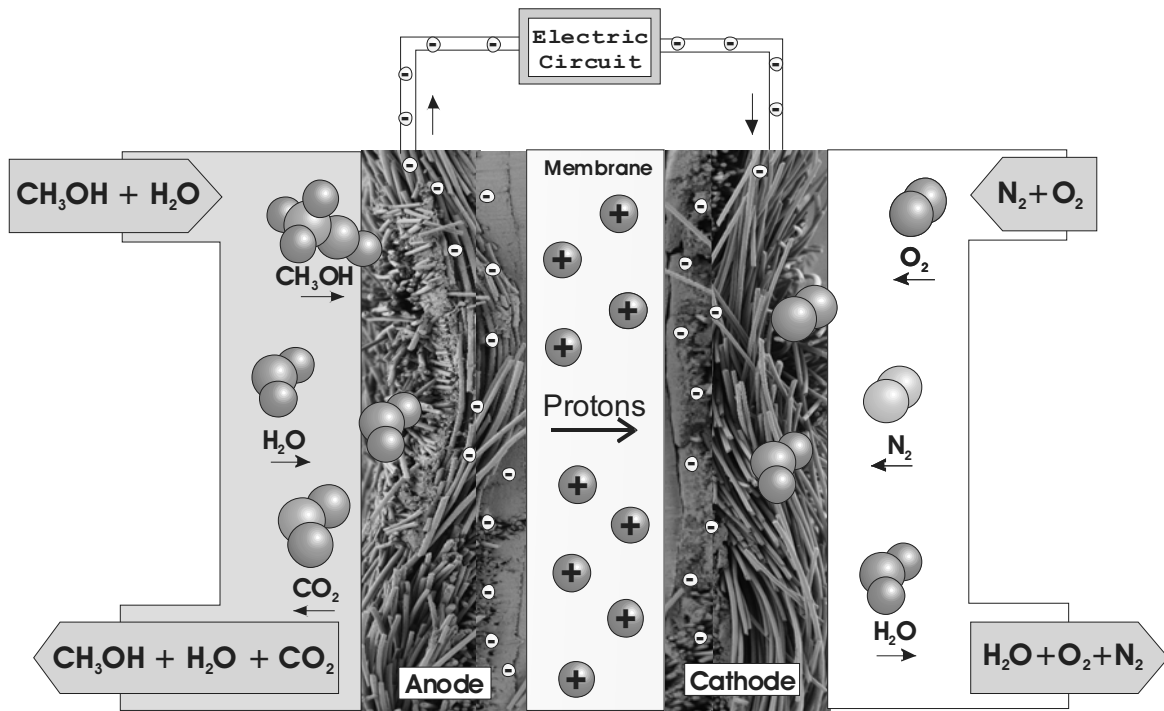


Fig. 1.1. Sketch of the DMFC illustrating the mass transport of the different species ( $\text{H}_2\text{O}$ ,  $\text{CH}_3\text{OH}$ ,  $\text{N}_2$ ,  $\text{O}_2$ ,  $\text{CO}_2$ ).

### 1.2.1. Thermodynamic background

In an electrochemical cell, operating at isothermal conditions, if the enthalpy energy of both anode and cathode reactions could be fully converted into electric work, the enthalpic cell voltage,  $U_H$ , obtained would be:

$$U_H = -\frac{\Delta H_R}{zF} \quad (1.4)$$

where  $z$  is the number of electrons involved in the electrochemical reaction (6 electrons for the DMFC),  $F$  is the Faraday constant ( $96484.6 \text{ C mol}^{-1}$ ) and  $\Delta H_R$  is the overall reaction enthalpy at standard conditions (Table 1.2).

However, according to the second law of thermodynamics, if an electrochemical cell operates reversibly (concerning the energy conversion) [1], there will be a variation of the system entropy (released heat). Thus, the maximal electric work of an electrochemical cell is obtained from the Gibb's free energy variation,  $\Delta G_R$ , and the maximal fuel cell voltage,  $U_{rev}$ , is obtained as follows:

$$U_{rev} = -\frac{\Delta G_R}{zF} = -\frac{\Delta H_R - T\Delta S_R}{zF} \quad (1.5)$$

where  $T$  is the system absolute temperature and  $\Delta S_R$  is the variation of the system entropy for standard conditions (Table 1.2).

Table 1.2. Thermodynamic data and overall enthalpic and reversible voltage for the direct methanol fuel cell reactions (standard conditions,  $P = 1$  atm and  $T = 298.15$ K; Anode: methanol oxidation reaction; Cathode: oxygen reduction reaction) [10].

Reaction	$\Delta H_R$ [kJ mol <sup>-1</sup> ]	$\Delta S_R$ [J mol <sup>-1</sup> K <sup>-1</sup> ]	$\Delta G_R$ [kJ mol <sup>-1</sup> ]	$U_H$ [V]	$U_{rev}$ [V]
Methanol oxidation	110.69	-79.11	134.28	-0.19	-0.23
Oxygen reduction	-857.49	-97.98	-828.28	1.48	1.43
Overall Cell	-746.80	-177.09	-694.00	1.29	1.20

Since not all the fuel chemical energy in a DMFC is converted into electric work, the thermodynamic fuel cell efficiency is limited by the fuel intrinsic properties. Therefore the maximum thermodynamic efficiency that can be achieved by a DMFC electrochemical cell can be obtained by the following equation:

$$\eta_{th} = \frac{U_{rev}}{U_H} = \frac{\Delta G_R}{\Delta H_R} \quad (1.6)$$

From the data presented in Table 1.2, the maximal thermodynamic efficiency of 92.9% for the DMFC (at standard conditions) can be obtained.

### 1.2.2. Polarization behavior

The classical experimental procedure to evaluate the performance of a fuel cell is to measure the stationary current-voltage behavior (Fig. 1.2). The S-shape curve, which is typical for a fuel cell

system, reflects the different limiting mechanisms occurring during the operation of the fuel cell [5]. From Fig. 1.2, it can be observed that at zero current the cell presents the maximum experimental voltage value (open circuit voltage, OCV). The DMFC experimental open circuit voltage differs from the reversible DMFC voltage due, essentially, to fuel losses (methanol crossover from the anode to the cathode) [11]. The transport of methanol from the anode to the cathode is associated to the problematic high permeability of PEM towards methanol. The permeated methanol reacts with oxygen at the cathode side forming a mixed potential that decreases the open circuit voltage. This DMFC limitation will be further discussed in next sections.

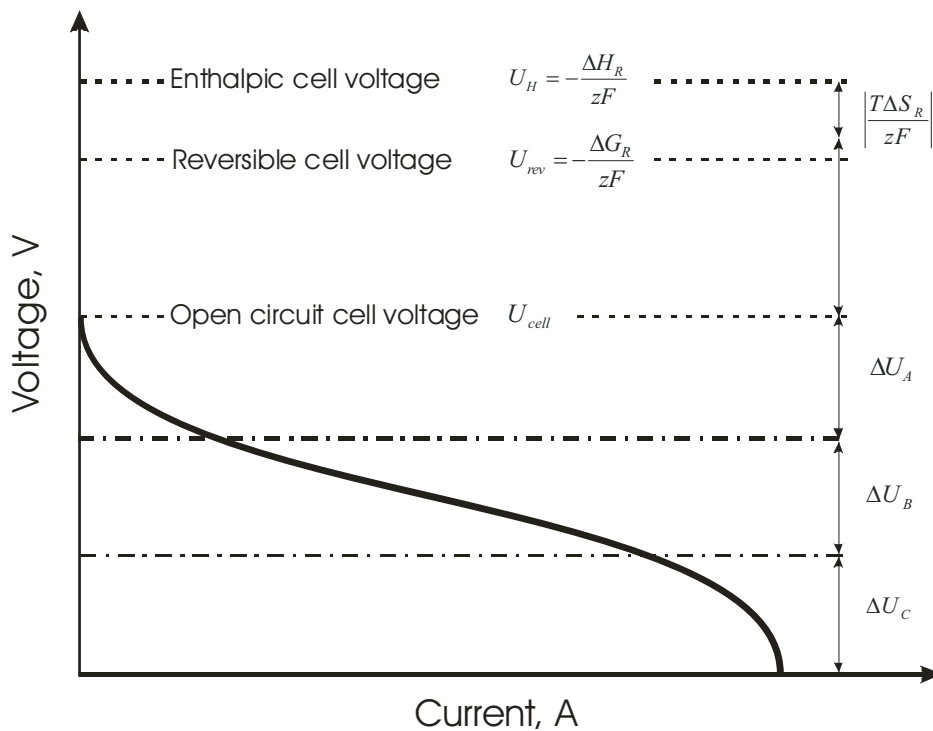


Fig. 1.2. Typical current-voltage behavior of a DMFC.

For low current densities, the cell voltage loss is mainly influenced by the kinetic limitations of the reactions involved at the anode and cathode (Fig. 1.2). The so called activation polarization,  $\Delta U_A$ , is mainly due to the energy reaction barrier (mostly the methanol electro-oxidation reaction), which must be overcome for the electrochemical reaction occur. For the DMFC, the methanol oxidation is one of the most limiting aspects due to the poor electro-oxidation kinetics [4-7]. Indeed, an overall of six electrons are formed (Eq. 1.1); consequently many surface-bound reaction intermediates can be expected [5]. At high current densities, mass transport limitations dominate the process, increasing the potential loss due to cell fuel or oxidant starvation,  $\Delta U_C$  (Fig. 1.2). For a certain current (limiting current) the cell voltage drops to zero. In between A and C regions, lies the

so called resistance polarization region,  $\Delta U_B$ , in which the voltage variation shows more or less an ohmic behavior (Fig. 1.2). This potential loss is mainly associated with the transport of electrons and protons through the electrodes and electrolyte, respectively. The electrodes usually have low resistance for the transport of electrons. However, the proton exchange membrane has much higher resistance for the transport of protons (ionic resistance) from the anode to the cathode, being the dominant factor in the ohmic voltage loss [5].

### 1.2.3. Membrane electrode assembly

The membrane electrode assembly (MEA) consists in the association of anode and cathode catalyst layers, ion-exchange polymer membrane and anode and cathode electrode backing/gas diffusion layers (Fig. 1.3) [1]. The functions of the three basic components are intimately related, and the interfaces formed between them and with the plates flow fields are critical for maximum fuel cell performance [12].

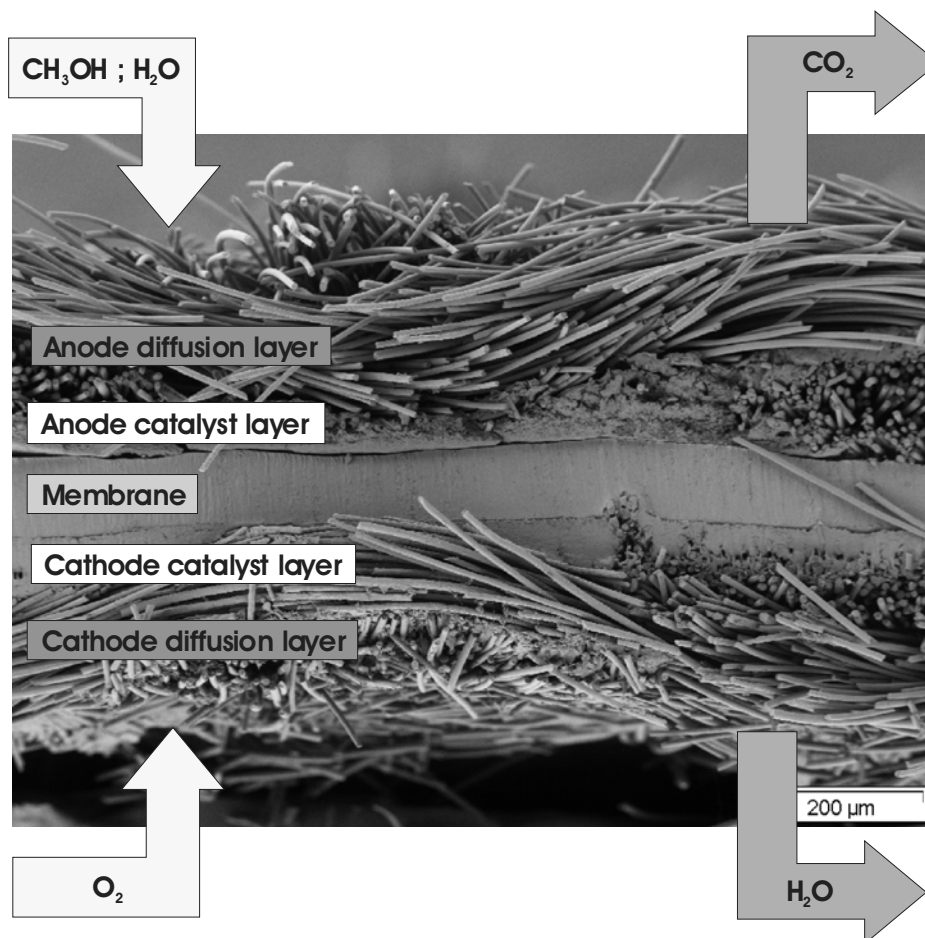


Fig. 1.3. Scanning electron micrograph of a MEA.

The diffusion layers are made of a carbon cloth that plays a key role on the transport of species and MEA structure integrity (Fig. 1.3) [4, 5, 12]. The porous backing, apart from allowing the transport of methanol and oxygen to the anode and cathode catalyst layers, respectively, also allows the conduction of electrical current out of the cell and provides the MEA's mechanical stability by holding the catalyst porous film-like structure [12]. Also, the carbon cloth structure allows the effective reactions products transport, carbon dioxide and water at the anode and cathode, respectively, in order to prevent the blockage of the transport paths in the electrodes. Usually, the diffusion layers are hydrophobized with polytetrafluoroethylene (PTFE) to prevent the flooding of the carbon cloth channels and to promote the gas transport [4].

On the other hand, the catalyst layer is where the chemical reactions are promoted. The catalyst layers have a film-like structure (Fig. 1.3) consisting of the following materials: 1) carbon black particles (usually Vulcan XC72) as electric conductor and catalyst support (if the catalyst is used as supported); 2) PTFE as hydrophobic element that also provides mechanical stability (holding the carbon particles) and 3) an ionomer (usually Nafion<sup>®</sup>) to promote the proton transport to the electrolyte and contact between electrodes and electrolyte polymer [4, 5, 12]. The catalyst can be used either unsupported or supported in carbon particles. It should have a high active surface area, poisoning-proof towards carbon monoxide and high dispersion. It is well known that the electro-oxidation, in Pt-based catalysts, of low molecular weight organic molecules, such as methanol, gives rise to the formation of strongly adsorbed CO species in linear or bridge-bounded form [4]. Accordingly to much work dedicated to the electro-oxidation of methanol, the most successful results up to date have been achieved using a binary alloy of platinum with ruthenium (Pt-Ru) [4]. The success of this alloy can be explained by the bifunctional effect of the Pt-Ru catalyst for DMFC [13]. The dehydrogenation steps take place at Pt surfaces sites, whereas Ru sites assume the role of providing the oxide/hydroxide species required to complete the oxidation of surface CO [13]. It is worth noting that the rate of methanol oxidation at Pt-Ru is strongly dependent on the temperature, with high performance being obtained near and above 100°C [14]. On the other hand, just like in a hydrogen fuel cell, the cathode reaction in a DMFC requires platinum to act as oxygen reduction electro-catalyst.

Finally, the proton exchange membrane plays a decisive role in the DMFC by isolating electronically the anode from the cathode, preventing the loss of methanol and oxygen and, mainly, enabling the transport of protons from the anode to the cathode. A critical analysis of the PEM characteristics for DMFC applications will be further discussed in detail below.

### 1.2.4. DMFC test system

The research and development of the direct methanol fuel cell requires intensive experimental work [15]. An experimentation platform should allow a wide range of parameters variation and ensure enough reproducibility. A simplified flow sheet of a DMFC test facility is presented in Figure 1.4. In this case, a tank is used to store the aqueous methanol solution (usually 1.5 M). A speed adjusted pump sucks the aqueous anode feed and pumps it into the closed circuit. A density meter enables the evaluation of the mixture density in order to verify the methanol concentration loss during DMFC operation. Usually the anode feed tank has a total volume higher than 2 liters in order to prevent the excessive variation in methanol concentration during one day experiment (less than 5%). To ensure the supply of aqueous methanol solution in liquid phase at temperatures higher than the methanol boiling point ( $64.7^{\circ}\text{C}$ ), the feed tank is pressurized with nitrogen. The feed tank pressure is controlled to adjust pressure fluctuations caused, for example, by the production of carbon dioxide at the anode side, using a venting valve (V1).

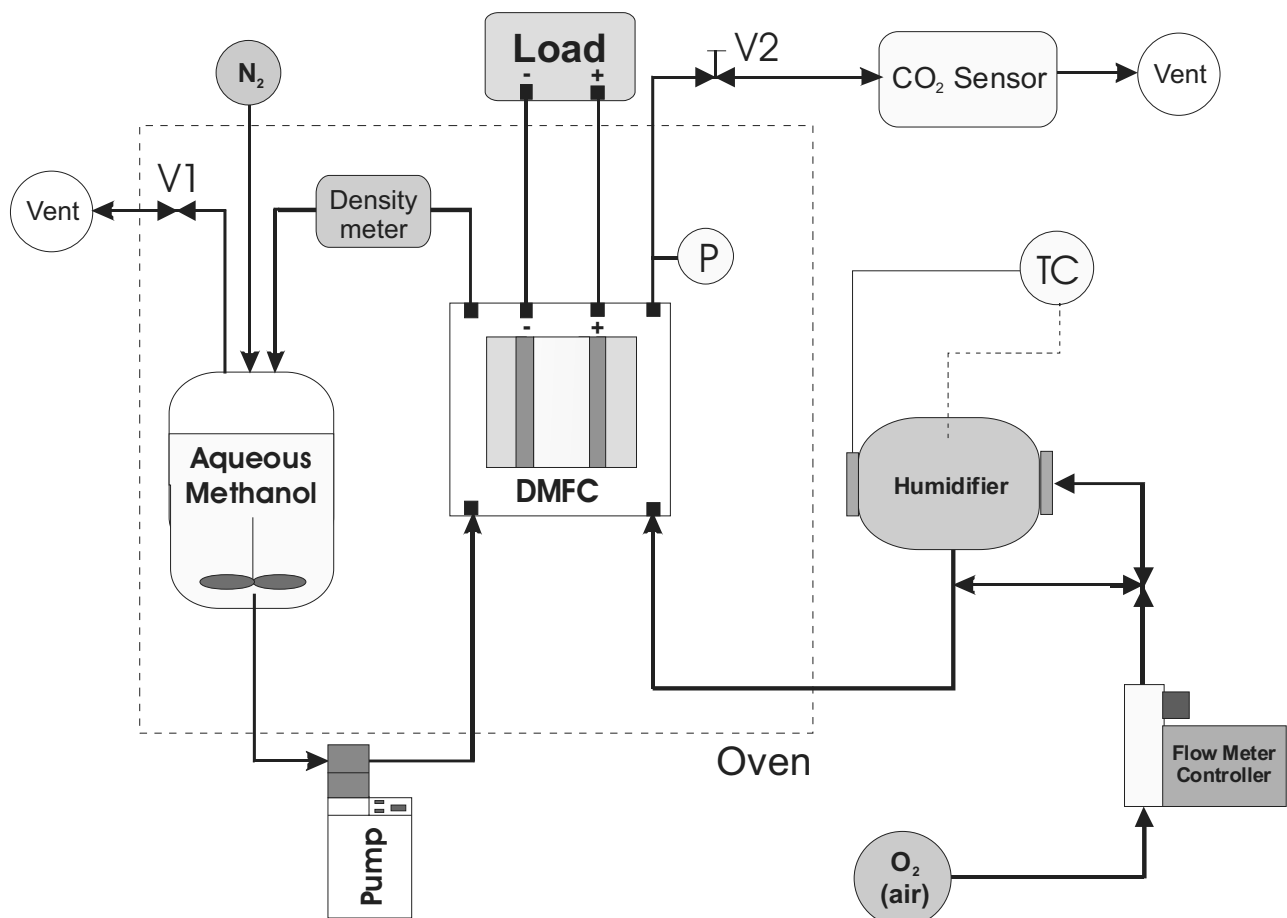


Fig. 1.4. Simplified flow sheet of a direct methanol fuel cell test facility.

The oxidant gas supply to the cathode can be either pure oxygen or air. A flow meter controller maintains constant the gas flow. A further option is the possibility of humidifying the cathode gas inlet. This can be achieved by bubbling this gas stream through a heated water container, the humidifier. Humidity control is obtained by regulating the temperature of the humidifier (temperature controller, TC). At the exit of the cathode a needle valve (V2) provides the required pressure ratios in the cell. For the determination of the methanol crossover at the cathode outlet, the CO<sub>2</sub> concentration is measured using an IR sensor [15].

For adjusting the electronic load of the cell and for measuring the current-voltage behavior, an electronic load is integrated in the DMFC flow sheet. This load can be operated potentiostatically or galvanostatically. The cell current is measured by a shunt, which is a precisely defined resistance that enables a certain voltage drop, proportional to the cell current. A more detailed description of a fully automatic DMFC test facility is described elsewhere [15].

### 1.3. R&D regarding the proton exchange membrane

The research and development of novel proton exchange membranes is known to be one of the most challenging issues regarding the direct methanol fuel cell technology [4-7, 16]. Usually mentioned as the heart of the DMFC, the membrane should ideally combine high proton conductivity (electrolyte properties) and low permeability towards DMFC species (barrier properties). Additionally, it should have a very high chemical and thermal stability in order to enable the DMFC operating at up to 150°C [4-7].

Nowadays, although involving high cost, perfluorinated ion-exchange polymers, such as Nafion<sup>®</sup> from Dupont, are still the most commonly used for DMFC applications (Fig. 1.5) [16]. This kind of membranes combines the extremely high hydrophobicity of the perfluorinated backbone with the extremely high hydrophilicity of the sulfonic acid functional groups [16]. For Nafion<sup>®</sup>, excellent characteristics in terms of chemical and thermal stability are ensured by the well known Teflon<sup>®</sup>-like perfluorinated backbone (Fig. 1.5). However, Nafion<sup>®</sup> only has a good proton conductor behavior when swollen in water and, consequently, the sulfonic groups are solvated.

In the presence of water, the distinct characteristics of both hydrophilic and hydrophobic characters of Nafion<sup>®</sup> are even more pronounced due to the aggregation of the hydrophilic domains (nano-separation) [16]. Consequently, DMFC species are readily transported across perfluorosulfonic acid membranes (mostly methanol and water) [4, 16-18]. This results in the drawback of methanol crossover from the anode to the cathode, which is mostly performed by: 1)

diffusion through the water-filled channels within the Nafion<sup>®</sup> structure and 2) active transport together with protons and their solvate water molecules during DMFC operation (electro-osmotic drag). The crossover methanol is chemically oxidized to CO<sub>2</sub> and H<sub>2</sub>O at the cathode, decreasing the fuel utilization efficiency and depolarizing the cathode. Apart from this, it can also adversely affect the cathode performance due to the consumption of oxygen by the parasitic methanol oxidation at the cathode catalyst layer, lowering its partial pressure [19]. It is believed that the methanol crossover from the anode to the cathode leads to a DMFC efficiency reduction down to 35% [18]. On the other hand, the high water permeability in perfluorinated membranes can also cause cathode flooding and, thus, lower cathode performance due to mass transport limitations [4]. The loss of oxygen from the cathode to the anode is also detrimental for the DMFC efficiency, although it can be neglected in comparison with the effect of the methanol crossover. In contrast, nitrogen and carbon dioxide mass transfer in the proton exchange membrane does not affect significantly the DMFC performance.

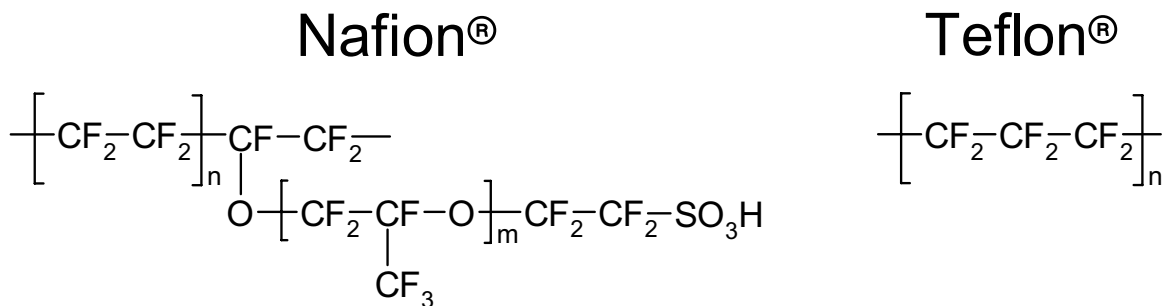


Fig. 1.5. Chemical structure of Nafion<sup>®</sup> and Teflon<sup>®</sup> (PTFE).

### 1.3.1. Novel materials

The key of the PEM research for direct methanol fuel cell applications is to overcome the strong link between proton conductivity and methanol permeability through the development of new materials or modification of the existing ones. The R&D schemes attempted so far have been mostly focused on either modifying the perfluorinated membranes by addition of highly hydrophilic oxides, or varying the polymer nano-pore network structure by modifying the polymers chemical nature [4-7], e.g. the use of SiO<sub>2</sub> entrapped particles in Nafion<sup>®</sup> polymeric structure [20], which work as a physical barrier for methanol crossover. However, as expected, the membrane ohmic resistance increases, depending on the concentration of silica. Another approach is the inorganic incorporation of zirconium phosphate in perfluorinated membranes (23wt.%) [21]. This membrane

shows lower methanol crossover when compared to recast Nafion<sup>®</sup> modified with SiO<sub>2</sub> (3wt.%) due to the higher content of inorganic compound (higher diffusion barrier characteristics). Yet, larger ohmic resistances were observed due to reduced proton mobility inside the Nafion<sup>®</sup> channels.

Nowadays, there are several alternative novel materials that show promising properties for DMFC applications. Some of the investigated membranes so far are: sulfonated poly(ether ether ketone) [22-26], poly(ether sulfone) [27], polyvinylidene fluoride [28], styrene grafted and sulfonated membranes [29], zeolite gel films and membranes doped with heteropolyanions [30]. Apart from enabling different preparation or modification approaches, the characteristics of these novel materials allows completely distinct mass transport mechanisms and much lower costs when compared to Nafion<sup>®</sup>. Non-fluorinated membranes based on sulfonated poly(ether ether ketones) (sPEEK) proved already to have promising characteristics in terms of barrier and electrolyte properties for DMFC applications [22, 26]. The plain poly(ether ether ketone) (PEEK) can be easily made hydrophilic by sulfonation reactions, being the sulfonation degree (SD) controlled by the reaction time and temperature (Fig. 1.6).

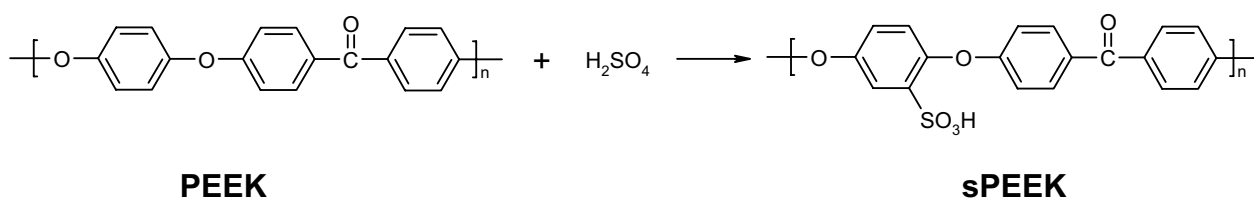


Fig. 1.6. Sulfonation reaction of the poly(ether ether ketone).

The sulfonation degree can optimize the hydrophobic-hydrophilic balance, acting directly on the electrolyte and barrier properties, as well as in the chemical and thermal stability of the polymer [22-26]. Higher sulfonation degrees increase the polymer proton conductivity and tend to improve the DMFC performance. However, the permeability towards methanol also increases concurrently, decreasing the fuel cell overall efficiency [22]. On the other hand, the polymer stability tends to progressively deteriorate with the sulfonation degree. Recently, Li et al. reported better DMFC performances for the sPEEK membranes (SD = 39 and 47%) compared to Nafion<sup>®</sup> 115, at 80°C [31]. Similar results were obtained by us for a sPEEK membrane with SD = 42% and thickness ranging from 25 to 55 μm (data not published).

Non-fluorinated PEM properties regarding proton conductivity and methanol permeation can be also improved by the preparation of hybrid or composite membranes incorporating inorganic-ceramic materials [32-42]. For an optimized composition, the hybrid or composite material may have superior performance as compared to the plain polymer [32]. For DMFC

applications operating at medium temperatures (up to 130°C), promising results were obtained for sPEEK composite membrane with SD=68% modified with 20.0wt.% of zirconium phosphate (ZrPh) pre-treated with *n*-propylamine and 11.2wt.% of polybenzimidazole (PBI) [35, 36]. This membrane proved to have a good balance between proton conductivity, aqueous methanol swelling and permeability. In addition, DMFC tests for this membrane showed similar current density output and higher open circuit voltage compared to that of sPEEK with SD=42%, but with much lower CO<sub>2</sub> concentration at the cathode outlet (thus higher global efficiency) and higher thermal/chemical stability.

Another approach is the incorporation of heteropolyacids in plain polymers [40, 41]. Heteropolyacids are well known for being proton conductors when in the crystalline form with a certain number of water molecules in their structure [43-45]. However, it is also well known that these electrolytes usually leach out of the polymer, decreasing the fuel cell performance [43, 46, 47]. Finally, the modification of sPEEK polymer with zirconium oxide incorporated via *in situ* hydrolysis proved to be very promising for decreasing the hybrid membrane permeability towards methanol (improved barrier properties) and for increasing the chemical/thermal stability of the polymer [37-39]. The drawback of the incorporation of ZrO<sub>2</sub> is the fact that it has also high impact on the proton conductivity, decreasing therefore the fuel cell performance [39].

### 1.3.2. Characterization methods

In order to select the proper PEM material for direct methanol fuel cell applications, characterization methods play an important role in DMFC research. Ideally, the obtained characteristics of the specific material should be used as a selection criterion: they should allow researchers to forecast the corresponding DMFC performance [48]. For example, instead of conducting DMFC experiments, which are time and money-consuming, the characterization results should be used to estimate qualitatively the fuel cell performance, for a given PEM [39]. Apart from this, the characterization results should also allow the identification of critical parameters regarding the application of certain materials in DMFC. The various membrane characterization methods normally involved in PEM research for DMFC applications can be classified as: (a) related to electrical or conductive properties; (b) related to the permeation of the DMFC species; (c) related to thermal and chemical stability and (d) related to the membrane morphology and elemental analysis.

At present, several characterization methods are used to obtain the critical parameters for DMFC application [39, 48, 49]. The three most common characterization methods for PEM research for DMFC applications are listed and described below.

### 1.3.2.1. Swelling measurements

The water or methanol solubility in the membrane is closely related to its basic properties and plays an essential role on its behavior. Proton conductivity depends to a large extent on the amount of sorbed water and even the proton transport is influenced by it [50]. On the other hand, the methanol crossover is also associated to higher water concentration in the membrane [51]. Apart from this, the sorbed water also influences the ionomer microstructure, cluster and channel size and modifies the membrane mechanical properties [52, 53]. The membrane properties in terms of swelling are usually evaluated using batch experiments in liquid solutions at room temperature [25, 26, 34-39, 49, 54]. The water or methanol uptake,  $W_{uptake}$ , is usually obtained using the following relation:

$$W_{uptake} = \frac{w_{wet} - w_{dry}}{w_{dry}} \quad (1.7)$$

where  $w_{wet}$  is the membrane sample wet weight after a certain time in the solution (up to the equilibrium) and  $w_{dry}$  is the initial dry weight of the sample after the drying process (usually in a oven with vacuum).

### 1.3.2.2. Conductivity measurements

The proton conductivity of a specific material is strictly related with the ohmic losses associated to the membrane during DMFC operation. The key for PEM research is to develop membranes with improved proton transport properties in order to have a minimum voltage drop, mainly for fuel cells operation at high current densities. This property is usually evaluated by impedance spectroscopy, using a membrane immersed in an acid solution or just hydrated in different values of relative humidity [25, 26, 33-42, 48, 49]. From impedance spectroscopy

experiments, the membrane proton conductivity,  $k_M$ , is obtained determining the impedance modulus at null phase shift [55],  $|Z_M|_{\alpha=0}$ , using the following equation:

$$k_M = \frac{d_M}{A \cdot |Z_M|_{\alpha=0}} \quad (1.8)$$

where  $d_M$  is the membrane thickness and  $A$  is the contact area membrane/electrodes.

### 1.3.2.3. Permeability measurements

The study of the methanol mass transport through DMFC membranes is very common due to its detrimental effect on the DMFC performance as discussed before. Even not accounting for the anode catalytic reaction and the electro-osmotic drag mass transfer, the permeability is usually evaluated by pervaporation [33-41, 48, 49] and diffusion cell experiments [56-58]. Pervaporation experiments consist on measuring the amount of permeated methanol and water through the membrane for a certain experiment time. The permeability coefficient,  $P_i$ , of species  $i$  (water or methanol) is obtained from the species flux according to

$$P_i = \frac{J_i \cdot d_M}{\gamma_{i,L} \cdot x_{i,L} \cdot p_i^{sat}} \quad (1.9)$$

where  $J_i$  is the molar flux,  $\gamma_i$  is the activity coefficient,  $x_{i,L}$  is the molar fraction in the liquid phase and  $p_i^{sat}$  is the equilibrium vapor pressure of species  $i$ .

Apart from studying the liquid species mass transport, researchers started also to characterize the permeation of gaseous species through the proton exchange membrane [35, 38]. Since the carbon dioxide concentration at the cathode outlet is usually used as an experimental measure of the methanol crossover, its transport through the electrolyte membrane should be also considered. The permeability of the gaseous species is usually evaluated through the pressure rise method, in the presence of water vapor (swollen membrane). As stated in [59], the permeability coefficient of species  $i$  can be obtained from pressure rise experiments using the following equation:

$$P_i = \frac{V \cdot d_M}{R \cdot T \cdot A} \ln \left( \frac{p_{i,F} - p_{i,Px}}{p_{i,F} - p_{i,Px+1}} \right) (t_{x+1} - t_x)^{-1} \quad (1.10)$$

where  $V$  is the permeate volume,  $R$  is the gas constant,  $p_{i,F}$  is the species  $i$  partial pressure in the feed stream,  $p_{i,P}$  is the species  $i$  partial pressure in the permeate side and  $t$  is the experiment time. The subscripts  $x$  and  $x+1$  refer to time instant  $x$  and time instant after  $x$ , respectively.

Other characterization methods are applied as well to give information on the chemical structure (determination of ion-exchange capacity, IEC, Fourier transform infrared spectroscopy, FTIR, nuclear magnetic resonance, NMR [60-63]), stability (thermo gravimetric analysis, TGA) and morphology (scanning electron microscopy, SEM, small angle x-ray scattering, SAXS, transmission electron microscopy, TEM).

With respect to the validation of the standard characterization data, results recently published by us showed a good qualitative agreement between them and the DMFC performance [39]. From this study it was possible to verify that characterization results obtained by impedance spectroscopy, water uptake and pervaporation experiments can be effectively used as critical parameters for the selection of proton electrolyte membranes for DMFC application purposes [39].

### 1.3.3. DMFC tests

DMFC tests can be performed to study the behavior of a certain material as electrolyte for real fuel cell operating conditions [12, 15]. These tests are normally implemented for a certain collection of membranes previously selected based on the characterization methods results described above. Usually, the experimental operation conditions of the DMFC test cell are selected in order to focus mainly on the membrane properties [15]. As an example, the DMFC test should be performed with a constant cathode flow rate, enough to prevent the electrodes flooding and oxygen starvation. Also, the used electrodes for the MEA preparation should always be the same (usually Etek<sup>®</sup> ELAT electrodes). Low amounts of catalyst in the electrodes are preferred in order to increase the methanol crossover detrimental effect and to study the membrane barrier properties for more unfavorable conditions (usually, 1 mg/cm<sup>2</sup> PtRu and 0.4 mg/cm<sup>2</sup> Pt in the anode and cathode catalyst layers, respectively). When preparing the MEA, the pressing conditions are selected in order to enable a good contact between the membrane and electrodes (practically negligible contact resistance).

The record of the current-voltage and power density characteristics of the DMFC is the most important and common fuel cell characterization method (Fig. 1.7) [1-6]. Usually, the DMFC polarization behavior is measured potentiostatically, with voltage steps of 50mV during 2 minutes (quasi-steady-state conditions), ranging from the open circuit voltage down to 50mV and back to the open circuit voltage [15]. For a specific material, the characteristic polarization is predominantly controlled by the methanol crossover through the membrane from the anode to the cathode, by the PEM proton conductivity and, finally, by the kinetics of methanol electro-oxidation at the anode catalyst layer [14, 64-71].

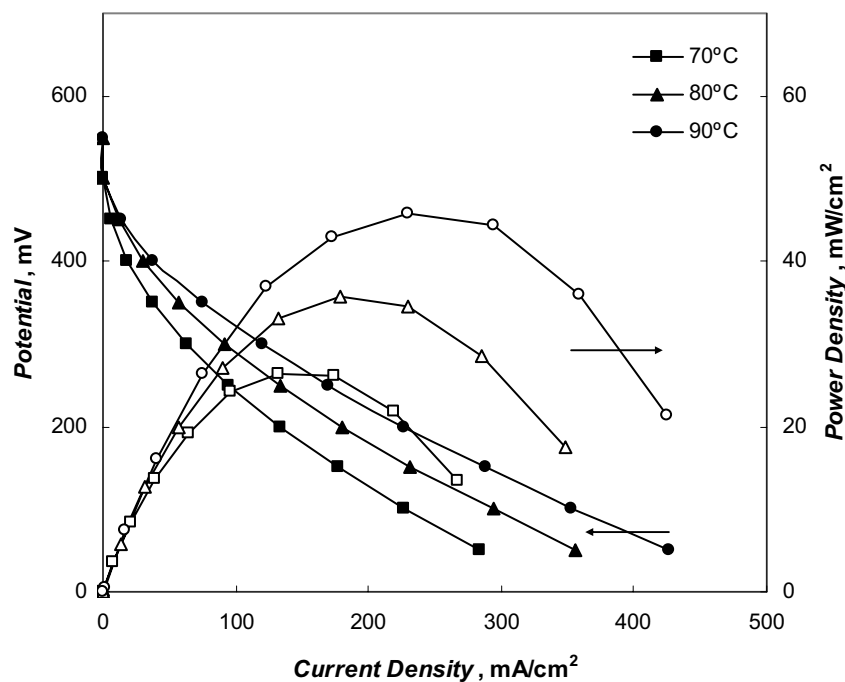


Fig. 1.7. Current-voltage and power density plots of the DMFC using a sPEEK membrane with  $SD=42\%$  ( $d_M = 40\mu\text{m}$ ).

Usually, DMFC tests involve also the measurement of the open circuit voltage. The main propose for this measurement is to infer about the cell voltage loss that is essentially due to the methanol permeation from the anode to the cathode. During OCV experiments, the concentration of methanol at the anode-membrane interface is maximal because no methanol is being consumed (no current output). Consequently, the methanol crossover is higher due to a larger mass transfer gradient across the membrane, making the detrimental effect of the methanol crossover more noticeable for OCV experiments [72].

In order to study the DMFC behavior under high load, experimental tests are also performed measuring the current density for constant voltage (CV) experiments, at 35mV. This measurement is performed in order to infer about the cell voltage loss associated to the PEM proton conductivity (ohmic losses) and methanol crossover effect for high load conditions. When the DMFC is under load conditions, there will be a consumption of methanol at the anode catalyst layer and, consequently, the methanol mass transfer gradient across the membrane decreases (leading to lower CO<sub>2</sub> concentrations at the cathode outlet).

Since the membrane development involves the characterization of materials with distinct swelling properties and this factor is known to strongly influence the performance of the DMFC, researchers also measure the cell impedance in order to diagnose the membrane state in terms of sorbed water content. The cell impedance measurement is commonly performed at high frequency, such as 10kHz, in order to measure the impedance for null phase conditions [15]. At null phase frequency, the impedance is dominated by the ohmic resistance in the cell and thus by the membrane conductivity and the contact resistances.

#### 1.3.4. DMFC efficiency

As mentioned before, the methanol crossover from the anode to the cathode during DMFC tests can be estimated by the CO<sub>2</sub> content at the cathode outlet [15]. However, this CO<sub>2</sub> content does not give an absolute amount of the methanol that permeates through the membrane. One must also quantify the CO<sub>2</sub> that permeates through the membrane during the fuel cell operation. In addition, it should be expected that the crossover methanol is not completely oxidized to CO<sub>2</sub> at the cathode catalyst layer. A detailed method for evaluating the absolute CO<sub>2</sub> amount at the cathode outlet due to the permeation of methanol was recently presented [36], accounting to the membrane permeability towards CO<sub>2</sub>. The effect of the non-converted crossover methanol at the cathode outlet was not considered because from gas chromatography analysis it was verified that the methanol molar fraction is usually less than 0.5% in this stream.

Therefore, from the predicted carbon dioxide molar flow rate due to the parasitic methanol oxidation at the cathode,  $N_{CO_2}^{MeOH}$ , and assuming the Faraday law, the current density loss due to methanol crossover,  $I_{MeOH}$ , can be evaluated through the following equation:

$$I_{MeOH} = \frac{N_{CO_2}^{MeOH} \cdot 6 \cdot F}{A_{cell}} \quad (1.11)$$

where  $A_{cell}$  is the DMFC effective area.

In order to study the ratio of the converted fuel to electric power (anode) to the total amount of converted fuel (anode and cathode), researchers usually calculate the DMFC Faraday efficiency,  $\eta_F$ , using the following equation:

$$\eta_F = \frac{I_{i,cell}}{I_{i,cell} + I_{i,MeOH}} \quad (1.12)$$

where  $I_{i,cell}$  is the DMFC measured current density.

On the other hand, in order to study the fuel cell polarization loss behavior, the potential efficiency,  $\eta_E$ , is also calculated. It is defined as the DMFC cell voltage divided by the reversible cell voltage:

$$\eta_E = \frac{U_{i,cell}}{U_{rev}} \quad (1.13)$$

in which  $U_{i,cell}$  is the measured cell voltage during the polarization curve evaluation.

The global DMFC efficiency,  $\eta_{DMFC}$ , is defined as the product of the thermodynamic, Faraday and potential efficiencies (Fig. 1.8). Since the thermodynamic efficiency of the DMFC is constant and independent of the material, usually PEM researchers neglect this term in the DMFC overall efficiency [4, 22, 36]. Therefore, the global DMFC efficiency is given by the following equation:

$$\eta_{DMFC} = \eta_{th} \cdot \eta_E \cdot \eta_F \quad (1.14)$$

The maximal value of global DMFC efficiency is achieved for intermediate current density due to the improved balance between potential and Faraday efficiencies (Fig. 1.8). Low current density is associated to high potential efficiency (higher voltage) and lower Faraday efficiency (higher methanol permeation). In contrast, high current density is associated to lower potential efficiency (lower voltage) and higher Faraday efficiency (lower methanol crossover).

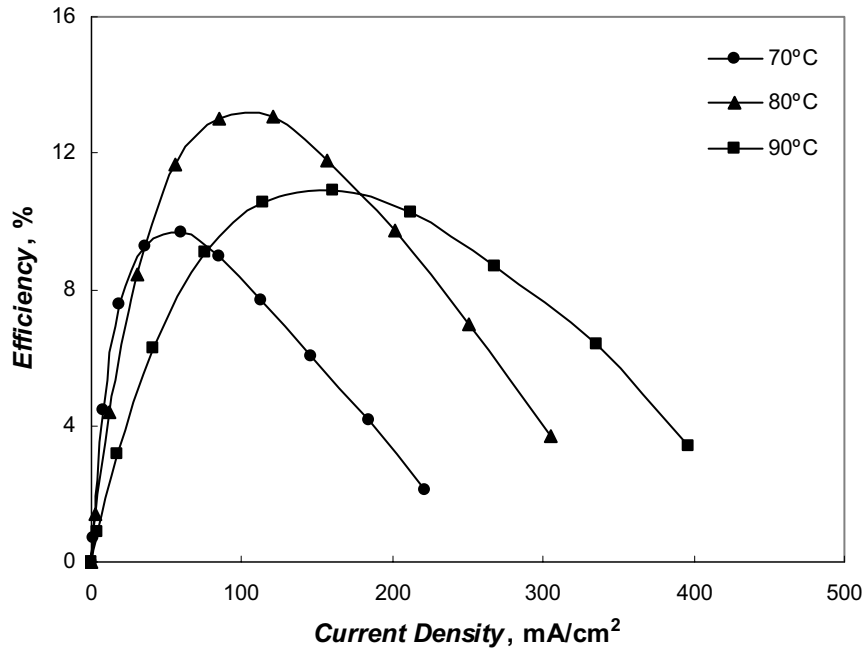


Fig. 1.8. Estimated overall efficiency of the DMFC using a sPEEK membrane with SD=42% ( $d_M = 40\mu\text{m}$ ).

### 1.3.5. PEM modeling

As mentioned before, in order to infer about the PEM properties and select the proper materials for DMFC applications, researchers usually apply standard characterization methods such as impedance spectroscopy, pervaporation and swelling experiments [39, 48, 49]. The results obtained from PEM characterization allow a qualitative first screening of the membranes properties for DMFC applications [39]. However, the application of standard characterization methods and DMFC tests are not enough to answer some questions, especially in terms of which is the optimal PEM development strategy that should be targeted, having in mind a compromise between proton conductivity (electrolyte requirements) and methanol and water transport (barrier requirements). In order to answer these questions, we believe that it is of decisive importance to develop novel R&D tools that could be complementary to the PEM standard characterization methods and DMFC tests.

Mathematical modeling seems to be very useful for these purposes since it allows the prediction of the DMFC performance for distinct materials and operation conditions. Unfortunately, much of the developed DMFC modeling research has focused extensively on Nafion<sup>®</sup> [73]. These models use data taken from literature that are usually impossible to reproduce by membrane research groups and, in many cases, these parameters hardly represent the properties of membranes

under development. Therefore, the developed mathematical models have limited usefulness for membrane development proposes regarding the direct methanol fuel cell.

Recently, in order to fulfill this lack, a semi-empirical mathematical model that enables the prediction of the DMFC performance using inputs obtained by easy-to-implement characterization methods was developed by us [74]. The applied standard characterization methods were: impedance spectroscopy (proton conductivity), water uptake (water sorption), pervaporation (permeability towards methanol and water) and gas permeation (permeability towards oxygen, nitrogen and carbon dioxide). For PEM development proposes, the present mathematical model proved to be very useful for selecting the right modifications that should be performed in order to prepare optimized materials that can improve the DMFC overall performance [75]. This model will be used to assist the PEM development and, consequently, to reduce the applied efforts to find the optimal material/conditions for DMFC applications.

## **1.4. Conclusions**

Nowadays, most of the world energy requirements are obtained by burning fossil fuels in generally low efficiency thermal processes. Associated consequences, such as, atmospheric pollution, global warming and green house effects are the main driving forces for the development of new power sources and converters. In this regard, it is widely recognized that fuel cells are becoming suitable for replacing common combustion processes in the near future.

The direct methanol fuel cell has good potentialities for portable application. Devices based on this technology eliminate the need of a complex reformer unit and avoids thermal and humidification problems (simplicity). However, one of the main drawbacks associated to the DMFC is the methanol crossover across the proton exchange membrane (where Nafion<sup>®</sup> is commonly used). The methanol crossover from the anode to the cathode decreases the fuel utilization efficiency and affects detrimentally the cathode performance. Therefore, the development of new PEMs with improved barrier and electrolyte properties is known to be one of the most challenging aims regarding the DMFC technology.

The present chapter gives an overview of the PEM development process, which comprises the following steps: materials preparation, characterization, DMFC test, modeling and simulation. The recent developments achieved by us concerning these aspects are emphasized. New materials using poly(ether ether ketone) as matrix polymer, modified inorganically with zirconium oxide or zirconium phosphate pre-treated with *n*-propylamine and polybenzimidazole are mentioned.

Membranes with improved relation between barrier and electrolyte properties were prepared, in comparison with that of Nafion<sup>®</sup>. In addition, a research work regarding the characterization methods validation is mentioned in terms of DMFC qualitative performance prediction. In this study it is shown that impedance spectroscopy (proton conductivity), water uptake (water swelling) and pervaporation (permeability towards methanol and water) can be effectively used as critical parameters for the PEM selection aiming the DMFC application. On the other hand, the importance of developing DMFC mathematical models based on characterization data is emphasized. These modeling tools proved to have a promising potential on assisting the PEM development by answering basic questions concerning novel materials with the best compromise between proton conductance (electrolyte properties) and methanol crossover (barrier properties).

## Acknowledgements

The work of Vasco Silva was supported by FCT (Grant SFRH/BD/6818/2001). Financial support by the HGF-Vernetzungsfonds is gratefully acknowledged. The present work was partially supported by FCT projects POCTI/EQU/38075/2001 and POCTI/EQU/45225/2002. The authors would like to acknowledge R. Reissner at Deutsches Zentrum für Luft-und Raumfahrt (DLR) for the MEA characterization in the DMFC. The authors wish to thank M. Schossig-Tiedemann and M. Adherhold for making the microscope analysis and Dr. S. Vetter for sulfonating the poly(ether ether ketone) polymer.

## References

- [1] K. Kordesch and G. Simader, Fuel cells and their applications, VCH Publishers, (1996).
- [2] M. Cappadonia, U. Stimming, K. Kordesch and J.C. Oliveira, Fuel cells, Ullmann's Encyclopedia of Industrial Chemistry, John Wiley & Sons, Inc., (2000).
- [3] J. Larminie, Fuel cells, Kirk-Othmer Encyclopedia of Chemical Technology, John Wiley & Sons, Inc., (2002).
- [4] A. S. Aricò, S. Srinivasan and V. Antonucci, DMFCs: From fundamental aspects to technology development, Fuel Cells 1 (2001) 133.
- [5] T. Schultz, S. Zhou and K. Sundmacher, Current status of and recent developments in direct methanol fuel cell, Chem. Eng. Technol. 24 (2001) 12.

- [6] R. Dillon, S. Srinivasan, A.S. Aricò and V. Antonucci, International activities in DMFC R&D: status of technologies and potential applications, *J. Power Sources* 127 (2004) 112.
- [7] P. Piela and P. Zelenay, Researchers redefine the DMFC roadmap, *The Fuel Cells Review* 1(2) (2004) 17.
- [8] R. Harris, D. Book, P. Anderson and P. Edwards, Hydrogen storage: the grand challenge, *The Fuel Cells Review* 1(1) (2004) 17.
- [9] S. Gottesfeld, DMFCs power up for portable devices, *The Fuel Cells Review* 1(2) (2004) 25.
- [10] P. W. Atkins, *Physical chemistry*, VCH Publishers (1990).
- [11] G. Hoogers, *Fuel Cell Technology Handbook*, CRC Press (2002).
- [12] E. Gülzow, T. Kaz, R. Reissner, H. Sander, L. Schilling and M. V. Bradke, Study of membrane electrode assemblies for direct methanol fuel cells, *J. Power Sources* 105 (2002) 261.
- [13] Y. Tong, H. S. Kim, P. K. Babu, P. Waszczuk, A. Wieckowski and E. Oldfield, An NMR investigation of CO tolerance in a Pt/Ru fuel cell catalyst, *J. Am. Chem. Soc.* 124 (2002) 468.
- [14] X. Ren, M. S. Wilson and S. Gottesfeld, High performance direct methanol polymer electrolyte fuel cells, *J. Electrochem. Soc.* 143 (1996) L12.
- [15] E. Gülzow, S. Weißhaar, R. Reissner and W. Schröder, Fully automatic test facilities for the characterization of DMFC and PEFC MEAs, *J. Power Sources* 118 (2003) 405.
- [16] K. A. Kreuer, On the development of proton conducting polymer membranes for hydrogen and methanol fuel cells, *J. Membr. Sci.* 185 (2001) 3.
- [17] J. Cruickshank and K. Scott, The degree and effect of methanol crossover in the direct methanol fuel cell, *J. Power Sources* 70 (1998) 40.
- [18] F. R. Kalhammer, P. R. Prokopius and V. P. Voeks, Status and prospects of fuel cells as automobile engines, State of California Air Resources Board, California, 1998.
- [19] D. Chu and S. Gilman, The influence of methanol on O<sub>2</sub> electroreduction at a rotating Pt disk electrode in acid electrolyte, *J. Electrochem. Soc.* 141 (1994) 1770.
- [20] A.S. Aricò, P. Cretì, P.L. Antonucci and V. Antonucci, Comparison of ethanol and methanol oxidation in a liquid-feed solid polymer electrolyte fuel cell at high temperature, *Electrochem. Solid-State Lett.* 1 (1998) 66.
- [21] C. Yang, S. Srinivasan, A.S. Aricò, P. Cretì, V. Baglio and V. Antonucci, Composite Nafion/Zirconium phosphate membranes for direct methanol fuel cell operation at high temperature, *Electrochem. Solid-State Lett.* 4 (2001) 31.
- [22] V.S. Silva, B. Ruffmann, S. Vetter, M. Boaventura, A. Mendes, M. Madeira and S. Nunes, Mass transport of direct methanol fuel cell species in sulfonated poly(ether ether ketone) membranes, *Chem. Eng. Sci.* (submitted, 2005).

- [23] X. Jin, M. T. Bishop, T. S. Ellis and F. Karasz, A sulphonated poly(aryl ether ketone), *Br. Polym. J.* 17 (1985) 4.
- [24] T. Kobayashi, M. Rikukawa, K. Sanui and N. Ogata, Proton-conducting polymers derived from poly(ether-etherketone) and poly(4-phenoxybenzoyl-1,4-phenylene), *Solid State Ionics* 106 (1998) 219.
- [25] S. M. J. Zaidi, S. D. Mikailenko, G. P. Robertson, M. D. Guiver and S. Kaliaguine, Proton conducting composite membranes for polyether ether ketone and heteropolyacids for fuel cell applications, *J. Membr. Sci.* 173 (2000) 17.
- [26] S. D. Mikhailenko, S. M. J. Zaidi and S. Kaliaguine, Sulfonated polyether ether ketone composite polymer electrolyte membranes, *Catal. Today* 67 (2001) 225.
- [27] B. Bauer, D. J. Jones, J. Roziere, L. Tchicaya, G. Alberti, M. Casciola, I. Massinelli, A. Peraio, S. Besse and E. Ramunni, Electrochemical characterisation of sulfonated polyetherketone membranes, *J. New Mater. Electrochem. Systems* 3 (2000) 93.
- [28] E. Peled, T. Duvdevani, A. Aharon and A. Melman, A direct methanol fuel cell based on a novel low-cost nanoporous proton-conducting membrane, *Electrochem. Solid-State Lett.* 3 (2000) 525.
- [29] S. Hietala, K. Koel, E. Skou, M. Elomaa and F. Sundholm, Thermal stability of styrene grafted and sulfonated proton conducting membranes based on poly(vinylidene fluoride), *J. Mater. Chem.* 8 (1998) 1127.
- [30] A.S. Aricò, P.L. Antonucci, N. Giordano and V. Antonucci, Ionic conductivity in heteropolyacid-tin mordenite composite electrolytes, *Material Letters* 24 (1995) 399.
- [31] L. Li, J. Zhang and Y. Wang, Sulfonated poly(ether ether ketone) membranes for direct methanol fuel cell, *J. Membr. Sci.* 226 (2003) 159.
- [32] B. Kumar and J. P. Fellner, Polymer-ceramic composite protonic conductors, *J. Power Sources* 123 (2003) 132.
- [33] S. P. Nunes, B. Ruffmann, E. Rikowsky, S. Vetter and K. Richau, Inorganic modification of proton conductive polymer membranes for direct methanol fuel cells, *J. Membr. Sci.* 203 (2002) 215.
- [34] B. Ruffmann, H. Silva, B. Schulte and S. Nunes, Organic/inorganic composite membranes for application in DMFC, *Solid State Ionics*, 162-163 (2003) 269.
- [35] V. S. Silva, B. Ruffmann, S. Vetter, A. Mendes, L. M. Madeira and S. P. Nunes, Characterization and application of composite membranes in DMFC, *Catalysis Today*, (in press, 2005).

- [36] V.S. Silva, S. Weisshaar, R. Reissner, B. Ruffman, S. Vetter, A. Mendes, L.M. Madeira, S.P. Nunes, Performance and efficiency of a DMFC using non-fluorinated composite membranes operating at low/medium temperatures, *J. Power Sources* (in press, 2005).
- [37] V. Silva, B. Ruffmann, H. Silva, A. Mendes, M. Madeira and S. Nunes, Zirconium oxide modified sulfonated poly(ether ether ketone) membranes for direct methanol fuel cell applications, *Mater. Sci. Forum* 455-456 (2004) 587.
- [38] V.S. Silva, B. Ruffmann, H. Silva, Y. A. Gallego, A. Mendes, L. M. Madeira and S. P. Nunes, Proton electrolyte membrane properties and direct methanol fuel cell performance. I. Characterization of hybrid sulfonated poly(ether ether ketone)/zirconium oxide membranes, *J. Power Sources* 140 (2005) 34.
- [39] V.S. Silva, J. Schirmer, R. Reissner, B. Ruffman, H. Silva, A. Mendes, L.M. Madeira and S.P. Nunes, Polymer electrolyte membrane properties and direct methanol fuel cell performance. II. Fuel cell performance and membrane properties effects, *J. Power Sources* 140 (2005) 41.
- [40] M. L. Ponce, L.A.S.de A. Prado, B. Ruffmann, K. Richau, R. Mohr and S. P. Nunes, Reduction of methanol permeability in polyetherketone-heteropolyacid membranes, *J. Membr. Sci.* 217 (2003) 5.
- [41] M.L Ponce, L.A.S.de A. Prado, V. Silva and S. P. Nunes, Membranes for direct methanol fuel cell based on modified heteropolyacids, *Desalination* 162 (2004) 383.
- [42] G. Alberti, M. Casciola, L. Massinelli and B. Bauer, Polymeric proton conducting membranes for medium temperature fuel cells (110-160°C), *J. Membr. Sci.* 185 (2001) 73.
- [43] P. Staiti, A.S. Aricò, V. Antonucci, S. Hocevar. Morphological variation of platinum catalysts in phosphotungstic acid fuel cell, *J. Power Sources* 70 (1998) 91.
- [44] O. Nakamura, T. Kodama, I. Ogino and Y. Miyake, High-conductivity solid proton conductors – dodecamolybdophosphoric acid and dodecatungstophosphoric acid crystals, *Chem. Lett.* 1 (1979) 17.
- [45] D.E. Katsoulis, A survey of applications of polyoxometalates, *Chem. Rev.* 98 (1998) 359.
- [46] P. Saiti, S. Hocevar and N. Giordano, Fuel cells with  $H_3PW_{12}O_{40} \cdot 29H_2O$  as solid electrolyte, *Int. Hydrogen Energy* 22 (1997) 809.
- [47] N. Giordano, P. Saiti, S. Hocevar and A.S. Aricò, High performance fuel cell based on phosphotungstic acid as proton conducting electrolyte, *Electrochimica Acta* 41 (1996) 397.
- [48] C. Manea and M. Mulder, Characterization of polymer blends of polyethersulfone/sulfonated polysulfone and polyethersulfone/sulfonated polyetheretherketone for direct methanol fuel cell applications, *J. Membr. Sci.* 206 (2002) 443.

- [49] P. Dimitrova, K. A. Friedrich, B. Vogt and U. Stimming, Transport properties of ionomers composite membranes for direct methanol fuel cells, *J. Electroanal. Chem.* 532 (2002) 75.
- [50] T. Zawodzinski, T. Springer, F. Uribe and S. Gottesfeld, Characterization of polymer electrolytes for fuel cell applications, *Solid State Ionics* 60 (1993) 199.
- [51] X. Ren, T.E. Springer and S. Gottesfeld, Water and methanol uptakes in Nafion membranes and membrane effects on direct methanol cell performance, *J. Electrochem. Soc.* 147 (2000) 92.
- [52] G. Pourcelly and C. Gavach, In proton conductors, in: P. Colomban (Ed.), *Chemistry of solid state materials*, Cambridge University Press, Cambridge (1992) 294.
- [53] P. J. James, J. A. Elliott, T.J. McMaster, J.M. Newton, A.M.S. Elliott, S. Hanna and M.J. Limes, Hydration of Nafion<sup>®</sup> studied by AFM and X-ray scattering, *J. Mater. Sci.* 35 (2000) 5111.
- [54] M. C. Wijers, Supported liquid membranes for removal of heavy metals, PhD Dissertation, University of Twente, The Netherlands, 1996.
- [55] J. R. Macdonald and W. R. Kenan, *Impedance spectroscopy: emphasizing solid materials and systems*, John Wiley & Sons, Inc., (1987).
- [56] L. Li, J. Zhang and Y. Wang, Sulfonated poly(ether ether ketone) membranes for direct methanol fuel cell, *J. Membr. Sci.* 226 (2003) 159.
- [57] L. Li, L. Xu and Y. X. Wang, Novel proton conducting composite membranes for direct methanol fuel cell, *Mater. Lett.* 57 (2003) 1406.
- [58] L. Li, L. Xu and Y. X. Wang, A hybrid membrane of poly(vinyl alcohol) and phosphotungstic acid fuel cells, *Chin. J. Chem. Eng.* 10 (2002) 614.
- [59] M. Mulder, *Basic Principles of Membrane Technology*, Kluwer Academic Publishers, (1997).
- [60] J. Kerres, A. Ulrich, F. Meier and T. Haring, Synthesis and characterization of novel acid–base polymer blends for application in membrane fuel cells, *Solid State Ionics* 125 (1999) 243.
- [61] J. Kerres, W. Cui, R. Disson and W. Neubrand, Development and characterization of crosslinked ionomer membranes based upon sulfonated and sulfonated PSU crosslinked PSU blend membranes by disproportionation of sulfinic acid groups, *J. Membr. Sci.* 139 (1998) 211.
- [62] J. Benavente, J. M. Garcia, R. Riley, A. E. Lozano and J. de Abajo, Sulfonated poly(ether ether sulfones): Characterization and study of dielectrical properties by impedance spectroscopy, *J. Membr. Sci.* 175 (2000) 43.
- [63] J. Kerres, A. Ulrich, Th. Haring, M. Baldauf, U. Gebhardt and W. Preidel, Preparation, characterization, and fuel cell application of new acid-base blend membranes, *J. New Mat. Electrochem. Syst.* 3 (2000) 129.
- [64] M.K. Ravikumar and A.K. Shukla, Effect of methanol crossover in a liquid-feed polymer-electrolyte direct methanol fuel cell, *J. Electrochem. Soc.* 143 (1996) 2601.

- [65] A. S. Aricò, P. Cretì, V. Baglio, E. Modica and V. Antonucci, Influence of flow field design on the performance of a direct methanol fuel cell, *J. Power Sources* 91 (2000) 202.
- [66] R. M. Moore, S. Gottesfeld and P. Zeleny in Proton conducting membrane fuel cells – Second International Symposium, (Eds. S. Gottesfeld, T. F. Fuller), Proceeding Volume 98-27, Electrochemical Society, Pennington, New Jersey (1999) 365.
- [67] S.R. Narayanan, W. Chun, T.I. Valdez, B. Jeffries-Nakamura, H. Frank, S. Surampudi, G. Halpert, J. Kosek, C. Cropley, A.B. LaConti, M. Smart, Q. Wang, G. Surya Prakash and G.A. Olah, Program and Abstracts, Fuel Cell Seminar (1996) 525.
- [68] M. Baldauf and W. Preidel, Status of the development of a direct methanol fuel cell, *J. Power Sources* 84 (1999) 161.
- [69] A.K. Shukla, P.A. Christensen, A. Hamnett and M.P. Hogarth, A vapor-feed direct-methanol fuel cell with proton-exchange membrane electrolyte, *J. Power Sources* 55 (1995) 87.
- [70] K. Scott, W.M. Taama, P. Argyropoulos and K. Sundmacher, The impact of mass transport and methanol crossover on the direct methanol fuel cell, *J. Power Sources* 83 (1999) 204.
- [71] D.H. Jung, C.H. Lee, C.S. Kim and D.R. Shin, Performance of a direct methanol polymer electrolyte fuel cell, *J. Power Sources* 71 (1998) 169.
- [72] J.-T. Wang, S. Wasmus and R. F. Savinell, Real-time mass spectrometric study of the methanol crossover in a direct methanol fuel cell, *J. Electrochem. Soc.* 143 (1996) 1239.
- [73] K.Z. Yao, K. Karan, K.B. McAuley, P. Oosthuizen, B. Peppley and T. Xie, A review of mathematical models for hydrogen and direct methanol polymer electrolyte membrane fuel cells, *Fuel Cells* 4 (2004) 3.
- [74] V.S. Silva, J. Schirmer, R. Reissner, B. Ruffman, A. Mendes, L.M. Madeira and S.P. Nunes, Direct methanol fuel cell modeling using proton exchange membrane properties evaluated by standard characterization methods, *Chem. Eng. Sci.* (submitted, 2005).
- [75] V.S. Silva, A. Mendes, L.M. Madeira, S.P. Nunes, Proton exchange membranes for direct methanol fuel cells: Properties critical study concerning methanol crossover and proton conductivity, *J. Membr. Sci.* (submitted, 2005).

## PART TWO

---

### **Sulfonated poly(ether ether ketone) membranes**



## Chapter 2. Mass transport of direct methanol fuel cell species in sulfonated poly(ether ether ketone) membranes \*

### Abstract

Homogeneous membranes based on sulfonated poly(ether ether ketone) (sPEEK) with different sulfonation degrees (SD) were prepared and characterized. In order to perform a critical analysis of the SD effect on the polymer barrier and mass transport properties towards direct methanol fuel cell species, proton conductivity, water/methanol pervaporation and nitrogen/oxygen/carbon dioxide pressure rise method experiments are proposed. This procedure allows the evaluation of the individual permeability coefficients in hydrated sPEEK membranes with different sulfonation degrees. Nafion<sup>®</sup> 112 was used as reference material. DMFC tests were also performed at 50°C. It was observed that the proton conductivity and the permeability coefficients of water, methanol, oxygen and carbon dioxide increase with the sPEEK sulfonation degree. In contrast, the SD seems to not affect the nitrogen permeability coefficient. In terms of selectivity, it was observed that the selectivity towards carbon dioxide/oxygen increases with the sPEEK SD. In contrast, the selectivity towards nitrogen/oxygen decreases. In terms of barrier properties for preventing the DMFC reactants loss, the polymer electrolyte membrane based on the sulfonated poly(ether ether ketone) with SD lower or equal to 71%, although having slightly lower proton conductivity, presented much better characteristics for fuel cell applications compared with the well known Nafion<sup>®</sup> 112. In terms of the DMFC tests of the studied membranes at low temperature, the sPEEK membrane with SD = 71% showed to have similar performance, or even better, as that of Nafion<sup>®</sup> 112. However, the highest DMFC overall efficiency was achieved using sPEEK membrane with SD = 52%.

---

\* V.S. Silva, B. Ruffmann, S. Vetter, M. Boaventura, A. Mendes, L.M. Madeira and S.P. Nunes, (submitted, 2005).

## 2.1. Introduction

At present, the direct liquid methanol fuel cell (DMFC) is one of the most promising power supply candidates for portable electric devices [1-3]. Methanol has the advantage as energy carrier of having a significant electro-activity and being easily oxidized directly to water and carbon dioxide in catalyst alloys. Apart from that, it is easy to handle and transport (liquid at room temperature), is used in low concentrations in the DMFC (typically 2%) and is less dangerous than hydrogen. Furthermore, it can be produced from a variety of sources (natural gas, coal, wood) and is biodegradable [2].

One of the main obstacles for the development of the DMFC is that usually it employs the same proton exchange membranes that are used in the hydrogen fuel cell [3]. The most common are the perfluorinated ion-exchange polymers, such as Nafion<sup>®</sup> from Dupont (Fig. 2.1) or Nafion-like polymers supplied by Dow, Asahi and some other companies. This kind of membranes combines the extremely high hydrophobicity of the perfluorinated backbone with the extremely high hydrophilicity of the sulfonic acid functional groups [4]. In the presence of water, this effect is even more pronounced due to the aggregation of the hydrophilic domains (nano-separation) [4]. Consequently, methanol and water are readily transported across perfluorosulfonic acid membranes [1, 5-6]. Methanol crossover from the anode to the cathode is detrimental to DMFC performance as it reduces the efficiency and cell voltage, leading to an efficiency reduction down to 35% [6]. On the other hand, the high water permeability in perfluorinated membranes can cause cathode flooding and thus, lower cathode performance [5]. The loss of oxygen from the cathode to the anode is also detrimental for the DMFC efficiency, although it can be neglected in comparison with the effect of the methanol crossover. Nitrogen and carbon dioxide mass transfer in the proton exchange membrane does not affect significantly the DMFC performance. However, the knowledge of the membrane permeability towards DMFC species can be useful for modeling purposes, enabling the calculation of their total concentration profiles in the fuel cell. Furthermore, it can be also helpful for evaluating the fuel cell total efficiency, where the knowledge of the carbon dioxide mass balance (with CO<sub>2</sub> resulting from methanol oxidation at the cathode catalyst layer) plays a significant role [5].

In order to improve the performance of the DMFC, it is necessary to develop and test new materials that eliminate or, at least, reduce the reactants loss without decreasing in the same degree the proton conductivity [7]. Non-fluorinated membranes based on the hydrophobic poly(oxi-1,4-phenylene-oxy-1,4-phenylene-carbonyl-1,4-phenylene) (PEEK) have been presented as base

membrane materials with excellent chemical and mechanical resistance [8-11]. This polymer can be easily made hydrophilic by sulfonation reactions (Fig. 2.2), being the sulfonation degree (SD) controlled by the reaction time and temperature. The sulfonation degree can control the hydrophobic-hydrophilic balance, acting directly in the proton conductivity, as well as in the mechanical, chemical and thermal stability of the polymer [12]. The mechanical and chemical properties of PEEK tend to progressively deteriorate with the sulfonation degree, which makes the long term stability of highly sulfonated polymer questionable [11]. On the other hand, the low sulfonated PEEK membranes are quite stable but their proton conductivity is very low for fuel cell applications.

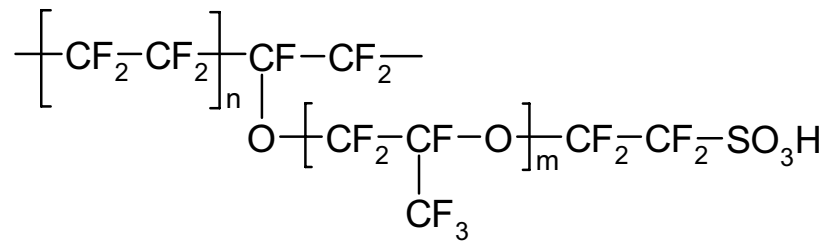


Fig. 2.1. Chemical structure of Nafion<sup>®</sup>.

The transport properties and morphological stability of the sulfonated poly(ether ether ketone) (sPEEK) polymer were found to be distinctly different from those of the perfluorinated polymer [4]. The separation of the hydrophilic-hydrophobic domains is less pronounced as a result of the less hydrophobic backbone (aromatic rings with ether, -O-, and carbonyl, -CO-, linkages), less acidic sulfonic acid functional group (linked to the aromatic ring) and smaller flexibility of the polymer backbone [9]. It has been reported that the hydrated sulfonated poly(aryl ether ketone) has narrower water channels, less separated and more branched with dead-end “pockets” compared to Nafion<sup>®</sup> [4]. Consequently, the permeation coefficients and electro-osmotic drag for the sulfonated poly(aryl ether ketone) polymer are below that of Nafion<sup>®</sup> [4]. These aspects result as an advantage in direct methanol fuel cells applications because they can reduce the loss of reactants, increasing the efficiency of the system. Apart from that, the sPEEK polymer allows direct casting from organic solutions, which is by far a less expensive process compared to the manufacturing of perfluorosulfonic membranes. However, having a weaker hydrophobic domain, the sPEEK polymer is less morphologically stable [11].

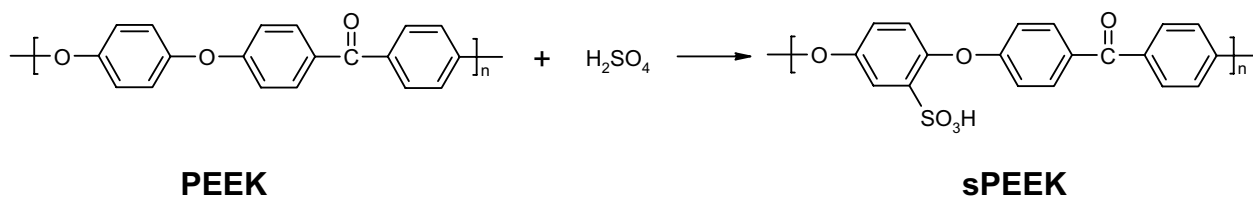


Fig. 2.2. Sulfonation reaction of poly(ether ether ketone).

The present work focuses on the evaluation of the permeability coefficients and mass transport properties of DMFC species in sulfonated poly(ether ether ketone) polymer with different sulfonation degrees. In this study the proton conductivity was obtained via impedance spectroscopy, using sulfuric acid 0.33M as electrolyte. Water and methanol permeability coefficients were evaluated by pervaporation experiments. On the other hand, nitrogen, oxygen and carbon dioxide permeability coefficients were obtained by a pressure rise method in presence of water vapor (swollen membrane). Apart from this, the studied membranes were also tested in real DMFC experiments, and the corresponding polarizations curves obtained. It was also performed a prediction of the fuel cell efficiency for each studied membrane, using the evaluation method as described in [12]. Nafion<sup>®</sup> 112 was used as reference material.

## 2.2. Experimental

### 2.2.1. Materials and methods

Sulfonated poly(ether ether ketone) (sPEEK) polymers with sulfonation degrees of 47, 52, 71 and 78% were prepared following the procedure described in [13]. Poly(ether ether ketone) was supplied as pellets by Victrex. The sulfonation degree was determined by elemental analysis and by H-NMR. Commercially available Nafion<sup>®</sup> 112 was purchased from Aldrich.

### 2.2.2. Membrane preparation

Sulfonated poly(ether ether ketone) polymers were dissolved in dimethylsulfoxide (6%, w/w) and left to stir for one day. The sPEEK polymers with lower sulfonation degrees (SD=47 and 52%) were dissolved by increasing the temperature to 50-70°C, while the others were dissolved at room temperature. After filtration, the final solutions were cast in a hydrophobised glass plate heated to 70°C. After casting, the membranes were stored in a vacuum oven for 24 hours at 90°C.

The thickness of the prepared membranes with sulfonation degrees of 47, 52, 71 and 78% were 87, 55, 52 and 59  $\mu\text{m}$ , respectively.

### 2.2.3. Characterization methods

#### 2.2.3.1. Proton conductivity

Conductivity measurements were carried out at 25°C in the cell described in [14], using an impedance spectroscopy. A membrane sample was placed in a liquid electrolyte solution (0.33M  $\text{H}_2\text{SO}_4$ ) between two platinum electrodes, which have a diameter of 2.8 cm and a distance between them of about 2 mm. The minimum phase angle impedance corresponding to the system membrane/electrolyte was measured after 18 hours of stabilization. As pretreatment, samples were immersed in water at room temperature during 3 days to ensure total leaching. One hour before the measurement, the samples were immersed in 0.33M  $\text{H}_2\text{SO}_4$ . The spectrometer used was a HP 4284A working in the frequency range between 100 and  $10^5$  Hz.

#### 2.2.3.2. Liquid permeability measurements

Permeabilities towards water and methanol were evaluated through pervaporation experiments at 25°C with a 20 wt % methanol aqueous solution. The pervaporation setup is described elsewhere [14]. Prior to all measurements, samples were immersed in the feed solution at room temperature for 1 hour.

The performance of a pervaporation process can be described by the flux through the membrane and the separation factor [15]. Assuming ideal mixing in the feed and permeate sides, the mass transfer during liquid permeation can be divided into three consecutive steps [16]:

- Selective sorption of molecules into the membrane at the feed side.
- Selective diffusion through the membrane.
- Selective desorption into the vapor phase at the permeate side.

According to Binning et al. [17], the selective diffusion through the membrane is the slowest step in the pervaporation process and, therefore, it can be assumed that the mass transfer of species through the membrane is practically not affected by sorption and desorption steps. Thus, the species' permeability coefficients in pervaporation processes can be obtained from the solution-diffusion model proposed by Lonsdale et al. for the transport of liquids through homogenous

membranes [18]. Applying the sorption-diffusion model stated by Lee [19], assuming that sorption is well described by the Henry's law [20] and steady-state diffusion across a non-porous one-dimensional membrane, the molar flux of species  $i$ ,  $J_i$ , is given by

$$J_i = \frac{P_i}{p_i^{sat} d_M} (\gamma_{i,L} x_{i,L} p_i^{sat} - \gamma_{i,V} x_{i,V} p_i) \quad (2.1)$$

in which  $P_i$  is the permeability coefficient,  $d_M$  is the membrane thickness,  $p_i$  is the permeate pressure,  $\gamma_i$  is the activity coefficient,  $x_i$  is the molar fraction and  $p_i^{sat}$  is the equilibrium vapor pressure of species  $i$ . Subscripts  $L$  and  $V$  refer to feed (liquid) and permeate (gas), respectively.

Rearranging the previous equation leads to

$$P_i' = \frac{J_i d_M}{\gamma_{i,L} x_{i,L} p_i^{sat} - \gamma_{i,V} x_{i,V} p_i} \quad (2.2)$$

where  $P_i'$  is the species  $i$  permeability coefficient divided by the equilibrium vapor pressure, in order to be expressed in mole  $\text{m}^{-1} \text{s}^{-1} \text{Pa}^{-1}$ .

In the present study it was verified that the permeate pressure was always less than 1 mbar and, therefore, it is assumed that  $p_i \cong 0$ . The saturation pressure was calculated from the Antoine equation and the liquid phase activity coefficient from the Wilson equation using data from [21]. In the present study the permeability coefficient is expressed in Barrer units ( $10^{10} \text{ cm}^3_{\text{STP}} \text{ cm cm}^{-2} \text{ s}^{-1} \text{ cmHg}^{-1}$ ).

Finally, the membrane selectivity towards components  $i$  and  $j$ ,  $\alpha_{i,j}$ , is defined as

$$\alpha_{i,j} = \frac{P_i'}{P_j'} \quad (2.3)$$

### 2.2.3.3. Gas permeability measurements

Nitrogen, oxygen and carbon dioxide permeability coefficients were evaluated at 20°C using the pressure rise method [22]. The permeation measurements were carried as described by E. Drioli et al. [22]. The gas feed was previously humidified (100% relative humidity) and fed to a Millipore cell with a 47 mm membrane diameter. The pressure in the permeate vessel was measured using a 100 mbar pressure sensor. Experiments were stopped when the permeate pressure was 25 mbar (for fast permeation species) or after 15 hours (for slow permeation species). Prior to all measurements, membranes were conditioned with the feed stream for 12 hours. This procedure ensured that membranes were in the swollen stationary state.

## 2.2.4. DMFC tests

The membrane electrode assemblies (MEAs) were prepared by hot pressing the membrane samples between two Etek<sup>®</sup> ELAT electrodes. Supported PtRu (0.5 mg/cm<sup>2</sup> 20wt.% PtRu (1:1) on carbon with 0.6-0.8 mg/cm<sup>2</sup> Nafion<sup>®</sup>/PTFE) and Pt (0.5 mg/cm<sup>2</sup> 30wt.% Pt on carbon with 0.6-0.8 mg/cm<sup>2</sup> Nafion<sup>®</sup>/PTFE) were used as anode and cathode electrodes, respectively. The membranes were conditioned in boiling water for 1 hour and then pressed with the electrodes at 80°C and 74 bar for 2 minutes. The DMFC experimental set-up is described elsewhere [23]. The DMFC with the prepared MEAs (25 cm<sup>2</sup>) was operated with an aqueous 0.5M methanol solution (26ml/min, 2.5bar) on the anode side and humidified air (600 sccm/min, 3 bar, 100% relative humidity) on the cathode side. The cell temperature was maintained at 50°C. The MEAs' characterization was performed measuring the DMFC current-voltage polarization curves and the CO<sub>2</sub> concentration at the cathode outlet at constant voltage current (CV, 50mV) and open circuit voltage (OCV). The CO<sub>2</sub> concentration at the cathode outlet was monitored as a measure of the methanol crossover during DMFC operation [24]. The potential, Faraday and overall DMFC efficiencies were evaluated as described in [12]. The Faraday efficiency is defined as the ratio of the converted fuel for current production (anode) to the total amount of converted fuel (anode and cathode). On the other hand, the potential efficiency is defined as the voltage loss of the DMFC compared to the standard cell voltage due to the overall potential losses. Finally, the overall DMFC efficiency is the combination of both Faraday and potential efficiencies.

## 2.3. Results and discussion

### 2.3.1. Proton conductivity

It is known that the main function of a polymer electrolyte membrane in the DMFC is to conduct protons from the anode to the cathode, while preventing the reactants loss. The effect of the sPEEK sulfonation degree on the conductivity of the studied membranes is shown in Fig. 2.3. As expected, the proton conductivity increases with the sulfonation degree of the sPEEK polymer. As a consequence of the higher number of sulfonated sites (Fig. 2.2), the amount of sorbed water by the polymer is higher, leading to the formation of water mediated pathways for protons. On the other hand, the proton conductivity measured for Nafion<sup>®</sup> 112 at 25°C was 88.6 mS/cm (Table 2.1),

which is approximately 18% higher than that of the sPEEK polymer with the highest sulfonation degree studied (SD = 78%). This fact can be explained based on the distinct transport properties due to morphological aspects [4]. As mentioned before, due to the smaller hydrophilic/hydrophobic difference, the hydrated sulfonated poly(ether ether ketone) has narrower and less separated water channels compared to those of Nafion<sup>®</sup> [4]. Therefore, for the sPEEK polymer a smaller water dynamic assisted proton conductance is expected. In order to reach higher conductivities, the sulfonation degree of the sPEEK polymer should be increased, but the mechanical and chemical properties will tend also to progressively deteriorate.

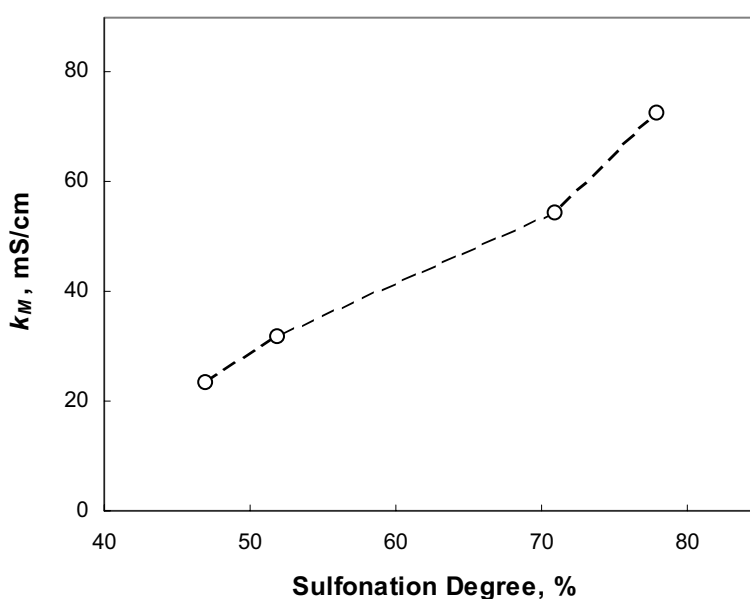


Fig. 2.3. Proton conductivity of the sPEEK polymer as a function of the sulfonation degree (25°C in 0.33M H<sub>2</sub>SO<sub>4</sub>).

Table 2.1. Proton conductivity, methanol and water permeability coefficients and selectivity towards water/methanol of Nafion<sup>®</sup> 112 (pervaporation experiments at 25°C).

Polymer	Thickness ( $\mu\text{m}$ )	$k_M$ (mS/cm)	$P_{MeOH}$ (Barrer)	$P_{Water}$ (Barrer)	$P_{Water}/P_{MeOH}$
Nafion <sup>®</sup> 112	56	88.6	$2.07 \times 10^5$	$4.16 \times 10^6$	20.1

### 2.3.2. Permeability towards water and methanol

Transport of water and methanol in polymer electrolyte membranes depends on the complex interactions between permeates and the polymeric membrane matrix [25]. In sPEEK membranes, it can be assumed that three distinct environments for mass transport of water and methanol exist:

- hydrophilic environment formed by highly polar sulfonic acid groups (-SO<sub>3</sub>H);
- hydrophobic environment formed by the polymeric matrix, which is the less polar part of the polymer (aromatic rings with ether, -O-, and carbonyl, -CO-, linkages);
- water/methanol bulk environment in the filled channels (hydrophobic/hydrophilic nano-separation).

Water preferentially interacts with the polymer sulfonic acid groups and with methanol (coupling effect) rather than with the polymer matrix, due to its chemical polarity. On the other hand, methanol interacts with all environments (-CH<sub>3</sub> non-polar; -OH polar).

The computed methanol and water permeability coefficients are given in Fig. 2.4. It can be noticed that the increase of the sulfonation degree leads to an increase in the permeability, although the effect is more pronounced for the higher sulfonation degrees. When increasing the sulfonation degree, the polymer becomes more hydrophilic and sorbs more water and methanol, which facilitates their mass transport [25, 4, 9]. Apart from increasing the number of sulfonic acid moieties, the sulfonation allows the formation of wider water mediated pathways for mass transport and also leads to a decrease on the polymer crystallinity, resulting in an excessive swelling for higher sulfonation degrees (polymer leaching) [25]. Thus, for SD=78%, the polymer starts becoming morphologically unstable to the feed solution and, therefore, the flux of water and methanol becomes extremely high. On the other hand, the values also indicate that the methanol permeability coefficients are much smaller than that of water. The corresponding values obtained for Nafion<sup>®</sup> 112 are given in Table 2.1. Nafion<sup>®</sup> shows permeability coefficients lower than that of the sPEEK membrane with SD=78% and higher than that with SD=71%.

In terms of selectivity towards water/methanol permeation (Fig. 2.5), it can be seen that it is practically not affected by the SD for the low sPEEK sulfonation degrees (SD≤71%). Since the methanol molecule is less polar than water, increasing the number of sulfonic groups should lead to an increase in the selectivity towards water/methanol because water is preferentially transported in the ionic moieties [25]. However, due to the high molecular interaction between methanol and water, the sulfonation degree seems to not affect the selectivity. It can be assumed that the hydrogen-bonding interaction between water and methanol competes with the sulfonic acid groups

assisted mass transfer. In the particular case of the sPEEK membrane with SD=78%, the selectivity decreases to the lowest level. This can be explained by the excessive swelling of the membrane due to the high sulfonation degree.

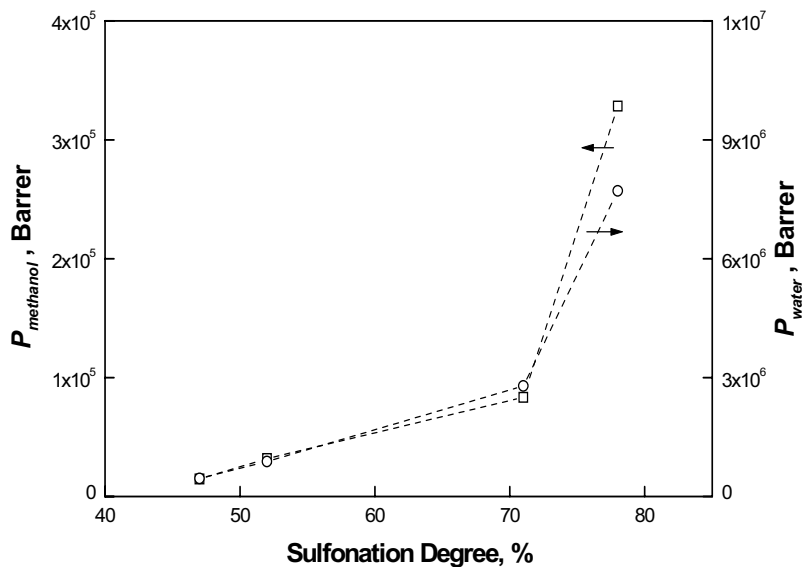


Fig. 2.4. Methanol and water permeability coefficients of sPEEK membranes as a function of the sulfonation degree (pervaporation experiments at 25°C).

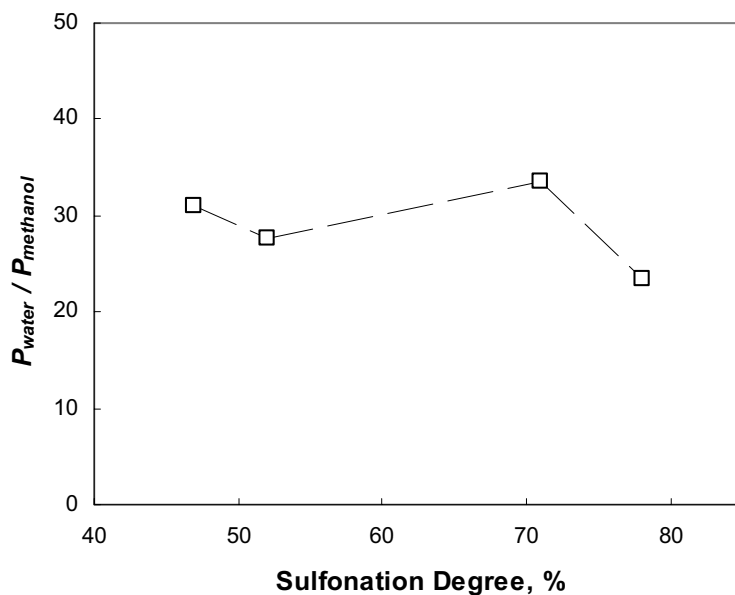


Fig. 2.5. Selectivity towards water/methanol of sPEEK membranes as a function of the sulfonation degree (pervaporation experiments at 25°C).

In comparison to Nafion<sup>®</sup> 112 (Table 2.1), the sPEEK polymer is always more selective towards water/methanol. As before, this fact can be explained by the previously mentioned distinct transport properties [4]. Due to the sPEEK narrower and less separated water channels compared to those of Nafion<sup>®</sup> [4], higher electrostatic interactions between water/methanol and –SO<sub>3</sub>H groups occurs. Therefore, the hydrogen-bonding interactions between water and methanol will probably be higher for Nafion<sup>®</sup> in comparison with those of sPEEK, decreasing its selectivity towards water permeation.

### 2.3.3. Permeability towards nitrogen, oxygen and carbon dioxide

Transport phenomenon involved in the permeation of nitrogen, oxygen and carbon dioxide in the swollen polymer electrolyte membrane depends on the interactions between permeates with the polymeric membrane matrix and sorbed water. Depending on the sulfonation degree, the polymer will have a certain degree of swelling and, therefore, the amount of sorbed water will influence the gas permeation. The nature of the polymer is also important due to the acidity associated with the sulfonic groups.

The computed nitrogen, oxygen and carbon dioxide permeability coefficients are given in Fig. 2.6. It shows that the oxygen and carbon dioxide permeability coefficients increases with the sPEEK sulfonation degree. In contrast, it can be noticed that the membrane permeability to nitrogen is almost not affected. For low sulfonation degrees the permeability towards oxygen is almost the same as the one for nitrogen. Apart from that, for all sulfonation degrees the permeability towards carbon dioxide is much higher compared with that of the other gases.

Fig. 2.7 shows that the nitrogen/oxygen selectivity decreases with the sPEEK sulfonation degree. This fact indicates that the membrane permeability towards oxygen relatively to nitrogen increases with the concentration of sulfonic acid sites and water swelling. Along with, the carbon dioxide/oxygen selectivity also increases with the sulfonation degree (Fig. 2.7).

Comparing the ratio between the molar solubility of these three species in water, at 25°C and 1 atm [20], let us call them the “solubility selectivity”, the values of 0.47 and 25.45, for the nitrogen/oxygen and carbon dioxide/oxygen systems, respectively, were obtained. These values are in agreement with the results found in the present study regarding the permeation selectivities. For example, the carbon dioxide/oxygen selectivity increases to values near the solubility selectivity as the water content increases in the sPEEK membrane (Fig. 2.7). This fact indicates that the sorbed water in the polymer might play an important role in the mass transfer properties of these species.

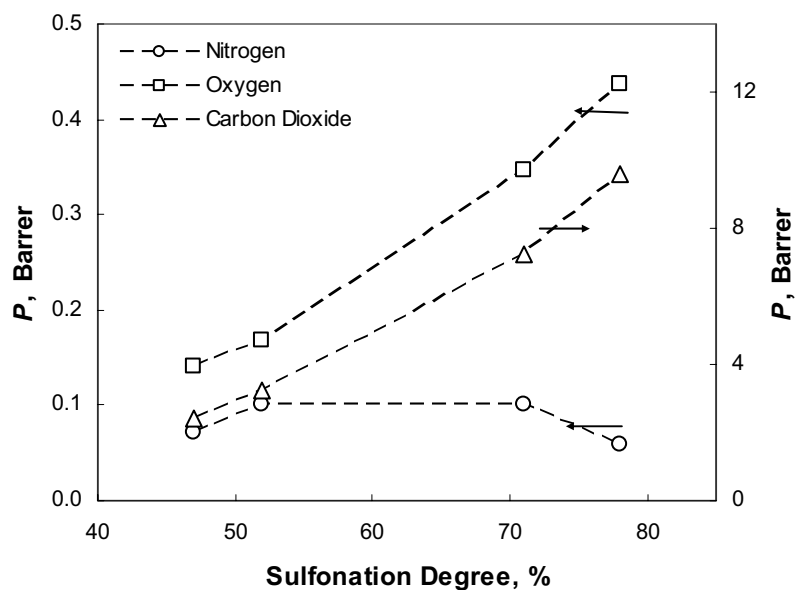


Fig. 2.6. Permeability coefficients of nitrogen, oxygen and carbon dioxide as a function of the sPEEK membrane sulfonation degree (pressure rise experiments at 20°C).

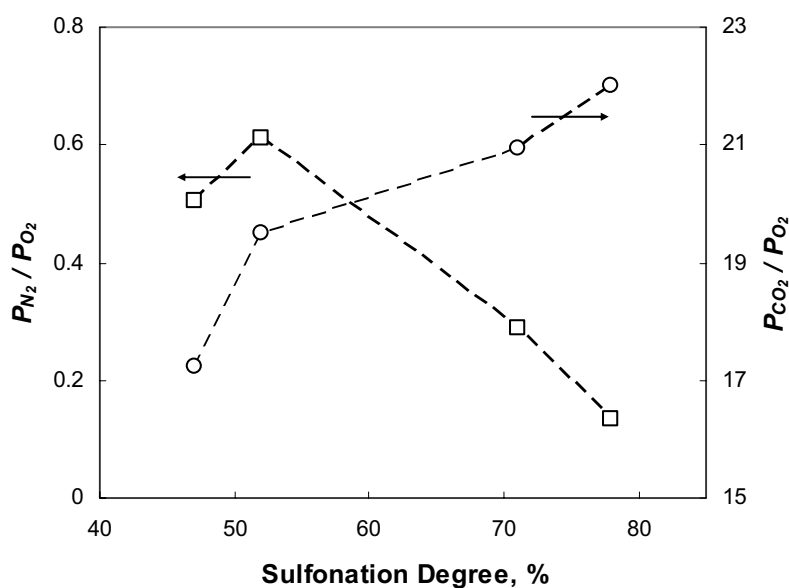


Fig. 2.7. Selectivity towards  $N_2/O_2$  and  $CO_2/O_2$  of sPEEK membranes as a function of the sulfonation degree (pressure rise experiments at 20°C).

In Table 2.2 are given the values obtained in the present study for Nafion<sup>®</sup> 112 with respect to gas permeation. It can be seen that the permeabilities are more than an order of magnitude higher than those obtained for sPEEK polymer (Fig. 2.6). As mentioned previously, these high permeation

ratios can be explained by the wider and more separated water filled channels of Nafion<sup>®</sup> compared with the sPEEK polymer. In terms of selectivity it can be seen that the nitrogen/oxygen selectivity has the same order of magnitude as the one calculated for sPEEK polymer (Fig. 2.7). In contrast, the carbon dioxide/oxygen selectivity is smaller than the one obtained for the sPEEK polymer. According to the theory of the narrower water filled channels in the swollen sPEEK membrane and, consequently, larger contact surface between the molecules of dissolved gas and the hydrophobic/hydrophilic interface [4], the acid behavior of carbon dioxide and its possible interaction with the  $-\text{SO}_3\text{H}$  groups can be suggested as the reason for the higher selectivity towards carbon dioxide in comparison with Nafion<sup>®</sup>. Thus, in the case of carbon dioxide it can be assumed that the mass transport is firstly governed by the solubility/diffusion of the gas in the sorbed water contained in the polymer channels and, secondly, by the interaction with the acid sulfonic groups. In contrast, for oxygen and nitrogen the mass transport is governed mostly by the solubility/diffusion in the water sorbed in the polymer channels because the wider/narrower channels seems to not affect the mass transport.

Table 2.2. Carbon dioxide, nitrogen and oxygen permeability coefficients and selectivity towards  $\text{N}_2/\text{O}_2$  and  $\text{CO}_2/\text{O}_2$  of Nafion<sup>®</sup> 112 (pressure rise experiments at 20°C).

Polymer	$P_{\text{CO}_2}$ (Barrer)	$P_{\text{N}_2}$ (Barrer)	$P_{\text{O}_2}$ (Barrer)	$P_{\text{N}_2}/P_{\text{O}_2}$	$P_{\text{CO}_2}/P_{\text{O}_2}$
Nafion <sup>®</sup> 112	110.18	3.39	8.48	0.40	12.99

#### 2.3.4. DMFC tests

The current density-voltage and current density-power density plots of MEAs obtained from sPEEK membranes with SD=52 and 71% at 50°C are shown in Fig. 2.8. The curves corresponding to the membrane with SD=47% are not presented because this membrane showed high resistance at the test temperature. On the other hand, the plots corresponding to the sPEEK membrane with SD=78% are not presented because this membrane proved to be not stable for DMFC applications at 50°C (excessive swelling). From Fig. 2.8 it can be observed that the DMFC performance increases with the sPEEK SD. The results also show that a DMFC using a sPEEK membrane with SD=71% shows higher performance compared with Nafion<sup>®</sup> 112. The maximum power output

achieved for that membrane was  $1.19\text{mW}/\text{cm}^2$  at  $8.67\text{mA}/\text{cm}^2$ , in comparison with  $1.16\text{mW}/\text{cm}^2$  at  $6.88\text{mA}/\text{cm}^2$  for Nafion<sup>®</sup> 112.

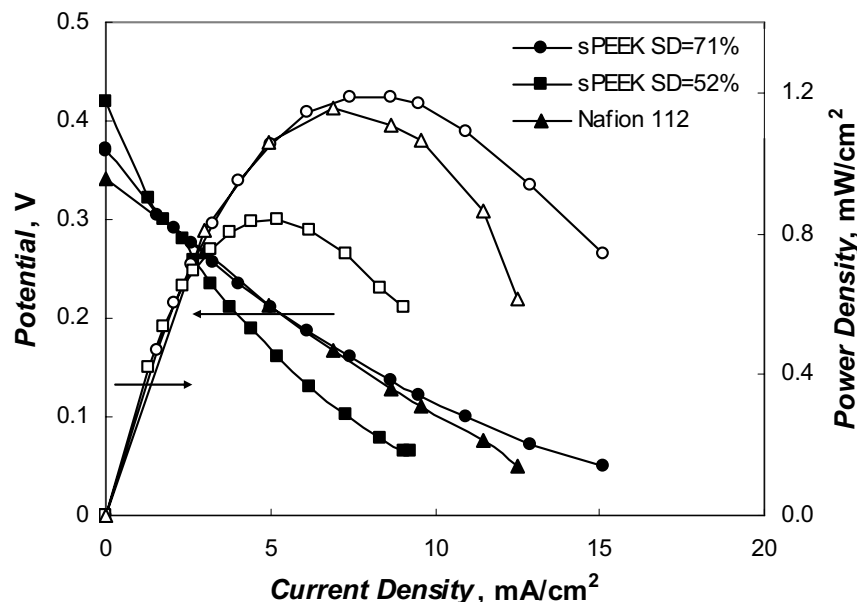


Fig. 2.8. Current density-voltage and power density plots of the DMFC using sPEEK membranes with SD= 52 and 71%, at 50°C. Nafion<sup>®</sup> 112 given as reference.

Apart from this, from the plots presented in Fig. 2.8 it can be also seen that the open circuit voltage (null current density) increases with the decrease of the sPEEK SD. This fact can be explained by the lower methanol crossover (lower potential loss) due to the improved barriers properties of the membranes with lower SD (Fig. 2.4). In terms of Nafion<sup>®</sup> 112, it can be observed that the DMFC using this membrane presents the lowest open circuit voltage (OCV) of the studied membranes (high methanol permeability).

In Fig. 2.9, both DMFC potential and Faraday efficiencies are given for the selected membranes as a function of current density. From these plots, it can be seen that the membrane with SD=52% presents improved properties in terms of Faraday efficiency (improved fuel utilization). Furthermore, the DMFC using this membrane has the highest potential efficiency for open circuit voltage (null current density) but when current density increases this efficiency decreases to the lowest level. On the other hand, from Fig. 2.9 it can be also observed that the DMFC using sPEEK membrane with SD=71%, although presenting always higher potential efficiency than that of Nafion<sup>®</sup> 112, it presents the lowest Faraday efficiency of the studied membranes. We believe that this fact can be explained by the effect of temperature on the permeability towards methanol of the

sPEEK membrane. Although having lower methanol permeability towards methanol than that of Nafion<sup>®</sup> 112 at 25°C (Fig. 2.4 and Table 2.1), for DMFC operation at 50°C this membrane presents lower barrier properties compared to Nafion<sup>®</sup> 112 (evidenced by the higher CO<sub>2</sub> concentrations at the cathode outlet – data not shown).

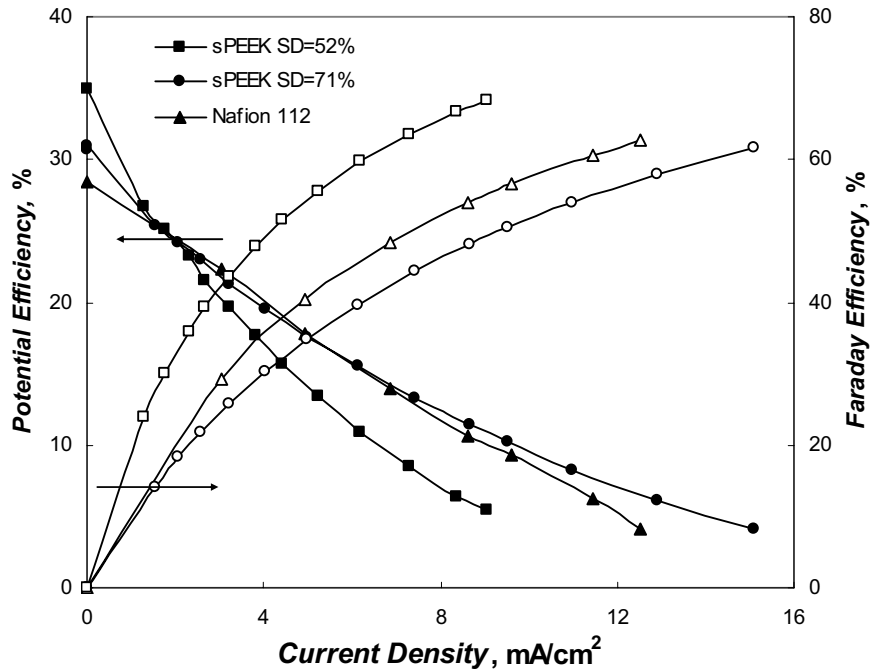


Fig. 2.9. Predicted potential and Faraday DMFC efficiencies during operation using sPEEK membranes with SD= 52 and 71%, at 50°C. Nafion<sup>®</sup> 112 given as reference.

The predicted overall DMFC performance using the studied membranes is presented in Fig. 2.10. It can be seen that the DMFC using sPEEK membrane with SD=52% presents the highest overall efficiency of the studied membranes. This fact derived from the improved membrane characteristics in terms of barrier properties that enable an improved fuel utilization (Faraday efficiency) and, not less important, enough proton conductivity (potential efficiency). However, the highest DMFC overall efficiencies are achieved using this membrane only for current densities lower than 5.32 mA/cm<sup>2</sup> (mainly due to the potential efficiency decrease shown in Fig. 2.9). From 5.32 to 9.63 mA/cm<sup>2</sup> the highest DMFC overall efficiency value is achieved using Nafion<sup>®</sup> 112 and between 9.63 and 15.08 mA/cm<sup>2</sup> using sPEEK with SD=71%.

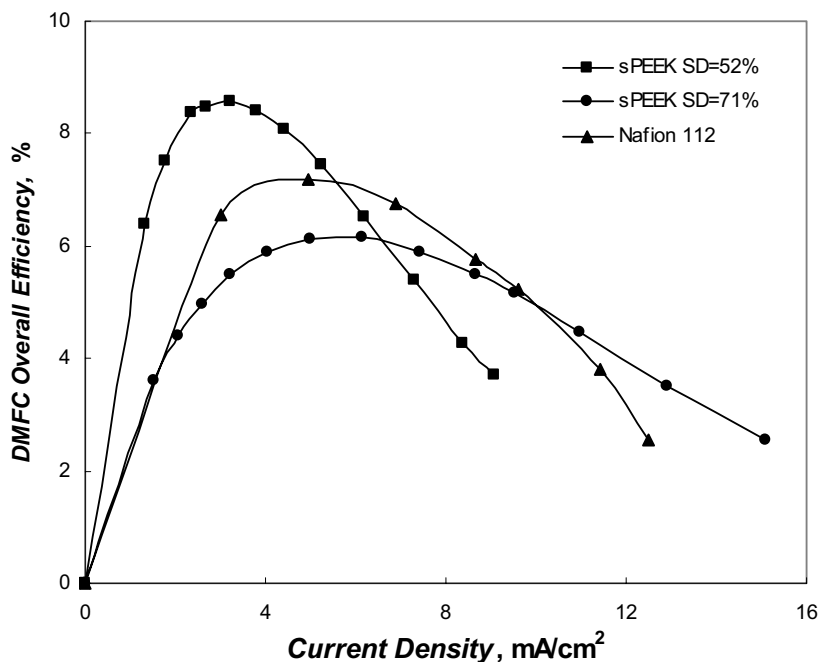


Fig. 2.10. Predicted overall DMFC efficiency during operation using sPEEK membranes with SD= 52 and 71%, at 50°C. Nafion<sup>®</sup> 112 given as reference.

## 2.4. Conclusions

In order to study the mass transport of DMFC species, various sulfonated poly(ether ether ketone) membranes with different sulfonation degrees have been prepared and characterized. The mass transport mechanisms of these species were compared with those for Nafion<sup>®</sup> 112.

Impedance spectroscopy measurements at 25°C using an acid electrolyte (H<sub>2</sub>SO<sub>4</sub>, 0.33M) showed that the proton conductivity increases with the sulfonation degree of the sPEEK polymer. On the other hand, pervaporation experiments at 25°C and 20 wt % methanol feed showed that the permeability coefficients of both water and methanol also increase with the sulfonation degree. It was observed that the sPEEK membranes with sulfonation degrees less than 71% have higher water/methanol selectivity and lower water and methanol fluxes compared to Nafion<sup>®</sup> 112. The sPEEK polymer with sulfonation degree of 78% provided high methanol and water fluxes and lower selectivity due to its lower morphological stability (excessive swelling). In terms of the membrane gas permeability towards nitrogen, oxygen and carbon dioxide in the presence of water vapor (100% r.h.), experimental results obtained by the pressure rise method, at 20°C, showed that the permeability coefficients of carbon dioxide and oxygen increase with the sulfonation degree of the sPEEK polymer. The effect in the nitrogen permeability coefficient is mostly negligible. It was

also found that the carbon dioxide/oxygen selectivity increases with the sulfonation degree. The opposite trend is verified for nitrogen/oxygen selectivity. From the DMFC tests it was observed that the fuel cell performance increases with the sulfonation degree. The results showed that the DMFC using a sPEEK membrane with sulfonation degree of 71% achieves a better performance than when using Nafion<sup>®</sup> 112. Apart from this, from the polarization curves it could be noticed that the open circuit voltage (null current density) decreases with the sPEEK SD (higher methanol crossover). DMFC operation using sPEEK membranes with SD lower than 71% provided a higher open circuit voltage than that of Nafion<sup>®</sup> 112. It was also observed that the potential efficiency decreases with the sPEEK SD. On the other hand, it was found that the Faraday efficiency (fuel effective utilization) increases when decreasing the sPEEK SD. From the predicted overall DMFC efficiency using the studied membranes, it was observed that the maximum efficiency is achieved for the lowest sPEEK SD tested. Although achieving the highest DMFC performance when using sPEEK membranes with SD=71%, the application of this membrane proved to be less efficient in the DMFC due to higher methanol crossover (lower Faraday efficiency).

Based on the criterion of the reactants loss minimization, chemical stability along with enough proton conductivity, the sPEEK membrane proved to be a potential material for DMFC applications. Depending on the sulfonation degree, the sPEEK membrane exhibits characteristics that can improve the DMFC performance and the global efficiency when compared to Nafion<sup>®</sup> 112.

## Acknowledgements

The work of Vasco Silva was supported by FCT (Grant SFRH/BD/6818/2001). The authors would like to acknowledge both FCT and GKSS for the grant assigned to V. Silva for his stay at GKSS Forschungszentrum GmbH. The present work was partially supported by FCT projects POCTI/EQU/38075/2001 and POCTI/EQU/45225/2002.

## Nomenclature

$A$	Membrane area ( $\text{m}^2$ )
$d$	Thickness (m)
$J$	Molar flux ( $\text{mol m}^{-2} \text{s}^{-1}$ )
$k$	Proton conductivity ( $\text{mS cm}^{-1}$ )
$p$	Pressure (Pa)

$P$	Permeability coefficient (Barrer, 1 Barrer = $10^{-10}$ cm <sup>3</sup> [STP] cm / (cm <sup>2</sup> s cmHg))
$R$	Ideal gas constant (J mol <sup>-1</sup> K <sup>-1</sup> )
$T$	Temperature (K)
$x$	Molar fraction

#### Greek letters

$\alpha$	Overall selectivity
$\gamma$	Activity coefficient

#### Subscripts

$i$	Species $i$
$j$	Species $j$
$L$	Liquid phase
$M$	Membrane
$V$	Vapor phase

#### Superscripts

$sat$	equilibrium state
-------	-------------------

## References

- [1] B. Gurau and E. S. Smotkin, Methanol crossover in direct methanol fuel cells: a link between power and energy density, *J. Power Sources* 112 (2002) 339.
- [2] L. Jörissen, V. Gogel, J. Kerres and J. Garche, New membranes for direct methanol fuel cells, *J. Power Sources* 105 (2002) 267.
- [3] J. Kerres, W. Zhang, L. Jörissen and V. Gogel, Application of different types of polyaryl-blend-membranes in DMFC, *J. New Mater. Electrochem. Systems* 5 (2002) 97.
- [4] K. A. Kreuer, On the development of proton conducting polymer membranes for hydrogen and methanol fuel cells, *J. Membr. Sci.* 185 (2001) 3.

- [5] J. Cruickshank and K. Scott, The degree and effect of methanol crossover in the direct methanol fuel cell, *J. Power Sources* 70 (1998) 40.
- [6] F. R. Kalhammer, P. R. Prokopius and V. P. Voecks, Status and prospects of fuel cells as automobile engines, State of California Air Resources Board, California, 1998.
- [7] K. A. Kreuer, On the development of proton conducting materials for technological applications, *Solid State Ionics* 97 (1997) 1.
- [8] X. Jin, M. T. Bishop, T. S. Ellis and F. Karasz, A sulphonated poly(aryl ether ketone), *Br. Polym. J.* 17 (1985) 4.
- [9] T. Kobayashi, M. Rikukawa, K. Sanui and N. Ogata, Proton-conducting polymers derived from poly(ether-etherketone) and poly(4-phenoxybenzoyl-1,4-phenylene), *Solid State Ionics* 106 (1998) 219.
- [10] S. M. J. Zaidi, S. D. Mikailenko, G. P. Robertson, M. D. Guiver and S. Kaliaguine, Proton conducting composite membranes for polyether ether ketone and heteropolyacids for fuel cell applications, *J. Membr. Sci.* 173 (2000) 17.
- [11] S.D. Mikhailenko, S.M.J. Zaidi and S. Kaliaguine, Sulfonated polyether ether ketone composite polymer electrolyte membranes, *Catal. Today* 67 (2001) 225.
- [12] V.S. Silva, S. Weisshaar, R. Reissner, B. Ruffman, S. Vetter, A. Mendes, L.M. Madeira and S.P. Nunes, Performance and efficiency of a DMFC using non-fluorinated composite membranes operating at low/medium temperatures, *J. Power Sources* (in press, 2005).
- [13] M. C. Wijers, Supported liquid membranes for removal of heavy metals, PhD Dissertation, University of Twente, The Netherlands, 1996.
- [14] S. P. Nunes, B. Ruffmann, E. Rikowsky, S. Vetter and K. Richau, Inorganic modification of proton conductive polymer membranes for direct methanol fuel cells, *J. Membr. Sci.* 203 (2002) 215.
- [15] E. E. B. Meuleman, J. H. A. Willemsen, M. H. V. Mulder and H. Strathmann, EPDM as a selective membrane material in pervaporation, *J. Membr. Sci.* 188 (2001) 235.
- [16] J. Olsson, G. Tragardh and C. Tragardh, Pervaporation of volatile organics from water II. Influence of permeate pressure on partial fluxes, *J. Membr. Sci.* 186 (2001) 239.
- [17] R. C. Binning, R. J. Lee, J. F. Jennings and E. C. Martin, Separation of liquid mixtures by permeation, *Ind. Eng. Chem.* 53 (1961) 45.
- [18] H. K. Lonsdale, U. Merten and R. L. Riley, Transport properties of cellulose acetate osmotic membranes, *J. Appl. Polym. Sci.* 9 (1965) 1341.
- [19] C. H. Lee, Theory of reverse osmosis and some other membrane permeation operations, *J. Appl. Polym. Sci.* 19 (1975) 83.

- [20] R. C. Reid, J. M. Prausnitz and B. E. Polling, *The properties of gases and liquids*, Mc-Graw Hill, (1976) 332.
- [21] J. Gmehling and B. Kolbe, *Thermodynamik*, George Thime Verlag, (1988).
- [22] E. Drioli, A. Regina, M. Casciola, A. Oliveti, F. Tratta and T. Massari, Sulfonated PEEK-WC membranes for possible fuel cell applications, *J. Membr. Sci.* 228 (2004) 139.
- [23] S. Vetter, B. Ruffmann, I. Buder and S.P. Nunes, Proton conductive membranes of sulfonated poly(ether ketone ketone), *J. Membr. Sci.* (in press, 2005).
- [24] Z. Qi and A. Kaufman, Open circuit voltage and methanol crossover in DMFCs, *J. Power Sources* 110 (2002) 177.
- [25] R. Y. M. Huang, P. Shao, X. Feng and C. B. Burns, Pervaporation separation of water/isopropanol mixture using sulfonated poly(ether ether ketone) (sPEEK) membranes: transport mechanism and separation performance, *J. Membr. Sci.* 192 (2001) 115.

PART THREE

---

**sPEEK composite membranes based on  
zirconium oxide**



## Chapter 3. Zirconium oxide modified sulfonated poly(ether ether ketone) membranes for direct methanol fuel cell applications \*

### Abstract

In order to perform a critical analysis of the zirconium oxide effects in sulfonated poly(ether ether ketone) (sPEEK) membranes with two sulfonation degrees (SD), 71 and 87%, the characterization of composite membranes prepared with a systematic variation of the inorganic content is proposed. The method involved the preparation of inorganic composite membranes with a wide range of properties which concern water swelling, chemical and thermal stability, methanol and water permeations and, finally, proton conductivity. A good balance between high proton conductivity, good chemical stability and low methanol permeability was reached for the sPEEK polymer with a 7.5% (w/w) ZrO<sub>2</sub> content and SD=87%. Compared to Nafion<sup>®</sup> 112, this membrane proved to be 3-times more selective towards water/methanol permeation and to have a similar proton conductivity (81.5 compared to 88.6 mS/cm).

\*V. Silva, B. Ruffmann, H. Silva, A. Mendes, M. Madeira and S. Nunes, *Mater. Sci. Forum* 455-456 (2004) 587.

### 3.1. Introduction

There is nowadays a growing interest in new materials for direct methanol fuel cell (DMFC) polyelectrolyte membranes that have good barrier properties for methanol, high proton conductivity and good thermal and chemical stability. DMFC require membranes that allow protons to move from the anode to the cathode and prevent the methanol crossover. Today, perfluorinated ion-exchange polymers, such as Nafion<sup>®</sup> from Dupont and Flemion<sup>®</sup> from Asahi Chemical, are the most commonly used for DMFC. However, it has been reported that methanol is readily transported across perfluorosulfonic acid membranes [1-4]. Methanol crossover from the anode to the cathode is detrimental to DMFC performance as it reduces the Faraday efficiency and cell voltage. It has been shown that the methanol crossover during fuel cell operation leads to an efficiency reduction down to 35% [5]. On the other hand, the water permeability should be minimized because it may cause cathode flooding and, thus, lower cathode performance [4].

In order to improve the performance of the DMFC, it is necessary to eliminate or, at least, to reduce the methanol crossover without decreasing the proton conductivity. Non-fluorinated membranes based on sulfonated poly(ether ether ketone) (sPEEK) have been presented in some studies [6-7] as being promising for fuel cells applications. However, for high sulfonation degrees (SD) the methanol permeability is in many cases still relatively high. Nevertheless, sPEEK has also been used as a matrix for the inclusion of inorganic oxides and proton conductors [8-10], which may lead to a reduction in methanol permeability. However, the analysis of the incorporation of zirconium oxide via sol-gel chemistry in high sulfonation degree sPEEK was not yet reported.

The present work focuses on the characterization of organic-inorganic composite membranes based on sulfonated poly(ether ether ketone) modified by the incorporation of zirconium oxide via sol-gel chemistry. The *in situ* generation of inorganic alkoxides via sol-gel chemistry enables wide possibilities of material processing [11-12]. The systematic variation of the inorganic content can be used to obtain a wide range of modifications on polymer electrolyte membranes' properties. For instance, by changing the zirconium oxide content in the composite membrane, water swelling, chemical and thermal stability, methanol and water permeations and, finally, proton conductivity can be affected. The aim of this study is to perform a critical analysis of the zirconium oxide effects in sPEEK membranes with two high sulfonation degrees, 71 and 87%, and to achieve a good balance between high proton conductivity, good chemical stability and low methanol permeability. Nafion<sup>®</sup> 112 was used as a reference material.

## 3.2. Experimental

### 3.2.1. Materials and methods

Sulfonated poly(ether ether ketone) (sPEEK) polymer with sulfonation degrees of 71 and 87% (ion exchange capacity = 1.97 and 2.31 meq/g, respectively) was prepared following the procedure reported in the literature [4]. Poly(ether ether ketone) was supplied as pellets by Victrex. Zirconium tetrapropylate (70% solution in iso-propanol) and acetyl acetone (ACAC) were purchased from Gelest. Commercially available Nafion<sup>®</sup> 112 was purchased from Aldrich.

### 3.2.2. Membrane preparation

sPEEK polymer was dissolved in dimethylsulfoxide (8%, w/w). The zirconium oxide modification was performed by hydrolysis of  $Zr(OPr)_4$  [11]. Acetyl acetone (ACAC) was used as chelating agent to avoid the precipitation of the inorganic compound. The proportion of ACAC compared to alkoxide ranged from 2:1 to 3:1. The polymer/ACAC solution was left to stir for three hours before adding the zirconium tetrapropylate in order to have a good mixture. To accomplish hydrolysis, 0.1g of water per g of polymer was added to the solution and stirred for about 16 h at room temperature. After filtration, the final solutions were cast in a hydrophobised glass plate heated to 70°C. After casting, the membranes were stored in a vacuum oven for 24 hours at 90 °C. Thickness of the prepared membranes varied from 110 to 190  $\mu\text{m}$ .

### 3.2.3. Methanol and water permeability measurements

The water and methanol permeabilities were evaluated through pervaporation measurements at 55°C with a 20 % (w/w) methanol solution. In the pervaporation setup, a Millipore cell with a 47 mm membrane diameter was used. The permeate was collected in a glass trap immersed in liquid nitrogen, at time intervals ranging from 1 to 2 hours. Then, the permeate was weighted and the composition determined by refractive index measurements. The selectivity of the membranes towards water/methanol was evaluated dividing the ratios between the water and methanol molar fraction in the permeate by the ratio in the feed. Prior to all measurements, samples were immersed in deionized water at room temperature for 3 days. Both plain sPEEK membranes (SD = 71 and

87%) were not tested in the pervaporation setup because they proved to be soluble in the 20% (w/w) aqueous methanol solution, at 55°C.

### **3.2.4. Proton conductivity measurements**

Conductivity measurements were carried out at 25°C using ac impedance spectroscopy, determining the impedance at null phase shift. A membrane sample was placed in a 0.33M H<sub>2</sub>SO<sub>4</sub> solution between two platinum electrodes, which have a diameter of 2.8 cm and a distance between them of about 2 mm. As pretreatment, samples were immersed in water at room temperature during 3 days to ensure total leaching. One hour before the measurement, the samples were immersed for 1 hour in 0.33M H<sub>2</sub>SO<sub>4</sub>. The spectrometer used was a HP 4284A working in the frequency range between 100 and 10<sup>5</sup> Hz.

### **3.2.5. Water swelling and chemical stability studies**

Swelling studies were performed on dry samples of the prepared membranes. The pretreatment procedure was started by drying the samples in a vacuum oven at 90 °C for 5 hours. After drying, four samples of each membrane were weighted, immersed in deionized water and equilibrated for 3 days at room temperature. The swollen membranes weights were measured after carefully removing the water from both surfaces. Water uptake (%) was evaluated calculating the ratio between the difference of the wet and dry weight and the dry weight. The average error obtained with the four samples analysis procedure was 4.7% (*t* distribution, 95% confidence level). The chemical stability of the membranes was evaluated qualitatively immersing the membrane samples in a 20 % (w/w) methanol solution (6M) at 60°C.

## **3.3. Results and discussion**

### **3.3.1. Water uptake and chemical stability of the composite membranes**

The water uptake is a measure of the water solubility in the membrane. It is usually correlated by several groups to the water permeability across the membrane. Solubility is one of the main factors that contribute to the permeability, but it is not the only one. Pervaporation may provide a more direct estimation of methanol and water crossover. But water uptake can

additionally give a good indication on how the membrane dimension may change in the cell when humidified. This is an important factor when preparing membrane-electrode-assemblies. High water uptake is usually a sign for low stability in DMFC operation. The proton conductivity in many cases [13] can be well correlated to the water uptake. In the case of sulfonated polymers, higher sulfonation degree not only means higher water solubility (water uptake), but also more acid sites for proton transport.

Fig. 3.1 shows the water uptake of the membranes at room temperature. It can be seen that sPEEK membranes with SD = 87% always exhibit a higher water uptake than those with SD=71%. As reported in [7], sulfonation of the PEEK polymer makes it more hydrophilic by increasing the protonated sites (-SO<sub>3</sub>H). It can be also observed that the amount of ZrO<sub>2</sub> in the sPEEK composite membrane has a large impact on the swelling properties of the composites. For the 87% sulfonated sPEEK membrane, introduction of 7.5% (w/w) ZrO<sub>2</sub> leads to a water uptake decrease of nearly 85%. On the other hand, for the sPEEK membrane with SD=71%, the incorporation of 7.5% of inorganic compound results in a composite membrane that practically doesn't sorb water.

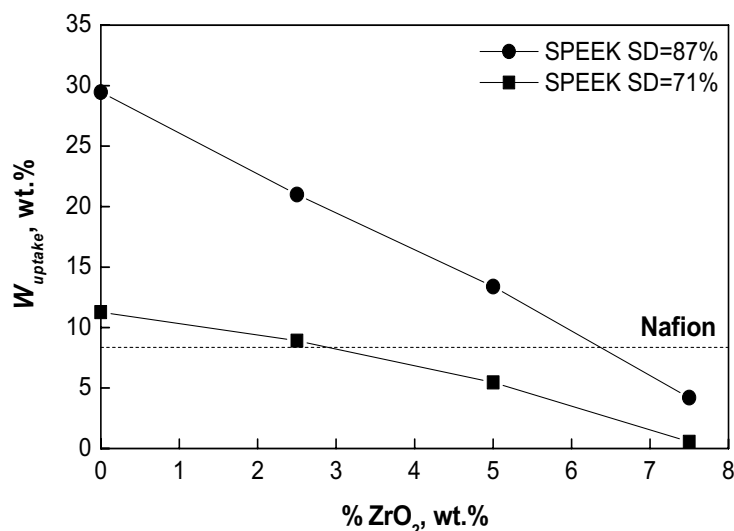


Fig. 3.1. Water uptake of sPEEK membranes as a function of ZrO<sub>2</sub> content (data at room temperature). Nafion<sup>®</sup> 112 given as reference.

In terms of chemical stability, it was observed that for ZrO<sub>2</sub> contents over 5% (w/w) for SD=87% and over 2.5% (w/w) for SD=71%, the membranes become stable in 6M methanol aqueous solution at 60°C. It is worth noting that the standard methanol concentration in a DMFC is 1.5 M, although for the qualitative test a more active solution was chosen.

### 3.3.2. Proton conductivity measurements

One of the more important characterization methods that can be applied to select the right material for fuel cells application is the proton conductivity technique. It is known that the main function of a polymer electrolyte membrane in the DMFC is to conduct protons while preventing reactants crossover from the anode to the cathode. The well known and characterized Nafion<sup>®</sup> can be used as a standard material in terms of conductivity and stability [14].

The effect of the zirconium oxide content in the proton conductivity of sPEEK membranes is shown in Fig. 3.2. The plots indicate an almost linear decrease of the membrane's conductivity with the zirconium oxide content. As mentioned previously, decreasing the hydrophilicity of the membranes leads to an increase in proton transfer resistance and, consequently, the conductivity decreases. In comparison with Nafion<sup>®</sup> 112, the incorporation of 5% (w/w) ZrO<sub>2</sub> in the sPEEK membrane with SD=87% leads to a higher proton conductivity – 94.0 compared to 88.6 mS/cm (Fig. 3.2). For the sPEEK membrane with SD=71%, the proton conductivity observed was always lower than that obtained for Nafion<sup>®</sup> 112.

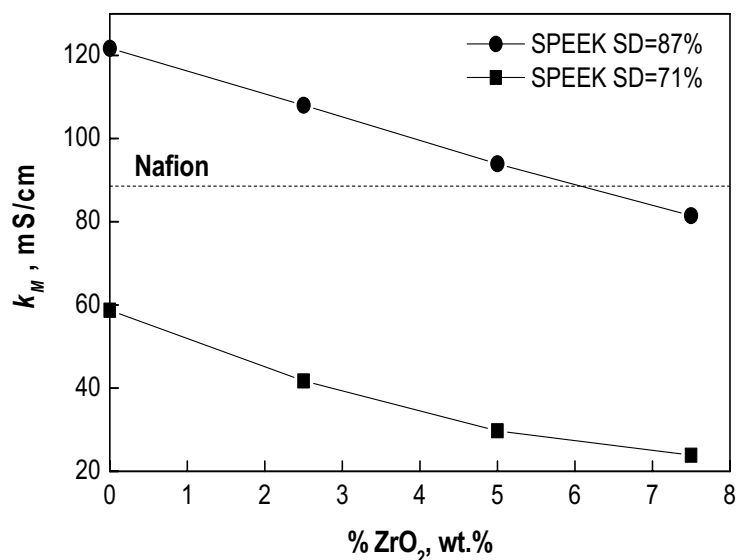


Fig. 3.2. Proton conductivity of sPEEK membranes as a function of ZrO<sub>2</sub> content (25°C in 0.33M H<sub>2</sub>SO<sub>4</sub>). Nafion<sup>®</sup> 112 given as reference.

### 3.3.3. Permeability measurements

Transport of water and methanol in inorganic-organic membranes depends on the complex interactions between the permeates and the organic-inorganic materials [14]. The present main task by incorporating  $ZrO_2$  in the sPEEK polymer is to reduce the water and methanol permeation without decreasing the conductivity of the membrane.

Figs. 3.3 and 3.4 show the measured water and methanol fluxes in the membranes. For the two polymers analyzed, the introduction of  $ZrO_2$  in the range of 2.5% to 5% (w/w) led to a much higher reduction in water and methanol permeations than in the proton conductivity (Figs. 3.2-3.4). It can be also seen that water and methanol fluxes remained practically unchanged with the introduction of 5% or 7.5 % (w/w)  $ZrO_2$ . Comparatively with the fluxes obtained for Nafion<sup>®</sup> 112, the incorporation of 5% or 7.5 % (w/w)  $ZrO_2$  in the two polymeric matrixes led to a 3-times reduction of water and methanol fluxes.

In terms of selectivity to water/methanol permeation (Fig. 3.5), it can be noticed that the higher levels of zirconium oxide used proved to yield sPEEK membranes with water permeation selectivities in the range between 5 and 6. In comparison with Nafion<sup>®</sup> 112, for example, the 5% (w/w)  $ZrO_2$  sPEEK membrane with a sulfonation degree of 71 or 87% led to a 3-times more selective membrane. Even membranes with low  $ZrO_2$  contents present a higher selectivity than Nafion<sup>®</sup> 112.

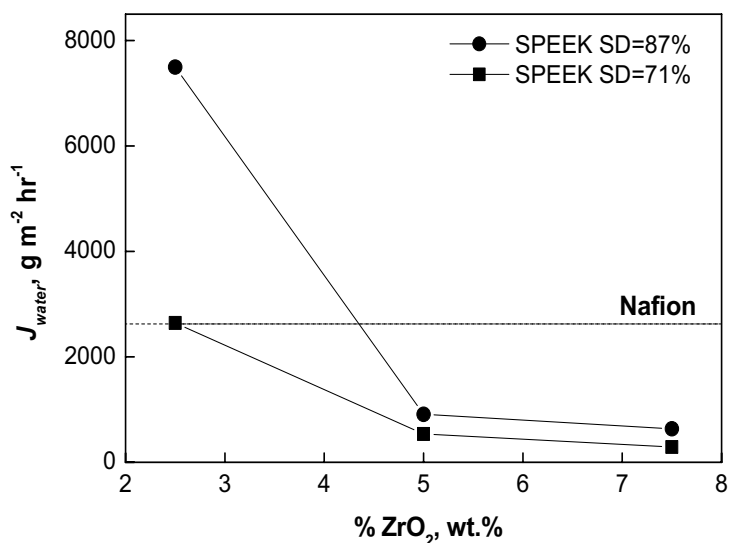


Fig. 3.3. Water flux through sPEEK membranes as a function of  $ZrO_2$  content (pervaporation experiments at 55 °C). Nafion<sup>®</sup> 112 given as reference.

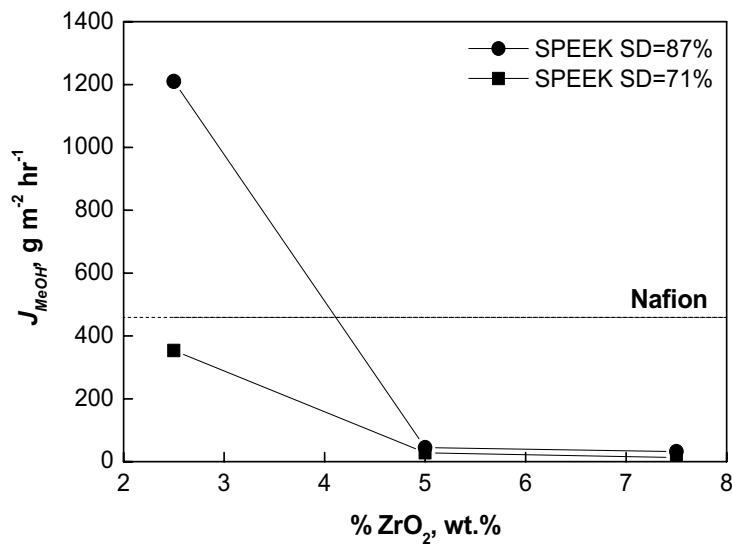


Fig. 3.4. Methanol flux through sPEEK membranes as a function of ZrO<sub>2</sub> content (pervaporation experiments at 55 °C). Nafion<sup>®</sup> 112 given as reference.

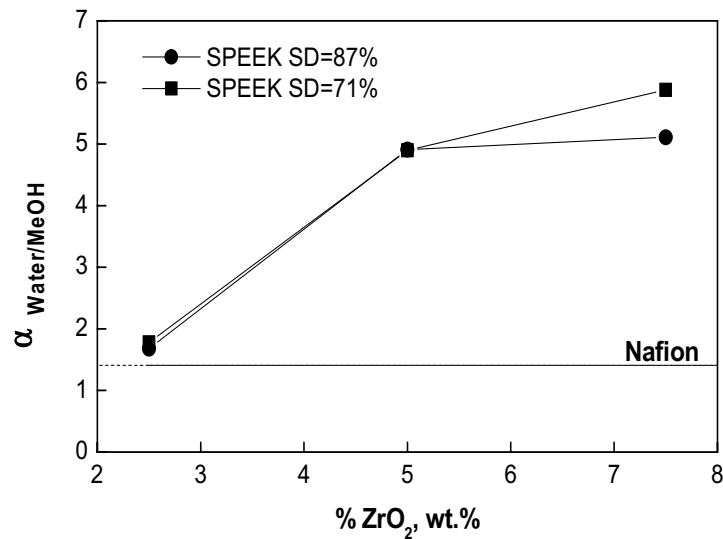


Fig. 3.5. Selectivity towards water/methanol of sPEEK membranes as a function of ZrO<sub>2</sub> content (pervaporation experiments at 55 °C). Nafion<sup>®</sup> 112 given as reference.

### 3.4. Conclusions

Several composite membranes with sulfonated poly(ether ether ketone) as polymeric matrix (with sulfonation degrees of 71 and 87%) and containing different amounts of ZrO<sub>2</sub> were prepared

and characterized. In order to select the proper level of  $ZrO_2$  in the sPEEK polymer for DMFC applications, the present study investigates the transport properties of the composite membranes as a function of the amount of zirconium oxide. The characterization methods used involved determination of: water swelling and chemical stability, methanol and water permeability, selectivity towards water/methanol permeation and proton conductivity.

It is observed that water swelling, proton conductivity and both water and methanol permeation decrease with the amount of  $ZrO_2$  in the composite membrane. However, the decrease observed in the permeability of water and methanol is much higher compared with the other analyzed parameters. In contrast, the chemical stability and the selectivity to water permeation of the composite membranes increase with the inorganic compound content. Based on the criterion of low methanol and water permeability, high proton conductivity, good chemical stability and low swelling, the incorporation of 7.5% (w/w)  $ZrO_2$  in the sPEEK membrane with SD=87% was found to be the most favorable and might be useful for DMFC applications.

## Acknowledgements

The work of Vasco Silva and Hugo Silva was supported by FCT (Grants SFRH/BD/6818/2001 and SFRH/3029/2000, respectively). The authors would like to acknowledge both FCT and GKSS for the grant assigned to V. Silva for his stay at GKSS Forschungszentrum GmbH.

## References

- [1] M.W. Verbrugge, Methanol diffusion in perfluorinated ion-exchange membranes, *J. Electrochem. Soc.* 136 (1989) 417.
- [2] P.S. Kauranen and E. Skou, Methanol permeability in perfluorosulphonate proton exchange membranes at elevated temperature, *J. Appl. Electrochem.* 26 (1996) 909.
- [3] X. Ren, T.E. Springer and S. Gottesfeld, Water and methanol uptakes in Nafion membranes and membrane effects on direct methanol cell performance, *J. Electrochem. Soc.* 147 (2000) 92.
- [4] J. Cruickshank and K. Scott, The degree and effect of methanol crossover in the direct methanol fuel, *J. Power Sources* 70 (1998) 40.
- [5] F.R. Kalhammer, P.R. Prokopius and V.P. Voecks, Status and prospects of fuel cells as automobile engines, State of California Air Resources Board, California, 1998.

- [6] D.J. Jones and J. Rozière, Recent advantages in the functionalisation of polybenzimidazole and polyetherketone for fuel cell applications, *J. Membrane Sci.* 185 (2001) 41.
- [7] S.D. Mikhailenko, S.M.J. Zaidi and S. Kaliaguine, Sulfonated polyether ether ketone based composite polymer electrolyte membranes, *Catal. Today* 67 (2001) 225.
- [8] B. Bonnet, D.J. Jones, J. Rozière, L. Tchicaya, G. Alberti, M. Casciola, L. Massinelli, D. Bauer, A. Peraio and E. Rammunni, Hybrid organic-inorganic membranes for a medium temperature fuel cell, *J. New Mater. Electrochem. Syst.* 3 (2000) 87.
- [9] J. Kjaer, S. Yde-Andersen, N.A. Knudsen and E. Skou, Solid state electrolyte membranes for direct methanol fuel cells, *Solid State Ionics* 46 (1991) 169.
- [10] S.P. Nunes, B. Ruffmann, E. Rikowsky, S. Vetter and K. Richau, Inorganic modification of proton conductive polymer membranes for direct methanol fuel cells, *J. Membrane Sci.* 2003 (2002) 215.
- [11] K.A. Mauritz, Organic-inorganic hybrid materials: perfluorinated ionomers as sol-gel polymerization templates for inorganic alkoxides, *Mat. Sci. and Eng. C* 6 (1998) 121.
- [12] P. Judeinstein and C. Sanchez, Hybrid organic-inorganic materials: a land of multi-disciplinarity, *J. Mater. Chem.* 6(4) (1996) 511.
- [13] P. Dimitrova, K.A. Friedrich, B. Vogt and U. Stimming, Modified Nafion-based membranes for use in direct methanol fuel cells, *J. Electroanal. Chem.* 532 (2002) 75.
- [14] J.A. Kerres, Development of ionomer membranes for fuel cells, *J. Membrane Sci.* 185 (2001) 3.

## Chapter 4. Proton electrolyte membrane properties and direct methanol fuel cell performance, I. Characterization of hybrid sulfonated poly(ether ether ketone)/zirconium oxide membranes\*

### Abstract

This chapter presents an evaluation of the zirconium oxide effects in sulfonated poly(ether ether ketone) (sPEEK) with sulfonation degree (SD) of 87%. A series of inorganic-organic hybrid membranes were prepared with a systematic variation of the zirconium oxide content via *in situ* zirconia formation (2.5, 5.0, 7.5, 10, 12.5 wt.%). This procedure enabled the preparation of proton electrolyte membranes (PEM) with a wide range of properties, which can be useful for evaluating the relationship between the PEM properties and the direct methanol fuel cell (DMFC) performance. The investigated properties are the proton conductivity, proton transport resistance, water uptake, water, methanol, oxygen, carbon dioxide and nitrogen permeability coefficients, morphology and elemental analysis. The results obtained show that the inorganic oxide network decreases the proton conductivity and water swelling. It is found that it leads also to a decrease of the water, methanol, carbon dioxide and oxygen permeability coefficients, an increase of the water/methanol selectivity and a decrease of the carbon dioxide/nitrogen and oxygen/nitrogen selectivities. In terms of morphology, it is found that *in situ* zirconium alkoxide hydrolysis enables the preparation of homogeneous membranes that present a good adhesion between inorganic domains and the polymer matrix.

\*V.S. Silva, B. Ruffmann, H. Silva, Y.A.-Gallego, A. Mendes, L.M. Madeira and S.P. Nunes, *J. Power Sources* 140 (2005) 34.

## 4.1. Introduction

In the last decade, the development of the direct methanol fuel cell (DMFC) has gained much interest mainly for portable power applications. It has the advantage of not requiring a fuel processor (more compact and simpler system) and, apart from that, it uses methanol, which has higher energy density compared to hydrogen at high pressures (360 atm) and is easier to handle and transport (liquid at room temperature) [1]. A DMFC consists in a proton electrolyte membrane (PEM) sandwiched between two porous electrodes that contain catalyst. To the fuel cell anode and cathode is fed a methanol solution (typically 1.5 mol/L) and oxygen (usually as air), respectively.

The PEM plays an important role in the development of the fuel cell technology. In the particular case of the direct methanol fuel cell, it should have a low permeability coefficient for the reactants (mainly methanol), exhibiting high proton conductivity, along with long term mechanical stability [1]. Species transport through the proton exchange membrane is illustrated in Fig. 4.1.

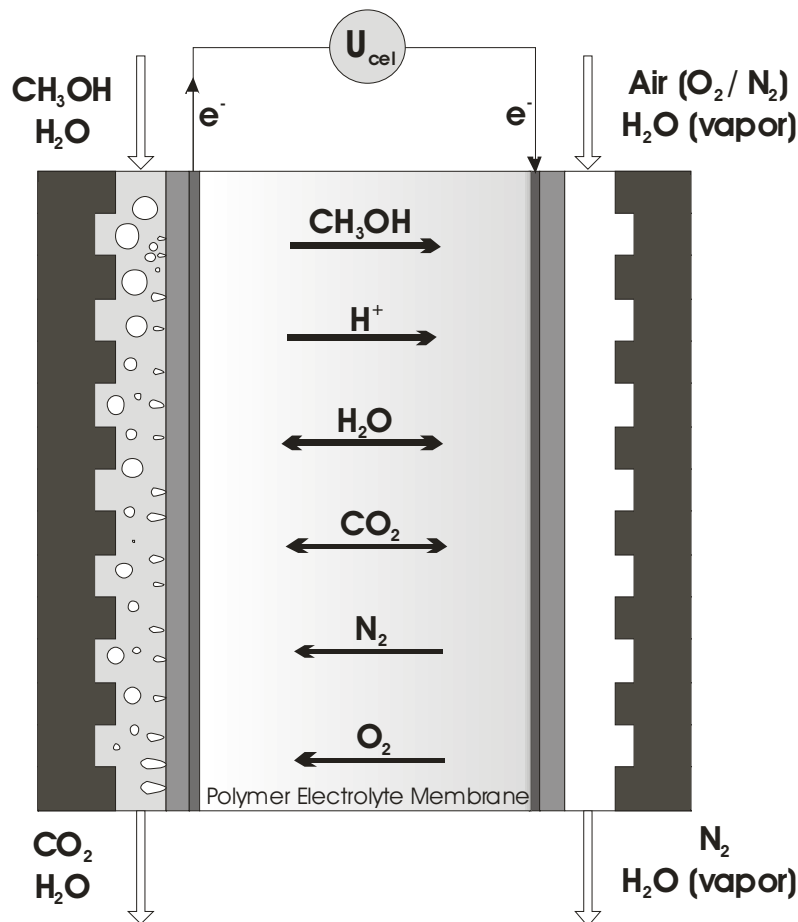


Fig. 4.1. Sketch of the DMFC illustrating the mass transport of the different species through the proton exchange membrane.

Although perfluorinated membranes, such as Nafion<sup>®</sup> or Flemion<sup>®</sup>, are very suitable for hydrogen fuel cells, they are not ideal for DMFC applications due to their high methanol and water permeability [2]. Methanol crossover from the anode to the cathode reduces the Faraday efficiency and cell voltage, leading to an overall efficiency reduction [3]. On the other hand, the high water permeability in perfluorinated membranes causes cathode flooding and, thus, lowers the cathode performance [4].

Non-fluorinated membranes based on sulfonated poly(ether ether ketone) (sPEEK) have been presented as promising materials due to their high proton conductivity [5-7]. Furthermore, in order to improve the membrane properties for DMFC applications, the single-phase pure polymer can be modified by the incorporation of a finely dispersed ceramic solid component.

Previous work focused on the influence of the zirconium oxide incorporation, via hydrolysis, on the proton, water and methanol transport in sulfonated poly(ether ether ketone) with several sulfonation degrees (SD = 71 and 87%) [8]. As a result of this study it was observed that the incorporation of increasing amounts of ZrO<sub>2</sub>, ranging from 2.5 to 7.5 wt.%, in the sPEEK polymer matrix, enabled the preparation of membranes with continuously decreasing water swelling, proton conductivity and water and methanol permeation fluxes. No results have been reported regarding DMFC performance using the studied composite membranes with the above mentioned ZrO<sub>2</sub> content. It was verified that some of these membranes (lower inorganic modification) were not morphologically stable in 20 wt.% aqueous methanol solutions at 60°C due to excessive swelling (high sulfonation degrees).

The present study aims at expanding the characterization of a series of novel organic-inorganic composite membranes with an extended range of zirconium oxide contents (2.5 to 12.5 wt.%), from standard characterization methods to field tests under DMFC conditions. Since the proton conductivity decreases with the amount of ZrO<sub>2</sub>, the sulfonated polymer with the highest sulfonation degree of the previous study (SD = 87%) was selected, in order to prepare membranes with enough proton conductivity [8]. Apart from taking advantage of the improved barrier properties of the composite membranes with respect to methanol permeation, the ZrO<sub>2</sub> also increases the membrane morphological stability (lower swelling). Therefore, it enables the use of high sulfonation sPEEK membranes in DMFC applications operating at temperatures up to 90°C.

## 4.2. Experimental

### 4.2.1. Materials and methods

Sulfonated poly(ether ether ketone) (sPEEK) polymers with sulfonation degree of 87% (ion exchange capacity = 2.31 meq/g) were prepared following the procedure reported in the literature [9]. Poly(ether ether ketone) was supplied as pellets by Victrex. The sulfonation degree was determined by elemental analysis and by H-NMR, as described by Nolte et al. [10].

### 4.2.2. Membrane preparation

The sPEEK composite membranes were prepared using *in situ* formation of zirconia with zirconium tetrapropylate as alkoxide and acetyl acetone as chelating agent. First, the sPEEK polymer was dissolved in dimethylsulfoxide (6 wt.% solution) and the incorporation of zirconium oxide was performed as described in detail elsewhere [8]. The water/alkoxide ratio was always maintained higher than 1 to ensure the formation of a finely dispersed inorganic phase in the polymer solution. The mixtures were cast in a hydrophobised glass plate heated to 70°C for solvent evaporation. Then, the membranes were stored in a vacuum oven for 24 hours at 90 °C. The thickness of the prepared membranes with 0.0, 2.5, 5.0, 7.5, 10.0, 12.5 wt.% of zirconium oxide were 188, 175, 133, 146, 128, 106  $\mu\text{m}$ , respectively. Membrane thickness was measured using a Micromaster system by TESA.

### 4.2.3. Characterization methods

#### 4.2.3.1. Conductivity

Proton conductivity and proton transport resistance were determined by impedance spectroscopy with two different set-ups, simulating the anode and cathode operation environment (liquid and vapor electrolyte). Both proton conductivity and proton transport resistance values were obtained from the impedance modulus at null phase shift (high frequency side). The proton transport resistance gives the specific resistance of the membrane with respect to proton transport.

The anode environment in the DMFC was simulated experimentally using a liquid acid electrolyte at 25°C [11]. The electrolyte used was liquid sulfuric acid (0.33M), ensuring a fully hydrated and protonated state of the measured samples. As pretreatment, samples were immersed in water at room temperature during 3 days to ensure total leaching. One hour before initiating the

measurement, the samples were immersed in the electrolyte solution. The spectrometer used was a HP 4284A, working in the frequency range between 100 and 10<sup>5</sup> Hz.

On the other hand, the cathode environment in the DMFC was simulated experimentally using water vapor as described by Alberti et al. [12]. Proton conductivity of the samples was determined at temperatures ranging from 50 to 110°C and 100% relative humidity. The samples were measured without pretreatment. The impedance measurements were carried on stacks containing up to 4 membranes (similar cumulative thickness, around 430 μm). This procedure was performed because the resistance of a single membrane with low ZrO<sub>2</sub> content (0, 2.5, 5.0wt.%) is close to the short-circuited cell's resistance. Obviously, the measured conductivity for the all stack is affected by the contact resistance between the membranes. The evaluation of the material resistance was performed subtracting such effect, as described by Alberti et al. [12]. The stacks were pressed between two Etek<sup>®</sup> electrodes to decrease the mass and charge transfer resistance between the membrane and the cell electrodes. The spectrometer used was a Zahner IM6 electrochemical workstation, working in the frequency range between 10 and 10<sup>6</sup> Hz. The plain sPEEK SD=87% membrane was not tested because it proved to be unstable in water vapor electrolyte at the experimented temperatures.

#### **4.2.3.2. Water swelling**

Water swelling studies were performed in batch experiments at room temperature as described elsewhere [8]. Relative water uptake (%) was evaluated calculating the ratio between the difference of the wet and dry weight and the dry weight of the membranes.

#### **4.2.3.3. Water and methanol pervaporation measurements**

Water and methanol permeability coefficients were evaluated from pervaporation measurements at 55°C with a 20 wt.% methanol solution. The pervaporation set-up is described elsewhere [13]. The evaluation of the permeability coefficients was performed using the method described by Manea and Mulder [2]. The water/methanol selectivity of the composite membranes was obtained as the ratio between water and methanol permeability coefficients. Prior to all measurements, samples were immersed in deionized water at room temperature for 3 days. The plain sPEEK SD=87% membrane was not tested because it proved to be unstable in the feed methanol aqueous solution at 55°C (excessive swelling).

#### **4.2.3.4. Nitrogen/Oxygen/Carbon dioxide permeability coefficients measurements**

Nitrogen, oxygen and carbon dioxide permeability coefficients were evaluated at 20°C using the pressure rise method. The permeation measurements were carried as described by E. Drioli et al. [14]. The feed gas was previously humidified and fed to a Millipore cell with a 47 mm membrane diameter. The pressure in the permeate vessel was measured using a 100 mbar pressure sensor. Experiments were stopped when the permeate pressure was 25 mbar (for fast permeation species) or after 15 hours (for slow permeation species). Prior to all measurements, membranes were conditioned with the feed stream for 12 hours. This procedure ensured that membranes were in the swollen stationary state.

#### **4.2.3.5. Membrane morphology**

The membrane morphology was investigated by field emission scanning electron microscopy in a LEO equipment, using both secondary and backscattered electron detectors. Samples were fractured in liquid nitrogen and sputtered with carbon in a penning sputtering equipment.

#### **4.2.3.6. Membrane elemental analysis**

The membrane elemental analysis was investigated by x-ray microfluorescence (XRMF) in an EDAX spectrometer. The samples were fractured in liquid nitrogen and sputtered with palladium in a penning sputtering equipment.

### **4.3. Results and discussion**

#### **4.3.1. Proton conductivity**

Fig. 4.2 shows the effects of the zirconium oxide incorporation in the sPEEK polymer on the proton conductivity and proton transport resistance measured at 25°C in an acid electrolyte (set-up

1, 0.33M H<sub>2</sub>SO<sub>4</sub>). The proton conductivity of the composite membranes decreases continuously with the inorganic content. The opposite behavior can be observed for the membrane resistance.

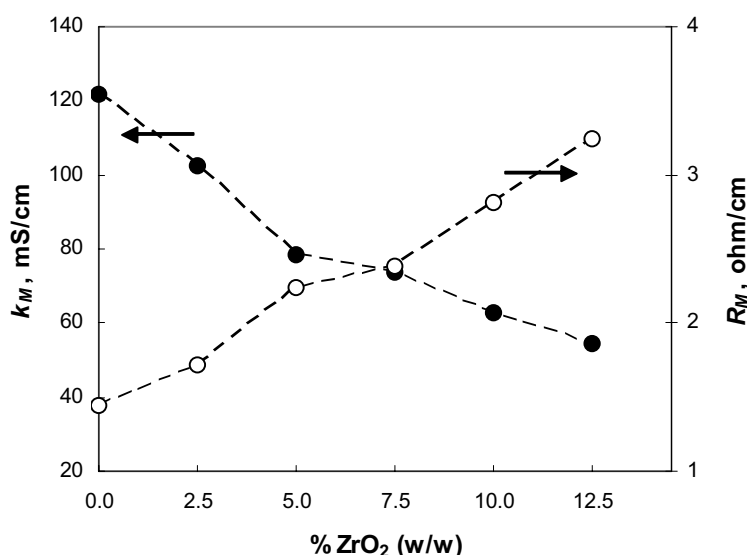


Fig. 4.2. Proton conductivity and impedance resistance of the sPEEK composite membranes in an acid electrolyte as a function of the ZrO<sub>2</sub> content (25°C in 0.33M H<sub>2</sub>SO<sub>4</sub>).

In terms of the membrane conductivity evaluated in the water vapor cell (Set-up 2, Fig. 4.3a), it can be seen that the proton conductivity also decreases with the amount of zirconium oxide. Furthermore, as observed for the acid electrolyte cell, it can be seen that the proton transport resistance increases with the amount of inorganic filler (Fig. 4.3b). It is worth noting that for the membrane with the highest content of inorganic incorporation (12.5 wt.% ZrO<sub>2</sub>), the resistance becomes very high. As expected, proton conductivity increases with temperature while resistance shows the opposite trend.

These results can be attributed to the possible chemical influence of the polymer functional groups nature in the inorganic oxide phase growth. As stated by Mauritz [15], it can be assumed that the hydrolysis reaction is catalyzed via pendant  $-\text{SO}_3\text{H}^+$  groups and, therefore, due to energetic preferences, the hydrolyzed alkoxides would preferentially migrate to the preformed membrane polar clusters. Consequently, the amount of sorbed electrolyte will be smaller (water vapor or aqueous sulfuric acid), decreasing the proton conductivity assisted by water [16]. However, the decrease of the proton conductivity is believed to derive mainly from the increased barrier properties of the membranes due to the incorporation of inorganic fillers [17].

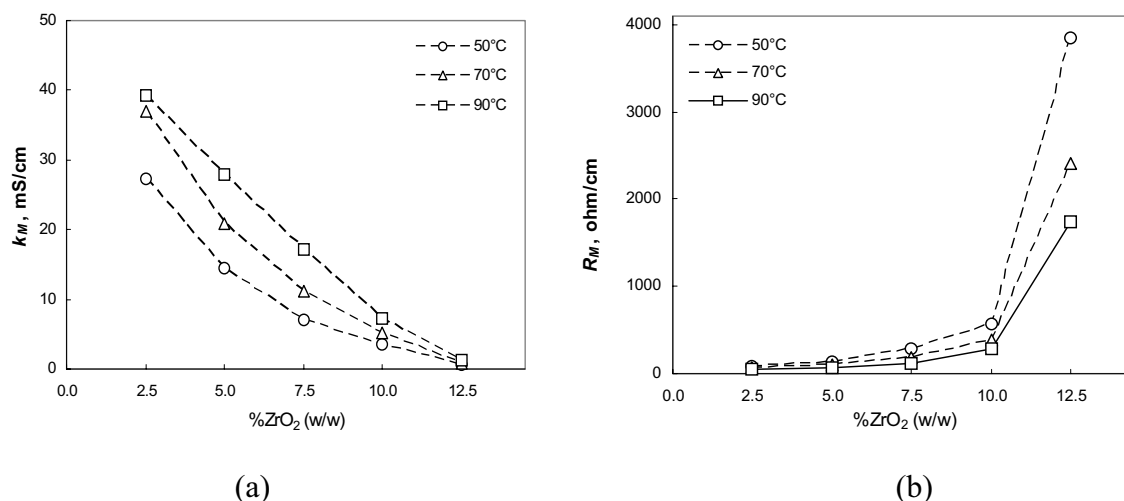


Fig. 4.3. Proton conductivity (a) and impedance resistance (b) of the sPEEK composite membranes in water vapor as a function of the ZrO<sub>2</sub> content (100% r.h.).

#### 4.3.2. Water uptake

From Fig. 4.4 it can be observed that, for the studied membranes, water uptake decreases to very low levels with the zirconium oxide incorporation. The observed variation is more pronounced for the lower ZrO<sub>2</sub> contents.

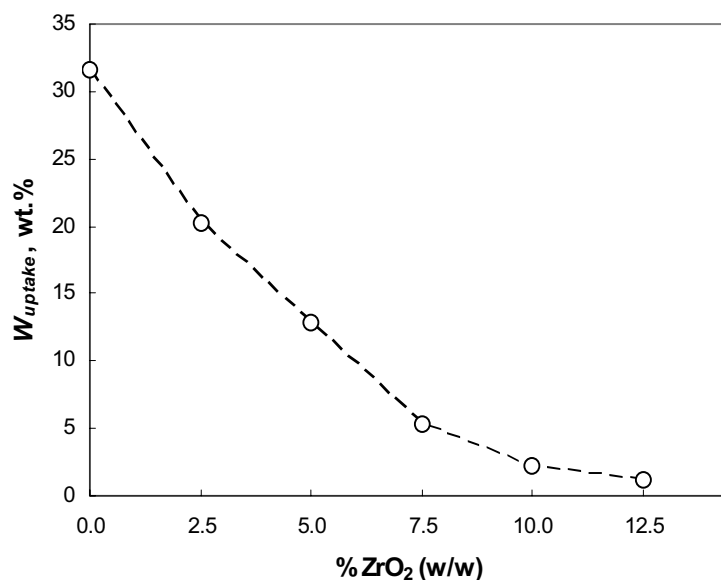


Fig. 4.4. Water uptake of sPEEK composite membranes as a function of the ZrO<sub>2</sub> content (room temperature).

Comparing the water uptake results (Fig. 4.4) and the corresponding proton conductivity (Figs. 4.2 and 4.3), it can be observed that higher water uptake leads to higher proton conductivity, showing the importance of sorbed water in the proton conductivity of sulfonated membranes, in agreement with previous studies [16]. However, it seems that for the acid electrolyte cell, a reduced water uptake does not mean reduced conductivity as it occurs for the water vapor cell. This fact shows that low sulfuric acid uptake leads to enough proton conductivity for the proton electrolyte membrane. In contrast, due to the absence of acid electrolyte in the water vapor cell, the conductivity decreases to very low values due to the low sorbed water in the polymer polar channels.

### 4.3.3. Permeabilities towards species present in DMFC

Pervaporation experiments at 55°C showed that the membranes permeability towards methanol decreases with the amount of zirconium oxide (Fig. 4.5). As observed previously for the water uptake and proton conductivity (vapor cell) properties, at lower ZrO<sub>2</sub> contents the effects in the permeability coefficients of water and methanol are much more pronounced. Moreover, from Fig. 4.5, it can be observed that the zirconium oxide content leads to an increase in the water/methanol selectivity.

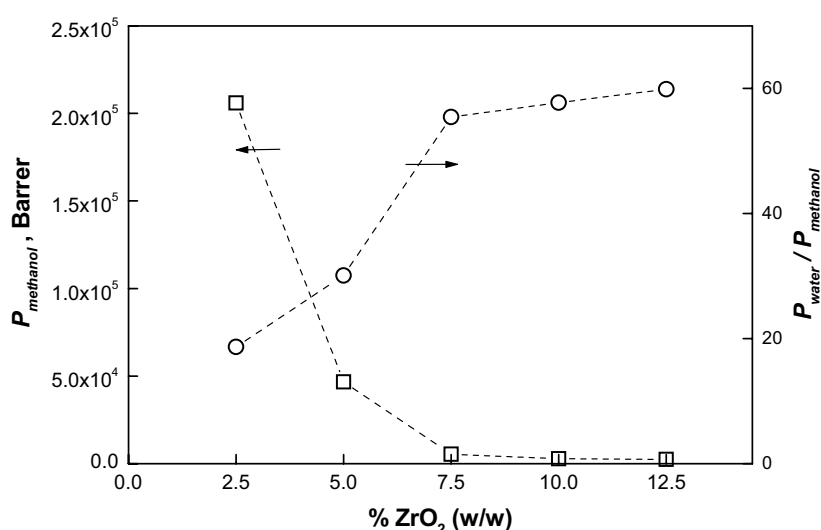


Fig. 4.5. Methanol permeability coefficients and water/methanol selectivity of the sPEEK composite membranes as a function of the ZrO<sub>2</sub> content (pervaporation experiments at 55°C, 1 Barrer = 10<sup>-10</sup> cm<sup>3</sup> [STP] cm / (cm<sup>2</sup> s cmHg)).

The membrane permeability towards nitrogen, oxygen and carbon dioxide as a function of the zirconium oxide content is given in Fig. 4.6. It can be observed that the oxygen and carbon dioxide permeability coefficients decrease with the amount of  $ZrO_2$ . In contrast, the inorganic modification resulted to have almost no noticeable effect on the nitrogen permeability coefficient. It seems that the less hydrophilic behavior of the higher  $ZrO_2$  content composite membranes results in lower permeability towards oxygen and carbon dioxide. It can be also noticed that the carbon dioxide permeability coefficient in the sPEEK composite membranes is much higher than that of oxygen or nitrogen. This fact can be explained by the higher ‘interactive’ behavior of  $CO_2$  with the polymer’s polar groups and sorbed water. Fig. 4.7 shows that the oxygen/nitrogen and carbon dioxide/nitrogen selectivities decrease with the  $ZrO_2$  content. These results are in agreement with previous data for DMFC species mass transfer in sPEEK polymer with several sulfonation degrees [14]. In that study, lower sPEEK sulfonation degrees resulted in lower hydrophilicity, lower water uptake and, finally, lower permeability towards  $CO_2$  and  $O_2$ . Therefore, the decreasing sorbed water by the polymer (Fig. 4.4) seems to decrease the oxygen/nitrogen and carbon dioxide/nitrogen selectivity. Additionally, it can be observed that the carbon dioxide/nitrogen selectivity is much higher compared with that corresponding to oxygen/nitrogen.

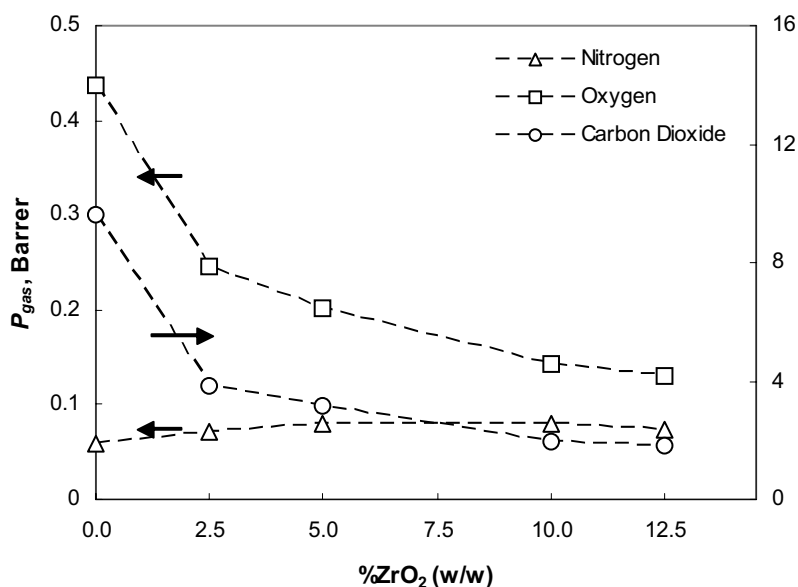


Fig. 4.6. Nitrogen, oxygen and carbon dioxide permeability coefficients of sPEEK composite membranes as a function of the  $ZrO_2$  content (pressure rise experiments at  $20^\circ C$ ).

The reduced permeability towards DMFC species of the  $ZrO_2$  modified composite membranes is believed to derive from the weaker hydrophilicity of the polymer, higher

concentration of rigid backscattering sites and increased tortuous pathways that molecules encounter during permeation due to the presence of inorganic particles [17]. Consequently, the barrier properties of the membranes increases with the ZrO<sub>2</sub> content, which can be assumed as an advantage for DMFC applications because it reduces the reactants loss and increases the overall fuel cell efficiency. Nevertheless, the verified proton conductivity decrease with the incorporation of ZrO<sub>2</sub> should be also taken in account. Finally, according to the results presented for proton conductivity, water uptake and liquid and gas permeability coefficients, it seems that these properties depend on the same transport phenomena.

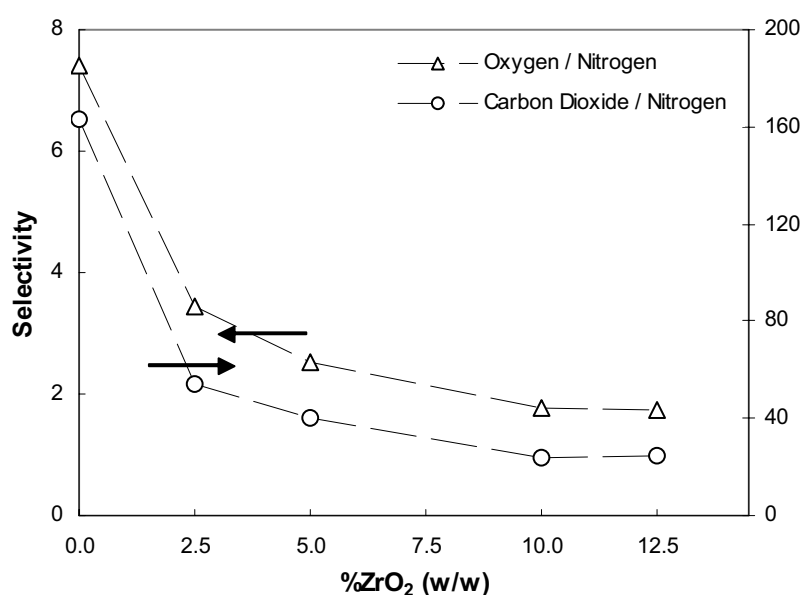


Fig. 4.7. Oxygen/nitrogen and carbon dioxide/nitrogen selectivities of the sPEEK composite membranes as a function of the ZrO<sub>2</sub> content (pressure rise experiments at 20°C).

#### 4.3.4. Microscopy and elemental analysis

Fig. 4.8 shows that the prepared membranes can be considered as homogeneous and dense (composite membrane with 2.5 wt.% ZrO<sub>2</sub>). Higher magnification electron micrograph shows a good adhesion between inorganic domains and the polymer matrix (Fig. 4.9). It can be observed that no cavities are present and that the ZrO<sub>2</sub> particles have dimensions smaller than ~100 nm.

Elemental analysis was performed by XRMF, in order to evaluate the effective incorporation of zirconium oxide on the composite membranes after the preparation procedure (mixing, filtration and casting). The analysis of the elemental content ratios between zirconium and

carbon or sulfur (Fig. 4.10) shows that both ratios increase linearly with the increased zirconium oxide content in the membrane.

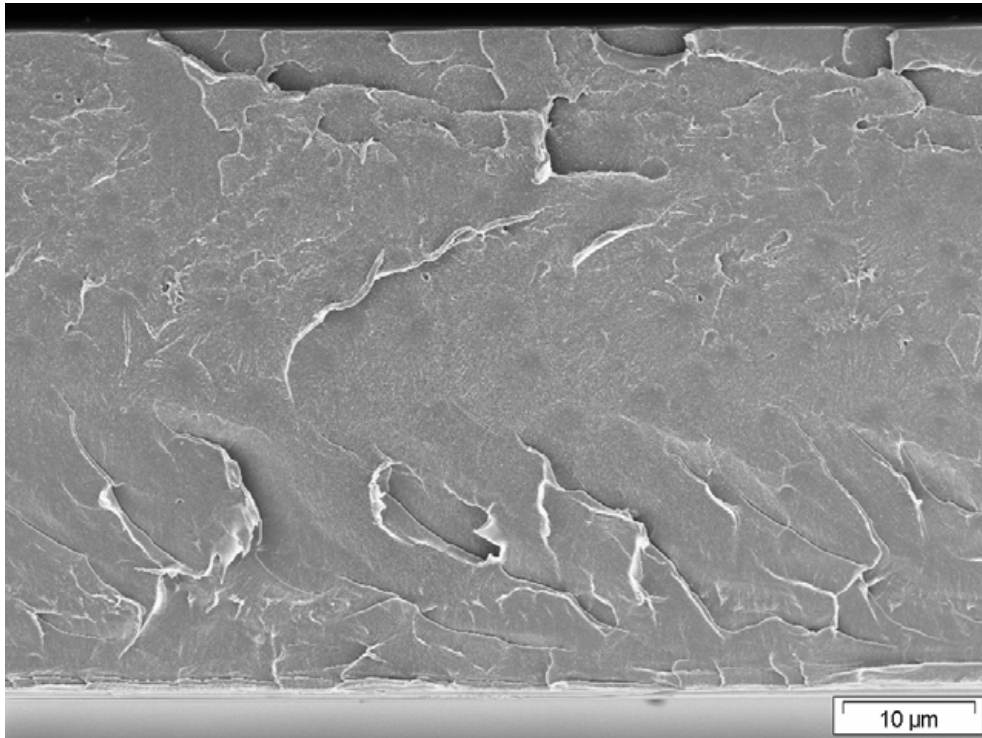


Fig. 4.8. Scanning electron micrograph of sPEEK composite membranes with 2.5 wt.% of ZrO<sub>2</sub>.

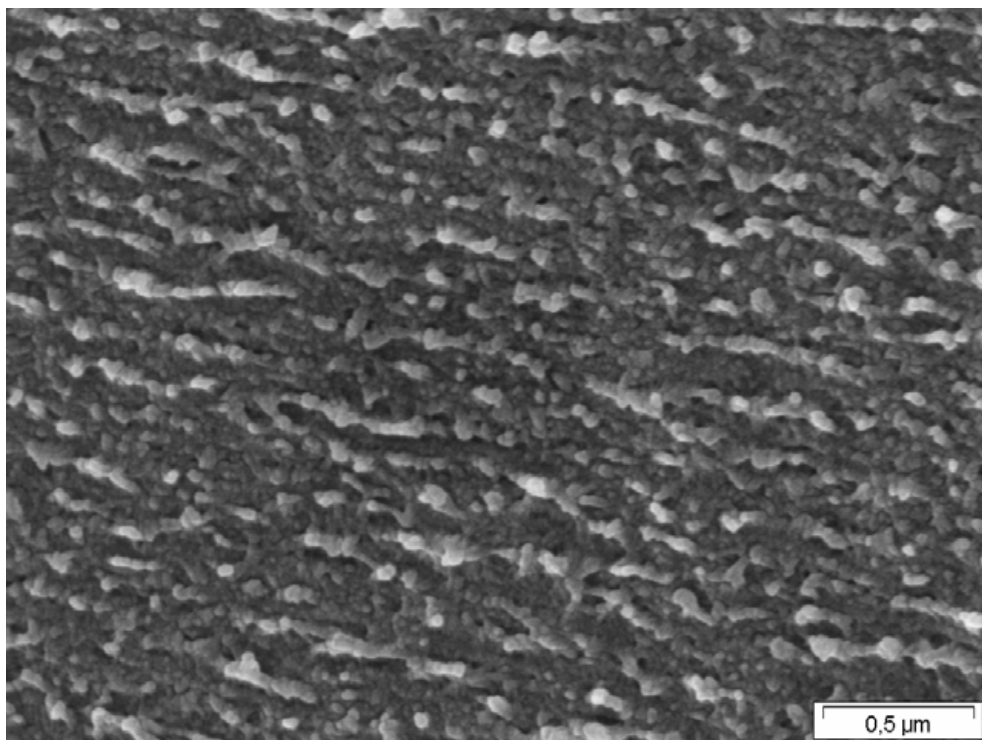


Fig. 4.9. Scanning electron micrograph showing the ZrO<sub>2</sub> particles finely dispersed in the sPEEK composite membrane with 5 wt.% of ZrO<sub>2</sub>.

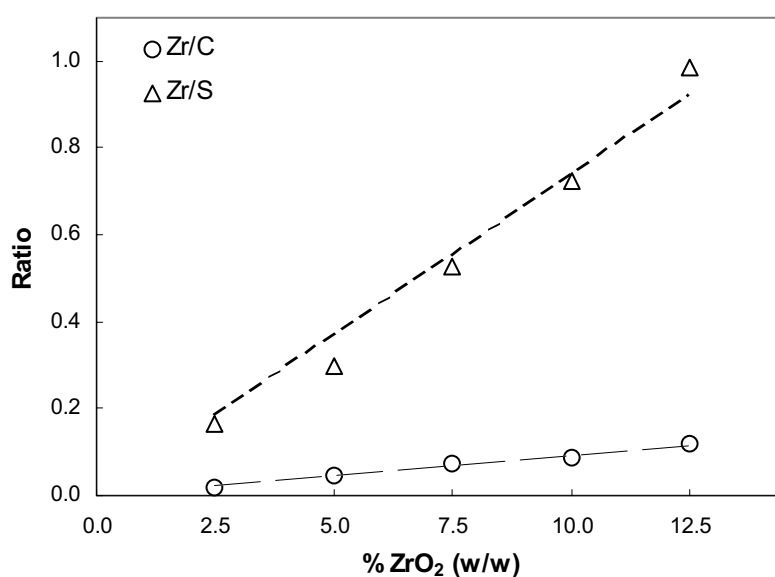


Fig. 4.10. Ratio between zirconium and carbon content of the sPEEK composite membranes as a function of the ZrO<sub>2</sub> content (elemental analysis by X-ray microfluorescence, EDAX).

#### 4.4. Conclusions

Composite membranes have been prepared using sPEEK polymer as organic matrix (SD = 87%) with different contents of zirconium oxide in the inorganic network (2.5, 5.0, 7.5, 10, 12.5 wt.%). Proton conductivity, water uptake, permeability towards species present in DMFC operation (CH<sub>3</sub>OH, H<sub>2</sub>O, N<sub>2</sub>, O<sub>2</sub> and CO<sub>2</sub>), morphology and elemental analysis of each membrane were obtained by standard characterization methods.

The results showed that increasing the zirconium oxide content in the sPEEK composite membranes leads to a decrease of the reactants permeability coefficients (except for nitrogen) and an increase of the water/methanol selectivity. The reason for these results is related with the increasing amount of inorganic filler in the membranes, which increases the membranes barrier properties in terms of mass transport. These features are advantages for the direct methanol fuel cell performance because they prevent reactants loss and increase the PEM long term stability. However, results showed that the zirconium oxide modification has the detrimental effect of decreasing the proton conductivity. The micrographs obtained by scanning electron microscopy showed a good adhesion between inorganic particles domains and the polymer matrix (no cavities) and that the particles have dimensions smaller than ~100 nm. On the other hand, elemental analysis performed by XRMF showed that the elemental content ratios between zirconium and oxygen and sulfur increase in agreement with the increased zirconium oxide amount in the membrane. These

results ensured that even after the complex preparation procedure (among others, filtration and solvent evaporation), the zirconium oxide content varied according to what was planned.

Furthermore, the different contents of zirconium oxide in the sPEEK polymer organic matrix enabled the preparation of composite membranes with a wide range of properties concerning proton conductivity, water uptake and methanol and water permeation. Therefore, these membranes can be used in the future to make a critical evaluation of the relationship between the proton electrolyte membrane properties and the DMFC performance. This will be discussed in the next chapter.

## **Acknowledgements**

Financial support by the HGF-Vernetzungsfonds is gratefully acknowledged. The authors wish to thank M. Schossig-Tiedemann and M. Adherhold for making the microscope analysis and Dr. S. Vetter for sulfonating the poly(ether ether ketone) polymer. The work of Vasco Silva and Hugo Silva was supported by FCT (grants SFRH/BD/6818/2001 and SFRH/3029/2000, respectively). Vasco Silva would like also to acknowledge both FCT and GKSS for the grant assigned for his stay at GKSS Forschungszentrum GmbH. The present work was in part supported by FCT/FEDER projects POCTI/EQU/38075/2001 and POCTI/EQU/45225/2002.

## **References**

- [1] L. Jörissen, V. Gogel, J. Kerres and J. Garche, New membranes for direct methanol fuel cells, *J. Power Sources* 105 (2002) 267.
- [2] C. Manea and M. Mulder, Characterization of polymer blends of polyethersulfone/sulfonated polysulfone and polyethersulfone/sulfonated polyetheretherketone for direct methanol fuel cell applications, *J. Membr. Sci.* 206 (2002) 443.
- [3] F.R. Kalhammer, P.R. Prokopius and V.P. Voecks, Status and prospects of fuel cells as automobile engines, State of California Air Resources Board, California, 1998.
- [4] J. Cruickshank and K. Scott, The degree and effect of methanol crossover in the direct methanol fuel cell, *J. Power Sources* 70 (1998) 40.
- [5] S.M. J. Zaidi, S. D. Mikailenko, G.P. Robertson, M.D. Guiver and S. Kaliaguine, Proton conducting composite membranes for polyether ether ketone and heteropolyacids for fuel cell applications, *J. Membr. Sci.* 173 (2000) 17.

- [6] S.D. Mikhailenko, S.M.J. Zaidi and S. Kaliaguine, Sulfonated polyether ether ketone composite polymer electrolyte membranes, *Catal. Today* 67 (2001) 225.
- [7] T. Kobayashi, M. Rikukawa, K. Sanui and N. Ogata, Proton-conducting polymers derived from poly(ether-etherketone) and poly(4-phenoxybenzoyl-1,4-phenylene), *Solid State Ionics* 106 (1998) 219.
- [8] V. Silva, B. Ruffmann, H. Silva, A. Mendes, M. Madeira and S. Nunes, Zirconium oxide modified sulfonated poly(ether ether ketone) membranes for direct methanol fuel cell applications, *Mater. Sci. Forum* 455-456 (2004) 587.
- [9] M. C. Wijers, Supported liquid membranes for removal of heavy metals, Dissertation, University of Twente, The Netherlands, 1996.
- [10] R. Nolte, K. Ledjeff, M. Bauer and R. Mulhapt, Partially sulfonated poly(arylene ether sulfone) – a versatile proton conducting membrane material for modern energy conversion technologies, *J. Membr. Sci.* 83 (1993) 211.
- [11] B. Ruffmann, H. Silva, B. Schulte and S. Nunes, Organic/inorganic composite membranes for application in DMFC, *Solid State Ionics*, 162-163 (2003) 269.
- [12] G. Alberti, M. Casciola, L. Massinelli and B. Bauer, Polymeric proton conducting membranes for medium temperature fuel cells (110-160°C), *J. Membr. Sci.* 185 (2001) 73.
- [13] S.P. Nunes, B. Ruffmann, E. Rikowsky, S. Vetter and K. Richau, Inorganic modification of proton conductive polymer membranes for direct methanol fuel cells, *J. Membr. Sci.* 203 (2002) 215.
- [14] E. Drioli, A. Regina, M. Casciola, A. Oliveti, F. Tratta and T. Massari, Sulfonated PEEK-WC membranes for possible fuel cell applications, *J. Membr. Sci.* 228 (2004) 139.
- [15] K.A. Mauritz, Organic-inorganic hybrid materials: perfluorinated ionomers as sol-gel polymerization templates for inorganic alkoxides, *Mater. Sci. and Eng. C* 6 (1998) 121.
- [16] K.A. Kreuer, On the development of proton conducting polymer membranes for hydrogen and methanol fuel cells, *J. Membr. Sci.* 185 (2001) 3.
- [17] B. Kumar and J.P. Fellner, Polymer-ceramic composite protonic conductors, *J. Power Sources* 123 (2003) 132.



## Chapter 5. Proton electrolyte membrane properties and direct methanol fuel cell performance, II. Fuel cell performance and membrane properties effects\*

### Abstract

In order to study the relationship between the properties of proton exchange membranes (PEM), obtained through standard characterization methods, and the direct methanol fuel cell (DMFC) performance, inorganic-organic hybrid membranes, modified via *in situ* hydrolysis, were used in a membrane electrolyte assembly (MEAs) for DMFC application. The membranes, the characterization of which was performed in the previous chapter, were based on sulfonated poly(ether ether ketone) (sPEEK) with a sulfonation degree (SD) of 87% and were loaded with different amounts of zirconium oxide (5.0, 7.5, 10.0, 12.5wt.%). The standard characterization methods applied were impedance spectroscopy (proton conductivity), water uptake, and pervaporation (permeability to methanol). The MEAs were characterized investigating the DMFC current-voltage polarization curves, constant voltage current (CV, 35mV), and open circuit voltage (OCV). The fuel cell ohmic resistance (null phase angle impedance, NPAI) and CO<sub>2</sub> concentration at the cathode outlet were also measured. The characterization results show that the incorporation of the inorganic oxide in the polymer network decreases the DMFC current density for CV experiments, CO<sub>2</sub> concentration at the cathode outlet for both OCV and CV experiments and, finally, the maximum power density output. The opposite effect was verified in terms of the NPAI (ohmic resistance) for both OCV and CV experiments. A good agreement was found between the studied DMFC performance parameters and the characterization results evaluated by impedance spectroscopy, water uptake and pervaporation experiments.

\*V.S. Silva, J. Schirmer, R. Reissner, B. Ruffmann, H. Silva, A. Mendes, L.M. Madeira and S.P. Nunes, *J. Power Sources* 140 (2005) 41.

## 5.1. Introduction

Liquid feed direct methanol fuel cells (DMFCs) operating at low temperatures and employing solid protonic electrolytes are promising candidates for portable power applications. DMFCs do not require fuel processing, allowing simple and compact designs. Apart from that, the use of methanol as fuel for portable applications has several advantages in comparison with hydrogen. In order to be competitive within the portable power applications market, the DMFC must be economical and capable of delivering high power densities [1]. Recent reports demonstrated a relatively high DMFC performance using solid polymer electrolytes such as Nafion<sup>®</sup> [2-7]. However, the use of perfluorinated membranes as polymer electrolyte increases appreciably the cost of the entire system [8-10]. Apart from the cost disadvantage, the use of Nafion<sup>®</sup>-like polymer electrolyte leads to a significant decrease in the fuel cell Faraday efficiency due to the methanol crossover from the anode to the cathode. Methanol uses cathode Pt sites (reducing the effective area of the cathode) for the direct reaction between methanol and oxygen, generating a mixed potential that reduces the cell voltage [11, 12]. However, these problems can be mitigated by developing new polymers, or modifying the existing ones, in order to achieve high ionic conductivity, low permeability to DMFC reactants, long-term stability under operating conditions and, not less important, low cost. Nowadays, non-perfluorinated polymers are being investigated by different groups [13-18]. Apart from the possibility of being directly applied to the DMFC, these polymers can be used as a polymeric matrix for organic/inorganic modifications, so that the properties of the final proton exchange membranes can be improved [15, 16, 19-21].

In order to select the proper material for direct methanol fuel cell applications, characterization methods play an important role in DMFC research. Ideally, the obtained characteristics of the specific material can be used as a selection criterion: they should allow us to forecast the corresponding DMFC performance. For example, instead of conducting DMFC experiments, the results of some characterization methods can be used to estimate the fuel cell performance for a given membrane. At present, several characterization methods are used to obtain critical parameters for DMFC application [21].

The three main characteristics considered by the standard characterization methods are (Fig. 5.1):

- Proton conductivity: gives an estimate of the H<sup>+</sup> conductivity, which is the main function of a proton exchange membrane. This property is usually evaluated with acid or water electrolytes (hydrated membranes) by impedance spectroscopy [14, 15, 18-30].

- Membrane permeability to methanol: the study of the methanol mass transport through DMFC membranes is very common due to its detrimental effect on the DMFC performance (reduced Faraday efficiency). Even if not accounting for the anode catalytic reaction and the electro-osmotic drag mass transfer, the permeability is usually evaluated by pervaporation [20, 21, 26-28] and diffusion cell experiments [29-31].
- Water swelling: gives a measure of the water solubility in the membrane. It is usually associated to improved proton conductivity but also to an increase in methanol crossover and morphological instability. Is usually evaluated using batch experiments in liquid solutions at room temperature [14, 15, 19-21, 27-29, 32].

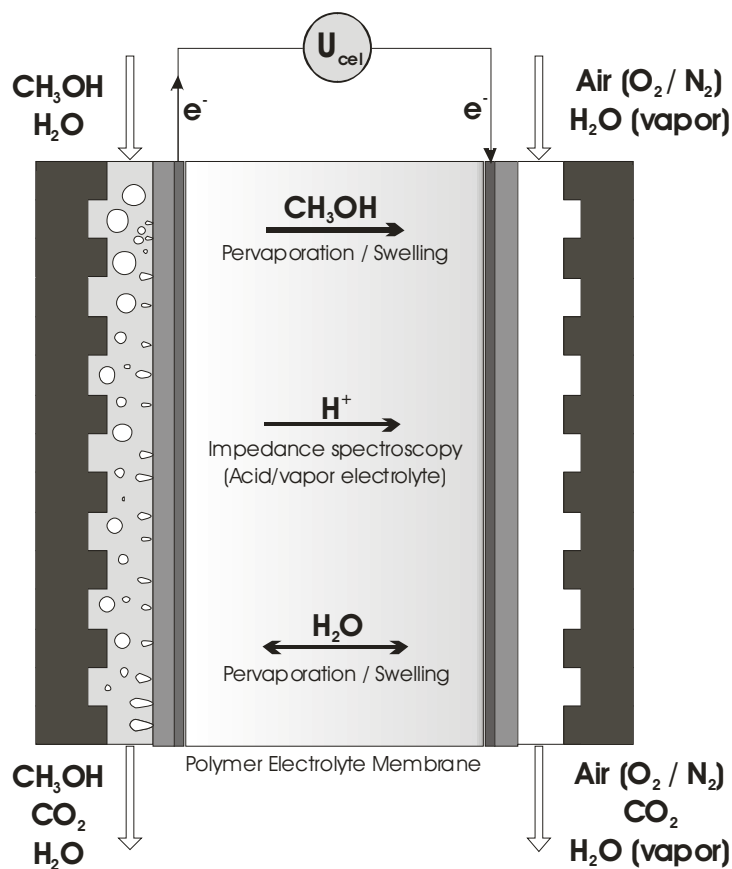


Fig. 5.1. Sketch of a DMFC illustrating proton, water and methanol permeation across the PEM and related characterization methods.

The lack of a systematic study that relates the membrane properties and the fuel cell energy output disables the validation of the characterization results, in terms of the fuel cell performance. Several DMFC research groups published promising data for new materials [14, 15, 18, 20, 21, 26-28]. However, a critical evaluation of the membrane properties implications in the direct methanol fuel cell performance is an important task to be done.

In this chapter we perform an analysis of the effect of the membrane properties on the DMFC performance for temperatures up to 90°C. We were able to prepare composite membranes with a wide variety of physical/chemical properties using a systematic variation of the inorganic content in the sulfonated poly(ether ether ketone) polymer (from 2.5 to 12.5wt.% of ZrO<sub>2</sub>) [33]. The incorporation of zirconium oxide in this polymer enabled the preparation of composite membranes with gradual decrease in water swelling, proton conductivity and permeability towards methanol and water [33]. Apart from taking advantage of the improved barrier properties of the composite membranes, the ZrO<sub>2</sub> incorporation enables also the preparation of membranes with improved morphological stability for DMFC application at temperatures up to 90°C, although using a sPEEK polymer with high sulfonation degree (higher proton conductivity). From the previous chapter results, the selected characterization methods for the analysis of the membrane properties effects were: impedance spectroscopy (proton conductivity and proton transport resistance), pervaporation (permeability to methanol) and water swelling. The proton transport resistance measures the specific resistance of the membrane with respect to proton transport (previous chapter). The aim of this study is to identify and study the main characterization parameters for DMFC research. These parameters should enable the right selection of materials for DMFC application purposes, by providing a first estimate of the corresponding fuel cell performance.

## 5.2. Experimental

The membrane electrode assemblies (MEAs) were prepared by hot pressing the membrane samples between two Etek<sup>®</sup> ELAT electrodes. Supported PtRu (1 mg/cm<sup>2</sup> 30wt.% PtRu (1:1) on carbon with 0.7 mg/cm<sup>2</sup> Nafion<sup>®</sup>/PTFE) and Pt (0.4 mg/cm<sup>2</sup> 20wt.% Pt on carbon with 0.7 mg/cm<sup>2</sup> Nafion<sup>®</sup>/PTFE) were used as anode and cathode electrodes, respectively. The membranes were humidified in water for 1 minute and then pressed with the electrodes at 100°C and 79 bar for 2 minutes. The DMFC experimental set-up is described elsewhere [34]. The MEAs (active cell area of 25 cm<sup>2</sup>) were conditioned at room temperature by feeding with an aqueous 0.25M methanol solution (4ml/min, 2.5bar) on the anode side and humidified air (600 sccm/min, 3 bar, 100% relative humidity) on the cathode side for two hours, and then operated with an aqueous 1.5M methanol solution (4ml/min, 2.5bar) on the anode side and humidified air (600sccm/min, 3bar, 100% relative humidity) on the cathode side. The cell temperature was varied from 40°C to 110°C. The MEAs' characterization was performed measuring the DMFC current-voltage polarization curves, constant voltage current (CV, 35mV), and open circuit voltage (OCV). The applied

procedures used in the MEAs' characterization are described elsewhere [34]. The last two parameters investigated also included the measurement of the cell impedance (null phase angle impedance, NPAI) and CO<sub>2</sub> concentration. The NPAI and CO<sub>2</sub> concentration at the cathode outlet were monitored as a measure of the MEA ohmic resistance and methanol crossover during DMFC operation, respectively [35]. In the present study only results from the first day were investigated.

The sPEEK (SD = 87%) membranes with zirconium oxide contents lower than 10.0wt.% were found to be stable at temperatures up to 90°C, despite having a high sulfonation polymer. For higher ZrO<sub>2</sub> contents, the thermal stability was even better. Therefore, in agreement with recent data [19, 33], these results show effectively that the zirconium oxide incorporation via *in situ* hydrolysis increases the chemical/thermal stability of the composite membranes. The thickness of the membranes used was between 100 and 150 μm (membranes with 5.0, 7.5, 10.0 and 12.5 wt.% of ZrO<sub>2</sub>: 113, 150, 108 and 100 μm, respectively). It is expected that the membranes thickness should influence the measurements in the fuel cell giving a lower current for 35mV, higher OCV, higher impedance and lower methanol permeation for a thicker membrane. The hybrid sPEEK membrane with 2.5wt.% of ZrO<sub>2</sub> was not studied because it proved to be unstable in methanol aqueous solutions due to its excessive swelling [33].

## 5.3. Results and discussion

### 5.3.1. DMFC performance

The current density-voltage and current density-power density plots of MEAs made from sPEEK composite membranes with 5.0, 7.5 and 10.0wt.% of ZrO<sub>2</sub> at different temperatures are shown in Fig. 5.2. The curves corresponding to the hybrid membrane with 12.5wt.% ZrO<sub>2</sub> are not presented because they could not be measured due to the high ohmic resistance of the corresponding MEA. From Fig. 5.2, it can be seen that the membrane with 5.0wt.% of ZrO<sub>2</sub> presents the best DMFC performance among all the studied MEAs. For 90°C, the 5.0wt.% ZrO<sub>2</sub> composite membrane achieves a maximum power density output of 16.4mW/cm<sup>2</sup> for a current density of 109.2mA/cm<sup>2</sup>. In comparison, for the same temperature, the 7.5wt.% zirconium oxide modified membrane achieves an output value of 8.0mW/cm<sup>2</sup> for 32.1 mA/cm<sup>2</sup>. On the other hand, due to its high ohmic resistance, the DMFC using a 10.0wt.% ZrO<sub>2</sub> composite membrane only provided a polarization curve at 110°C and a maximum power density of 2.7mW/cm<sup>2</sup> was achieved for a current density of 17.8mA/cm<sup>2</sup>.

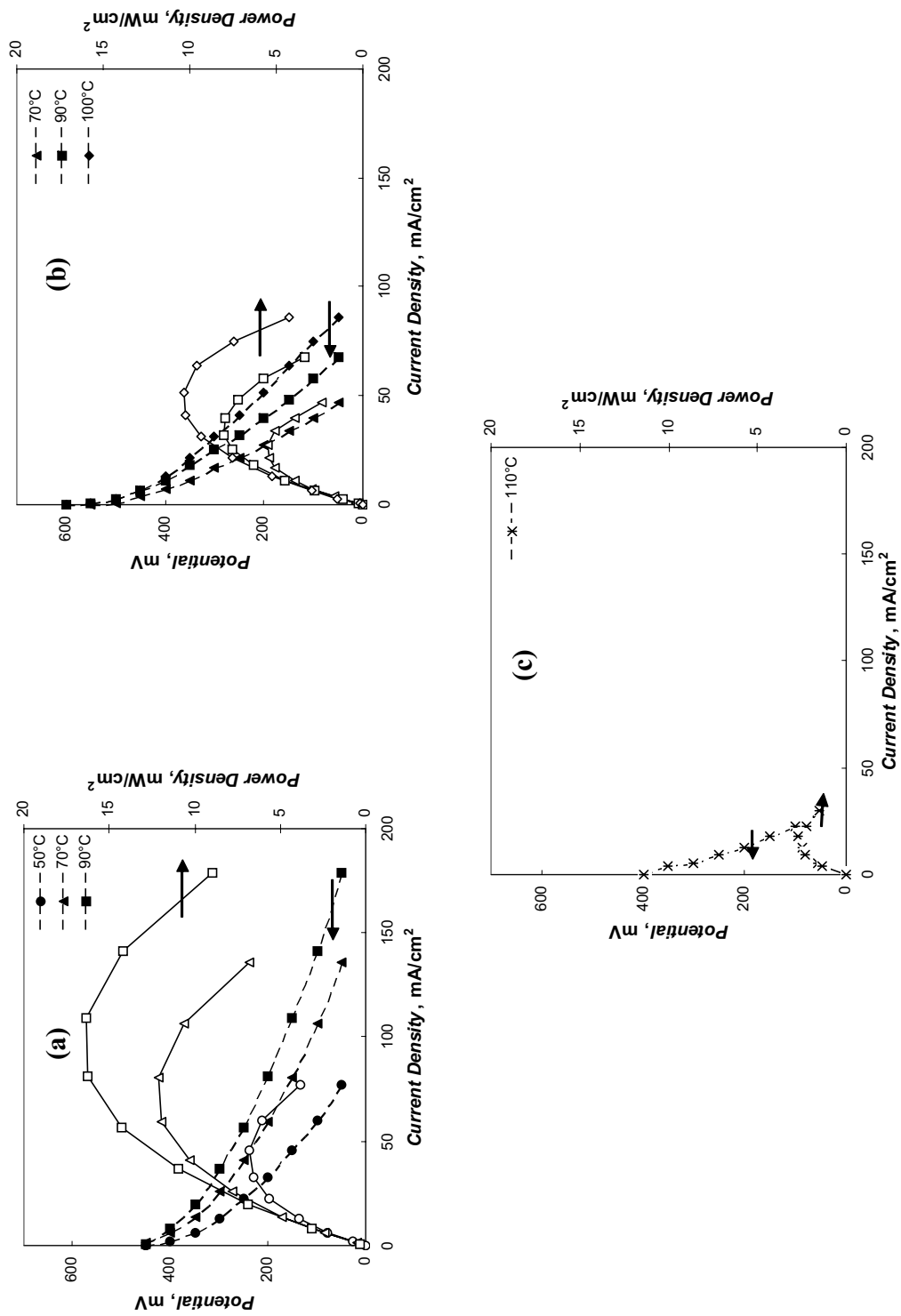


Fig. 5.2. Current density-voltage and power density plots of the DMFC using sPEEK composite membranes with: a) 5.0, b) 7.5 and c) 10wt.%ZrO<sub>2</sub>.

Apart from measuring the current density-voltage polarization curves, in the present study the current density, null phase angle impedance (NPAI) and CO<sub>2</sub> cathode outlet concentration were also evaluated for constant voltage (CV) experiments at 35mV (Fig. 5.3). It can be seen that the cell current density (Fig. 5.3b) and CO<sub>2</sub> cathode outlet concentration (Fig. 5.3c) decrease when increasing the sPEEK zirconium oxide content. The opposite effect can be seen for the NPAI (Fig. 5.3a), i.e., the ohmic resistance of the MEAs increases with the amount of ZrO<sub>2</sub> in the polymer matrix. This means that hybrid membranes with higher ZrO<sub>2</sub> contents present lower permeability towards protons and methanol, increasing the MEAs ohmic resistance (NPAI) and reducing both DMFC output current and CO<sub>2</sub> concentration at the cathode outlet, in good agreement with the characterization data obtained previously [33].

Analogous results were found for open circuit voltage (OCV) experiments in terms of NPAI (Fig. 5.4a) and CO<sub>2</sub> concentration at the cathode outlet (Fig. 5.4c). However, the open circuit potential seems to show a maximum value for the hybrid membrane with 7.5wt.% ZrO<sub>2</sub> (Fig. 5.4b). This should happen due to the direct relationship between OCV and the methanol crossover and membrane ohmic resistance [11, 12]. During OCV experiments, the concentration of methanol at the anode-membrane interface is maximal because no methanol is being consumed (no current output). Consequently, the methanol crossover is higher due to a larger mass transfer gradient across the membrane, making the detrimental effect of the methanol crossover more noticeable for OCV experiments [38]. Thus, the 5.0wt.% ZrO<sub>2</sub> membrane presents lower OCV than that of the 7.5wt.% because it has a higher methanol crossover [33]. The OCV increase should continue for higher ZrO<sub>2</sub> contents. However the measurements of the open cell voltage cannot be conducted without any cell current flowing. Because for both 10.0 and 12.5wt.% ZrO<sub>2</sub> hybrid membranes, the ohmic resistance increases a lot with the amounts of inorganic incorporation (proton conductivity near zero [33]), the very small current flowing during the OCV measurement is sufficient to give a high voltage loss and consequently, OCV decreases.

In summary, from the DMFC characterization results it can be observed that even having a high methanol crossover and, consequently, higher CO<sub>2</sub> concentration at the cathode, the sPEEK inorganically modified membrane with 5.0wt.% ZrO<sub>2</sub> presents the best DMFC performance among the studied membranes, in terms of output energy, mainly due to its high proton conductivity. However, as mentioned before, this membrane turned out to be the least stable one.

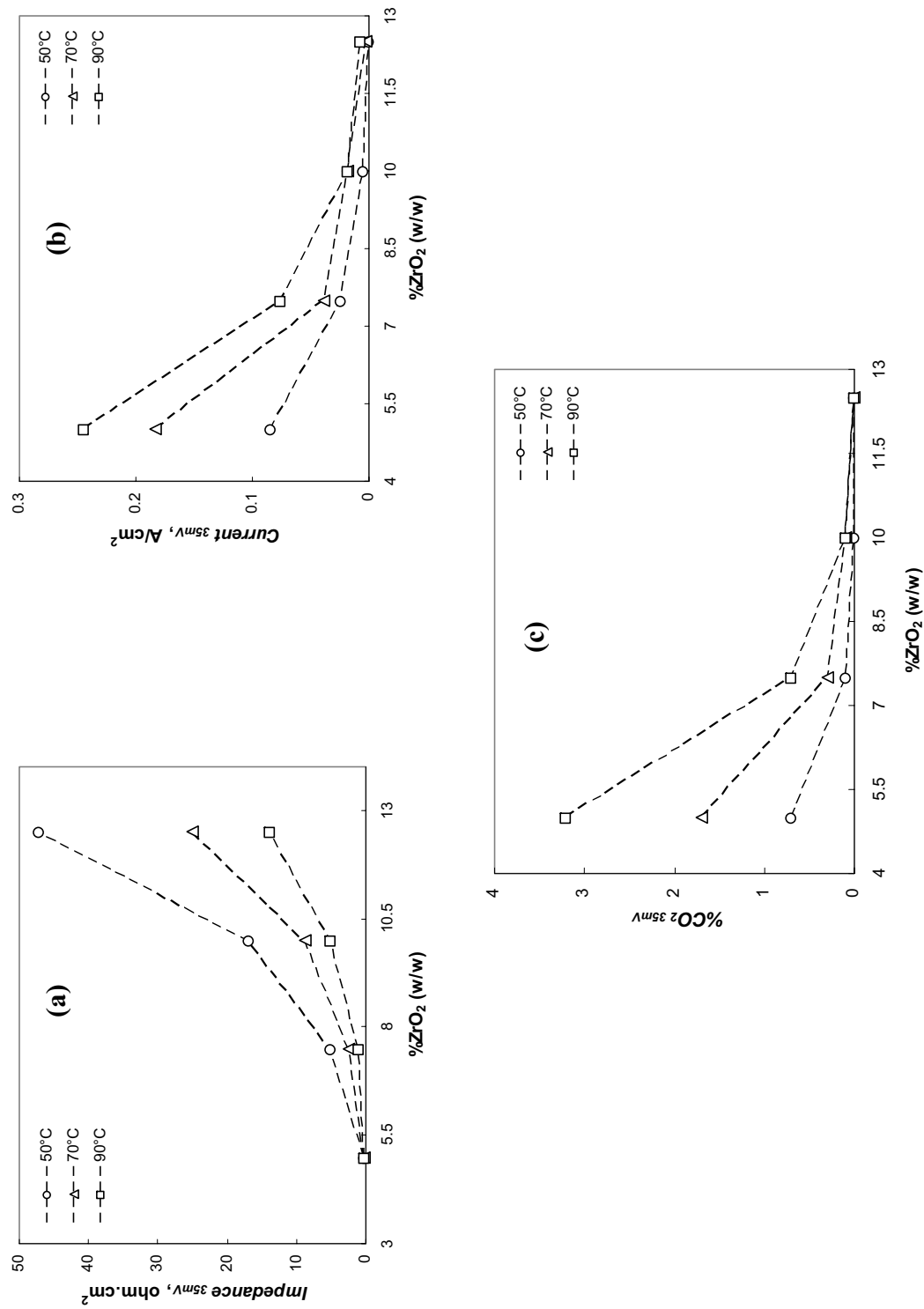


Fig. 5.3. Null phase angle impedance (a), current density (b) and CO<sub>2</sub> concentration at the cathode outlet (c) for constant voltage DMFC experiments (35mV) as a function of the ZrO<sub>2</sub> content.

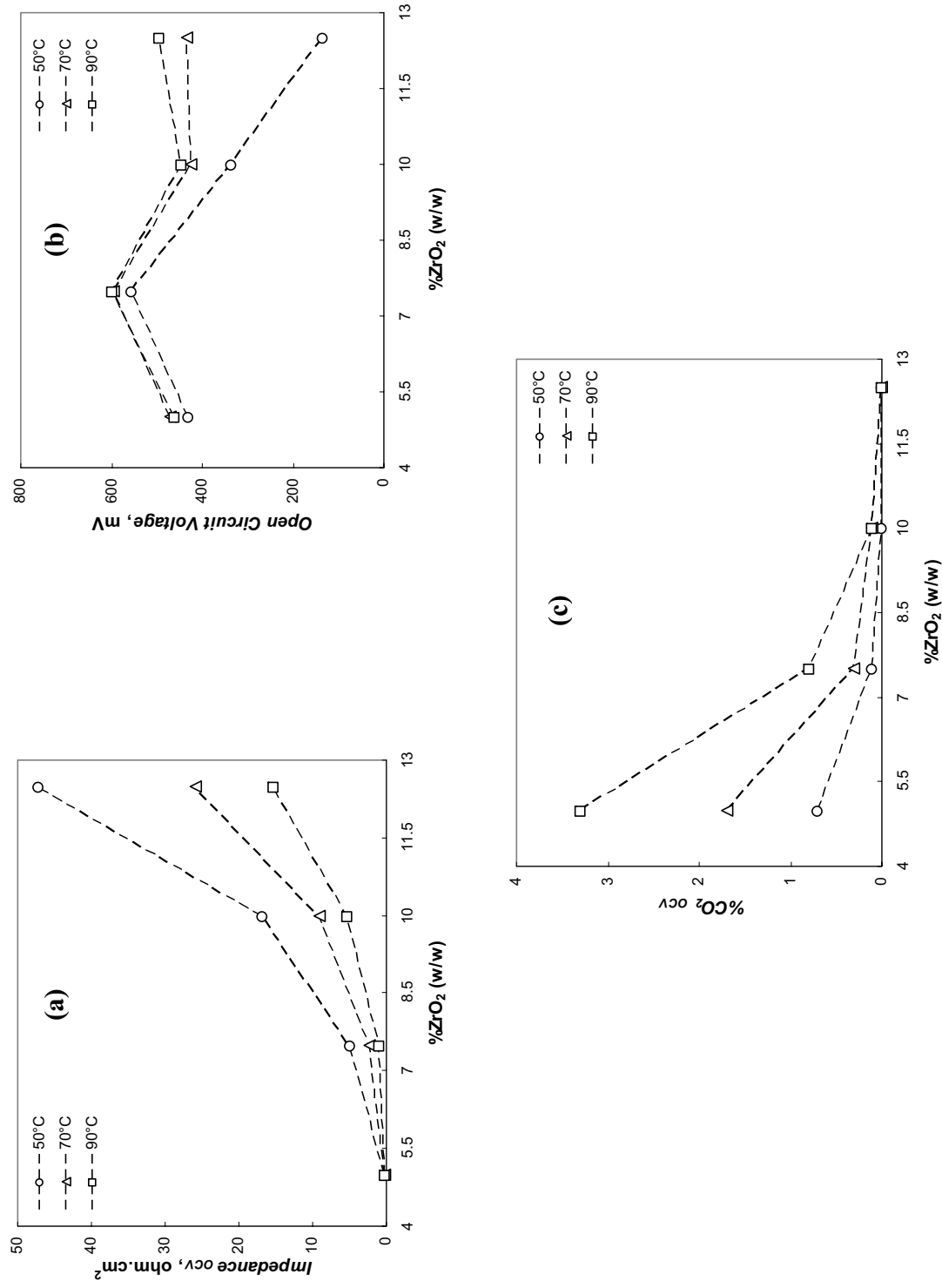


Fig. 5.4. Null phase angle impedance (a), voltage (b) and CO<sub>2</sub> concentration at the cathode outlet (c) for open circuit DMFC experiments as a function of the ZrO<sub>2</sub> content.

### 5.3.2. Membranes characterization results versus DMFC performance

In Fig. 5.5 the output current for CV experiments (35mV) is plotted as a function of the proton conductivity, evaluated in the acid electrolyte cell (25°C). It can be verified that for values lower than 75 mS/cm, current increases slightly with proton conductivity. In comparison, higher values of proton conductivity lead to a strong increase in the DMFC current output (Fig. 5.5).

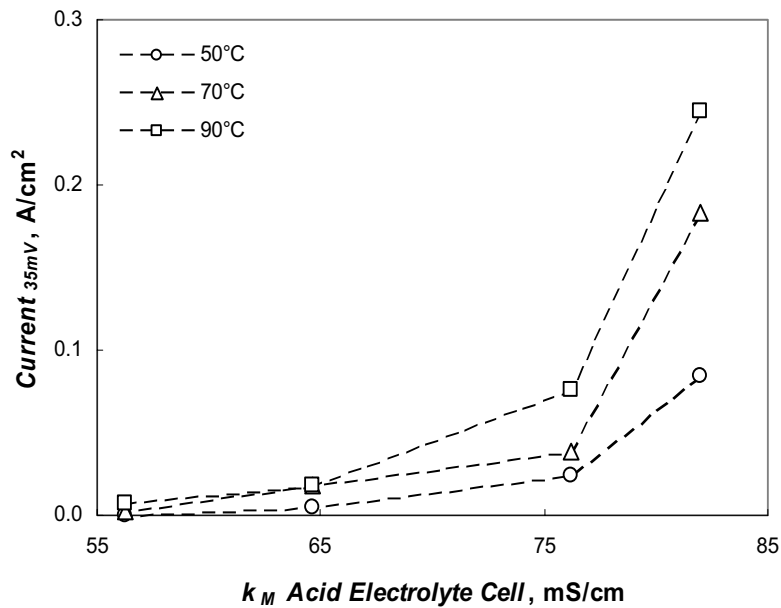


Fig. 5.5. DMFC current density for constant voltage experiments (35mV) as a function of proton conductivity evaluated in the acid electrolyte cell (25°C).

In terms of the null phase angle impedance variation as a function of the proton transport resistance, evaluated in the acid electrolyte cell (Fig. 5.6), it seems that the DMFC resistance increases with the proton transport resistance, as expected.

On the other hand, for the output current density plot versus the membrane proton conductivity, evaluated in the cell using water vapor (Fig. 5.7), an analogous variation as noticed in Fig. 5.5 is observed for higher conductivities (strong current output increase), although the effect is not as pronounced as for the previous cell. Furthermore, for this cell the NPAI also increases with the proton transport resistance (Fig. 5.8). In general, the impedance spectroscopy in acid and vapor electrolytes seems to be a good criterion for selecting the right membranes for DMFC use. It seems that improved DMFC performance in terms of energy output occurs (current density) for conductivities above 75 and 20mS/cm in the acid and vapor electrolyte cells, respectively. For the

studied membranes, proton conductivities lower than these values lead to poor DMFC performance.

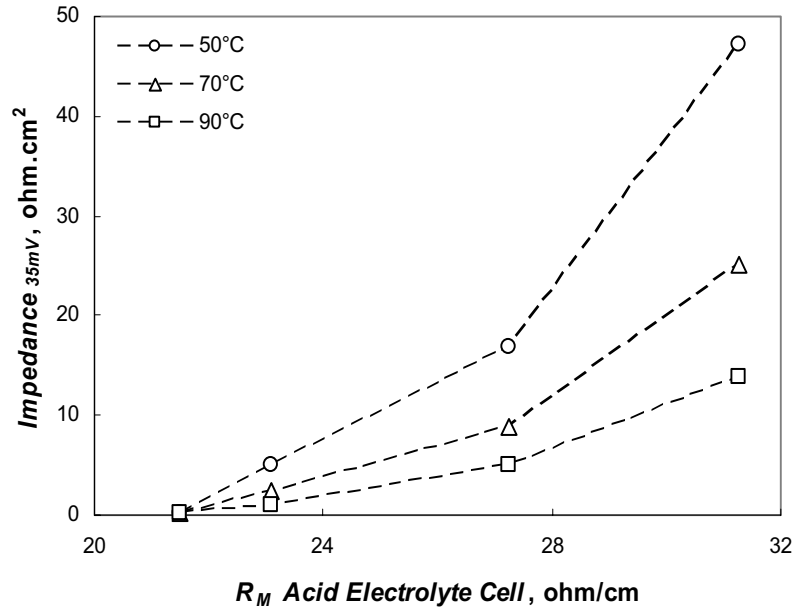


Fig. 5.6. DMFC null phase angle impedance for constant voltage experiments (35mV) as a function of proton transport resistance evaluated in the acid electrolyte cell (25°C).

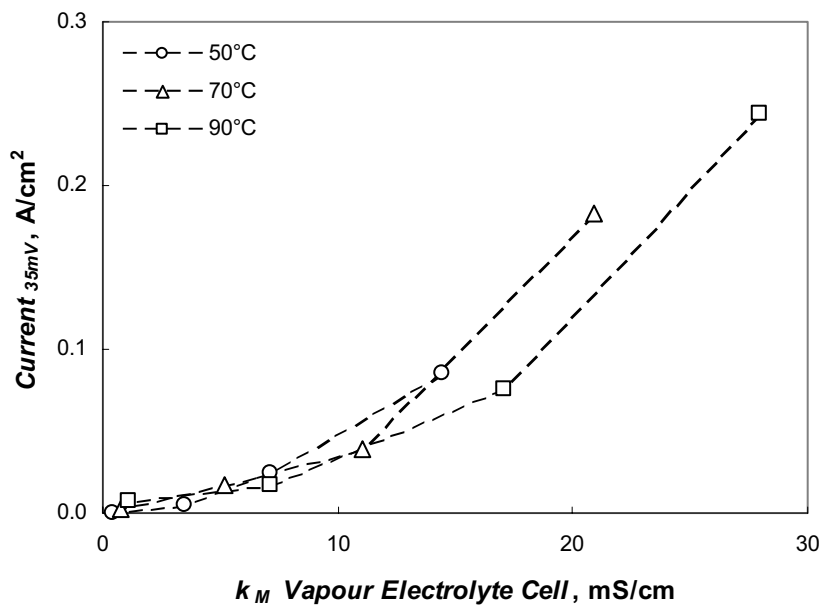


Fig. 5.7. DMFC current density for constant voltage experiments (35mV) as a function of proton conductivity evaluated in the vapor cell (50, 70 and 90°C).

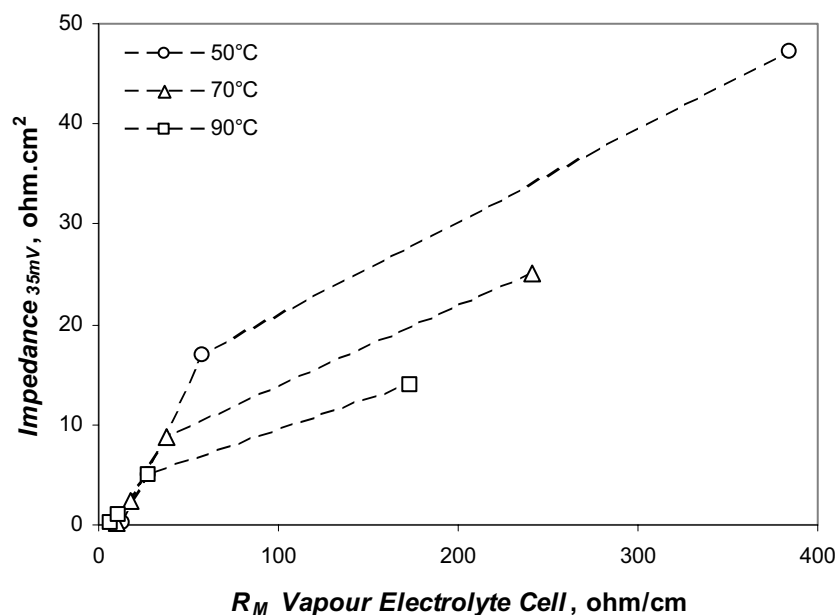


Fig. 5.8. DMFC null phase angle impedance for constant voltage experiments (35mV) as a function of proton transport resistance evaluated in the vapor cell (50, 70 and 90°C).

In the particular case of the water uptake characterization method, Fig. 5.9 demonstrates that the electric current density, for experiments performed at 35mV, increases almost linearly with the water uptake (room temperature), showing that this characterization method is well related with such DMFC output. In contrast, the DMFC ohmic resistance seems to vary in a distinct way with the proton exchange membranes' water uptake (Fig. 5.9). Low values for the membrane water uptake result in a strong increase in the NPAI while higher amounts of sorbed water seem to affect slightly the ohmic resistance.

The carbon dioxide concentration at the cathode outlet was monitored as a measure of the methanol loss through the membrane during the fuel cell operation. Assuming that all methanol transferred to the cathode is oxidized to  $\text{CO}_2$ , the amount of methanol permeation can be calculated. This procedure neglects the unreacted methanol in the cathode (especially for lower temperatures) and the  $\text{CO}_2$  permeation through the membrane. The unreacted methanol at the cathode outlet would mean that the methanol permeation value calculated from the  $\text{CO}_2$  content would be too low. In contrast, the  $\text{CO}_2$  permeation from the anode to the cathode would mean higher concentrations of  $\text{CO}_2$  at the cathode outlet and, therefore, the calculated methanol permeation value would be too high. Even considering different membranes and using the same electrodes and the same operating conditions, the relative methanol permeation calculated from the  $\text{CO}_2$  content at the cathode outlet can be used for comparison.

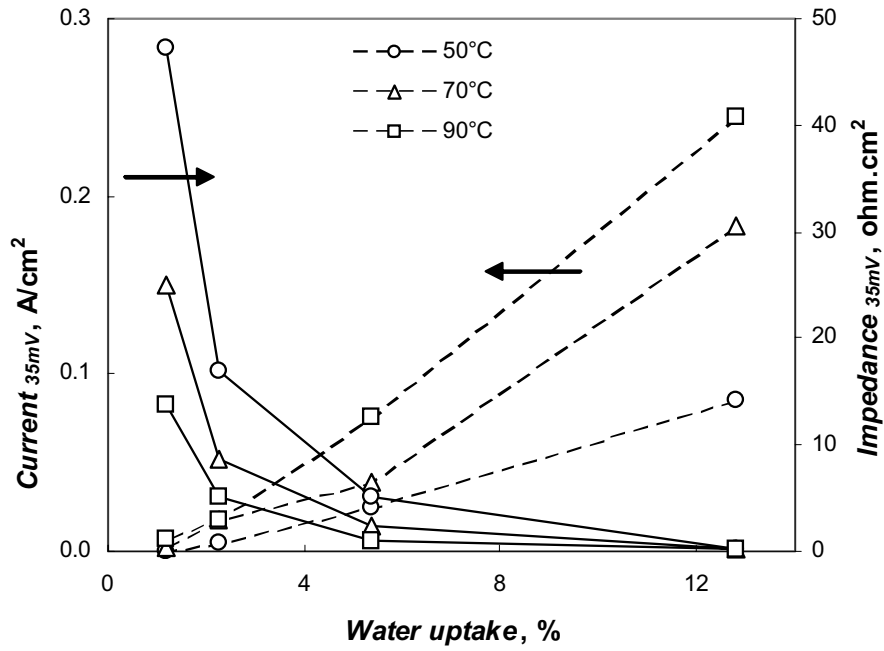


Fig. 5.9. DMFC current density and null phase angle impedance for constant voltage experiments (35mV) as a function of water uptake evaluated by batch experiments (room temperature).

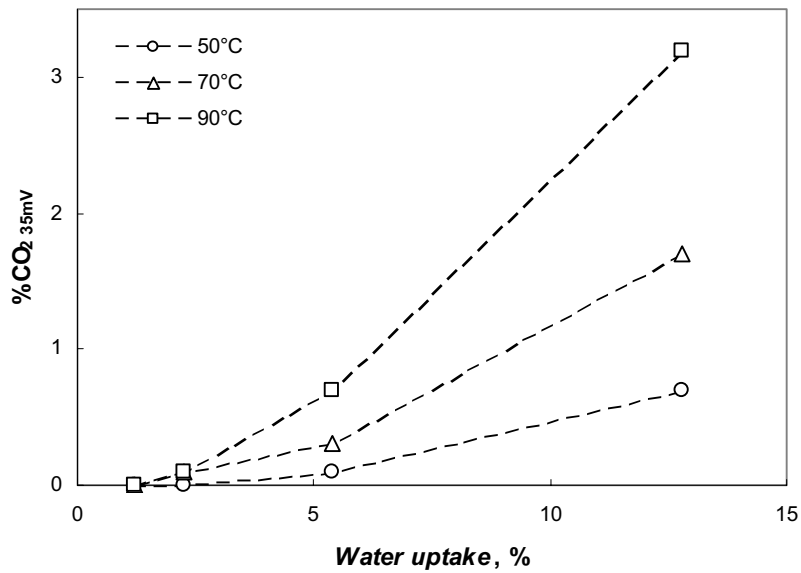


Fig. 5.10. Carbon dioxide concentration (%) at the cathode outlet for constant voltage experiments (35mV) as a function of water uptake evaluated by batch experiments (room temperature).

Good agreement is found between the  $\text{CO}_2$  concentration at the cathode outlet and the water uptake (Fig. 5.10). The global analysis of these results shows the important role that sorbed water in the membrane plays in DMFC performance. It seems that sorbed water improves the DMFC energy output because it increases the membrane conductivity by assisting the proton transfer in the polymer hydrated microstructure [16]. However, it leads also to increased methanol crossover and, consequently, lower total efficiency with increased fuel loss and cathode depolarization [35-37].

Finally, in terms of the membrane permeability towards methanol, obtained by pervaporation experiments at  $55^\circ\text{C}$ , it can be seen that it is in agreement with the  $\text{CO}_2$  concentration at the cathode outlet (Fig. 5.11). For the lowest temperature ( $50^\circ\text{C}$ ), it seems that the  $\text{CO}_2$  concentration increases almost lineally with the methanol permeability coefficient. In contrast, for both  $70$  and  $90^\circ\text{C}$ , the values for the highest methanol permeation are not as high as expected for a linear curve. This could mean that either the methanol transfer through the membrane is so high that it cannot be completely converted to  $\text{CO}_2$ , or so much methanol is consumed in the anode that the concentration gradient from anode to cathode and hence the methanol permeation is lower. In general, it can be assumed that even without accounting for the anode catalytic reaction and the electro-osmotic drag mass transfer, the permeability coefficients evaluated by pervaporation experiments are in good agreement with methanol crossover (Fig. 5.11).

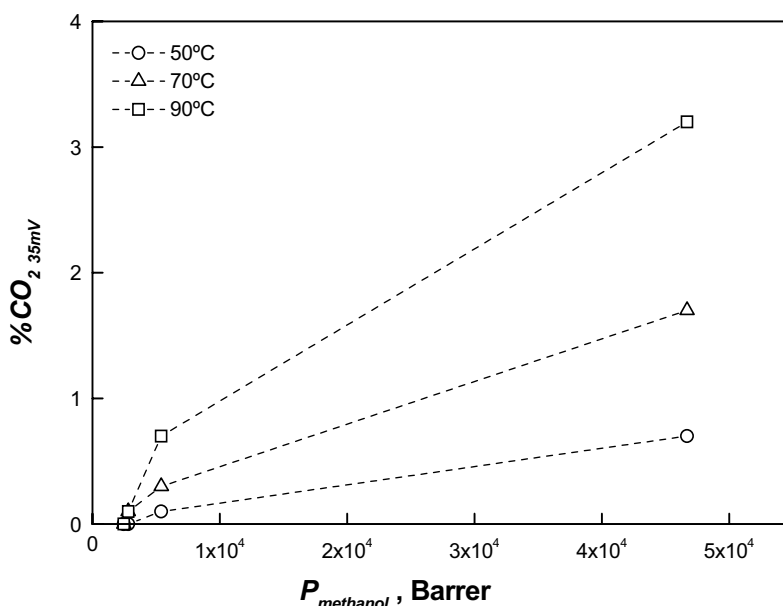


Fig. 5.11. Carbon dioxide concentration (%) at the cathode outlet for constant voltage experiments (35mV) as a function of the methanol permeability coefficient evaluated by pervaporation experiments ( $55^\circ\text{C}$ ).

As a whole, from the present study, it can be seen that characterization methods such as impedance spectroscopy, water uptake and pervaporation experiments can be used effectively for selecting the appropriate materials for DMFC application purposes and for estimating the fuel cell performance.

## 5.4. Conclusions

In order to perform a critical analysis of the relationship between the results obtained from characterization methods and DMFC performance, several hybrid membranes based on sPEEK polymer (SD = 87%) with different contents of zirconium oxide (5.0, 7.5, 10, 12.5wt.%) were evaluated in a DMFC bench test. The selected characterization methods for the analysis were impedance spectroscopy (proton conductivity), pervaporation (permeability to methanol) and water swelling. The DMFC characterization consisted in investigating the current-voltage polarization curves, constant voltage current (CV, 35mV), and open circuit voltage (OCV).

The results showed that increasing the zirconium oxide content in the sPEEK composite membranes leads to a decrease in the DMFC current density for CV experiments, CO<sub>2</sub> concentration at the cathode exhaust for both OCV and CV experiments and, finally, maximum power density output. The opposite effect was verified in terms of the NPAI (ohmic resistance). Bench test results showed also that the sPEEK based hybrid membrane with 7.5wt.% ZrO<sub>2</sub> presents the highest open circuit potential due to its better ratio between methanol crossover and ohmic resistance in comparison with the other studied membranes. With respect to the validation of the characterization methods, results showed a co-current variation between proton conductivity, evaluated by impedance spectroscopy (acid electrolyte and water vapor cells), and DMFC output current density. The same behavior was observed regarding the proton transport resistance, evaluated in characterization cells, and the DMFC null phase angle impedance for CV experiments. A strong increase of the output current density for conductivities higher than 75 and 20mS/cm was found in the acid electrolyte and vapor cells, respectively. On the other hand, an almost linear variation was detected between the water uptake and the DMFC output current density for CV experiments. The fuel cell ohmic resistance seems to increase strongly for membranes with low water uptake, while it is almost independent for higher values of this property. Finally, our results showed a good agreement between the membranes' methanol permeability coefficients obtained by pervaporation experiments and the CO<sub>2</sub> concentration at the cathode outlet.

The present chapter shows that characterization results obtained by impedance spectroscopy, water uptake and pervaporation experiments can be used as critical parameters for the selection of proton electrolyte membranes for DMFC application purposes.

## **Acknowledgements**

Financial support by the HGF-Vernetzungsfonds is gratefully acknowledged. The work of Vasco Silva and Hugo Silva was supported by FCT (Grants SFRH/BD/6818/2001 and SFRH/3029/2000, respectively). Vasco Silva would also like to acknowledge both FCT and GKSS for the grant assigned for his stay at GKSS Forschungszentrum GmbH. The present work was partially supported by FCT/FEDER projects POCTI/EQU/38075/2001 and POCTI/EQU/45225/2002.

## **References**

- [1] A. S. Aricò, S. Srinivasan and V. Antonucci, DMFCs: From fundamental aspects to technology development, *Fuel Cells* 1 (2001) 133.
- [2] C. Lamy, J. M. Leger and S. Srinivasan, in: J.O'M. Bockris, B. E. Conway, R. E. White (Eds.), *Direct methanol fuel cells: From a twentieth century electrochemist's dream to a twenty-first century emerging technology. Modern aspects of electrochemistry*, Vol. 34, Kluwer Academic Publishers/Plenum Press, Dordrecht/New York, 2001, 33.
- [3] X. Ren, M. S. Wilson and S. Gottesfeld, High performance direct methanol polymer electrolyte fuel cells, *J. Electrochem. Soc.* 143 (1996) L12.
- [4] P. Argyropoulos, K. Scott and W. M. Taama, One-dimensional thermal model for direct methanol fuel cell stacks: Part II. Model based parametric analysis and predicted temperature profiles, *J. Power Sources* 79 (1999) 184.
- [6] F.R. Kalhammer, P.R. Prokopius and V.P. Voecks, *Status and prospects of fuel cells as automobile engines*, State of California Air Resources Board, California, 1998.
- [7] E.S. Steigerwalt, G.A. Deluga, D.E. Cliffler and C.M. Lukehart, A Pt-Ru/graphitic carbon nanofiber nanocomposite exhibiting high relative performance as a direct-methanol fuel cell anode catalyst, *J. Phys. Chem. B* 105 (2001) 8097.

- [8] C. Yang, S. Srinivasan, A. S. Aricò, P. Creti, V. Baglio and V. Antonucci, Composite nafion/zirconium phosphate membranes for direct methanol fuel cell operation at high temperature, *Electrochem. Solid State Lett.* 4 (2001) A31.
- [9] B.D. McNicol, D. A. J. Rand and K. R. Williams, Direct methanol–air fuel cells for road transportation, *J. Power Sources* 83 (1999) 15.
- [10] S. Wasmus and A. Kluver, Methanol oxidation and direct methanol fuel cells: a selective review, *J. Electroanal. Chemistry* 461 (1999) 150.
- [11] J.-T. Wang, S. Wasmus and R.F. Savinell, Real-time mass spectrometric study of the methanol crossover in a direct methanol fuel cell, *J. Electrochem. Soc.* 143 (1996) 1239.
- [12] K. Kordesch and G. Simader, *Fuel cells and their applications*, VCH, Weinheim, 1996.
- [13] B. Bauer, D. J. Jones, J. Roziere, L. Tchicaya, G. Alberti, M. Casciola, I. Massinelli, A. Peraio, S. Besse and E. Ramunni, Electrochemical characterisation of sulfonated polyetherketone membranes, *J. New Mater. Electrochem. Systems* 3 (2000) 93.
- [14] S.M.J. Zaidi, S.D. Mikailenko, G.P. Robertson, M.D. Guiver and S. Kaliaguine, Proton conducting composite membranes for polyether ether ketone and heteropolyacids for fuel cell applications, *J. Membr. Sci.* 173 (2000) 17.
- [15] S.D. Mikhailenko, S.M.J. Zaidi and S. Kaliaguine, Sulfonated polyether ether ketone composite polymer electrolyte membranes, *Catal. Today* 67 (2001) 225.
- [16] K. A. Kreuer, On the development of proton conducting polymer membranes for hydrogen and methanol fuel cells, *J. Membr. Sci.* 185 (2001) 3.
- [17] J. Kerres, W. Zhang, L. Jörisen and V. Gogel, Application of different types of polyarylblend-membranes in DMFC, *J. New Mater. Electrochem. Systems* 5 (2002) 97.
- [18] G. Alberti, M. Casciola, L. Massinelli and B. Bauer, Polymeric proton conducting membranes for medium temperature fuel cells (110-160°C), *J. Membr. Sci.* 185 (2001) 73
- [19] V. Silva, B. Ruffmann, H. Silva, A. Mendes, M. Madeira and S. Nunes, Zirconium oxide modified sulfonated poly(ether ether ketone) membranes for direct methanol fuel cell applications, *Mater. Sci. Forum* 455-456 (2004) 587.
- [20] M.L. Ponce, L. Prado, B. Ruffmann, K. Richau, R. Mohr and S.P. Nunes, Reduction of methanol permeability in polyetherketone-heteropolyacid membranes, *J. Membr. Sci.* 217 (2003) 5.
- [21] C. Manea and M. Mulder, Characterization of polymer blends of polyethersulfone/sulfonated polysulfone and polyethersulfone/sulfonated polyetheretherketone for direct methanol fuel cell applications, *J. Membr. Sci.* 206 (2002) 443.

- [22] J. Kerres, A. Ulrich, F. Meier and T. Haring, Synthesis and characterization of novel acid–base polymer blends for application in membrane fuel cells, *Solid State Ionics* 125 (1999) 243.
- [23] J. Kerres, W. Cui, R. Disson and W. Neubrand, Development and characterization of crosslinked ionomer membranes based upon sulfinated and sulfonated PSU crosslinked PSU blend membranes by disproportionation of sulfinic acid groups, *J. Membr. Sci.* 139 (1998) 211.
- [24] J. Benavente, J. M. Garcia, R. Riley, A. E. Lozano and J. de Abajo, Sulfonated poly(ether ether sulfones): Characterization and study of dielectrical properties by impedance spectroscopy, *J. Membr. Sci.* 175 (2000) 43.
- [25] J. Kerres, A. Ulrich, Th. Haring, M. Baldauf, U. Gebhardt and W. Preidel, Preparation, characterization, and fuel cell application of new acid-base blend membranes, *J. New Mat. Electrochem. Syst.* 3 (2000) 129.
- [26] S.P. Nunes, B. Ruffmann, E. Rikowsky, S. Vetter and K. Richau, Inorganic modification of proton conductive polymer membranes for direct methanol fuel cells, *J. Membr. Sci.* 203 (2002) 215.
- [27] B. Ruffmann, H. Silva, B. Schulte and S. Nunes, Organic/inorganic composite membranes for application in DMFC, *Solid State Ionics*, 162-163 (2003) 269.
- [28] P. Dimitrova, K.A. Friedrich, B. Vogt and U. Stimming, Transport properties of ionomers composite membranes for direct methanol fuel cells, *J. Electroanal. Chem.* 532 (2002) 75.
- [29] L. Li, J. Zhang and Y. Wang, Sulfonated poly(ether ether ketone) membranes for direct methanol fuel cell, *J. Membr. Sci.* 226 (2003) 159.
- [30] L. Li, L. Xu and Y.X. Wang, Novel proton conducting composite membranes for direct methanol fuel cell, *Mater. Lett.* 57 (2003) 1406.
- [31] L. Li, L. Xu and Y.X. Wang, A hybrid membrane of poly(vinyl alcohol) and phosphotungstic acid fuel cells, *Chin. J. Chem. Eng.* 10 (2002) 614.
- [32] M.C. Wijers, Supported liquid membranes for removal of heavy metals, PhD Dissertation, University of Twente, The Netherlands, 1996.
- [33] V.S. Silva, B. Ruffmann, H. Silva, Y. Alvarez, A. Mendes, L. M. Madeira and S.P. Nunes, Proton electrolyte membrane properties and the direct methanol fuel cell performance. I. Hybrid sulfonated poly(ether ether ketone)/zirconium oxide membranes characterization, *J. Power Sources* 140 (2005) 34.
- [34] E. Gulzow, T. Kaz, R. Reissner, H. Sander, L. Schilling and M. V. Bradke, Study of membrane electrode assemblies for direct methanol fuel cells, *J. Power Sources* 105 (2002) 261.
- [35] Z. Qi and A. Kaufman, Open circuit voltage and methanol crossover in DMFCs, *J. Power Sources* 110 (2002) 177.

[36] B. Gurau and E. S. Smotkin, Methanol crossover in direct methanol fuel cells: a link between power and energy density, *J. Power Sources* 112 (2002) 339.

[37] A. Kuver, I. Vogel and W. Vielstich, Distinct performance evaluation of a direct methanol SPE fuel cell. A new method using a dynamic hydrogen reference electrode, *J. Power Sources* 52 (1994) 77.



## Chapter 6. Direct methanol fuel cell modeling using proton exchange membrane properties evaluated by standard characterization methods<sup>\*</sup>

### Abstract

A one-dimensional semi-empirical mathematical model is presented enabling the prediction of the direct methanol fuel cell (DMFC) performance using different proton exchange membranes (PEM) through parameters obtained from easy-to-implement standard PEM characterization methods. The applied standard characterization methods are: impedance spectroscopy (proton conductivity), water uptake (water sorption), pervaporation (permeability towards methanol and water) and gas permeation experiments (permeability towards oxygen, nitrogen and carbon dioxide). The DMFC model was experimentally validated using the DMFC results obtained with membranes based on sulfonated poly(ether ether ketone) (sPEEK) polymer modified via *in situ* incorporation of zirconium oxide. The development of a theoretical model based on the characteristics of these membranes enables the simulation of the DMFC using membranes with a wide variety of physical/chemical properties. The model predicts accurately the DMFC polarization curves and effectively differentiates the DMFC performance in terms of open circuit voltage, current density at 35mV and CO<sub>2</sub> concentration at the cathode exhaust according to the membrane properties. These facts confirm that the simulator can successfully predict the DMFC performance, using the standard characterization data as model input parameters.

<sup>\*</sup>*V.S. Silva, J. Schirmer, R. Reissner, B. Ruffmann, A. Mendes, L.M. Madeira and S.P. Nunes, (submitted, 2005).*

## 6.1. Introduction

The proton exchange membrane (PEM) is a key issue in the development of the direct methanol fuel cell (DMFC) technology. The PEM for DMFC applications should have low permeability coefficients for the reactants (particularly for methanol), exhibit high proton conductivity, along with long term mechanical stability and, not less important, low cost [1]. Nowadays, the commercially available membrane electrode assemblies (MEAs) for DMFC applications use plain perfluorinated membranes, such as Nafion<sup>®</sup> or Flemion<sup>®</sup>, that have high proton conductivity and sufficient mechanical stability [1]. However, it is known that apart from being costly, these membranes are not ideal for DMFC applications due to their high methanol and water permeability [2-3]. The methanol transport across the perfluorinated membranes decreases the Faraday efficiency for methanol consumption by as much as 20% under practical operation conditions [4].

These problems can be mitigated by developing new polymers, or modifying the existing ones, in order to prepare PEMs with improved properties compared to perfluorinated membranes. In the last decade, significant progress regarding membrane development for DMFC applications has been achieved [2, 5-11]. However, there are still many open questions, especially concerning the optimal PEM properties that should be targeted, having in mind a compromise between proton conductivity (electrolyte requirements) and methanol and water transport (barrier requirements). In order to infer about the PEM properties and select the proper materials for DMFC applications, researchers usually apply some standard characterization methods such as impedance spectroscopy and swelling experiments [12]. These and others characterization methods enable the evaluation of membrane properties such as: proton conductivity, permeability coefficients, water and methanol swelling, morphology and chemical stability.

Ideally, the obtained characteristics of a given membrane should be used as inputs in a mathematical model to predict the corresponding DMFC performance. Thus, instead of having only a qualitative forecast of the DMFC performance based on the research experience and characterization results, this type of model should enable a quantitative prediction. However, much of the developed DMFC modeling research has focused extensively on Nafion<sup>®</sup> using many parameters from literature [13]. Until now, no results have been reported regarding the application of these models for general PEM research. Therefore, the development of a mathematical model that enables the prediction of the DMFC performance with different membranes using inputs obtained from characterization methods, which are easy to implement is an important task. Apart

from that, the formulation of a detailed model helps in a critical evaluation of the transport mechanisms in the proton exchange membrane during DMFC operation.

The present chapter focuses on the development of a semi-empirical mathematical model to predict the DMFC performance using inputs obtained by characterization methods, such as impedance spectroscopy and pervaporation. As mentioned in previous studies [12, 14], the incorporation of zirconium oxide in sulfonated poly(ether ether ketone) allows the preparation of composite membranes with a gradual decrease in water swelling, proton conductivity and permeability towards methanol and water [12]. A well defined change in the DMFC performance was quantified using these membranes with different  $ZrO_2$  concentrations [14]. Therefore, the development of a mathematical model that predicts the steady-state DMFC performances using these composite membranes enables the simulation of a wide variety of physical/chemical membrane properties. In summary, the aim of this study is to develop a simulator that can effectively reduce our efforts to find the material with the best compromise between proton conductivity and water and methanol permeation.

## 6.2. Mathematical modeling

Until now, the developed DMFC mathematical models focused mainly on the fuel cell operating conditions using perfluorinated membranes as PEM [13]. Unfortunately, these models use data taken from literature that are usually impossible to reproduce by membrane development research groups and, in many cases, these parameters hardly represent the properties of membranes under development, therefore limiting the success of the models. In order to provide a useful tool for predicting the DMFC performance for a certain material, the present chapter presents a detailed semi-empirical mathematical model for the DMFC using PEM properties obtained from standard characterization results. This one-dimensional steady-state model was developed comprising the multi-layer structure of the MEA (Fig. 6.1), taking into account the multi-component transport ( $CH_3OH$ ,  $H_2O$ ,  $O_2$ ,  $CO_2$  and  $N_2$ ) and the detailed electrochemical reactions. The model used PEM data obtained by the following characterization methods reported in [12]:

### *Pervaporation experiments*

- Permeability towards methanol (1) and water (2),  $P_1^M$  and  $P_2^M$ , respectively.

### *Gas permeation experiments*

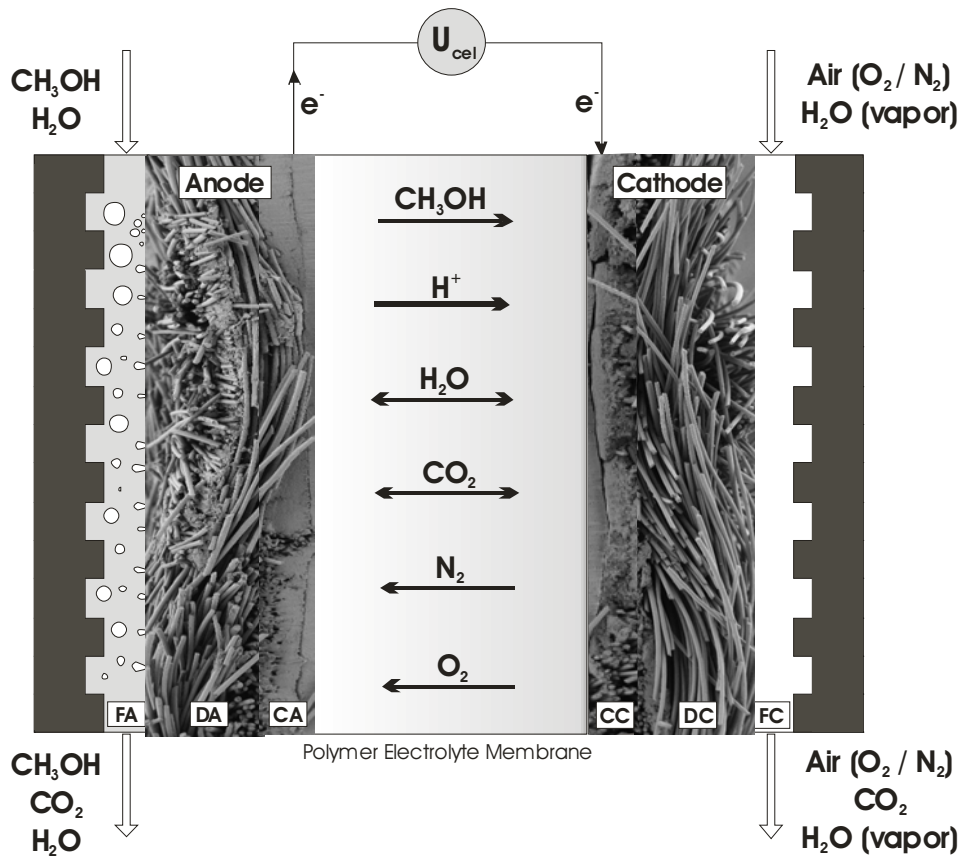
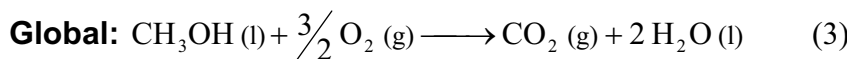
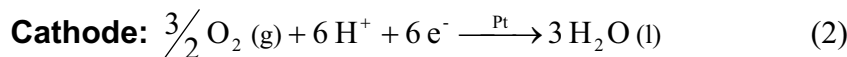
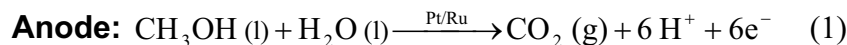
- Permeability towards oxygen (3), carbon dioxide (4) and nitrogen (5),  $P_3^M$ ,  $P_4^M$  and  $P_5^M$ , respectively.

*Swelling experiments*

- Swelling in liquid water,  $S_{2,L}^M$ .

*Impedance spectroscopy*

- Proton conductivity,  $k_M$ .

**Reactions****Legend**

- FA – Anode compartment
- DA – Anode diffusion layer
- CA – Anode catalyst layer
- CC – Cathode catalyst layer
- DC – Cathode diffusion layer
- FC – Cathode compartment

Fig. 6.1. Sketch of the DMFC illustrating the mass transport of the different species through the proton exchange membrane and the characterization methods used for fuel cell modeling.

All parameters regarding species mass transport through the electrodes and kinetics of the electrochemical reactions were taken from the literature (Table 6.1). The model was implemented within the ordinary differential equations solver tool LSODA [28]. This routine solves initial

condition problems for stiff and non-stiff systems of first-order ODEs. The anode and cathode diffusion and reaction layers and the proton exchange membrane were discretized in one dimension using the finite volume method [28]. The experimental DMFC performance presented by us elsewhere [14] was used as model validation data. Methanol and carbon dioxide transport in the multi-layer structure and the prediction of the polarization curves, open circuit voltage and carbon dioxide concentration at the cathode exhaust are modeled.

### 6.2.1. Governing equations

Anode

The anode compartment is assumed to be a continuously stirred tank reactor (CSTR), where the governing equation related to mass balance is

$$N_i^{DA} = Q^{FA} C_T (x_i^{FA} - x_i^A) \quad (6.1)$$

where  $Q^{FA}$  is the anode volumetric flow rate,  $N_i^{DA}$  is the molar flow rate of species  $i$  in the diffusion layer of the anode,  $C_T$  is the total concentration,  $x_i^{FA}$  is the molar fraction of species  $i$  in the anode feed and  $x_i^A$  is the molar fraction of species  $i$  in the anode outlet. In the model equations, fluxes are considered as positive in the direction from the anode to the cathode.

The mass transport of methanol (1) and water (2) through the anode diffusion and reaction layer (DA and CA, respectively), Fig. 6.1, considers both diffusion and convection transport mechanisms. In this model it is assumed that the convective term is due to the transport of water, i.e., consumption of water at the anode catalyst layer,  $\frac{I_{cell}}{6F}$  (reaction 1, Fig. 6.1) and water permeation through the membrane,  $N_2^M$  [21, 29].

Therefore, the molar flow rate of methanol and water through the anode diffusion layer and reaction layer can be expressed as

$$N_i = -A_{cell} D_i^{L,eff} C_T \frac{dx_i}{dz} + x_i \left( \frac{I_{cell}}{6F} + N_2^M \right), \quad i = 1, 2 \quad (6.2)$$

where  $A_{cell}$  is the reaction area (fuel cell active area),  $D_i^{L,eff}$  is the effective diffusion coefficient of species  $i$  in the anode layers (liquid phase),  $I_{cell}$  is the fuel cell current density,  $F$  is the Faraday constant,  $z$  is the axial coordinate and  $x_i$  is the molar fraction of species  $i$ .

Table 6.1. Model parameters and constants

Parameter	Symbol	Value	Reference
Anodic transfer coefficient	$\alpha_A$	0.75	[15]
Reference exchange current density of anode	$i_{A,ref}$	$94.25 \cdot e^{\frac{35570}{R} \left( \frac{1}{273.15+80.0} - \frac{1}{T} \right)}$ , A m <sup>-2</sup>	[16]
Cathode transfer coefficient	$\alpha_C$	0.875	[17]
Reference exchange current density of cathode	$i_{C,ref}$	$0.04222 \cdot e^{\frac{73200}{R} \left( \frac{1}{273.15+80.0} - \frac{1}{T} \right)}$ , A m <sup>-2</sup>	[18]
Reaction order at the anode	$\gamma_A$	1.0	[19]
Reaction order at the cathode	$\gamma_C$	0.4	[20]
Reaction order for methanol	$\gamma_{MeOH}$	1.0	[19]
Reference molar concentration of methanol at the anode	$C_{1,ref}^{CA}$	$1 \times 10^3$ , mol m <sup>-3</sup>	[19]
Reference partial pressure of oxygen at the cathode	$p_{3,ref}^{CC}$	$5 \times 10^5$ , Pa	[18]
Reference molar concentration of methanol at the cathode	$C_{1,ref}^{CC}$	$1 \times 10^3$ , mol m <sup>-3</sup>	[19]
Porosity of anode and cathode diffusion layers	$\varepsilon_D$	0.7	[21]
Porosity of anode and cathode catalyst layer	$\varepsilon_C$	0.4	[21]
Diffusion coefficient of $i$ in liquid (assumed as in water)	$D_{i,2}^L$	$\frac{7.4 \times 10^{-12} \cdot (1.9 \cdot M_i)^{1/2} \cdot T}{\mu_2 \cdot V_2^M}$ , m <sup>2</sup> s <sup>-1</sup>	[22]
Diffusion coefficient of $i$ in gas (assumed as in nitrogen)	$D_{i,5}^G$	$1.86 \times 10^{-3} \cdot \frac{T^{1.5}}{p \cdot \sigma_{i,5} \cdot \Omega_{i,5}} \cdot \sqrt{\frac{1}{M_i} + \frac{1}{M_5}}$ , m <sup>2</sup> s <sup>-1</sup>	[22]
Henry coefficient for O <sub>2</sub>	$H_3$	$9.01 \times 10^{-10}$ , Pa <sup>-1</sup>	[23]
Henry coefficient for CO <sub>2</sub>	$H_4$	$2.22 \times 10^{-9}$ , Pa <sup>-1</sup>	[24]
Henry coefficient for N <sub>2</sub>	$H_5$	$9.01 \times 10^{-10}$ , Pa <sup>-1</sup>	Assumed
Total concentration	$C_T$	$1 \times 10^3$ , mol m <sup>-3</sup>	Assumed
Electro-osmotic drag coefficient of water	$n_{drag,2}$	3.16	[25]
Electro-osmotic drag coefficient of methanol	$n_{drag,1}$	$3.16 x_1$	[26]
Proton molar fraction depending on boundary conditions (BC)	$x_{H^+}$	$\left\{ \begin{array}{l} \frac{1}{S_{2,L}^M + 2}, BC_{Anode} \\ \frac{1}{(0.18 - 0.015 \cdot \%ZrO_2) + 2}, BC_{Cathode} \end{array} \right.$	[27]
Contact resistance	$R_{contact}$	0.0, $\Omega$ m <sup>2</sup>	Assumed
DMFC electrode area	$A_{cell}$	$25 \times 10^{-4}$ , m <sup>2</sup>	[21]
Gas constant	$R$	8.314 J mol <sup>-1</sup> K <sup>-1</sup>	[21]
Faraday constant	$F$	96485 C mol <sup>-1</sup>	[21]

In terms of the oxygen (3), carbon dioxide (4) and nitrogen (5) transport in these regions, diffusion and convection transport mechanisms are also assumed. However, for these species, the Henry's law constant,  $H_i$ , is incorporated in the convective term, since it is assumed that their convective transport proceeds as dissolved gases [30]. As a first approximation, the solubility of species  $i$  in pure water was used since the methanol feed stream concentration is very low (5wt.%) [14].

$$N_i = -A_{cell} D_i^{L,eff} C_T \frac{dx_i}{dz} + p_i^A H_i \left( \frac{I_{cell}}{6F} + N_2^M \right), \quad i = 3, 4, 5 \quad (6.3)$$

where  $p_i^A$  is the partial pressure of species  $i$  in the anode.

The effective diffusion coefficient of species  $i$  in the anode diffusion and reaction layers can be derived from the bulk diffusion coefficient,  $D_i^L$ , and the void fraction of both layers,  $\varepsilon_A^{DA}$  and  $\varepsilon_A^{CA}$ , respectively, using the *Bruggeman* correction [31, 32].

$$D_i^{L,eff} = (\varepsilon_A)^{3/2} D_i^L \quad (6.4)$$

On the other hand, the consumption of water and methanol and the formation of carbon dioxide will also occur in the anode reaction layer. Therefore, at steady state conditions, the variation of the molar flow rates of the species  $i$  is affected by the anode electrochemical reaction rate as follows:

$$\frac{dN_i^{CA}}{dz} = \nu_{1,i} \frac{i_A}{6F}, \quad i = 1, 2, 4 \quad (6.5)$$

where  $i_A$  the local anodic proton exchange current and  $\nu_{1,i}$  is the stoichiometric coefficient of species  $i$  in reaction 1 (Fig. 6.1).

### Proton Exchange Membrane

As mentioned before, the core of the present chapter is the prediction of the transport phenomenon in the PEM using parameters such as proton conductivity, swelling and permeability coefficients obtained by standard characterization methods [12]. As in conventional DMFC models, it is assumed that water and methanol permeate through the membrane due to the electro-osmotic drag (convective term: resulting from the cell current density) and to the species concentration gradient (diffusive term: resulting from distinct hydration state of the membrane). The electro-osmotic species flux is assumed to be driven by the proton concentration gradient [27] and parameterized by the water transport number,  $n_{drag,i}$ , and the proton conductivity,  $k_M$  (obtained

by impedance spectroscopy). The water transport number is assumed to be the same as that for Nafion<sup>®</sup> [25]. The proton concentration gradient is parameterized by the PEM water and vapor swelling as described in [27, 29]. On the other hand, the diffusion term is parameterized by the permeability coefficient,  $P_i$ , evaluated by pervaporation experiments [12]: this parameter is an approximation of the commonly used membrane hydraulic permeability [29, 33]. Therefore, the water and methanol transport through the membrane was expressed as

$$N_i^M = -n_{drag,i} \frac{RTk_M}{F^2} \frac{dx_{H^+}^M}{dz} - A_{cell} P_i \frac{dx_i^M}{dz}, \quad i = 1, 2 \quad (6.6)$$

where  $R$  is the gas constant,  $T$  is the operation temperature,  $x_i^M$  is the molar fraction of species  $i$  in the membrane and  $x_{H^+}^M$  is the molar fraction of protons in the membrane.

Regarding the transport of oxygen, carbon dioxide and nitrogen through the membrane, it is also assumed both diffusion and convection mechanisms. However, for these species, the convection is superimposed by the water flux in the membrane. Furthermore, as for the anode regions, it is assumed that the transport of these species across the membrane occur as dissolved gases, and thus the Henry's law constant was included in the convective term. The diffusion term is parameterized using the permeability coefficients evaluated by gas permeation experiments:

$$N_i^M = H_i P_i^M N_2^M - A_{cell} P_i \frac{dx_i^M}{dz}, \quad i = 3, 4, 5 \quad (6.7)$$

The use of parameters evaluated by standard characterization methods to simulate the permeation of protons and all other species is a rough estimate because real values for DMFC operation depend on the operation conditions through the entire MEA. In real DMFC operation, the concentration of species and protons in both anode and cathode changes with the applied load and, therefore, different mass transport conditions exist compared to those in standard characterization methods such as impedance spectroscopy, pervaporation and gas permeation.

## Cathode

The cathode compartment is also assumed to behave as a CSTR, where the governing equation related to the mass balance is

$$N_i^{DC} = Q^{FC} C_T (y_i^{FC} - y_i^C) \quad (6.8)$$

where  $Q^{FC}$  is the cathode volumetric flow rate,  $N_i^{DC}$  is the molar flow rate of species  $i$  in the diffusion layer of the cathode,  $y_i^{FC}$  is the gas phase molar fraction of species  $i$  in the cathode feed and  $y_i^C$  is the gas phase molar fraction of species  $i$  at the cathode outlet.

The mass transport of all species in the gas phase through the cathode diffusion and reaction layers (DC and CC, respectively), Fig. 6.1, is modeled using the *Fickian* diffusion approximation and can be expressed as

$$N_i = -A_{cell} C_T D_i^{G,eff} \frac{dy_i}{dz} \quad (6.9)$$

where  $D_i^{G,eff}$  is the effective diffusion coefficient of species  $i$  in the cathode layers (gas phase).

In the cathode reaction layer, the consumption and formation of species  $i$  occurs through the reduction of oxygen and the parasitic oxidation of methanol. Therefore, at steady-state, the variation of the molar fluxes of the species is affected by the cathode electrochemical reactions as follows:

$$\frac{dN_i^{CC}}{dz} = \frac{1}{C_T A_{cell} 6F} (v_{2,i} i_C + v_{3,i} i_{MeOH}) \quad (6.10)$$

where  $i_{MeOH}$  is the parasitic exchange current due to the methanol reaction in the Pt catalyst at the cathode catalytic layer,  $i_C$  is the cathode proton exchange density and, finally,  $N_i^{CC}$  is the molar flow rate of species  $i$  in the cathode catalytic layer.

### 6.2.2. Electrochemical kinetics

Anode

The rate of the electrochemical reaction at the anode catalyst layer can be described using the *Butler-Volmer* rate expression [33]. This is then simplified to give a *Tafel* type equation in terms of the methanol concentration,

$$i_A(z) = i_{A,ref} \left( \frac{x_1^{CA}(z) C_T}{C_{1,ref}^{CA}} \right)^{\gamma_A} \exp\left( \frac{\alpha_A F}{RT} \eta_A \right) \quad (6.11)$$

where  $i_{A,ref}$  is the reference proton exchange current density of the methanol oxidation (anode),  $x_1^{CA}$  is the local molar fraction of methanol,  $C_{1,ref}^{CA}$  is the reference methanol molar concentration,

$\alpha_A$  is the charge transfer coefficient,  $\eta_A$  is the local anode overpotential and  $\gamma_A$  is the chemical reaction order for methanol oxidation in the anode.

The integration of the local volumetric reaction rate over the whole catalyst layer thickness,  $l_C$ , yields the overall current density,  $I_A^{overall}$ :

$$I_A^{overall} = \int_0^{l_C} i_A(z) dz \quad (6.12)$$

Due to losses associated with the conduction of both electrons in the solid phase and protons in the electrolyte, there will be a locally changing overpotential (voltage loss) during the DMFC operation. Therefore, the overall voltage loss in the anode catalyst layer can be evaluated using the following equation:

$$\eta_A^{overall} = \frac{1}{I_{cell}} \int_0^{l_C} i_A(z) \eta_A(z) dz \quad (6.13)$$

More detailed information regarding the kinetic parameters used is given in Table 6.1.

## Cathode

At the cathode, the electrochemical reactions are also modeled using the *Tafel* equations for both the oxygen reduction reaction and the methanol parasitic oxidation on platinum [33]:

$$i_C(z) = i_{C,ref} \left( \frac{p_3^{CC}(z)}{p_{3,ref}^{CC}} \right)^{\gamma_C} \exp \left[ -\frac{\alpha_C F}{RT} \eta_C \right] \quad (6.14)$$

$$i_{MeOH}(z) = i_{MeOH,ref} \left( \frac{C_1^{CC}(z)}{C_{1,ref}^{CC}} \right)^{\gamma_{MeOH}} \exp \left[ -\frac{\alpha_{MeOH} F}{RT} \eta_{MeOH} \right] \quad (6.15)$$

where  $i_{c,ref}$  is the reference proton exchange current density of the oxygen reduction (cathode),  $p_{3,ref}^{CC}$  is the reference oxygen partial pressure,  $p_3^{CC}$  is the oxygen partial pressure,  $\alpha_C$  is the charge transfer coefficient in the cathode,  $\eta_c$  is the local cathode overpotential,  $\gamma_C$  is the chemical reaction order for oxygen reduction in the cathode,  $i_{MeOH,ref}$  is the reference proton exchange current density for the methanol oxidation (cathode),  $C_{1,ref}^{CC}$  is the reference molar concentration of methanol at the cathode,  $C_1^{CC}$  is the molar concentration of methanol at the cathode,  $\alpha_{MeOH}$  is the charge transfer coefficient,  $\eta_{MeOH}$  is the voltage loss due to the parasitic reaction and  $\gamma_{MeOH}$  is the corresponding chemical reaction order.

The evaluation of the cathode overall current density,  $I_C^{overall}$ , and the overall voltage loss in the cathode catalyst layer,  $\eta_C^{overall}$ , was performed using equations analogous to Eqs. (6.12) and (6.13), respectively. On the other hand, the overall current density loss due to the oxidation reaction of methanol in the cathode catalyst layer,  $I_{MeOH}^{overall}$ , was evaluated using the Faraday's law:

$$I_{MeOH}^{overall} = N_1^M 6F \quad (6.16)$$

The overpotential loss associated with methanol crossover,  $\eta_{MeOH}^{overall}$ , was obtained using the *Tafel* equation for zero order reaction [33]:

$$\eta_{MeOH}^{overall} = -\frac{RT}{\alpha_{MeOH} F} \ln \left[ \frac{I_{MeOH}^{overall}}{I_{MeOH,ref}} \right] \quad (6.17)$$

where  $I_{MeOH,ref}$  is the reference current density for the reaction of methanol in the cathode catalyst layer.

### 6.2.3. Cell voltage

The DMFC output voltage is the result of the open circuit cell voltage (OCV),  $U_{cell}^o$ , the overall overpotentials at the anode and cathode (oxygen and methanol reactions) and the ohmic loss due to the PEM resistance and contacts between plates, electrodes and membrane [33]. The ohmic loss due to the PEM is parameterized using the membrane proton conductivity obtained by impedance spectroscopy characterization. Therefore, the cell voltage can be determined as follows

$$U_{cell} = U_{cell}^o - \eta_A^{overall} + \eta_C^{overall} + \eta_{MeOH}^{overall} - \frac{d_M}{k_M} I_{cell} - R_{contact} I_{cell} \quad (6.18)$$

where  $d_M$  is the proton exchange membrane thickness and  $R_{contact}$  is the DMFC contact resistance.

As an initial estimate of the open circuit voltage, it was assumed that this value was calculated by the standard DMFC voltage (1.21V) subtracted by the overpotential loss associated with the methanol crossover at open circuit operation conditions [34]. Therefore, one should expect the highest value for OCV using a membrane that has practically no permeability towards methanol ( $\eta_{MeOH}^{overall} \cong 0$ ). However, this procedure proved to fail regarding the prediction of the experimental OCV. This happens because it does not take into account the decreased proton conductivity associated with lower permeability towards methanol of the PEM. In fact, when OCV experimental measurement is performed, there exists current flowing from the anode to the cathode due to non-idealities of the voltmeter (usually  $I_{cell} \leq 1\text{mA/cm}^2$ ). Ideally, one should expect an infinite

resistance for the voltmeter when measuring the open circuit voltage. However, it is known that real voltmeters have finite resistance ( $R_v > 10M\Omega$ ), which allow some current to flow. Thus, if the membrane has very low proton conductivity ( $k_M \cong 0$ ), it could exhibit a significant ohmic loss that decreases the OCV value. This fact was often verified experimentally by us for membranes with high inorganic modifications. Therefore, in the present model we assumed a current density of  $0.1\text{mA}/\text{cm}^2$  for open circuit conditions (based on experimental test with the applied voltmeter), in order to account the ohmic drop due to the application of membranes with lower electrolyte properties. It is worth noting that assuming this current density, the obtained anode and cathode overpotentials,  $\eta_A^{overall}$  and  $\eta_C^{overall}$ , respectively, evaluated through the *Butler-Volmer* rate expression are negligible for the DMFC operating at open circuit conditions (practically no reaction occurs apart from the parasitic oxidation of the crossover methanol in the cathode catalyst layer).

#### 6.2.4. Cell efficiency

The DMFC efficiency depends strongly on the permeability of the proton exchange membranes towards methanol. The methanol permeation from the anode to the cathode through the PEM promotes the methanol oxidation at the cathode, leading to a loss of potential. Apart from that, it leads also to a loss of reactant and therefore lowers the DMFC efficiency. Usually the DMFC efficiency can be obtained from the Faraday and potential efficiencies [35]. The Faraday efficiency,  $\eta_F$ , is defined as the ratio between the converted fuel for current production (anode) and the total amount of converted fuel (anode and cathode). Therefore, it is obtained from the following equation:

$$\eta_F = \frac{I_{cell}}{I_{MeOH}^{overall} + I_{cell}} \quad (6.19)$$

On the other hand, the potential efficiency,  $\eta_P$ , is defined as the voltage of the DMFC compared to the standard cell voltage due to the overall potential losses and is obtained from the following equation:

$$\eta_P = \frac{U_{cell}}{U_{cell}^{rev}} \quad (6.20)$$

Finally, the overall DMFC efficiency,  $\eta_{DMFC}$ , is obtained using the following equation:

$$\eta_{DMFC} = \eta_F \eta_P \quad (6.21)$$

### 6.3. Experimental

In order to predict the proton concentration gradient in the membrane during DMFC operation as reported in [27], the vapor sorption of the studied membranes must be known (cathode boundary conditions). Therefore, extra-experiments were performed, at 90°C, to evaluate this property using a magnetic suspension balance by *Rubotherm*, as presented in [36]. Since it was possible to evaluate this property only for two membranes (0.0 and 5.0wt.% ZrO<sub>2</sub>; evaluation results: 2.07 and 0.11wt.%, respectively), a linear variation of the vapor sorption with the amount of ZrO<sub>2</sub> incorporation between 5.0 and 12.5wt.% was assumed (Table 6.1). Apart from this, it was also considered that the membrane with higher amount of inorganic modification experienced no swelling in water vapor at 90°C due to its low hydrophilic character. Since the permeability towards methanol was only experimentally obtained at 55°C [12], in the model it is assumed an activation energy of 34.1 kJ mol<sup>-1</sup> (assuming *Arrhenius* law). This activation energy was experimentally evaluated through pervaporation experiments at 40, 55 and 70°C for sPEEK membranes with sulfonation degree of 42%.

The DMFC experimental results used for validating the model simulations were obtained using Etek<sup>®</sup> ELAT electrodes [14]. As anode catalyst layer, supported PtRu (1 mg/cm<sup>2</sup> 30wt.% PtRu (1:1) on carbon with 0.7 mg/cm<sup>2</sup> Nafion<sup>®</sup>/PTFE) was used and as cathode Pt (0.4 mg/cm<sup>2</sup> 20wt.% Pt on carbon with 0.7 mg/cm<sup>2</sup> Nafion<sup>®</sup>/PTFE). The prepared MEAs (25 cm<sup>2</sup>) were operated with an aqueous 1.5M methanol solution (4ml/min, 2.5bar) on the anode side and humidified air (600sccm/min, 3bar, 100% relative humidity) on the cathode side. Other experimental specifications regarding the DMFC tests can be found in [14]. The suggested mathematical model was implemented to predict the DMFC current-voltage polarization curves, constant voltage current at 35mV (CV, 35mV), open circuit voltage (OCV) and CO<sub>2</sub> concentration at the cathode outlet.

In the present model, the kinetic parameters regarding the oxidation of methanol in the cathode catalyst layer,  $\alpha_{MeOH}$  and  $i_{MeOH,ref}$  were considered to be the same as  $\alpha_A$  and  $i_{A,ref}$ , respectively. In order to fit the experimental data, the reference proton exchange current density of the methanol oxidation at the anode,  $i_{A,ref}$ , the reference proton exchange current density of the oxygen reduction at the cathode,  $i_{C,ref}$  and the reference current density of the methanol crossover oxidation at the cathode,  $I_{MeOH,ref}$ , are adjusted in the present model. The values presented in Table

6.1 were used as initial estimative of the fitting parameters. The experimental data fitting was performed using trial and error method [37].

## 6.4. Results and discussion

### 6.4.1. Polarization curves

The simulation curves and experimental points for the current density-voltage and current density-power density plots using MEAs made from SPEEK composite membranes with 5.0, 7.5 and 10.0wt.% of ZrO<sub>2</sub> at different temperatures are shown in Fig. 6.2. It can be observed that the simulations show a good agreement with the experimental results for several temperatures and ZrO<sub>2</sub> incorporation loads. From Fig. 6.2, it can be seen that the model correctly predicts the decrease in the DMFC performance when the ZrO<sub>2</sub> incorporation increases from 5.0 to 10.0wt.%. Fig. 6.2a shows that, although having a slight deviation for the curves evaluated at 70°C (mainly for the current density-power density plot), the simulations show good agreement with the experimental data. For example, at 90°C, the model predicts that the MEA using a 5.0wt.% ZrO<sub>2</sub> composite membrane achieves a maximum power density output of 16.3mW/cm<sup>2</sup> for a current density of 109.2mA/cm<sup>2</sup>, while the experimental result is 16.4mW/cm<sup>2</sup> for a current density of 109.2mA/cm<sup>2</sup>. In contrast, for the 7.5wt.% zirconium oxide modified membrane (Fig. 6.2b), it can be seen that the simulations show a good agreement for 70 and 90°C and a slight deviation for 100°C. On the other hand, the model effectively predicted the low performance of the DMFC using a 10.0wt.% ZrO<sub>2</sub> composite membrane at 110°C, what is mainly due to the low membrane proton conductivity [12] (Fig. 6.2c). This fact shows the ability of the simulator to account for the ohmic resistance of a specific material when predicting the DMFC polarization curves.

### 6.4.2. Current density at constant voltage and open circuit voltage

Besides simulating the current density-voltage polarization curves, in the present study the current density and CO<sub>2</sub> concentration at the cathode outlet were also simulated for constant voltage (CV) experiments at 35mV (Fig. 6.3). It can be seen that the experimental DMFC cell current density decrease with ZrO<sub>2</sub> content and increase with temperature is well predicted by the simulations (Fig. 6.3a). However, a more significant deviation from the experimental results can be noticed when using a 5.0wt.% ZrO<sub>2</sub> composite membrane at 70 and 90°C.

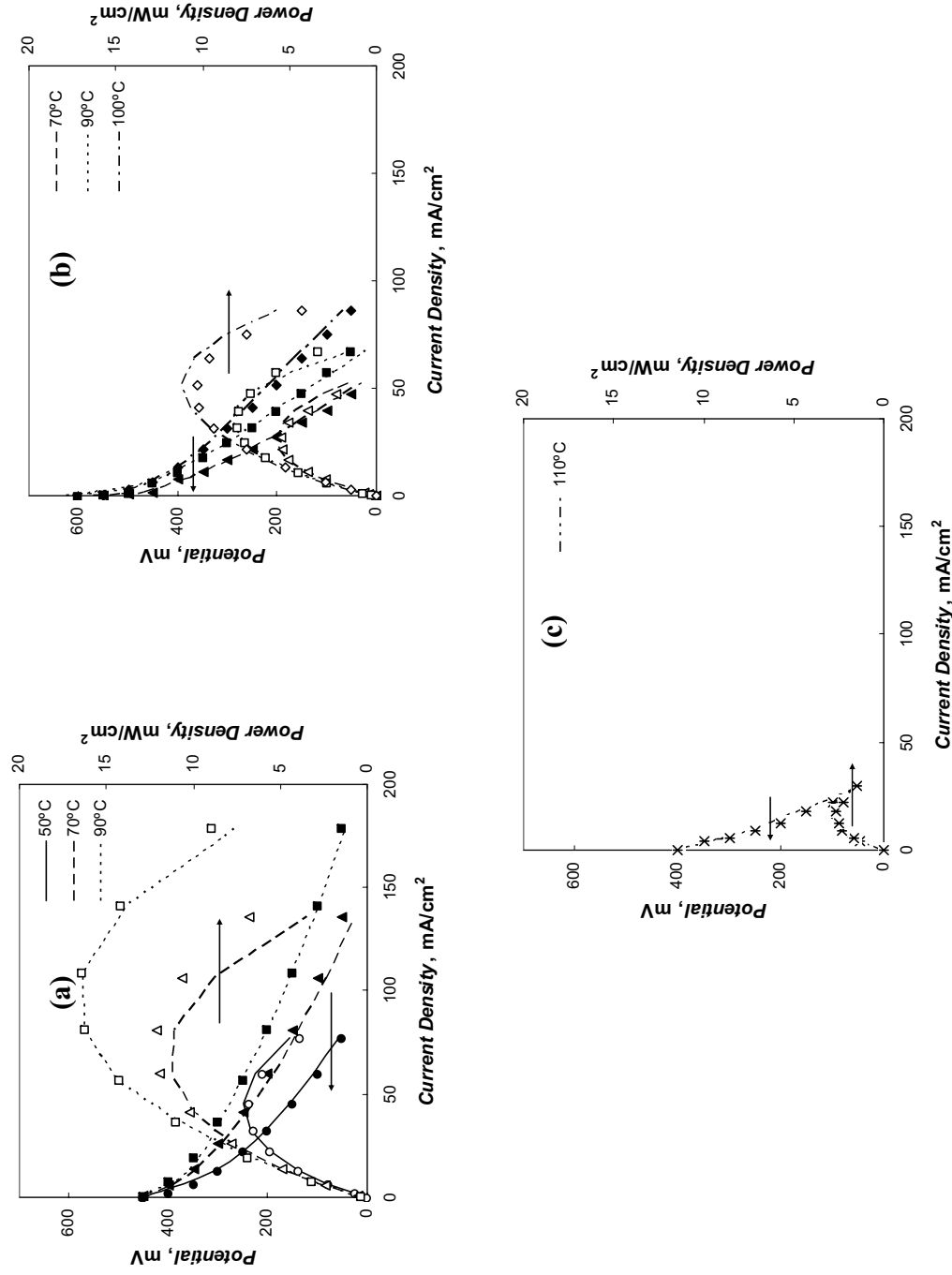


Fig. 6.2. Predicted (curves) and experimental (points: ● 50°C; ▲ 70°C; ■ 90°C; ◆ 100°C; ✱ 110°C) current density-voltage and power density plots for DMFC operation using sPEEK composite membranes with: a) 5.0, b) 7.5 and c) 10wt.%ZrO<sub>2</sub>.

On the other hand, the simulation deviations for 70 and 90°C seem to be higher when predicting the CO<sub>2</sub> concentration at the cathode outlet (Fig. 6.3b). This may be a consequence of the use of the permeability coefficients obtained by pervaporation and of the activation energy assumption. However, the simulations allowed the clear differentiation of the effect of different physical and chemical properties of the membranes on both current density and CO<sub>2</sub> concentration at the cathode outlet for constant voltage experiments (35mV, high current density). As expected, one can clearly verify from the simulation results that a higher methanol permeability coefficient, evaluated by pervaporation experiments (and recorded for low ZrO<sub>2</sub>-containing membranes), means higher CO<sub>2</sub> concentration at the cathode outlet and, therefore, lower DMFC fuel conversion efficiency (as shown below).

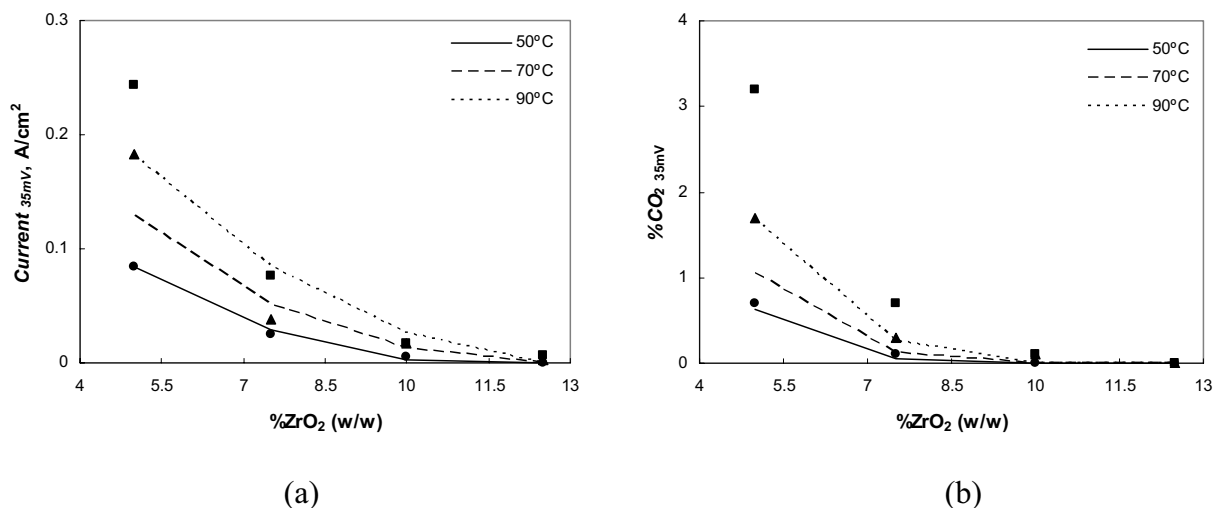


Fig. 6.3. Predicted (curves) and experimental (points: ● 50°C; ▲ 70°C; ■ 90°C) current density (a) and CO<sub>2</sub> concentration at the cathode outlet (b) for DMFC operation at constant voltage (35mV) as a function of the ZrO<sub>2</sub> content.

The simulation curves and experimental data for the open circuit voltage and corresponding CO<sub>2</sub> concentration at the cathode outlet, at different temperatures, are shown in Fig. 6.4. From Fig. 6.4a, it can be seen that the maximum experimental DMFC open circuit voltage for the hybrid membrane with 7.5wt.% ZrO<sub>2</sub> [14] is well predicted by the simulations. Apart from this, good OCV predictions are obtained for membranes with 5.0, 7.5 and 10wt.% for each studied temperature (except some deviation for the membrane with 10.0wt.% ZrO<sub>2</sub> at 50°C). In contrast, higher deviations can be observed for the membrane containing 12.5wt.% ZrO<sub>2</sub>. In terms of prediction of the CO<sub>2</sub> concentration at the cathode outlet (Fig. 6.4b), it can be observed that the deviations follow the same trend as those found for the constant voltage experiments (Fig. 6.3b). Although with lower

predicted values for the membranes with 5.0 and 7.5wt.% ZrO<sub>2</sub>, at 70 and 90°C, the effect of distinct membrane properties on the CO<sub>2</sub> concentration at the cathode outlet for open circuit experiments can be noticed.

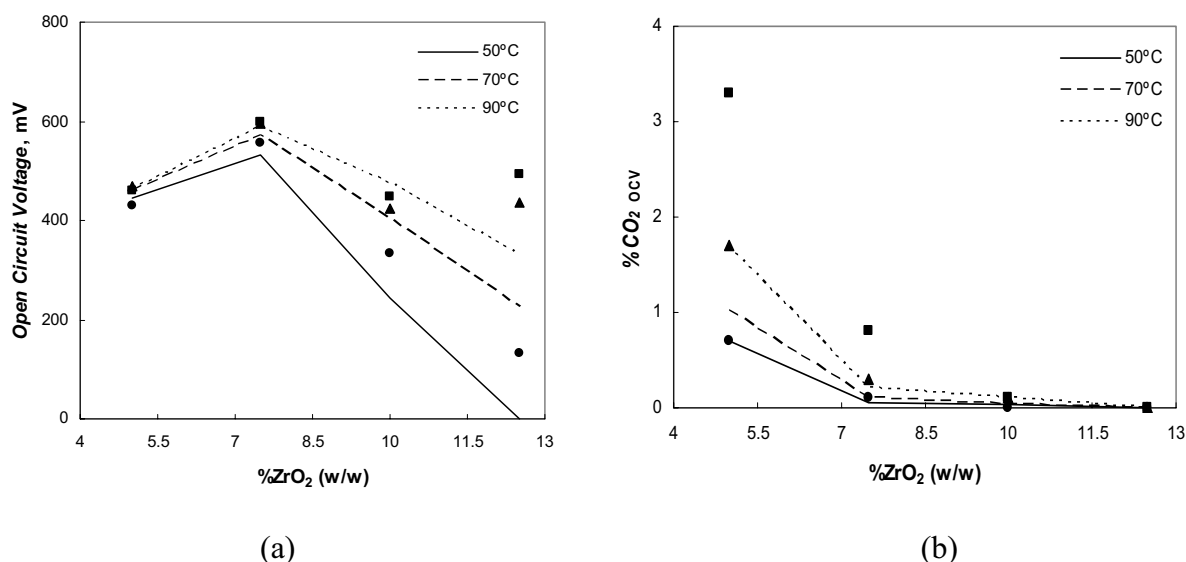


Fig. 6.4. Predicted (curves) and experimental (points: ● 50°C; ▲ 70°C; ■ 90°C) voltage (a) and CO<sub>2</sub> concentration at the cathode outlet (b) for open circuit DMFC operation as a function of the ZrO<sub>2</sub> content.

### 6.4.3. DMFC efficiency

In Fig. 6.5 the DMFC efficiencies using sPEEK composite membranes with 5.0wt.%ZrO<sub>2</sub> are plotted as a function of current density. From results presented in Fig. 6.5a, it is possible to observe that although increasing with current density, the ratio between the converted methanol for current production and the total converted methanol (Faraday efficiency) decreases with temperature. The increase with current density is directly related to the decrease of the driving force for methanol transport through the membrane (lower methanol concentration at the anode). On the other hand, we believe that the efficiency decrease with temperature is due to an increase of the membrane permeability towards methanol. For the same membrane, Fig. 6.5a demonstrates that the potential efficiency increases with the temperature and decreases with the current density. The potential efficiency increase with temperature is directly related with the anode and cathode overpotentials decrease. The potential efficiency decrease with current density is mainly due to the increase of the anode overpotential when larger amounts of electrons are produced. With respect to the overall DMFC efficiency using sPEEK composite membranes with 5.0wt.%ZrO<sub>2</sub>, from the plots

presented in Fig. 6.5b it can be observed that it increases with temperature and exhibits an optimum value of current density, which depends on the temperature employed.

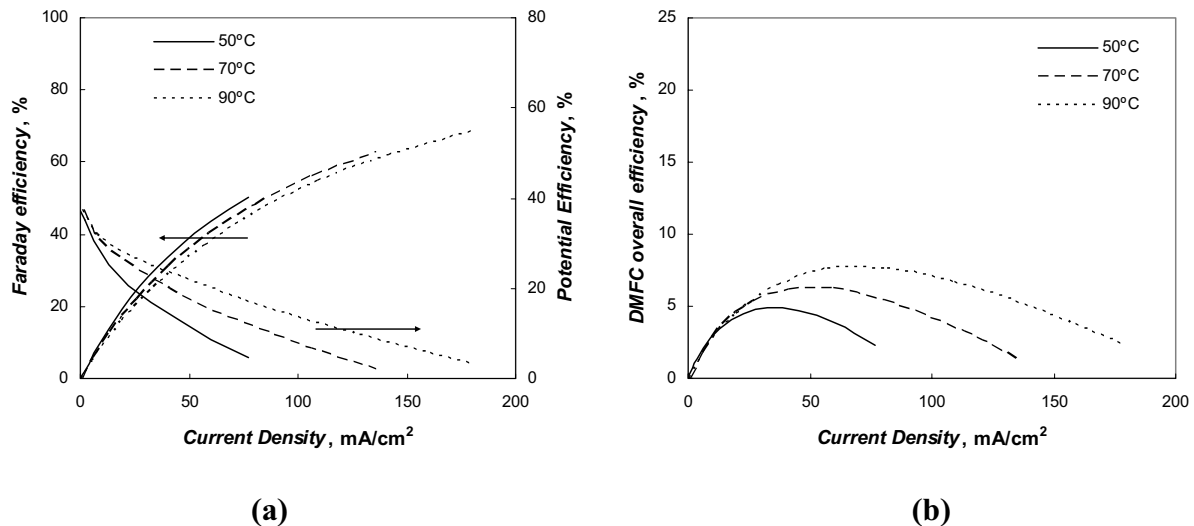


Fig. 6.5. Predicted DMFC efficiency using sPEEK composite membranes with 5.0wt.%ZrO<sub>2</sub>: Faraday and potential efficiencies (a) and overall efficiency (b).

In contrast, a distinct Faraday and overall efficiencies variation with temperature is observed using the sPEEK composite membranes with 7.5wt.%ZrO<sub>2</sub> (Fig. 6.6). For this membrane, the Faraday efficiency increases from 70°C until 90°C and then decreases when increasing the temperature to 100°C (Fig. 6.6a). Furthermore, at 100°C, the Faraday efficiency is even lower than that obtained at 70°C. Thus, the highest overall efficiency is obtained at 90°C (Fig. 6.6b). We believe that this effect is due to a change of the membrane structure at higher temperatures, increasing the membrane permeability towards methanol (thus decreasing the methanol utilization efficiency). In contrast, with respect to the variation with current density, the DMFC efficiencies using sPEEK composite membranes with 7.5 and 10.0wt.% of ZrO<sub>2</sub> (Figs. 6.6 and 6.7, respectively) are analogous to those obtained for the 5.0wt.% ZrO<sub>2</sub> membrane (Fig. 6.5).

Comparing the results presented in Figs. 6.5, 6.6 and 6.7, it can be observed that the DMFC using the composite membrane with 7.5wt.% ZrO<sub>2</sub> presents the highest overall efficiency of all studied membranes (Fig. 6.6b). This fact results from the improved membrane properties in terms of barrier properties that enable an improved fuel utilization (higher Faraday efficiency) and, not less important, enough proton conductivity (higher potential efficiency). It should be emphasized that the highest Faraday efficiency is achieved with the composite membrane with 10.0wt.% of ZrO<sub>2</sub> (Fig. 6.7a) because this membrane presents the best barrier properties of the studied materials

[12]. However, due to its very low proton conductivity it has very poor electrolyte properties (high potential losses due to membrane resistance).

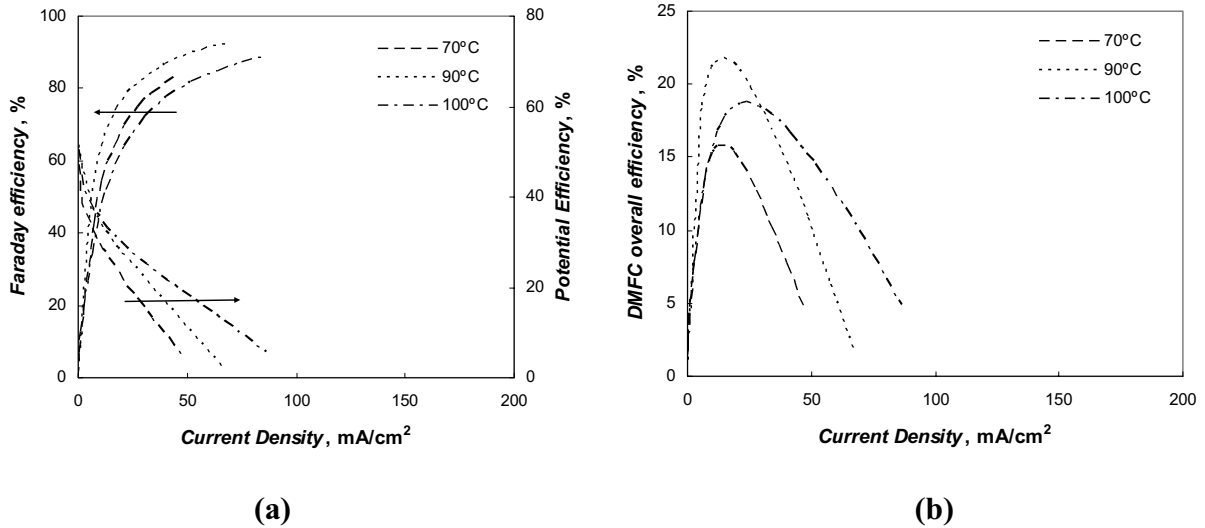


Fig. 6.6. Predicted DMFC efficiency using sPEEK composite membranes with 7.5wt.%ZrO<sub>2</sub>: Faraday and potential efficiencies (a) and overall efficiency (b).

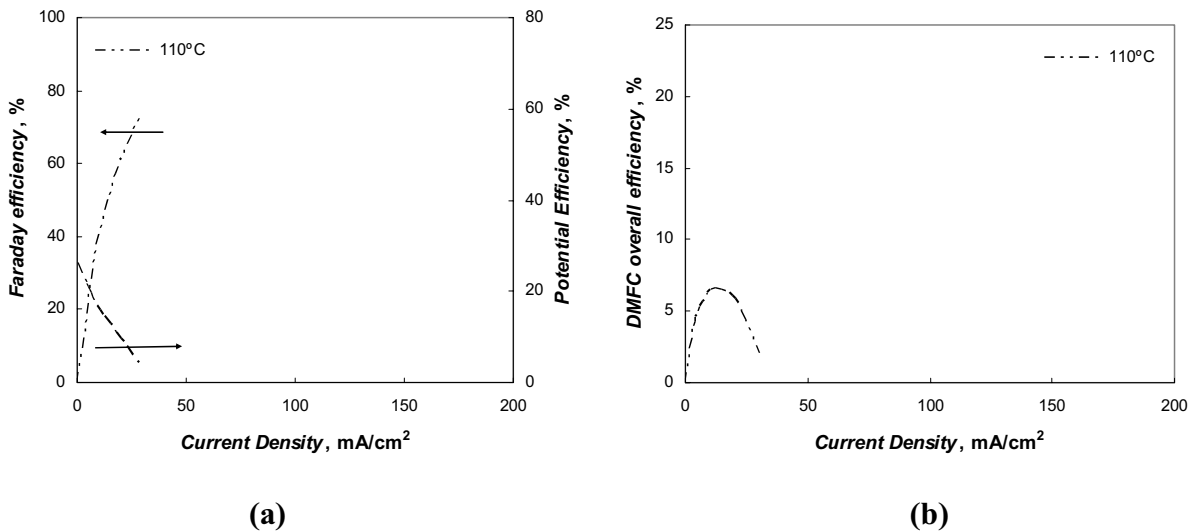


Fig. 6.7. Predicted DMFC efficiency using sPEEK composite membranes with 10.0wt.%ZrO<sub>2</sub>: Faraday and potential efficiencies (a) and overall efficiency (b).

## 6.5. Conclusions

In order to develop a useful modeling tool to predict the DMFC performance using as inputs membrane parameters obtained by PEM standard characterization methods, a set of sPEEK

composite membranes with different amounts of zirconium oxide (5.0, 7.5, 10.0 and 12.5wt.% ZrO<sub>2</sub>) was selected because of their wide range of physical/chemical properties. The selected and studied parameters obtained through easy-to-implement characterization methods to predict the PEM behavior during DMFC operation were: proton conductivity (from impedance spectroscopy), H<sub>2</sub>O sorption (from batch experiments), permeability towards H<sub>2</sub>O and CH<sub>3</sub>OH (from pervaporation) and permeability towards N<sub>2</sub>, O<sub>2</sub> and CO<sub>2</sub> (from gas permeation). The results showed that the simulations obtained using the proposed model present a good agreement with the experimental data for different temperatures and ZrO<sub>2</sub> incorporation loadings. The model predicts correctly the decrease of the DMFC performance when the ZrO<sub>2</sub> content increases from 5.0 to 10.0wt.% ZrO<sub>2</sub>. In terms of current density and CO<sub>2</sub> concentration at the cathode outlet for constant voltage experiments (35mV, high current density), the model proved to perform a good estimation of the DMFC behavior with reasonable prediction of the influence of different physical and chemical properties of the membranes. The same occurs for the prediction of the open circuit voltage and corresponding CO<sub>2</sub> concentration at the cathode outlet.

From the DMFC efficiency theoretical study, it was observed that the composite membrane with 7.5wt.% ZrO<sub>2</sub> presents the highest overall efficiency of the studied materials. Besides showing improved properties in terms of barrier properties (higher fuel utilization), this membrane also presents enough proton conductivity. In summary, the present research work shows the ability of the developed model to account for the membrane properties evaluated by standard characterization methods when predicting the DMFC current-voltage polarization curves, constant voltage current at 35mV (CV, 35mV), open circuit voltage (OCV) and CO<sub>2</sub> concentration at the cathode outlet. The present simulator will be used by us for membrane research and development. Apart from this, future research work will be focused on a critical study concerning the PEM properties for DMFC applications, taking into account the compromise between high proton conductivity and low methanol transport.

## **Acknowledgements**

Financial support by the HGF-Vernetzungsfonds is gratefully acknowledged. The work of Vasco Silva was supported by FCT (grant SFRH/BD/6818/2001). Vasco Silva would also like to acknowledge both FCT and GKSS for the grant assigned for his stay at GKSS Forschungszentrum GmbH. The authors would like to acknowledge H. Silva at GKSS for the vapor sorption measurements. The authors also acknowledge Paulo Cruz and João Santos at LEPAE for helping

with the implemented numerical methods. The present work was partially supported by FCT/FEDER projects POCTI/EQU/38075/2001 and POCTI/EQU/45225/2002.

## List of symbols

$A_{cell}$	Reaction area (fuel cell active area), $m^2$ .
$C_T$	Total concentration, $mol\ m^{-3}$ .
$D_i$	Diffusion coefficient of species $i$ , $m^2\ s^{-1}$ .
$d_M$	Membrane thickness, $m$ .
$F$	Faraday constant, $C\ mol^{-1}$ .
$H_i$	Henry's law constant, $Pa^{-1}$ .
$i$	Local proton exchange current density, $A\ m^{-2}$ .
$I$	Overall current density, $A\ m^{-2}$ .
$k_M$	Membrane proton conductivity, $S\ m^{-1}$ .
$l_C$	Catalyst layer thickness, $m$ .
$N_i$	Molar flow rate of species $i$ , $mol\ s^{-1}$ .
$n_{drag,i}$	Transport number (electro-osmotic drag) of species $i$ .
$p_i$	Partial pressure of species $i$ , $Pa$ .
$P_i$	Permeability towards species $i$ , $mol\ m^{-1}\ s^{-1}$ .
$Q^F$	Feed volumetric flow rate, $m^3\ s^{-1}$ .
$R_{contact}$	Fuel cell contact resistance, $\Omega\ m^2$ .
$R$	Ideal gas constant, $J\ mol^{-1}\ K^{-1}$ .
$S_i$	Membrane swelling in species $i$ , $g_{water}\ g_{polymer}^{-1}$ .
$T$	Temperature, $K$ .
$U_{cell}$	Fuel cell potential, $V$ .
$x_i$	Molar fraction of species $i$ in the liquid phase (anode and membrane).
$y_i$	Molar fraction of species $i$ in the gas phase (cathode).
$z$	Axial coordinate, $m$ .

**Greek letters**

$\nu_{r,i}$	Stoichiometric coefficient of species $i$ in reaction $r$ .
$\eta_F$	Faraday efficiency.
$\eta_P$	Potential efficiency.
$\eta_{DMFC}$	Overall DMFC efficiency.
$\gamma$	Chemical reaction order.
$\eta$	Overpotential, V.
$\mu$	Viscosity, N s m <sup>-2</sup> .
$\varepsilon$	Void fraction (porosity).

**Subscripts**

1	Methanol.
2	Water.
3	Oxygen.
4	Carbon dioxide.
5	Nitrogen.
A	Anode.
C	Cathode.
Cell	DMFC cell
$i$	Species $i$ .
L	Liquid phase.
M	Membrane.
MeOH	Methanol (cathode related, crossover).
$r$	Reaction $r$ presented in Fig. 6.1.
Ref	Reference.
T	Total.
V	Vapor phase.

## Superscripts

CA	Anode catalyst layer.
CC	Cathode catalyst layer.
DA	Anode diffusion layer.
DC	Cathode diffusion layer.
Eff	Effective.
FA	Anode compartment.
FC	Cathode compartment.
L	Liquid phase.
M	Membrane.
OCV	Open circuit voltage.
rev	Reversible reaction.
V	Vapor phase.

## References

- [1] A. S. Aricò, S. Srinivasan and V. Antonucci, DMFCs: From fundamental aspects to technology development, *Fuel Cells* 1 (2001) 133.
- [2] C. Manea and M. Mulder, Characterization of polymer blends of polyethersulfone/sulfonated polysulfone and polyethersulfone/sulfonated polyetheretherketone for direct methanol fuel cell applications, *J. Membr. Sci.* 206 (2002) 443.
- [3] J. Cruickshank and K. Scott, The degree and effect of methanol crossover in the direct methanol fuel cell, *J. Power Sources* 70 (1998) 40.
- [4] S. Cleghorn, X. Ren, S. Thomas and S. Gottesfeld, Book of extended abstracts, 1997 ISE-ECS Joint Symposium, Paris, Sept. 1997, Abstract n. 182, 218.
- [5] S. M. J. Zaidi, S. D. Mikailenko, G. P. Robertson, M. D. Guiver and S. Kaliaguine, Proton conducting composite membranes for polyether ether ketone and heteropolyacids for fuel cell applications, *J. Membr. Sci.* 173 (2000) 17.
- [6] K. A. Kreuer, On the development of proton conducting polymer membranes for hydrogen and methanol fuel cells, *J. Membr. Sci.* 185 (2001) 3.
- [7] J. Kerres, W. Zhang, L. Jörissen and V. Gogel, Application of different types of polyaryl-blend-membranes in DMFC, *J. New Mater. Electrochem. Systems* 5 (2002) 97.

- [8] G. Alberti, M. Casciola, L. Massinelli and B. Bauer, Polymeric proton conducting membranes for medium temperature fuel cells (110-160°C), *J. Membr. Sci.* 185 (2001) 73
- [9] V. S. Silva, B. Ruffmann, S. Vetter, A. Mendes, L. M. Madeira and S. P. Nunes, Characterization and application of composite membranes in DMFC, *Catalysis Today*, (in press, 2005).
- [10] M. L. Ponce, L. Prado, B. Ruffmann, K. Richau, R. Mohr and S. P. Nunes, Reduction of methanol permeability in polyetherketone-heteropolyacid membranes, *J. Membr. Sci.* 217 (2003) 5.
- [11] S. P. Nunes, B. Ruffmann, E. Rikowsky, S. Vetter and K. Richau, Inorganic modification of proton conductive polymer membranes for direct methanol fuel cells, *J. Membr. Sci.* 203 (2002) 215.
- [12] V.S. Silva, B. Ruffmann, H. Silva, Y. A. Gallego, A. Mendes, L. M. Madeira and S. P. Nunes, Proton electrolyte membrane properties and direct methanol fuel cell performance. I. Characterization of hybrid sulfonated poly(ether ether ketone)/zirconium oxide membranes, *J. Power Sources* 140 (2005) 34.
- [13] K.Z. Yao, K. Karan, K.B. McAuley, P. Oosthuizen, B. Peppley and T. Xie, A review of mathematical models for hydrogen and direct methanol polymer electrolyte membrane fuel cells, *Fuel Cells* 4 (2004) 3.
- [14] V.S. Silva, J. Schirmer, R. Reissner, B. Ruffman, H. Silva, A. Mendes, L.M. Madeira, S.P. Nunes, Polymer electrolyte membrane properties and direct methanol fuel cell performance. II. Fuel cell performance and membrane properties effects, *J. Power Sources* 140 (2005) 41.
- [15] H. Dohle, J. Divisek and R. Jung, Process engineering of the direct methanol fuel cell, *J. Power Sources* 86 (2000) 469.
- [16] X. Ren, T.E. Springer and S. Gottesfeld, Water and methanol uptakes in Nafion membranes and membrane effects on direct methanol cell performance, *J. Electrochem. Soc.* 147 (2000) 92.
- [17] S. Gottesfeld and T. A. Zawodzinski, in *Advances in electrochemical science and engineering*, Vol. 5, R.C. Alkire and D.M. Kolb, Editors, Wiley VCH, Weinheim (1997).
- [18] A. Parthasarathy, S. Srinivasan, A.J. Appleby and C.R. Martin, Temperature dependence of the electrode kinetics of oxygen reduction at the platinum/nafion interface – A microelectrode investigation, *J. Electrochem. Soc.* 139 (1992) 2530.
- [19] X. Ren, P. Zelenay, S. Thomas, J. Davey and S. Gottesfeld, Recent advances in direct methanol fuel cells at Los Alamos National Laboratory, *J. Power Sources* 86 (2000) 111.
- [20] V.S. Bagotsky and Y.B. Vasilyev, Some characteristics of oxidation reactions of organic compounds on platinum electrodes, *Electrochim. Acta* 9 (1964) 869.

- [21] K.T. Jeng, C.W. Chen, Modeling and simulation of a direct methanol fuel cell anode, *J. Power Sources* 112 (2002) 367.
- [22] R.B. Bird, W.E. Stewart and E.N. Lightfoot, *Transport phenomena*, 2nd ed., John Wiley & Sons, Inc., New York (2002).
- [23] J.T. Wang and R.F. Savinell, in *Electrode materials and processes for energy conversion and storage*, S. Srinivasan, D.D. MacDonald and A.C. Khandkar, Editors, The Electrochemical Society Proceedings Series, Pennington, NJ (1994).
- [24] M. Mench and C.Y. Wang, An in-situ method for determination of current distribution in PEM fuel cells applied to a direct methanol fuel cell, *J. Electrochem. Soc.* 150 (2003) A79.
- [25] X. Ren, W. Handerson and S. Gottesfeld, Electro-osmotic drag of water in ionomeric membranes. New measurement employing a direct methanol fuel cell, *J. Electrochem. Soc.* 144 (1997) L267.
- [26] X. Ren, T.E. Springer, T.A. Zawodzinski and S. Gottesfeld, Methanol transport through nafion membranes. Electro-osmotic drag effects on potential step measurements, *J. Electrochem. Soc.* 147 (2000) 466.
- [27] W. Neubrand, *Modellbildung und simulation von elektromembranverfahren*, PhD thesis, University of Stuttgart (1999).
- [28] L. Petzold, Automatic selection of methods for solving stiff and nonstiff systems of ordinary differential equation, *SIAM J. Sci. Stat. Comput.* (1983) 4.
- [29] A. Siebke, W. Schunurnberger, F. Meier and G. Eigenberger, Investigation of the limiting processes of a DMFC by mathematical modeling, *Fuel Cells* 3 (2003) 37.
- [30] H. Dohle, J. Divisek, J. Mergel, H.F. Oetjen, C. Zingler and D. Stolten, Recent developments of the measurement of the methanol permeation in a direct methanol fuel cell, *J. Power Sources* 105 (2002) 274.
- [31] J.J. Baschuk and X. Li, Modeling of polymer electrolyte fuel cells with variable degrees of water flooding, *J. Power Sources* 86 (2000) 181.
- [32] C. W. Tobias, *Advances in electrochemistry and electrochemical engineering*, John Wiley & Sons, Inc., New York (1962).
- [33] Z.H. Wang and C.Y. Wang, Mathematical modeling of liquid-feed direct methanol fuel cells, *J. Electrochem. Soc.* 150 (2003) A508.
- [34] V.M. Barragán and A. Heizel, Estimation of the membrane methanol diffusion coefficient from open circuit voltage measurements in a direct methanol fuel cell, *J. Power Sources* 104 (2002) 66.

- [35] V.S. Silva, S. Weisshaar, R. Reissner, B. Ruffman, S. Vetter, A. Mendes, L.M. Madeira, S.P. Nunes, Performance and efficiency of a DMFC using non-fluorinated composite membranes operating at low/medium temperatures, *J. Power Sources* (in press, 2005).
- [36] F. Dreisbach and H. W. Lösch, Magnetic suspension balance for simultaneous measurement of a sample and the density of the measuring fluid, *J. Therm. Anal. Calorim.* 62 (2000) 515.
- [37] A.A. Kulikovsky, The voltage-current curve of a direct methanol fuel cell: “exact” and fitting equations, *Electrochem. Commun.* 4 (2002) 939.

## **Chapter 7. Proton exchange membranes for direct methanol fuel cells: Properties critical study concerning methanol crossover and proton conductivity\***

### **Abstract**

Generally, standard R&D procedures regarding the proton exchange membrane (PEM) development for direct methanol fuel cell (DMFC) applications do not allow direct conclusions concerning the PEM limiting characteristics. In this regard, a recent developed DMFC model is used to predict the influence of the PEM proton conductivity and permeability towards methanol on the DMFC performance. In addition, the application of the present model was performed in order to answer some open questions regarding the PEM properties for DMFC applications. The mathematical model uses as inputs membrane properties obtained from easy-to-implement standard characterization methods. From the simulation results it was verified that the PEM electrolyte and barrier properties play a decisive role on the DMFC performance. The proton conductivity seems to influence mainly the DMFC current and power density and the cell efficiency regarding fuel conversion (Faraday efficiency). On the other hand, the permeability towards methanol was found to influence all the studied DMFC outputs as it is directly related to the fuel loss and parasitic reaction of methanol in the cathode catalyst layer. As expected, the simulations show that the optimal PEM properties for DMFC applications are high proton conductivity to reduce the ohmic losses and low permeability towards methanol in order to prevent the crossing over of methanol from the anode to the cathode.

\*V.S. Silva, A. Mendes, L.M. Madeira and S.P. Nunes (submitted, 2005).

## 7.1. Introduction

The research and development of novel proton exchange membranes (PEM) is known to be one of the most challenging issues regarding the direct methanol fuel cell (DMFC, Fig. 7.1) technology [1, 2]. The PEM is usually designated as the heart of the DMFC, and should ideally combine high proton conductivity (electrolyte properties) with low permeability towards DMFC species (barrier properties). Additionally it should have a very high chemical and thermal stability in order to enable the DMFC operation at up to 150°C [1, 2].

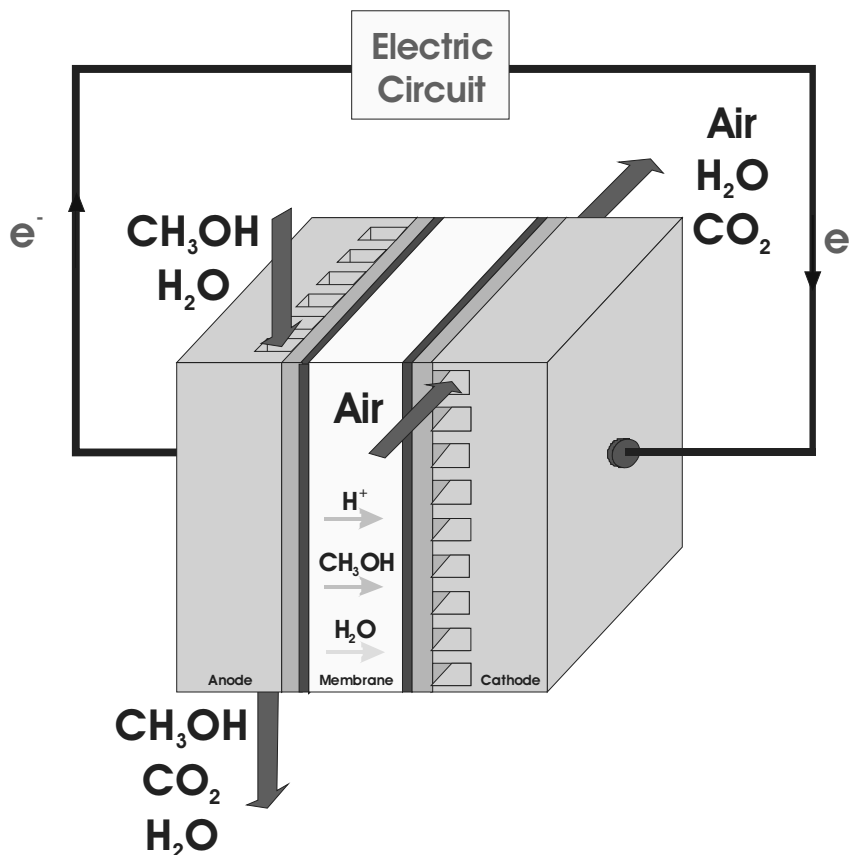


Fig. 7.1. Sketch of a DMFC illustrating protons, methanol and water transport through the proton exchange membrane.

Nowadays, perfluorinated ion-exchange polymers, such as Nafion<sup>®</sup> from Dupont and Flemion<sup>®</sup> from Asahi Chemical, are the most commonly used for DMFC applications [2]. This kind of membranes combines the extremely high hydrophobicity of the perfluorinated backbone (mechanical strength) with the extremely high hydrophilicity of the sulfonic acid functional groups (high proton conductivity) [2]. In the presence of water, this effect is even more pronounced due to the aggregation of the hydrophilic domains (nano-separation) [2]. Consequently, methanol and

water are readily transported across perfluorosulfonic acid membranes [1-4]. Therefore, in the DMFC, the permeated methanol is chemically oxidized to CO<sub>2</sub> and H<sub>2</sub>O at the cathode, decreasing the fuel efficiency and depolarizing the cathode. Apart from this, it can also adversely affect the cathode performance due to the consumption of oxygen through the parasitic methanol oxidation at the cathode catalyst layer, lowering the oxidant activity in this side of the cell [5].

Thus, it is necessary to develop and test new materials that eliminate or, at least, reduce the reactants loss without decreasing in the same degree the proton conductivity [6]. Recently, we characterized and tested non-fluorinated membranes based on sulfonated polyetherketones, used as plain polymer or modified with composites or proton conductors [7-10]. The polyetherketones can be easily made hydrophilic by sulfonation reactions, being the sulfonation degree (SD) controlled by the reaction time and temperature. The sulfonation degree can optimize the hydrophobic-hydrophilic balance, acting directly on the electrolyte and barrier properties, as well as in the chemical and thermal stability of the polymer [9-11]. Higher sulfonation degrees increase the polymer proton conductivity and tend to improve the DMFC performance (power output). However, the permeability towards methanol also increases concurrently, decreasing the fuel cell efficiency [12]. On the other hand, the polymer stability tends to progressively deteriorate with the sulfonation degree.

The PEM properties regarding proton conductivity and methanol permeation can be also improved by the preparation of composite membranes by the incorporation of inorganic-ceramic materials. For an optimized composition, the composite material may have superior performance as compared to the plain polymer [13]. The use of solid polymer-ceramic composite materials in fuel cell applications has several attributes of interest [13]. Mostly, the incorporation of inorganic-ceramic materials decreases the methanol permeability due to improved barrier properties. However, in most of the cases, the proton conductivity also decreases due to less hydrophilic characteristics (lower water swelling). On the other hand, the incorporation of inorganic-ceramic materials increases the membrane stability, providing better long-term structural stability and the possibility of operation at higher temperatures [14].

In the last decade, a significant progress has been achieved regarding membrane development for DMFC applications [2, 6-12, 15-20]. However, there are still many open questions, especially concerning the PEM formulation (e.g. sulfonation degree, inorganic material nature and content) that allows the preparation of membranes with an optimal compromise between electrolyte and barrier properties. In order to answer these open questions, we believe that it is of decisive importance to develop novel R&D tools that can be used as complementary to the membrane standard characterization methods and DMFC tests [21, 22]. A useful procedure should enable the

critical evaluation of the membrane proton conductivity and methanol permeability effects on the DMFC performance and efficiency.

Recently, we developed a semi-empirical mathematical model that enables the prediction of the DMFC performance using inputs obtained by easy-to-implement characterization methods [23]. In order to have a wide variety of physical/chemical properties, the model was developed using a set of sulfonated poly(ether ether ketone) (sPEEK) hybrid membranes with sulfonation degree of 87%, modified with different amounts of zirconium oxide (5.0, 7.5, 10.0 and 12.5wt.% ZrO<sub>2</sub>) [21]. The PEM properties ranged from high to very low proton conductivity and permeability towards methanol values.

The present chapter focuses on the use of the developed model to predict the DMFC performance for a wide range of proton conductivity and permeability towards methanol of the proton exchange membrane. The aim of this approach is to perform a critical study concerning the influence of the PEM electrolyte and barrier properties on the DMFC power output and efficiency. We believe that this approach will short tremendously our efforts for the design of new materials with optimal characteristics for DMFC applications.

## **7.2. Mathematical Model**

Until now, the developed mathematical models of the DMFC focused mainly on the fuel cell operating conditions using perfluorinated membranes as PEM [24]. Unfortunately, these models use data obtained from the literature that are usually impossible to reproduce by membrane development research groups and, in many cases, these parameters hardly represent the properties of membranes under development (thus limiting the success of the model) [23]. In order to provide a useful tool for predicting the DMFC performance for a certain material, we developed a semi-empirical mathematical model for the DMFC that uses standard characterization results as inputs. This one-dimensional steady-state model is described elsewhere [23]. The model uses PEM data obtained by the following characterization methods: pervaporation (liquid species permeability, CH<sub>3</sub>OH and H<sub>2</sub>O), gas permeation (gas species permeability, N<sub>2</sub>, O<sub>2</sub> and CO<sub>2</sub>), water uptake (water swelling) and impedance spectroscopy (proton conductivity). The model was validated using the experimental DMFC performance presented in a previous work [22], in which are also presented the detailed specifications regarding the cell tests. The present study is focused on the effect of the membrane electrolyte and barrier properties on the DMFC performance. Therefore, the cell operating temperature is assumed to be constant and equal to 70°C.

In the present study, proton conductivity and methanol permeability values ranging from 1.18 to 3.39 S m<sup>-1</sup> and 4.00·10<sup>-7</sup> to 1.32·10<sup>-5</sup> mol s<sup>-1</sup> m<sup>-1</sup>, respectively, were selected. These ranges were selected based on characterization data recently published elsewhere [17, 21]. In terms of methanol/water selectivity, since the model does not account the cathode flooding effect due to the permeation of water through the membrane, it was assumed a constant value of 0.1 for all the simulated properties. On the other hand, it was also assumed constant PEM permeabilities towards gaseous species (the data used were obtained for the sPEEK membrane with SD = 87% and 5.0wt.% ZrO<sub>2</sub>). The membrane thickness was assumed also to be constant for all simulations (133μm). In contrast, due to the much higher influence of the water uptake on the DMFC performance prediction [23], a linear variation of this property with the proton conductivity was assumed. From the experimental data obtained for the hybrid membranes used for the model validation, this assumption is considered a good approximation due to the intimate relation between water uptake and proton conductivity [21].

The mathematical model was implemented to predict the influence of the PEM proton conductivity and permeability towards methanol on the DMFC current-voltage polarization curves, constant voltage current at 35mV (CV, 35mV), open circuit voltage (OCV), CO<sub>2</sub> concentration at the cathode outlet for CV and OCV experiments. Apart from this, the model was also used for predicting the influence of the studied PEM properties on the DMFC potential, Faraday and global efficiencies. The potential efficiency is defined as the DMFC voltage divided by the standard cell voltage. On the other hand, the Faraday efficiency is defined as the ratio between the converted fuel for current production (anode) and the total amount of converted fuel (anode and cathode). The DMFC global efficiency evaluation is performed by combining both Faraday and potential efficiency as presented in [14].

## 7.3. Results and discussion

### 7.3.1. DMFC performance

Fig. 7.2 shows the predicted effect of the PEM proton conductivity and permeability towards methanol on the current density-voltage curves of the DMFC. From Fig. 7.2a it can be observed that when the PEM proton conductivity increases, the DMFC performance also increases (assuming a methanol permeability of 2.95×10<sup>-6</sup> mol s<sup>-1</sup> m<sup>-1</sup>). This fact can be explained by the lower PEM ohmic losses for higher membrane proton conductivity. As the current density increases, ohmic

losses due to the PEM start to limit the cell performance and, consequently, the membranes with higher proton conductivity yield the best DMFC performance. On the other hand, from Fig. 7.2b it can be seen that the DMFC performance decreases with the membrane permeability towards methanol (assuming a proton conductivity of  $2.98 \text{ S m}^{-1}$ ). These predicted results can be attributed to the higher DMFC overpotential loss associated to the methanol crossover (parasite reaction at the cathode). Furthermore, there is also the detrimental effect of the parasitic consumption of oxygen at the cathode catalyst layer (thus decreasing the  $\text{O}_2$  partial pressure). Since the reaction order of the oxygen reduction at the cathode catalyst layer is 0.4 [25], the extra consumption of oxygen from the methanol crossover results in a lower cell potential and, hence, a lower power density.

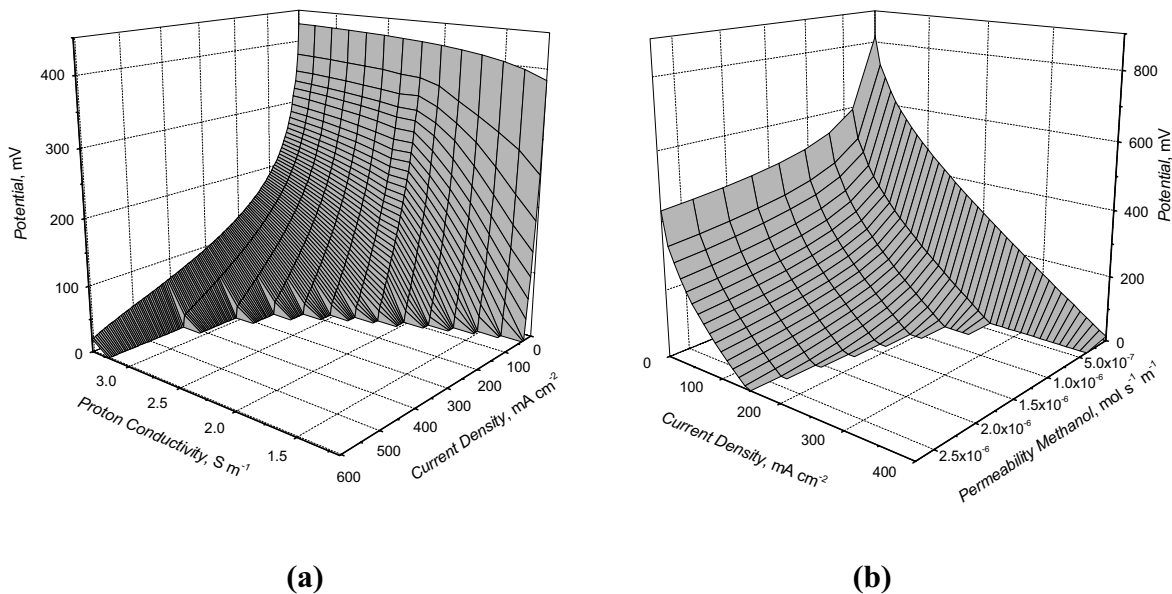


Fig. 7.2. Predicted current density-voltage plots of the DMFC, at  $70^\circ\text{C}$ , as a function of the PEM: (a) proton conductivity (permeability towards methanol of  $2.95 \times 10^{-6} \text{ mol s}^{-1} \text{ m}^{-1}$ ) and (b) permeability towards methanol (proton conductivity of  $2.98 \text{ S m}^{-1}$ ).

The model simulations regarding the effect of the PEM proton conductivity and methanol permeability on the open circuit voltage are presented in Fig. 7.3. As expected, it can be observed that the OCV decreases with the PEM permeability towards methanol. This is due to the direct relationship between OCV and the methanol crossover [26, 27]. In addition, it can be observed that the methanol permeability has a higher effect on OCV for values lower than  $4.00 \times 10^{-6} \text{ mol s}^{-1} \text{ m}^{-1}$ . This result can be attributed to the reduced methanol concentration in the cathode catalyst layer for low membrane permeability towards methanol, thus limiting the overpotential loss due to the methanol crossover. As expected, the maximum value for OCV is achieved for the lowest methanol

permeation. From Fig. 7.3, it can be also noticed a slight variation of the OCV with the proton conductivity, although with a more pronounced effect for lower proton conductivity. This fact can be explained by the model ability to predict the influence of the proton conductivity on the DMFC open circuit voltage [23]. It is known that the open cell voltage evaluation using standard fuel cell characterization potentiostats cannot be performed without any current flowing due to equipment resistance limitations (usually 0.01 A). Therefore, membranes with very low proton conductivity ( $k_M \cong 0 \text{ S m}^{-1}$ ) increase the DMFC ohmic losses, even for OCV operating conditions (low currents flowing) and, consequently, the fuel cell measured potential decreases. We verified this fact experimentally for several membranes with very low electrolyte properties [22].

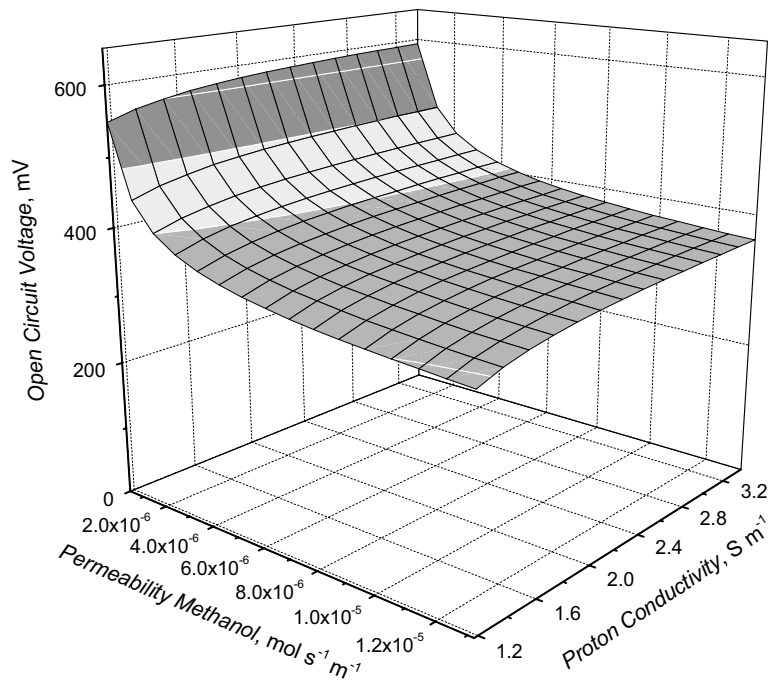


Fig. 7.3. Predicted open circuit voltage, at 70°C, as a function of the PEM proton conductivity and permeability towards methanol.

For open circuit voltage experiments, the  $\text{CO}_2$  concentration at the cathode outlet as a function of the PEM proton conductivity and methanol permeability is shown in Fig. 7.4. It can be seen that the permeability towards methanol has a much higher effect on the  $\text{CO}_2$  concentration than proton conductivity (which effect can be practically neglected). From this plots it can be observed that the  $\text{CO}_2$  concentration at the cathode outlet, for OCV experiments, starts to be constant for high methanol permeation. This fact can be explained by the limited reaction capacity of the cathode

catalyst layer for the methanol parasitic oxidation, leading to higher amounts of unreacted methanol at the cathode outlet for even higher PEM methanol permeability values.

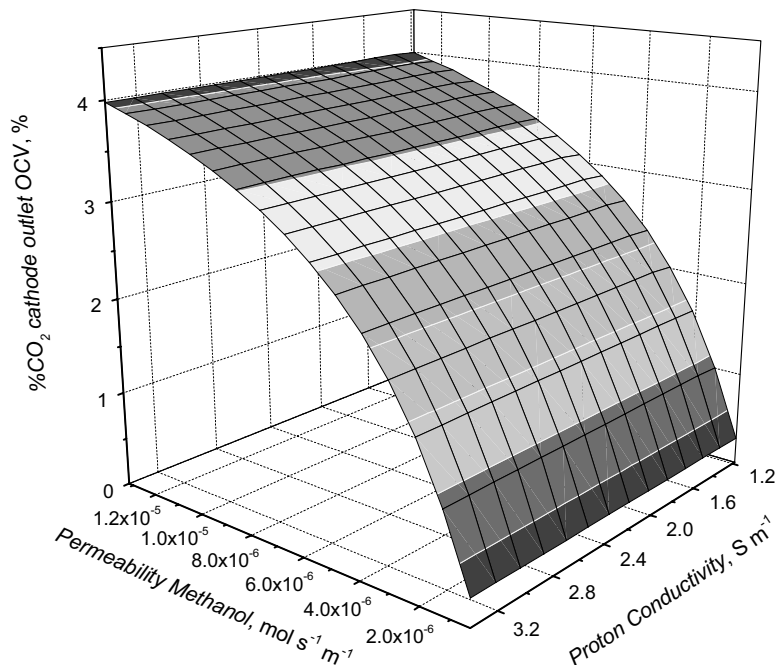


Fig. 7.4. Predicted CO<sub>2</sub> concentration at the cathode outlet for open circuit voltage experiments, at 70°C, as a function of the PEM proton conductivity and permeability towards methanol.

Apart from studying the current density-voltage polarization curves and open circuit voltage, in the present study the current density for constant voltage (CV) experiments, at 35mV, were also simulated (Fig. 7.5). It can be seen that the highest current density at 35mV is achieved for the lowest methanol permeability and highest proton conductivity. However, the current density at 35mV seems to be more affected by the PEM proton conductivity (Fig. 7.5). Even for high methanol permeation, the model predicts nearly 300mA cm<sup>-2</sup> for the highest proton conductivity (3.39 S m<sup>-1</sup>). This fact can be explained by lower ohmic losses associated to this membrane, although presenting a high parasitic overpotential due to the methanol crossover. An excellent example of a PEM with high proton conductivity and methanol permeation is the commonly used Nafion<sup>®</sup>. Although having high permeability towards methanol (thus lower methanol conversion efficiency), this membrane has a good performance in terms of energy production. However, it should be mentioned that for high proton conductivity, the DMFC current density output at 35mV can be almost doubled for improved barrier properties. On the other hand, for lower electrolyte

properties, the DMFC presents limited maximum current density at 35mV due to the dominant high ohmic losses. For these conditions, the barrier properties of the membrane have almost no influence on the DMFC performance because nearly no current is produced.

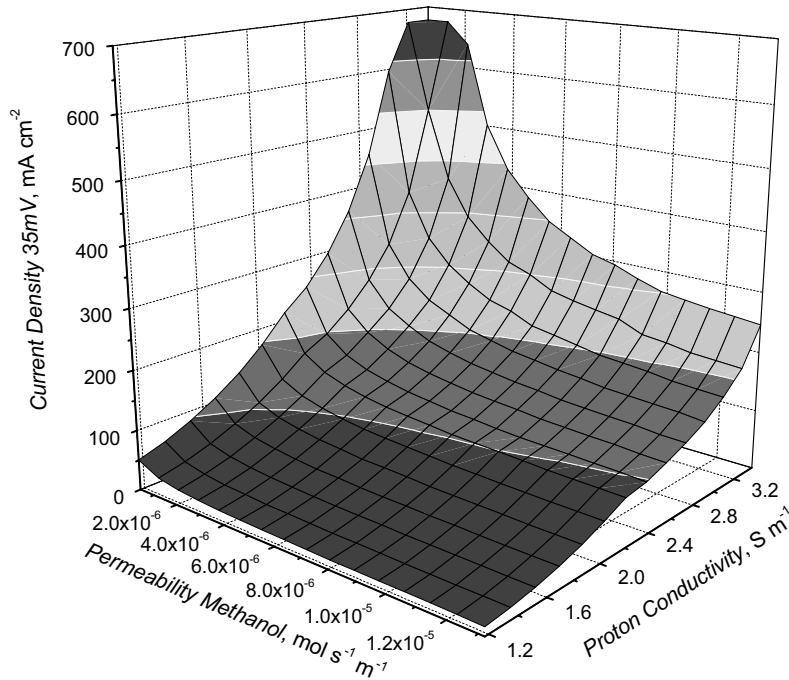


Fig. 7.5. Predicted current density (constant voltage experiments, 35mV), at 70°C, as a function of the PEM proton conductivity and permeability towards methanol.

The variation of the CO<sub>2</sub> concentration at the cathode outlet for constant voltage experiments at 35mV was also plotted as a function of the electrolyte and barrier PEM properties (Fig. 7.6). From these simulations it can be observed that the predicted CO<sub>2</sub> concentration at the cathode outlet for constant voltage experiments is lower compared to OCV experiments (Fig. 7.4). When the DMFC is under load conditions, there will be a consumption of methanol at the anode catalyst layer and, consequently, a lower methanol mass transfer gradient across the membrane is expected (leading to lower CO<sub>2</sub> concentrations). In contrast, during OCV experiments, the concentration of methanol at the anode-membrane interface is maximal because no methanol is being consumed (no current output). Consequently, the methanol crossover is higher due to a larger mass transfer driving force across the membrane, making the detrimental effect of the methanol crossover more noticeable for OCV experiments [26, 27]. Apart from this, Fig. 7.6 also shows that the CO<sub>2</sub> concentration decreases with proton conductivity, specially for higher permeability towards

methanol. This fact can be explained by the lower methanol concentration gradient due to the methanol consumption at the anode catalyst layer. For increased PEM proton conductivity one expects higher methanol transport by electro-osmotic drag (higher current density), leading to higher concentrations of  $\text{CO}_2$  at the cathode outlet. However, when a certain current density level is achieved, increased consumption of methanol at the anode catalyst layer leads to a shortage of methanol and then to a lower methanol diffusion rate;  $\text{CO}_2$  concentration at the cathode outlet then decreases.

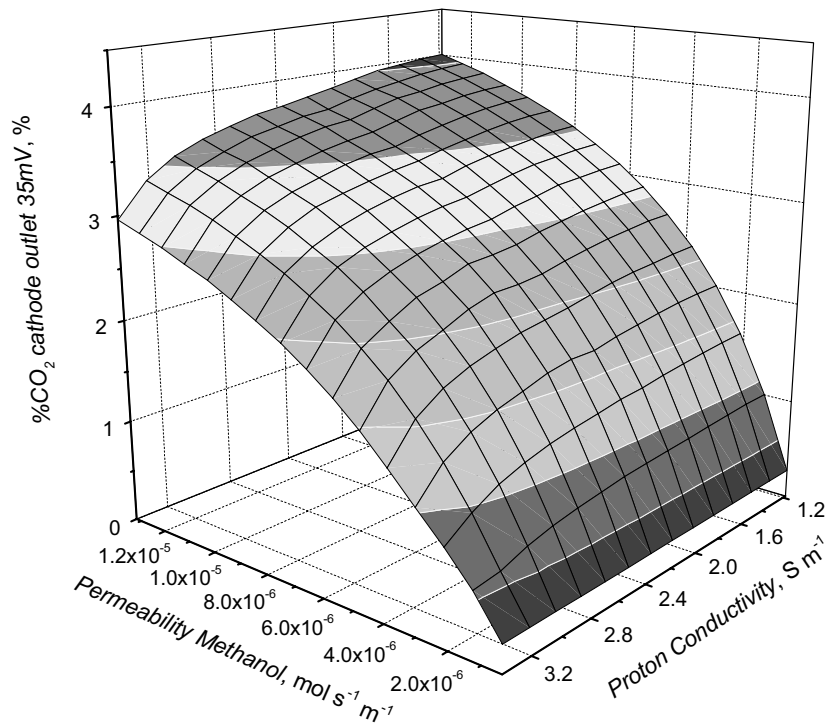


Fig. 7.6. Predicted  $\text{CO}_2$  concentration at the cathode outlet for constant voltage experiments, 35mV, at 70°C, as a function of the PEM proton conductivity and permeability towards methanol.

In terms of PEM properties influence on the DMFC maximum power density, from Fig. 7.7 it can be observed that the highest value is obtained for high proton conductivity and low permeability towards methanol. The simulations predict that a DMFC can achieve power densities higher than  $20 \text{ mW cm}^{-2}$  using membranes with proton conductivity higher than  $2.53 \text{ S m}^{-1}$  and permeability towards methanol lower than  $4.65 \times 10^{-6} \text{ mol s}^{-1} \text{ m}^{-1}$ . In fact, this power density may seem low for DMFC applications at 70°C. However, it should be noticed that the model was developed and validated using electrodes with low catalyst loadings [23].

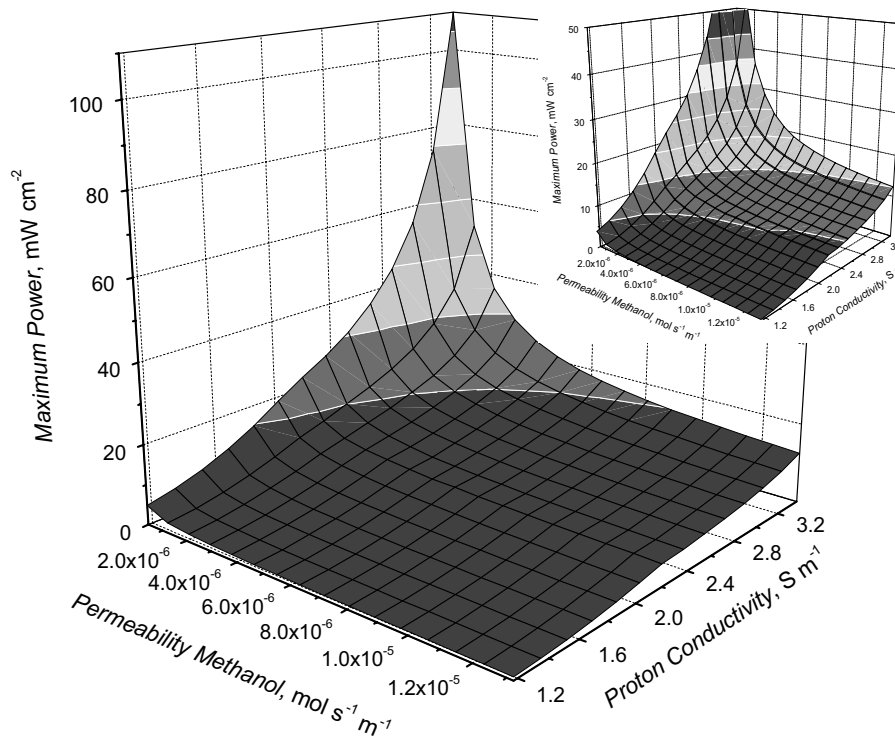


Fig. 7.7. Predicted maximum power density, at 70°C, as a function of the PEM proton conductivity and permeability towards methanol.

### 7.3.2. DMFC efficiency

The DMFC efficiency depends strongly on the two main factors: i) electro-catalytic kinetics of the methanol oxidation at the anode and ii) permeability of the proton exchange membrane towards methanol. The first limitation leads to considerable high anodic overpotentials, lowering the cell voltage significantly below the theoretically expected values. On the other hand, the high methanol permeation from the anode to the cathode through the proton exchange membrane promotes the methanol oxidation at the cathode, leading to a loss of potential due to the methanol/oxidation mixed potential and lower oxygen activity at the cathode. Apart from that, it leads also to a loss of reactant and, therefore, to lower DMFC efficiency. As mentioned before, in order to predict the effect of the proton conductivity and permeability towards methanol on the DMFC efficiency, the potential, Faraday and global DMFC efficiencies are considered.

Fig. 7.8 shows the maximum potential efficiency as a function of the PEM proton conductivity and permeability towards methanol. It should be noticed that the maximum potential efficiency is obtained for open circuit voltage because, as it is known, for this conditions the potential is maximal (lower overpotential losses). From Fig. 7.8 it can be seen that from the lowest

to the highest permeability towards methanol, the predicted maximum potential efficiency decreases approximately between 15 to 18%. The explanation of the electrolyte and barrier properties effects on the potential efficiency are the same as discussed before for the open circuit voltage (Fig. 7.3).

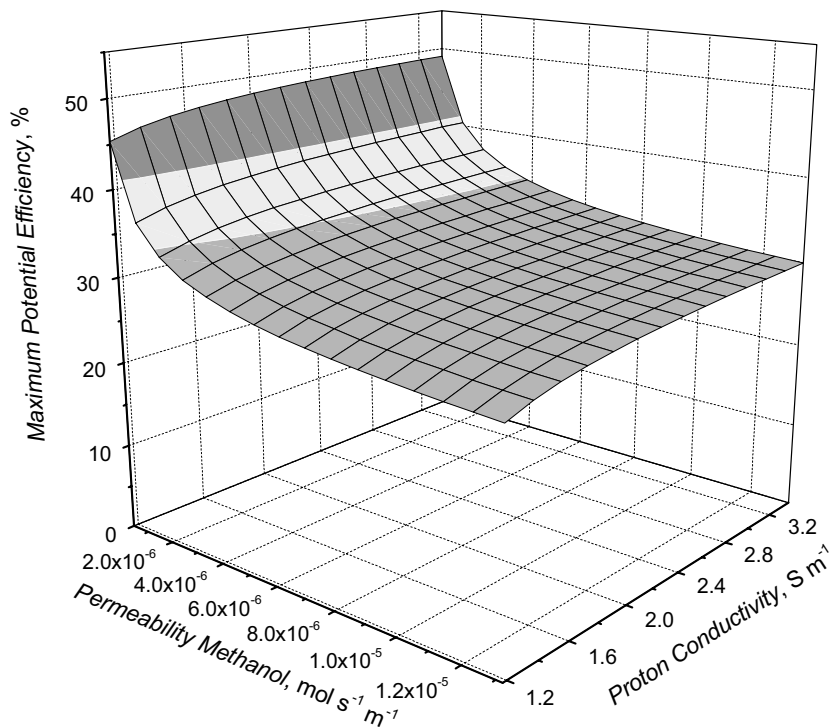


Fig. 7.8. Predicted maximum potential efficiency, at 70°C, as a function of the PEM proton conductivity and permeability towards methanol.

Regarding the maximum Faraday efficiency, the model simulations are presented in Fig. 7.9. The maximum Faraday efficiency is evaluated for the maximum current density due to the associated lower methanol losses. As expected, it can be observed that the fuel losses decrease for lower PEM methanol permeation. Moreover, the influence of permeability towards methanol seems to decrease with the increase of the proton conductivity. This fact can be explained by the decreasing methanol mass transfer gradient across the membrane for increasing current density. High proton conductivity decreases the DMFC ohmic loss and therefore higher current density is obtained (lower methanol concentration at the anode). Also, due to the same reason, the influence of the proton conductivity seems to be higher for high permeability towards methanol. In contrast, for low methanol permeation, the influence of the proton conductivity is nearly negligible because almost no methanol crossover exists (higher Faraday efficiency).

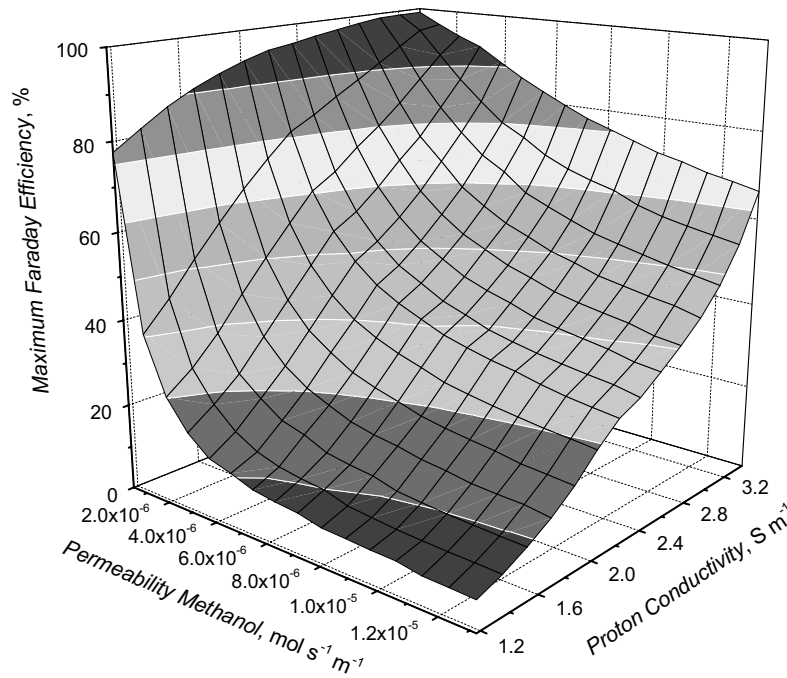


Fig. 7.9. Predicted maximum Faraday efficiency, at 70°C, as a function of the PEM proton conductivity and permeability towards methanol.

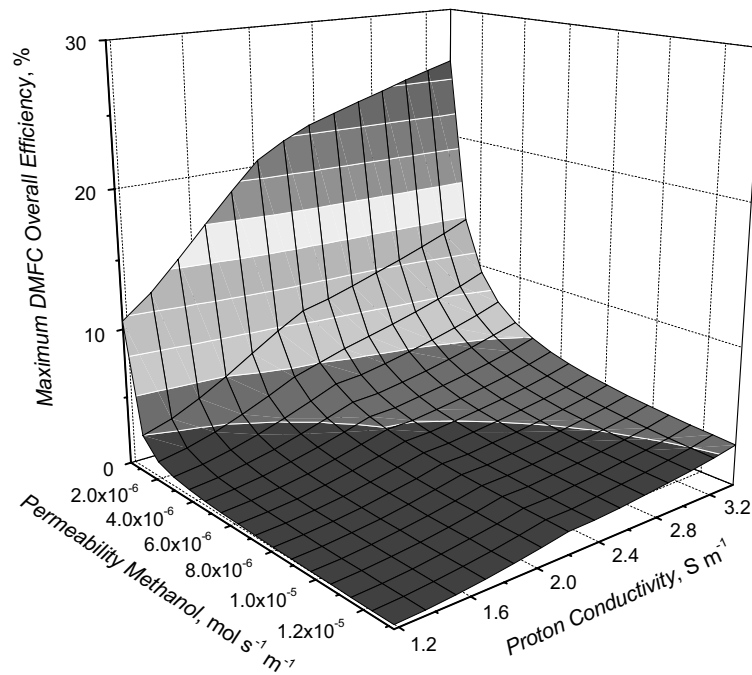


Fig. 7.10. Predicted maximum DMFC global efficiency, at 70°C, as a function of the PEM proton conductivity and permeability towards methanol.

Fig. 7.10 shows the maximum DMFC overall efficiency as a function of the electrolyte and barrier properties of the PEM. As expected, it can be seen that the lowest levels for the DMFC overall efficiency are obtained for low proton conductivity and high permeability towards methanol. For the studied range of the permeability towards methanol, this property seems to have very high influence on the DMFC overall efficiency, even for high PEM proton conductivity (high current density). On the other hand, the proton conductivity seems to have higher influence on the maximum overall DMFC efficiency for lower methanol permeations. This fact can be explained by the low potential losses due to the membrane ohmic resistance (Fig. 7.8). For high methanol permeations, the losses of efficiency are mainly due to the methanol crossover. As expected, the highest value for the maximum DMFC overall efficiency is achieved for the highest electrolyte and barrier properties.

### 7.3.3. Case study

In Table 7.1 are given some predicted and experimental results for membranes that were developed and tested previously [21]. It can be observed that, although assuming several approximations, as mentioned before, the model predictions show qualitative good agreement with the experimental results obtained for the membranes used on its validation (sPEEK SD=87% with 5.0 and 7.5wt.% of ZrO<sub>2</sub>). Even presenting some deviations concerning the prediction of the current density for constant voltage experiments, at 35mV, it can be observed that the model is able to clearly differentiate the influence of different physical and chemical properties of the membranes in all the studied DMFC outputs. Furthermore, the model is also able to predict, with acceptable agreement, the DMFC performance using other membranes, such as Nafion<sup>®</sup> 1135 and sPEEK with SD=42% (Table 7.1). The experimental results presented in Table 7.1 for the sPEEK SD=42% membrane were obtained using a PEM thickness of 55μm.

As an example of the usefulness of the present model, it can be mentioned a R&D case study regarding the sPEEK sulfonation degree optimization and possible inorganic modification in order to improve the barrier properties. After developing sPEEK membranes with a sulfonation degree of 42% that enabled DMFC performances similar as that obtained using Nafion<sup>®</sup> (Table 7.1), the modification of the polymer with 1.0wt.% of ZrO<sub>2</sub> was assumed as a potential mean of decreasing the methanol permeation [11, 21]. However, it is known that the incorporation of ZrO<sub>2</sub> also decreases the proton conductivity. Although not having the possibility to test this membrane in the set-up described in [28], the model prediction show that the incorporation of 1.0wt.% of ZrO<sub>2</sub> in

the sPEEK polymer with SD=42% decreases strongly the DMFC power output. The model shows that the detrimental decrease of the proton conductivity is much more influent on the DMFC performance than the advantages associated with the lower permeability towards methanol. Therefore, this trend shows that the incorporation of ZrO<sub>2</sub> as a stand alone inorganic charge is not favorable for the DMFC performance due to its high impact on the proton conductivity. In order to verify experimentally the model predictions, the membranes were tested in another test bench and it was verified good qualitative agreement with the model predictions (data not shown).

Table 7.1. Predicted and experimented (between branches, tested in set-up described in [28]) DMFC performance, at 70°C, using a selected series of PEMs.

Membrane	$W_{max}$ (mW cm <sup>-2</sup> )	$I_{corr,35mV}$ (mA cm <sup>-2</sup> )	%CO <sub>2</sub> 35mV (%)	OCV (mV)	%CO <sub>2</sub> OCV (%)
sPEEK SD=87% 5.0wt.% ZrO <sub>2</sub> *	9.7 (12.1)	114.8 (183.2)	1.4 (1.7)	447 (470)	1.4 (1.7)
sPEEK SD=87% 7.5wt.% ZrO <sub>2</sub> *	5.8 (5.7)	54.5 (38.8)	0.1 (0.3)	592 (596)	0.1 (0.3)
sPEEK SD=42%**	19.6 (21.3)	249.0 (215.2)	1.0 (0.2)	475 (539)	1.1 (0.5)
Nafion® 1135**	13.2 (38.3)	255.2 (293.8)	2.7 (0.9)	379 (516)	3.4 (1.9)
sPEEK SD=42% 1.0wt.% ZrO <sub>2</sub> **	3.3 (-)	41.6 (-)	0.9 (-)	458 (-)	0.9 (-)

\* Experimental data previously published elsewhere [21]

\*\* Data unpublished

In addition, in the present study it was also evaluated the potential, Faraday and overall efficiency for the studied membranes (Table 7.2). From this table it can be observed that the sPEEK hybrid membrane with sulfonation degree of 87% and 7.5wt.% of ZrO<sub>2</sub> presents the best results. This result can be explained by the improved membrane characteristics in terms of electrolyte and, mainly, barrier properties [17]. In fact, from recently published characterization results [17], it can be seen that when increasing the amount of ZrO<sub>2</sub> from 5.0 to 7.5wt.% for SD=87%, the impact on the proton conductivity is lower than that verified for the sPEEK with SD=42%, from 0.0 to 1.0wt.%. Moreover, the use of a high sulfonation sPEEK as polymer matrix allowed enough proton conductivity for DMFC proposes. However, it should be noticed that the DMFC using this membrane presents the second lowest energy output (Table 7.1).

Table 7.2. Predicted DMFC efficiencies, at 70°C, using a selected series of PEMs.

Membrane	<i>Maximum Potential Efficiency (%)</i>	<i>Maximum Faraday Efficiency (%)</i>	<i>Maximum Global Efficiency (%)</i>
sPEEK SD=87% 5.0wt.% ZrO <sub>2</sub>	37.0	61.4	5.6
sPEEK SD=87% 7.5wt.% ZrO <sub>2</sub>	49.0	89.1	17.2
sPEEK SD=42% Nafion <sup>®</sup> 1135	39.2	84.1	9.5
sPEEK SD=42% 1.0wt.% ZrO <sub>2</sub>	31.3	65.6	3.5
	37.9	46.1	3.5

The second most favorable PEM in terms of efficiency is the sPEEK polymer with SD=42%. This polymer, apart from presenting excellent proton conductivity, has also improved barrier properties in comparison with Nafion<sup>®</sup> 1135. As it is commonly accepted, it can be observed from the simulations that the main limitation of the perfluorinated membrane is the high permeability towards methanol. This characteristic decreases the open circuit voltage (higher methanol crossover overpotential), leading to a lower maximum potential efficiency. Apart from this, it increases also the methanol losses (higher methanol permeation), leading to lower maximum Faraday efficiency. In addition, from Table 7.2, it can be observed that the lowest DMFC efficiency is predicted for the sPEEK SD=42% membrane with 1.0wt.% ZrO<sub>2</sub>. As mentioned before, the main limitation of this membrane is the low proton conductivity that leads to lower current density (higher mass transfer gradient for methanol transport) and lower open circuit voltage associated to higher membrane ohmic losses.

## 7.4. Conclusions

In order to simulate the influence of the PEM electrolyte and barrier properties on the DMFC performance and efficiency, a mathematical model that uses as inputs membrane properties obtained by PEM standard characterization methods, was used. The study involved the DMFC simulation using PEMs with a wide range of properties concerning proton conductivity and permeability towards methanol. The mathematical model was implemented to predict the following

DMFC outputs: current-voltage polarization curves; constant voltage current at 35mV (CV, 35mV); open circuit voltage (OCV); CO<sub>2</sub> concentration at the cathode outlet for CV and OCV experiments. Apart from this, the model was also used for predicting the influence of the studied properties on the DMFC potential, Faraday and global efficiencies. The selection of the PEM properties range was performed according to characterization results evaluated previously. The simulation results showed that both PEM proton conductivity and permeability towards methanol play an important role on the DMFC overall performance. The proton conductivity seems to influence mainly the DMFC current and power density outputs and the cell efficiency regarding fuel conversion (Faraday efficiency). Moreover, very low proton conductivity seems to have high influence on the DMFC energy output due to limiting PEM properties concerning the cell ohmic losses. On the other hand, the permeability towards methanol was found to influence all the studied DMFC outputs as it is directly related to the fuel loss and parasitic reaction of methanol at the cathode catalyst layer. As expected, the simulations show that the optimal PEM properties for DMFC applications are high proton conductivity to reduce the ohmic losses and low permeability towards methanol in order to prevent the crossing over of methanol from the anode to the cathode. It is well known that high proton conductivity is commonly associated with high methanol permeations. However, improvements on the PEM properties can be achieved developing new materials with improved characteristics, acting on the hydrophilic/hydrophobic characteristics through polymer structural changes (ex. sulfonation degree) and by incorporating inorganic composites or proton conductors (ex. zirconium phosphate). For these PEM development proposes, the present mathematical model can be a very useful tool for selecting the right modifications that should be performed in order to prepare optimized materials that can improve the DMFC performance.

## **Acknowledgements**

The work of Vasco Silva was supported by FCT (Grant SFRH/BD/6818/2001). The authors would like to acknowledge J. Schirmer and R. Reissner at Deutsches Zentrum für Luft-und Raumfahrt (DLR) for the MEA characterization in the DMFC. The present work was in part supported by FCT projects POCTI/EQU/38075/2001 and POCTI/EQU/45225/2002.

## References

- [1] A. S. Aricò, S. Srinivasan and V. Antonucci, DMFCs: From fundamental aspects to technology development, *Fuel Cells* 1 (2001) 133.
- [2] K. A. Kreuer, On the development of proton conducting polymer membranes for hydrogen and methanol fuel cells, *J. Membr. Sci.* 185 (2001) 3.
- [3] J. Cruickshank and K. Scott, The degree and effect of methanol crossover in the direct methanol fuel cell, *J. Power Sources* 70 (1998) 40.
- [4] F. R. Kalhammer, P. R. Prokopius and V. P. Voecks, Status and prospects of fuel cells as automobile engines, State of California Air Resources Board, California, 1998.
- [5] D. Chu and S. Gilman, The influence of methanol on O<sub>2</sub> electroreduction at a rotating Pt disk electrode in acid electrolyte, *J. Electrochem. Soc.* 141 (1994) 1770.
- [6] K. A. Kreuer, On the development of proton conducting materials for technological applications, *Solid State Ionics* 97 (1997) 1.
- [7] X. Jin, M. T. Bishop, T. S. Ellis and F. Karasz, A sulphonated poly(aryl ether ketone), *Br. Polym. J.* 17 (1985) 4.
- [8] T. Kobayashi, M. Rikukawa, K. Sanui and N. Ogata, Proton-conducting polymers derived from poly(ether-etherketone) and poly(4-phenoxybenzoyl-1,4-phenylene), *Solid State Ionics* 106 (1998) 219.
- [9] S. M. J. Zaidi, S. D. Mikailenko, G. P. Robertson, M. D. Guiver and S. Kaliaguine, Proton conducting composite membranes for polyether ether ketone and heteropolyacids for fuel cell applications, *J. Membr. Sci.* 173 (2000) 17.
- [10] S. D. Mikhailenko, S. M. J. Zaidi and S. Kaliaguine, Sulfonated polyether ether ketone composite polymer electrolyte membranes, *Catal. Today* 67 (2001) 225.
- [11] V. Silva, B. Ruffmann, H. Silva, A. Mendes, M. Madeira and S. Nunes, Zirconium oxide modified sulfonated poly(ether ether ketone) membranes for direct methanol fuel cell applications, *Mater. Sci. Forum* 455-456 (2004) 587.
- [12] V. Silva, B. Ruffmann, H. Silva, A. Mendes, M. Madeira and S. Nunes, Mass transport of direct methanol fuel cell species in sulfonated poly(ether ether ketone) membranes, *Chem. Eng. Sci.* (submitted, 2005).
- [13] B. Kumar and J. P. Fellner, Polymer-ceramic composite protonic conductors, *J. Power Sources* 123 (2003) 132.

- [14] V.S. Silva, S. Weisshaar, R. Reissner, B. Ruffman, S. Vetter, A. Mendes, L.M. Madeira and S.P. Nunes, Performance and efficiency of a DMFC using non-fluorinated composite membranes operating at low/medium temperatures, *J. Power Sources* (in press, 2005).
- [15] J. Kerres, W. Zhang, L. Jörissen and V. Gogel, Application of different types of polyarylblend-membranes in DMFC, *J. New Mater. Electrochem. Systems* 5 (2002) 97.
- [16] G. Alberti, M. Casciola, L. Massinelli and B. Bauer, Polymeric proton conducting membranes for medium temperature fuel cells (110-160°C), *J. Membr. Sci.* 185 (2001) 73
- [17] V. S. Silva, B. Ruffmann, S. Vetter, A. Mendes, L. M. Madeira and S. P. Nunes, Characterization and application of composite membranes in DMFC, *Catalysis Today*, (in press, 2005).
- [18] M. L. Ponce, L. Prado, B. Ruffmann, K. Richau, R. Mohr and S. P. Nunes, Reduction of methanol permeability in polyetherketone-heteropolyacid membranes, *J. Membr. Sci.* 217 (2003) 5.
- [19] S. P. Nunes, B. Ruffmann, E. Rikowsky, S. Vetter and K. Richau, Inorganic modification of proton conductive polymer membranes for direct methanol fuel cells, *J. Membr. Sci.* 203 (2002) 215.
- [20] C. Manea and M. Mulder, Characterization of polymer blends of polyethersulfone/sulfonated polysulfone and polyethersulfone/sulfonated polyetheretherketone for direct methanol fuel cell applications, *J. Membr. Sci.* 206 (2002) 443.
- [21] V.S. Silva, B. Ruffmann, H. Silva, Y. A. Gallego, A. Mendes, L. M. Madeira and S. P. Nunes, Proton electrolyte membrane properties and direct methanol fuel cell performance. I. Characterization of hybrid sulfonated poly(ether ether ketone)/zirconium oxide membranes, *J. Power Sources* 140 (2005) 34.
- [22] V.S. Silva, J. Schirmer, R. Reissner, B. Ruffman, H. Silva, A. Mendes, L.M. Madeira and S.P. Nunes, Polymer electrolyte membrane properties and direct methanol fuel cell performance. II. Fuel cell performance and membrane properties effects, *J. Power Sources* 140 (2005) 41.
- [23] V.S. Silva, J. Schirmer, R. Reissner, B. Ruffman, A. Mendes, L.M. Madeira and S.P. Nunes, Direct methanol fuel cell modeling using proton exchange membrane properties evaluated by standard characterization methods, *Chem. Eng. Sci.* (submitted, 2005).
- [24] K.Z. Yao, K. Karan, K.B. McAuley, P. Oosthuizen B. Peppley and T. Xie, A review of mathematical models for hydrogen and direct methanol polymer electrolyte membrane fuel cells, *Fuel Cells* 4 (2004) 3.
- [25] V.S. Bagotsky and Y.B. Vasilyev, Some characteristics of oxidation reactions of organic compounds on platinum electrodes, *Electrochim. Acta* 9 (1964) 869.

[26] J.-T. Wang, S. Wasmus and R. F. Savinell, Real-time mass spectrometric study of the methanol crossover in a direct methanol fuel cell, *J. Electrochem. Soc.* 143 (1996) 1239.

[27] K. Kordesch and G. Simader, *Fuel cells and their applications*, VCH, Weinheim, 1996.

[28] E. Gulzow, T. Kaz, R. Reissner, H. Sander, L. Schilling and M. V. Bradke, Study of membrane electrode assemblies for direct methanol fuel cells, *J. Power Sources* 105 (2002) 261.

## PART FOUR

---

# **sPEEK composite membranes based on zirconium phosphate**



## Chapter 8. Characterization and application of composite membranes in DMFC\*

### Abstract

The present work focuses on the characterization of membranes for direct methanol fuel cells (DMFC), prepared using composites of sulfonated poly(ether ether ketone) (sPEEK, with sulfonation degree, SD, of 42 and 68%) as polymer matrix. This polymer was inorganically modified incorporating different amounts of zirconium phosphate (ZrPh) pretreated with *n*-propylamine and polybenzimidazole (PBI). The investigated properties were: proton conductivity, water and aqueous methanol swelling, permeability coefficients for DMFC species and morphology. DMFC tests were performed at 110°C with relative humidity (r.h.) in the cathode feed of 100 and 138%. The results obtained show that the inorganic modification of the polymer decreases the proton conductivity, water and aqueous methanol swelling and permeability towards DMFC species. In terms of morphology, it was found that the applied procedure enabled the preparation of membranes with good compatibility between inorganic and organic components. In terms of the DMFC tests of the composite membranes, working with the cathode feed at 100% r.h., the unmodified sPEEK membrane with SD = 42% proved to have the best performance, although with higher methanol crossover. In contrast, for r.h. of 138%, the best performance was achieved by the sPEEK composite membrane with SD = 68% and 20.0wt.% of ZrPh and 11.2wt.% of PBI.

\*V.S. Silva, B. Ruffmann, S. Vetter, A. Mendes, L.M. Madeira and S.P. Nunes, *Catalysis Today* (in press, 2005).

## 8.1. Introduction

The direct methanol fuel cell (DMFC) is a promising candidate system for portable electric devices [1-3]. Methanol as an energy carrier has the advantage of having a significant electro-activity and being easily oxidized directly to water and carbon dioxide in catalyst alloys without the need for a reformer. Apart from that, it is easy to handle and transport (liquid at room temperature), can be produced from a variety of sources (natural gas, coal or biogas) and is biodegradable [2].

One of the main obstacles for the development of the DMFC concerns the limitations associated with the usually employed proton exchange membranes [3]. Perfluorinated membranes, such as Nafion<sup>®</sup> or Flemion<sup>®</sup>, although very suitable for hydrogen fuel cells, are not appropriate for DMFC applications due to their high methanol and water permeability [4]. Methanol crossover from the anode to the cathode is detrimental for the DMFC performance as it reduces the Faraday efficiency and cell voltage, leading to an efficiency reduction down to 35% [5]. On the other hand, the high water permeability in perfluorinated membranes can cause cathode flooding and, thus, lower cathode performance [6].

In order to improve the performance of the DMFC, it is necessary to develop and test new materials that eliminate or, at least, reduce the reactants loss without decreasing in the same degree the proton conductivity [7]. Non-fluorinated membranes based on the hydrophobic poly(ether ether ketone) (PEEK) have been presented as materials with excellent chemical and mechanical resistance [8-11]. This polymer can be easily made hydrophilic by sulfonation reactions, being the sulfonation degree (SD) controlled by the reaction time and temperature. Recently, Li et al. reported better DMFC performances for the sPEEK membranes (SD = 39 and 47%) compared to Nafion<sup>®</sup> 115, at 80°C [12]. Similar results were obtained by us for a sPEEK membrane with SD = 42% and thickness ranging from 25 to 55  $\mu\text{m}$ . However, non-modified membranes resulted to be mechanically unstable due to excessive swelling when operated for periods longer than 4 days at medium temperatures (up to 110°C).

In order to improve the sPEEK membrane properties for DMFC applications at medium temperatures, composite membranes can be prepared by the incorporation of dispersed inorganic proton conductor particles such as  $\alpha$ -zirconium phosphate [13-17]. Layered inorganic  $\alpha$ -zirconium phosphate is well known for its ion exchange capacity [18-19] and proton conductivity [20-22], depending on its degree of crystallinity, since the protons are mainly transported on the particle surfaces. In order to improve its proton conductivity, the interlayer distance can be increased by the intercalation of alkyldiamines (exfoliation) [23]. These modified zirconium phosphate with

increased acidic surface area have been found to have a proton conductivity, at room temperature, that is two or three orders of magnitude higher than that of the original microcrystal [24]. With this objective in mind and also attempting to improve the compatibility between the sPEEK polymer and the zirconium phosphate particles, the ZrPh dispersion can be treated with *n*-propylamine and further with polybenzimidazole (PBI). Small-angle X-ray scattering (ASAX) and scanning electron microscopy (SEM) results showed that the pretreatment with *n*-propylamine/PBI of the zirconium phosphate dispersion prevents the formation of particles agglomerates and improves the compatibilization between the organic and inorganic phases [25].

The present work focuses on the characterization of composite membranes prepared using sulfonated poly(ether ether ketone) (SD = 42 and 68%) as polymer matrix, which has been modified with different amounts of ZrPh pretreated with *n*-propylamine and PBI. In this study the proton conductivity was evaluated via impedance spectroscopy and DMFC tests were performed at 110°C and with a cathode inlet feed relative humidity of 100 and 138%.

## 8.2. Experimental

### 8.2.1. Materials and methods

Sulfonated poly(ether ether ketone) (sPEEK) polymers with sulfonation degrees of 42 and 68% (ion exchange capacity = 1.27 and 1.90 meq/g, respectively) were prepared following the procedure reported in the literature [9-11, 26]. Poly(ether ether ketone) was supplied as pellets by Victrex. The sulfonation degree was determined by elemental analysis and by H-NMR as described by Nolte et al. [27].

### 8.2.2. Preparation of zirconium phosphate

The phosphate dispersion was prepared as described in the US Patent 5,932,361 [28]. Layered  $\alpha$ -zirconium phosphate (ZrPh) was synthesised using the method described elsewhere [13], in which  $ZrOCl_2$  is used as precursor of  $ZrO_2$ . The ZrPh solution (6 wt.% in dimethylformamide, DMF) was treated adding *n*-propylamine solution (1M in DMF) using the mass relation of 5.7g to 6.2g, respectively. After stirring for 3 days the dispersion of treated zirconium phosphate (ZrPh) at 60°C, 6.2 g of polybenzimidazole (PBI) solution (2.5 wt.% in DMF) were added and the dispersion further stirred for 6 days at the same temperature.

### **8.2.3. Membrane preparation**

The sPEEK polymer was dissolved in dimethylsulfoxide. Then the treated ZrPh dispersion solution was added and the final solution was left to stir for 3 days at 60°C. After filtration, the solution was cast in a hydrophobised glass plate heated at 70°C. Next, the membranes were stored in a vacuum oven for 24 hours at 90 °C.

### **8.2.4. Characterization methods**

#### **8.2.4.1. Proton conductivity**

Proton conductivity was determined by impedance spectroscopy with two different cells. With the first cell, the measurements were performed using sulfuric acid (0.33M) as electrolyte, at 25°C, and determining the impedance modulus at zero phase shift [16]. The spectrometer used was a HP 4284A, working in the frequency up to 100 Hz. As pretreatment, samples were immersed in water at room temperature during 3 days. One hour before initiating the measurement, the samples were immersed for 1 hour in the electrolyte solution.

On the other hand, with the second cell, the measurements were performed using water vapor as described by Alberti et al. [29]. Proton conductivity of the samples without pretreatment was determined at temperatures ranging from 50 to 110°C and 100% relative humidity. The spectrometer used was a Zahner IM6 electrochemical workstation, working in the frequency range between 10 and 10<sup>6</sup> Hz. The plain sPEEK membrane with SD=68% was not tested in the vapor cell (second cell) because it proved to be unstable at the tested temperatures.

#### **8.2.4.2. Swelling measurements**

Swelling studies were carried out by drying the samples in a vacuum oven at 90°C for 5 hours. After drying, four samples of each membrane were weighed and immersed in deionized water or 20wt.% aqueous methanol solution and equilibrated for 2 days at each temperature (room temperature, 40, 55 and 70°C). The weights of the swollen membranes were measured after carefully removing the solution from both surfaces. Membrane swelling (wt.%) was evaluated calculating the ratio between the difference of the wet and dry weight and the dry weight.

### 8.2.4.3. Water and methanol pervaporation measurements

The methanol and water permeability coefficients were evaluated by pervaporation measurements as described in [16]. The measurements were performed at 55°C with a 20wt.% aqueous methanol solution as feed. Prior to all measurements, samples were immersed in the feed solution for 1 hour. The water/methanol selectivity of the composite membranes was obtained dividing the water and methanol permeability coefficients. The plain sPEEK membranes with SD=68% was not tested in the pervaporation setup because it proved to be soluble in the 20% (w/w) aqueous methanol solution, at 55°C.

### 8.2.4.4. Nitrogen/Oxygen/Carbon dioxide permeability measurements

Nitrogen, oxygen and carbon dioxide permeability coefficients were evaluated at 20°C using the pressure rise method. The permeation measurements were carried as described by Drioli et al. [30]. Prior to all measurements, membranes were conditioned with the feed stream for 12 hours.

### 8.2.4.5. Membrane morphology

The membrane morphology was investigated by field emission scanning electron microscopy in a LEO 1550 equipment. Samples were fractured in liquid nitrogen and sputtered with Au/Pd.

## 8.2.5. DMFC tests

The membrane electrode assemblies (MEAs) were prepared by hot pressing the membrane samples between two Etek<sup>®</sup> ELAT electrodes. Supported PtRu (1 mg/cm<sup>2</sup> 30wt.% PtRu(1:1 a/o) on carbon with 0.7 mg/cm<sup>2</sup> Nafion<sup>®</sup>/PTFE) and Pt (0.4 mg/cm<sup>2</sup> 20wt.% Pt on carbon with 0.7 mg/cm<sup>2</sup> Nafion<sup>®</sup>/PTFE) were used as anode and cathode electrodes, respectively. The DMFC experimental set-up is described elsewhere [31]. The MEAs (25 cm<sup>2</sup>) were fed with an aqueous 1.5M methanol solution (4 ml/min, 2.5 bar) on the anode side and humidified air (600 sccm/min, 3 bar, 100 and 138% relative humidity) on the cathode side. The MEAs' characterization was performed measuring the DMFC current-voltage polarization curves at 110°C.

### 8.3. Results and discussion

#### 8.3.1. Proton conductivity

Table 8.1 shows the effects of the incorporation of zirconium phosphate, pretreated with *n*-propylamine/PBI, in the proton conductivity of the sPEEK polymer at 25°C in an acid electrolyte (0.33M H<sub>2</sub>SO<sub>4</sub>). It can be observed that the proton conductivity of the composite membranes decreases with the amount of inorganic incorporation. The ZrPh treatment with *n*-propylamine was expected to exfoliate the inorganic layers and, consequently, increase the acid surface area and thus the proton conductivity [23]. In a recently published work regarding sPEEK/ZrPh/PBI membranes analysis using SEM and ASAXS techniques [25], it was observed that addition of PBI to a zirconium phosphate dispersion previously treated with *n*-propylamine resulted in ZrPh with some extent of exfoliation. It was also found that the PBI treatment increased the compatibility of the ZrPh particles with the sPEEK polymer and improved the dispersion of the inorganic phase. However, it is believed that with the incorporation of PBI (base) the acid character of the sPEEK/ZrPh/PBI system is lower and, therefore, the proton conductivity may decrease.

Table 8.1. Proton conductivity of various sPEEK membranes in an acid electrolyte (25°C in 0.33M H<sub>2</sub>SO<sub>4</sub>).

<i>Membrane composition</i> sPEEK / ZrPh / PBI (wt.%)	<i>Thickness</i> ( $\mu\text{m}$ )	$k_M$ (mS/cm)
100.0 (SD=68%) / 0 / 0	75	46.3
84.4 (SD=68%) / 10.0 / 5.6	73	29.4
68.8 (SD=68%) / 20.0 / 11.2	84	18.2
100.0 (SD=42%) / 0 / 0	79	20.2
84.4 (SD=42%) / 10.0 / 5.6	63	11.5
68.8 (SD=42%) / 20.0 / 11.2	65	2.8

In terms of the membrane conductivity evaluated using the water vapor cell (Fig. 8.1), a similar trend as for the acid electrolyte cell (Table 8.1) was observed. The proton conductivity of the pure sPEEK membrane with SD=68% is not presented because of the high solubility of this polymer and therefore low stability of the unmodified membranes. For the compositions

investigated here, the unmodified sPEEK membrane with SD=42% resulted to be the most conductive membrane. Assuming that conductivity follows the Arrhenius law, it was found that the unmodified membrane presents the lowest proton transport activation energy (Table 8.2). The introduction of 10wt. % ZrPh /and 5.6wt.% PBI caused already a drastic reduction of conductivity.

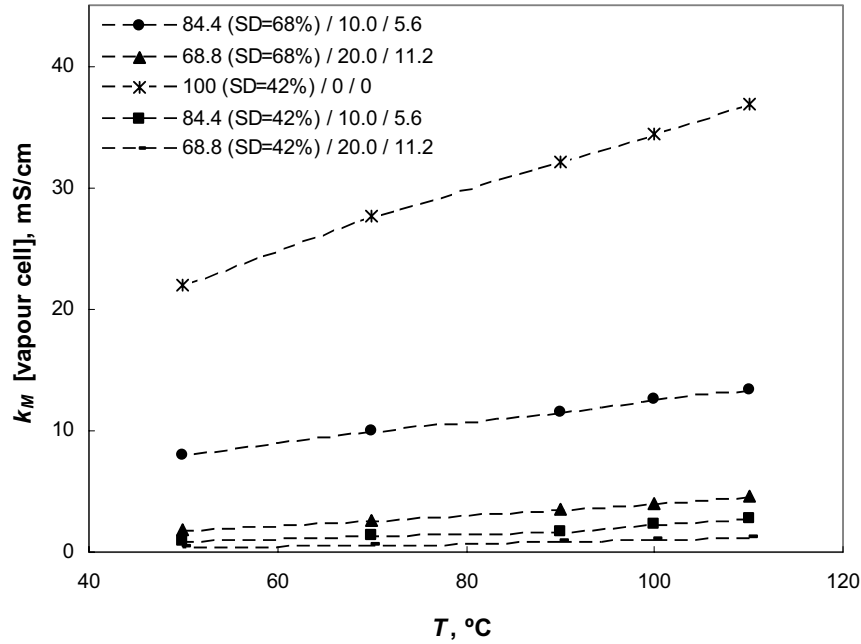


Fig. 8.1. Proton conductivity of various sPEEK membranes (sPEEK / ZrPh / PBI, wt.%) in the water vapor cell as a function of temperature (at 100% r.h.).

Table 8.2. Pre-exponential factors,  $A$ , and activation energy,  $E_a$ , of various sPEEK membranes in the water vapor cell.

Membrane composition sPEEK / ZrPh / PBI (wt.%)	$A$	$E_a$ (kJ/mol)
84.4 (SD=68%) / 10.0 / 5.6	204.7	11.7
68.8 (SD=68%) / 20.0 / 11.2	475.1	17.9
100.0 (SD=42%) / 0 / 0	557.6	11.7
84.4 (SD=42%) / 10.0 / 5.6	634.3	20.6
68.8 (SD=42%) / 20.0 / 11.2	152.4	18.5

### 8.3.2. Swelling measurements

From Table 8.3 it can be observed that the membrane swelling in water and methanol aqueous solution (20wt.%), at room temperature, decreases with the incorporation of pretreated phosphate. However, a slight increase of the swelling can be usually noticed when the amount of ZrPh and PBI is increased from 10.0wt.% to 20.0wt.% and 5.6wt.% to 11.2wt.%, respectively. From Table 8.3, it can be also noticed that the swelling in methanol aqueous solution is always higher than in pure water. This fact is even more pronounced for membranes prepared with sPEEK with SD=42% as polymer matrix.

Table 8.3. Swelling of membranes based on sPEEK composites when immersed in water and aqueous methanol (20wt.%) (batch experiments at room temperature).

<i>Membrane composition</i> sPEEK / ZrPh / PBI (wt.%)	<i>Swelling water</i> (wt %)	<i>Swelling methanol</i> 20wt.% solution (wt.%)
100.0 (SD=68%) / 0 / 0	17.4	-*
84.4 (SD=68%) / 10.0 / 5.6	9.4	11.6
68.8 (SD=68%) / 20.0 / 11.2	12.0	13.4
100.0 (SD=42%) / 0 / 0	10.1	15.0
84.4 (SD=42%) / 10.0 / 5.6	0.3	4.7
68.8 (SD=42%) / 20.0 / 11.2	0.6	4.0

\*partially soluble

Fig. 8.2 shows the swelling of the composite membranes as a function of temperature, when immersed in methanol aqueous solution (20wt.%). From this plot it can be noticed that swelling increases with temperature for all the studied membranes. The swelling is much higher for unmodified membranes. The unmodified sPEEK membrane with SD = 68 % is even soluble at the studied temperatures. For the composite membranes, the highest swelling was observed for the membrane with 10.0wt.% ZrPh 5.6wt% PBI. The results obtained for all composite membranes show improved stability properties in terms of swelling in aqueous methanol solution.

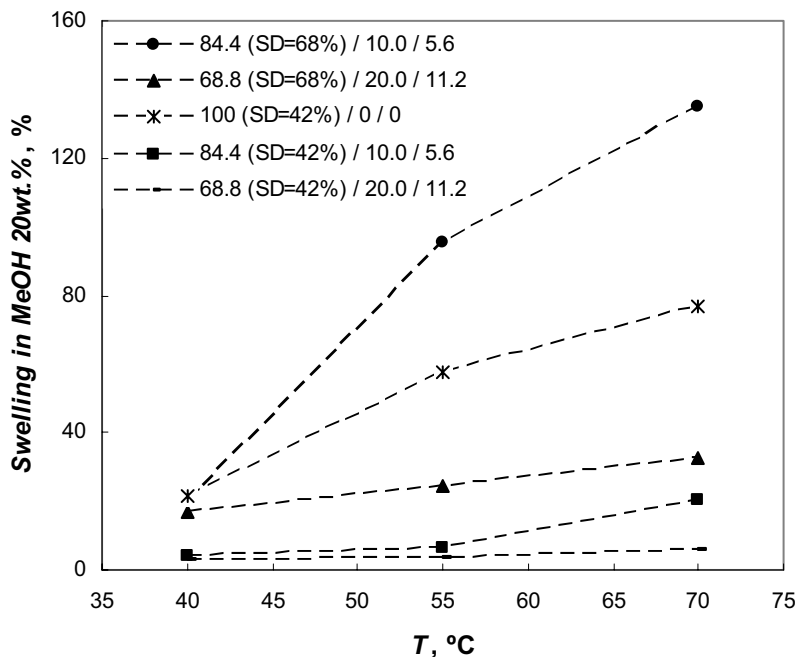


Fig. 8.2. Swelling in 20 wt.% methanol solution as a function of temperature.

### 8.3.3. Permeability towards species present in DMFC (methanol, water and gases)

In terms of membranes permeability towards methanol and water, pervaporation experiments at 55°C showed that it decreases with the amount of inorganic incorporation for both sulfonation degrees (Table 8.4). As a matter of fact, the membrane permeability towards water and methanol depends on the solubility and diffusivity of the species in the membrane. There is a good correlation between swelling in methanol aqueous solution (20wt.%, used as feed in the pervaporation experiments) and the total pervaporation flux, both at 55°C (Fig. 8.3). Moreover, it can be also observed that the incorporation of pretreated phosphate leads to an increase of the water/methanol selectivity (Table 8.4).

On the other hand, gas permeation experiments show that the composite membranes permeability towards nitrogen, oxygen and carbon dioxide decreases with the inorganic phosphate incorporation (Table 8.5). The values are in all cases low enough to consider the membranes a barrier for the gases. The permeability of CO<sub>2</sub> (and  $P_{CO_2/N_2}$ ) increased with the sulfonation degree, due to the higher content of acid groups. However the amount of CO<sub>2</sub> crossing the membrane is still very low compared to the methanol transport. It is reasonable to assume that practically all the

CO<sub>2</sub> detected in the cathode during DMFC experiments comes from the oxidation of methanol crossing the membrane.

Table 8.4. Methanol and water permeability coefficients and water/methanol selectivity of the sPEEK composite membranes (pervaporation experiments at 55°C with 20wt.% aqueous methanol solution used as feed, 1 Barrer = 10<sup>-10</sup> cm<sup>3</sup> [STP] cm / (cm<sup>2</sup> s cmHg))

<i>Membrane composition</i> sPEEK / ZrPh / PBI (wt.%)	$P_{MeOH}$ (Barrer)	$P_{Water}$ (Barrer)	$P_{Water}/P_{MeOH}$
84.4 (SD=68%) / 10.0 / 5.6	1.4×10 <sup>4</sup>	5.2×10 <sup>5</sup>	37.4
68.8 (SD=68%) / 20.0 / 11.2	4.7×10 <sup>3</sup>	2.1×10 <sup>5</sup>	44.2
100 (SD=42%) / 0 / 0	2.2×10 <sup>4</sup>	5.9×10 <sup>5</sup>	26.6
84.4 (SD=42%) / 10.0 / 5.6	4.0×10 <sup>3</sup>	1.3×10 <sup>5</sup>	32.5
68.8 (SD=42%) / 20.0 / 11.2	1.5×10 <sup>3</sup>	9.9×10 <sup>4</sup>	68.5

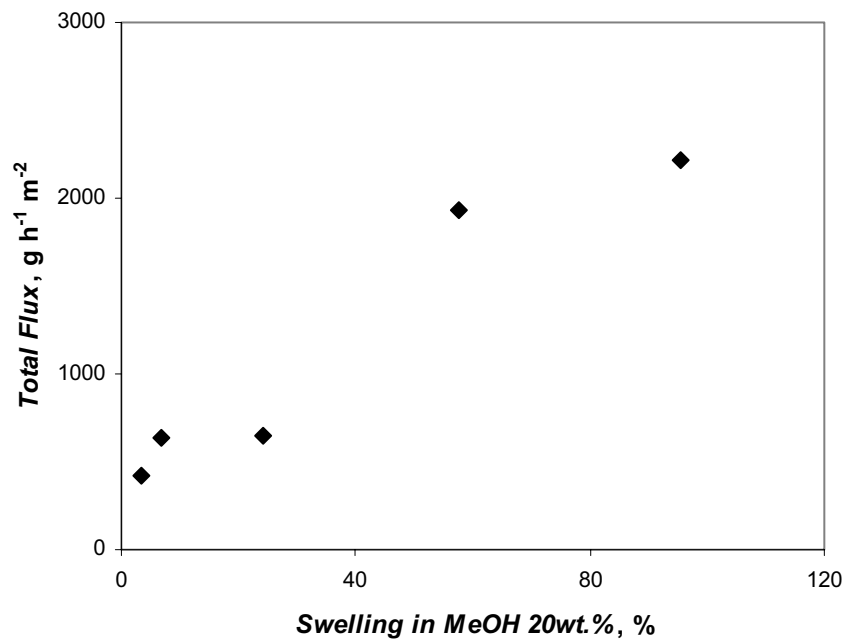


Fig. 8.3. Total flux from pervaporation measurements at 55°C as a function of swelling in 20 % methanol solution (batch experiments at pervaporation conditions).

Table 8.5. Nitrogen, oxygen and carbon dioxide permeability coefficients and oxygen/nitrogen and carbon dioxide/nitrogen selectivities of the various sPEEK membranes (pressure rise method at 20°C with swollen membranes).

<i>Membrane composition</i> sPEEK / ZrPh / PBI (wt.%)	$P_{N_2}$ (Barrer)	$P_{O_2}$ (Barrer)	$P_{CO_2}$ (Barrer)	$P_{O_2/N_2}$	$P_{CO_2/N_2}$
100.0 (SD=68%) / 0 / 0	$1.0 \times 10^{-1}$	$3.5 \times 10^{-1}$	7.4	3.5	72.5
84.4 (SD=68%) / 10.0 / 5.6	$4.4 \times 10^{-2}$	$1.3 \times 10^{-1}$	3.2	2.9	75.4
68.8 (SD=68%) / 20.0 / 11.2	$2.7 \times 10^{-2}$	$6.6 \times 10^{-2}$	$5.5 \times 10^{-2}$	2.5	20.6
100.0 (SD=42%) / 0 / 0	$7.1 \times 10^{-2}$	$1.4 \times 10^{-1}$	2.4	2.0	34.1
84.4 (SD=42%) / 10.0 / 5.6	$3.7 \times 10^{-2}$	$5.8 \times 10^{-2}$	$7.9 \times 10^{-1}$	1.6	21.3
68.8 (SD=42%) / 20.0 / 11.2	$4.2 \times 10^{-2}$	$6.2 \times 10^{-2}$	$6.1 \times 10^{-1}$	1.5	14.4

It is well known that the introduction of fillers with low (or none) permeability in a membrane leads to a reduction on the overall membrane permeability when the compatibilization between polymer and filler is good. This reduction is a function of the filler concentration and shape and has been described also previously for gas separation [32]. The interface between filler and polymer matrix is an important factor. In the case of the composite membranes investigated here, PBI strongly interacts with a fraction of the ionic acid groups of the sPEEK polymer and makes the membrane less hydrophilic. Consequently, the barrier properties of the prepared composite membranes increases, which can be assumed as an advantage for DMFC applications because it reduces the reactants loss and increases the overall fuel cell efficiency.

### 8.3.4. Membrane morphology

Fig. 8.4 shows that the treatment of zirconium phosphate with *n*-propylamine and PBI enabled good compatibility between the inorganic phase and the sPEEK polymer matrix. A reason for this is the basic character of PBI, which enables strong interactions with the acid phosphate particles surface and with the acid sulfonic groups of the sPEEK polymer.

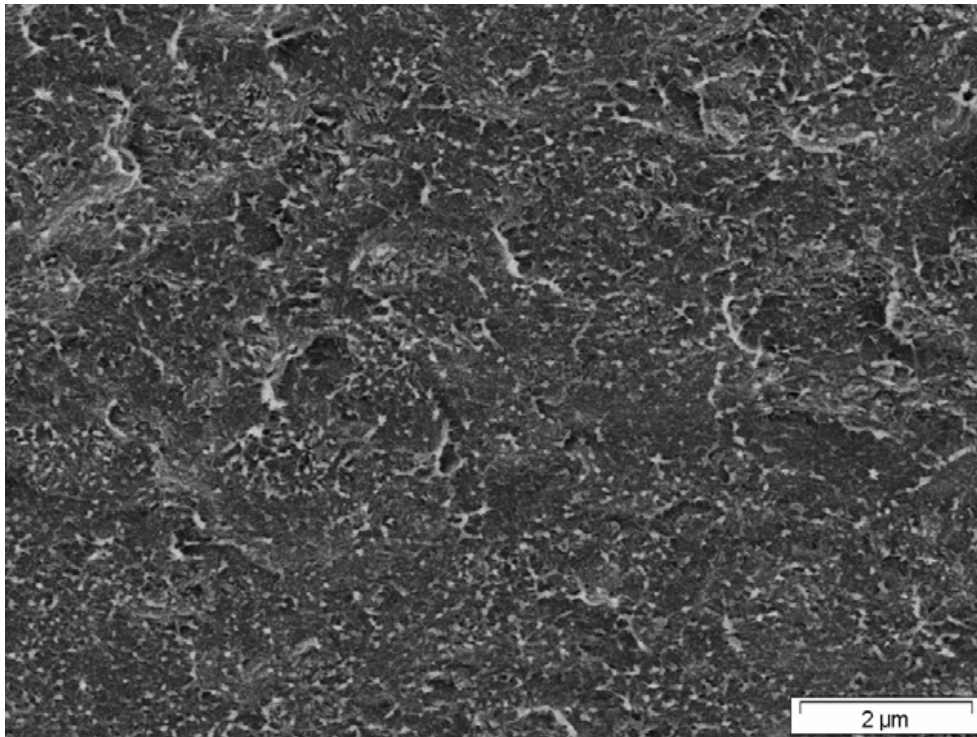


Fig. 8.4. Scanning electron micrograph of sPEEK (SD=42%) membrane with 20% ZrPh and 11.2% of PBI.

### 8.3.5. Polarization curves

The current density/power density plots of MEAs made with the investigated sPEEK composite membranes, at 110°C and 100% r.h. (cathode feed), are shown in Fig. 8.5. From these plots it can be observed that the unmodified sPEEK (SD=42%) membrane presented the maximum power density output. It achieved an output power density value of 10.4mW/cm<sup>2</sup> for 51.8mA/cm<sup>2</sup>. The unmodified membrane with SD = 68 % could not be characterized due to its instability (high swelling or even solubility). However, the sPEEK (SD = 68%) membrane with 20.0wt.% ZrPh and 11.2wt.% PBI had even higher power density than the membrane with SD = 42% for current densities lower than 25mA/cm<sup>2</sup>. When the relative humidity at the cathode feed was increased to 138% (Fig. 8.6), it could be observed that the sPEEK (SD = 68 %) membrane with 20.0wt.% ZrPh and 11.2wt.% PBI had the best performance. This membrane achieved an output power density value of 14.7mW/cm<sup>2</sup> for 58.8mA/cm<sup>2</sup>. When comparing the plain sPEEK SD=42 % membrane with its composites, for both r.h. values tested, the unmodified membrane had higher power density output. It is worth noting that for the same operation conditions (110°C and 138% cathode feed r.h.), in terms of amount of CO<sub>2</sub> at the cathode outlet obtained at 35mV, for the membranes with the best power density output performance (Fig. 8.6), the membrane with sPEEK (SD = 68 %),

20.0wt.% ZrPh and 11.2wt.% PBI exhibits a notable value of 0.1vol.%, in comparison with 1.9vol.% for the unmodified sPEEK membrane with SD=42%. However the filler addition to sPEEK (SD = 42 %) besides reducing the crossover had an excessive (negative) effect on the proton conductivity. As a whole the performance in the DMFC decreased too much after the modification of the low sulfonated membrane.

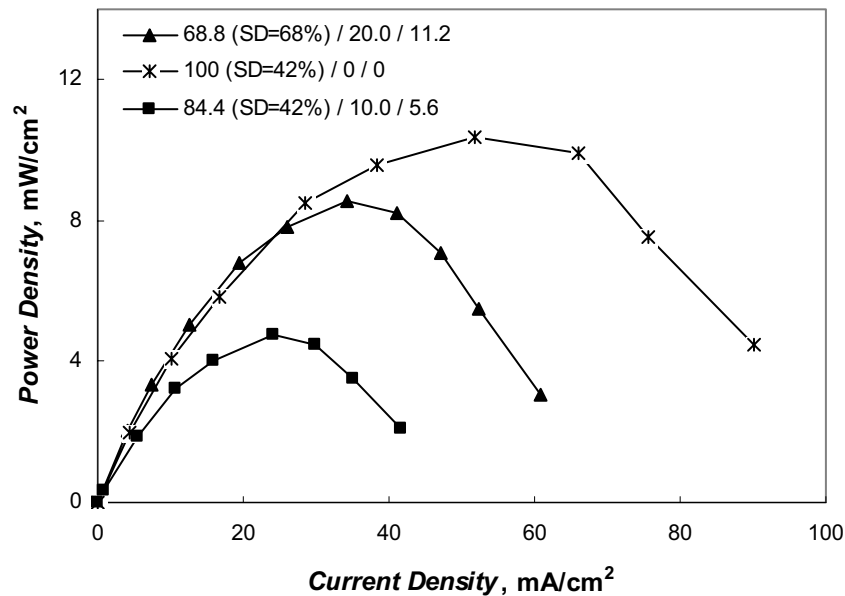


Fig. 8.5. Power density plots of the DMFC using various sPEEK membranes, at 110°C and 100% r.h. in the cathode feed.

The maximum output power density is plotted in Fig. 8.7, for both 100 and 138% r.h., at 110°C, as a function of the aqueous methanol swelling (evaluated at 70°C by batch experiments). It can be verified that the plot presents a maximum for both relative humidities. At 100% r.h., both composite membranes with the highest and lowest swelling in methanol present the lowest maximum output power density. This result shows the paramount influence of the membranes swelling in the DMFC performance. Low swelling leads to low proton conductivity (protons transport assisted by sorbed water) and excessive swelling leads to poor DMFC performance (high methanol and water crossover). Moreover, it can be seen that the DMFC performance increases operating at higher cathode feed humidity and, as expected, the performance improvement is higher for the low swelling membranes.

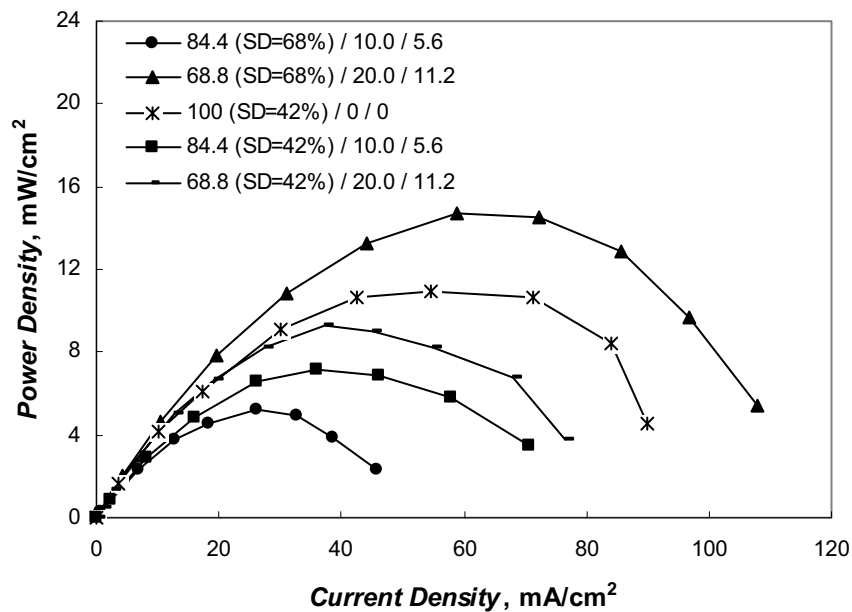


Fig. 8.6. Power density plots of the DMFC using sPEEK composite membranes, at 110°C and 138% r.h. in the cathode feed.

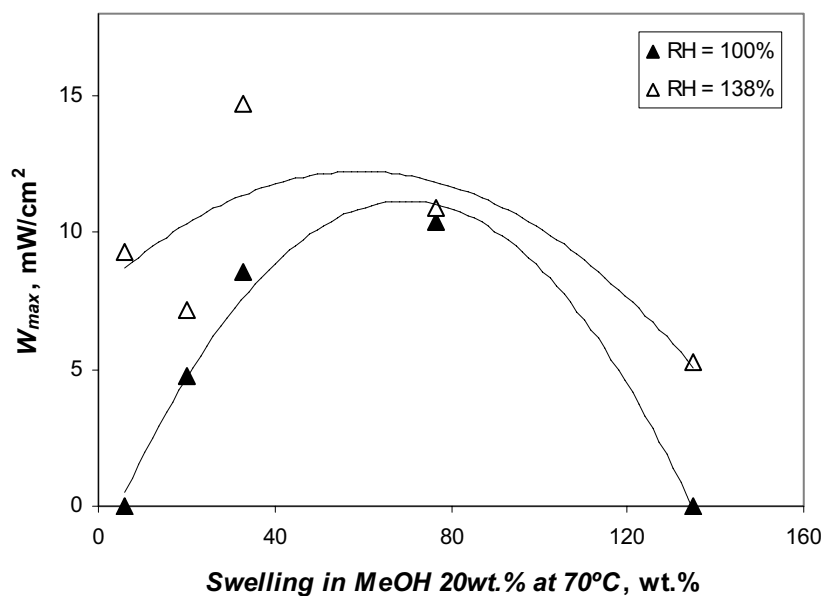


Fig. 8.7. Maximum power density of the DMFC (110°C and r.h. of 100 and 138%), as a function of swelling in 20wt.% methanol solution (lines are guides to the eye), evaluated through batch experiments at 70°C.

In the particular case of the maximum output power density variation with the proton conductivity evaluated in the acid electrolyte cell, Fig. 8.8 shows similar results as those obtained for swelling in methanol (Fig. 8.7). It can be seen that composite membranes with low proton conductivity present low DMFC performance. On the other hand, from Fig. 8.8 it can be also verified that high proton conductivity does not mean higher DMFC performance, due to the excessive swelling associated to this membranes (higher methanol and water crossover).

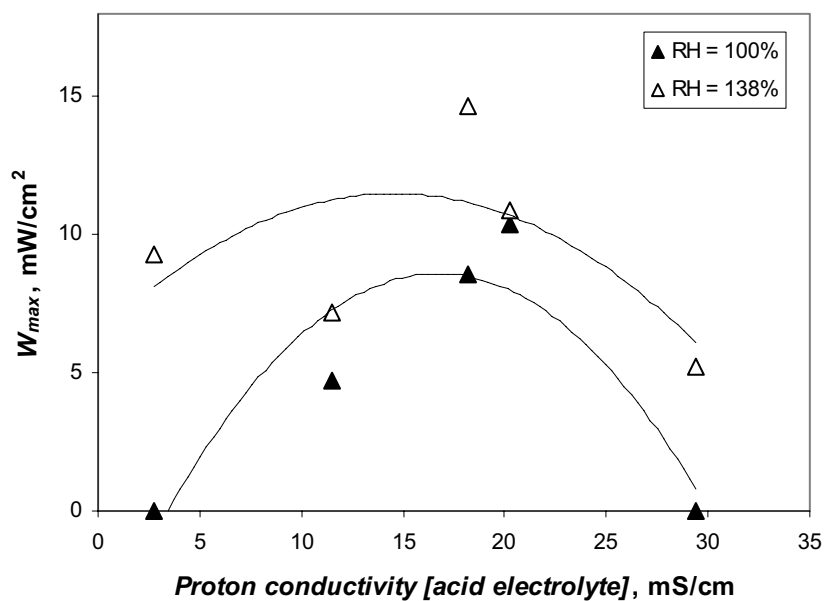


Fig. 8.8. Maximum power density of the DMFC (110°C and r.h. of 100 and 138%), as a function of the proton conductivity (lines are guides to the eye), evaluated in acid electrolyte (0.33M H<sub>2</sub>SO<sub>4</sub>, impedance spectroscopy at 25°C).

## 8.4. Conclusions

Composite membranes were prepared using sPEEK polymer as organic matrix (SD = 42 and 68%) with different contents of zirconium phosphate as inorganic network (10.0 and 20.0wt.%) pretreated with *n*-propylamine and polybenzimidazole (PBI, 5.6 and 11.2wt.%).

Impedance measurements showed, for the concentration range investigated, that increasing the ZrPh/PBI content in the sPEEK composite membranes leads to a decrease of the proton conductivity. On the other hand, from impedance characterization it was also observed that the temperature dependence of proton conductivity increases with the incorporation of inorganic content. In terms of the membranes swelling in water or methanol aqueous solution, batch

experiments showed that the inorganic incorporation decreased the swelling of the composite membranes. Moreover, it was observed that the unmodified membrane with SD=68% was soluble and with SD=42% had excessive swelling in 20wt.% aqueous methanol solution, at temperatures higher than 70°C. This was also the case for composite membranes prepared with sPEEK (SD = 68 %) and low inorganic content. All other composite membranes showed improved thermal and chemical stability in the methanol aqueous solution. Pervaporation (H<sub>2</sub>O, CH<sub>3</sub>OH) and pressure rise (N<sub>2</sub>, O<sub>2</sub>, CO<sub>2</sub>) experiments showed that the incorporation of ZrPh/PBI in the sPEEK polymer organic matrix decreased the DMFC species permeability coefficients. Micrographs obtained by scanning electron microscopy showed a good adhesion between inorganic particles domains and the polymer matrix. Finally, the results obtained from the DMFC tests, at 110°C, using the prepared composite membranes showed that the best performance was achieved by the unmodified sPEEK membrane (SD = 42 %) and sPEEK (SD = 68 %) composite membrane containing 20.0wt.% ZrPh and 11.2wt.% PBI, for cathode feed relative humidity of 100 and 138%, respectively. For 138% r.h., the DMFC using this composite membrane presented a much lower CO<sub>2</sub> emission (and therefore lower methanol crossover) at the cathode outlet (0.1vol.%), in comparison with the unmodified sPEEK (SD = 42 %) membrane (1.9vol.%). It is believed that this performance resulted from the best properties of this membrane in terms of swelling in methanol, proton conductivity and water and methanol permeation. Based on the results obtained for the PEM characterization and DMFC tests, among the investigated systems reported here, the incorporation of 20.0wt.% of ZrPh (pretreated with *n*-propylamine) and 11.2wt.% of PBI in the sPEEK polymer with SD=68% was found to be the most favorable for future application in DMFC systems working at temperature up to 110°C.

## Acknowledgements

Vasco Silva acknowledges both FCT (Grant SFRH/BD/6818/2001) and GKSS for the grant assigned for his stay at GKSS Forschungszentrum GmbH. The collaboration between GKSS and Deutsches Zentrum für Luft-und Raumfahrt (DLR) on the membrane development and MEA characterization was supported by the HGF-Strategiefonds project “Membranes and Electrodes for DMFC”. The present work was also partially supported by FCT/FEDER projects POCTI/EQU/38075/2001 and POCTI/EQU/45225/2002. The authors would like to acknowledge S. Weisshaar and R. Reissner at DLR for the MEA characterization in the DMFC. The authors also thank M. Schossig and M. Aderhold for the electron microscopy.

## References

- [1] B. Gurau and E.S. Smotkin, Methanol crossover in direct methanol fuel cells: a link between power and energy density, *J. Power Sources* 112 (2002) 339.
- [2] L. Jörissen, V. Gogel, J. Kerres and J. Garche, New membranes for direct methanol fuel cells, *J. Power Sources* 105 (2002) 267.
- [3] J. Kerres, W. Zhang, L. Jörissen and V. Gogel, Application of different types of polyaryl-blend-membranes in DMFC, *J. New Mater. Electrochem. Systems* 5 (2002) 97.
- [4] X. Ren, T.E. Springer, T.A. Zawodzinski and S. Gottesfeld, Methanol transport through nafion membranes: Electro-osmotic drag effects and potential step measurements, *J. Electrochem. Soc.* 147 (2000) 466.
- [5] F. R. Kalhammer, P.R. Prokopius and V.P. Voecks, Status and prospects of fuel cells as automobile engines, State of California Air Resources Board, California, 1998.
- [6] J. Cruickshank and K. Scott, The degree and effect of methanol crossover in the direct methanol fuel cell, *J. Power Sources* 70 (1998) 40.
- [7] K.A. Kreuer, On the development of proton conducting materials for technological applications, *Solid State Ionics* 97 (1997) 1.
- [8] X. Jin, M.T. Bishop, T.S. Ellis and F. Karasz, A sulphonated poly(aryl ether ketone), *Br. Polym. J.* 17 (1985) 4.
- [9] T. Kobayashi, M. Rikukawa, K. Sanui and N. Ogata, Proton-conducting polymers derived from poly(ether-etherketone) and poly(4-phenoxybenzoyl-1,4-phenylene), *Solid State Ionics* 106 (1998) 219.
- [10] S.M.J. Zaidi, S.D. Mikailenko, G.P. Robertson, M.D. Guiver and S. Kaliaguine, Proton conducting composite membranes for polyether ether ketone and heteropolyacids for fuel cell applications, *J. Membr. Sci.* 173 (2000) 17.
- [11] S.D. Mikhailenko, S.M.J. Zaidi and S. Kaliaguine, Sulfonated polyether ether ketone composite polymer electrolyte membranes, *Catal. Today* 67 (2001) 225.
- [12] L. Li, J. Zhang and Y. Wang, Sulfonated poly(ether ether ketone) membranes for direct methanol fuel cell, *J. Membr. Sci.* 226 (2003) 159.
- [13] B. Ruffmann, H. Silva, B. Schulte and S. Nunes, Organic/inorganic composite membranes for application in DMFC, *Solid State Ionics* 162-163 (2003) 269.

- [14] G. Alberti, R. Vivani and S.M. Mascarós, First structural determination of layered and pillared organic derivatives of  $\gamma$ -zirconium phosphate by X-ray powder diffraction data, *J. Molecular Structure* 470 (1998) 81.
- [15] B. Bonnet, D. J. Jones, T. Tchicaya, G. Alberti, M. Casciola, L. Massinelli, B. Bauer, A. Peraio and E. Ramunni, Hybrid organic-inorganic membranes for a medium temperature fuel cell, *J. New Mat. Electrochem. Syst.* 3 (2000) 87.
- [16] S.P. Nunes, B. Ruffmann, E. Rikowsky, S. Vetter and K. Richau, Inorganic modification of proton conductive polymer membranes for direct methanol fuel cells, *J. Membr. Sci.* 203 (2002) 215.
- [17] G. Alberti and M. Casciola, Solid state protonic conductors, present main applications and future prospects, *Solid State Ionics* 145 (2001) 3.
- [18] A. Clearfield, ed., in: *Inorganic ion exchange materials*, CRC Press, Boca Raton, FL, (1982) chapt. 1-3.
- [19] G. Alberti, M. Casciola and U. Costantino, Inorganic ion-exchange pellicles obtained by delamination of  $\alpha$ -zirconium phosphate crystals, *J. Coll. Interf. Sci.* 107 (1985) 256.
- [20] G. Alberti and M. Casciola, Layered metal<sup>IV</sup> phosphates, a large class of inorganic-organic proton conductors, *Solid State Ionics* 97 (1997) 177.
- [21] G. Alberti, L. Boccali, M. Casciola, L. Massinelli and E. Montoneri, Protonic conductivity of layered zirconium phosphonates containing  $-\text{SO}_3\text{H}$  groups, III. Preparation and characterization of  $\gamma$ -zirconium sulfoaryl phosphonates, *Solid State Ionics* 84 (1996) 97.
- [22] U. Costantino, M. Casciola, G. Pani, D. J. Jones and J. Rozière, Vibrational spectroscopic characterization of protonic conducting polyethyleneimine- $\alpha$ - and  $\gamma$ -zirconium phosphate nanocomposites, *Solid State Ionics* 97 (1997) 261.
- [23] M. Casciola, U. Costantino and F. Marmottini, Influence of guest molecules on the protonic conduction of anhydrous intercalation compounds of  $\alpha$ -zirconium hydrogen phosphate with diamines, *Solid State Ionics* 35 (1989) 67.
- [24] G. Alberti, M. Casciola, U. Costantino and F. Di Gregorio, Protonic conduction of polyhydrated phases obtained from colloidal dispersions of  $\alpha$ -zirconium phosphate, *Solid State Ionics* 32/33 (1989) 40.
- [25] L.A.S. de A. Prado, H. Wittich, K. Schulte, G. Goerigk, V. M. Garamus, R. Willumeit, S. Vetter, B. Ruffman and S.P. Nunes, Anomalous small-angle x-ray scattering characterization of composites based on sulfonated poly(ether ether ketone), zirconium phosphate, and zirconium oxide, *J. Polym. Sci. Part B: Polymer Phys.* 42 (2003) 567.

- [26] M.C. Wijers, Supported liquid membranes for removal of heavy metals, PhD Dissertation, University of Twente, The Netherlands, 1996.
- [27] R. Nolte, K. Ledjeff, M. Bauer and R. Mulhapt, Partially sulfonated poly(arylene ether sulfone) – a versatile proton conducting membrane material for modern energy conversion technologies, *J. Membr. Sci.* 83 (1993) 211.
- [28] V.N. Belyakov, V.M. Linkov, Ceramic based membranes, US Patent 5,932,361 (1999).
- [29] G. Alberti, M. Casciola, L. Massinelli and B. Bauer, Polymeric proton conducting membranes for medium temperature fuel cells (110-160°C), *J. Membr. Sci.* 185 (2001) 73.
- [30] E. Drioli, A. Regina, M. Casciola, A. Oliveti, F. Trotta and T. Massari, Sulfonated PEEK-WC membranes for possible fuel cell applications, *J. Membr. Sci.* 228 (2004) 139.
- [31] E. Gulzow, T. Kaz, R. Reissner, H. Sander, L. Schilling and M. V. Bradke, Study of membrane electrode assemblies for direct methanol fuel cells, *J. Power Sources* 105 (2002) 261.
- [32] B. Kumar and J. P. Fellner, Polymer-ceramic composite protonic conductors, *J. Power Sources* 123 (2003) 132.



## Chapter 9. Performance and efficiency of a DMFC using non-fluorinated composite membranes operating at low/medium temperatures \*

### Abstract

In order to increase the chemical/thermal stability of the sPEEK polymer for direct methanol fuel cell (DMFC) applications at medium temperatures (up to 130°C), novel inorganic-organic composite membranes were prepared using sPEEK polymer as organic matrix (sulfonation degree, SD, of 42 and 68%) modified with zirconium phosphate (ZrPh) pre-treated with *n*-propylamine and polybenzimidazole (PBI). The final compositions obtained were: 10.0wt.% ZrPh and 5.6wt.% PBI; 20.0wt.% ZrPh and 11.2wt.% PBI. These composite membranes were tested in DMFC at several temperatures by evaluating the current-voltage polarization curve, open circuit voltage (OCV) and constant voltage current (CV, 35mV). The fuel cell ohmic resistance (null phase angle impedance, NPAI) and CO<sub>2</sub> concentration at the cathode outlet were also measured. A method is also proposed to evaluate the fuel cell Faraday and global efficiency considering the CH<sub>3</sub>OH, CO<sub>2</sub>, H<sub>2</sub>O, O<sub>2</sub> and N<sub>2</sub> permeation through the proton exchange membrane (PEM) and parasitic oxidation of the crossover methanol in the cathode. In order to improve the analysis of the composite membrane properties, selected characterization results presented in [1] were also used in the present study. The unmodified sPEEK membrane with SD=42% (S42) was used as the reference material. In the present study, the composite membrane prepared with sPEEK SD=68% and inorganic composition of 20.0wt.%ZrPh and 11.2wt.%PBI proved to have a good relationship between proton conductivity, aqueous methanol swelling and permeability. DMFC tests results for this membrane showed similar current density output and higher open circuit voltage compared to that of sPEEK with SD=42%, but with much lower CO<sub>2</sub> concentration at the cathode outlet (thus higher global efficiency) and higher thermal/chemical stability. This membrane was also tested at 130°C with pure oxygen (cathode inlet) and achieved a maximum power density of 50.1 mW/cm<sup>2</sup> at 250.0 mA/cm<sup>2</sup>.

\*V.S. Silva, S. Weisshaar, R. Reissner, B. Ruffmann, S. Vetter, A. Mendes, L.M. Madeira and S.P. Nunes, *J. Power Sources (in press, 2005)*.

## 9.1. Introduction

Direct methanol fuel cells (DMFCs) based on solid polymer electrolyte are promising candidates for transport applications because they do not require any fuel processing equipment and can be operated at temperatures up to 140°C (Fig. 9.1) [2]. The main disadvantage of the DMFC system is the relative low power density compared to polymer electrolyte membrane fuel cells operating on hydrogen [3].

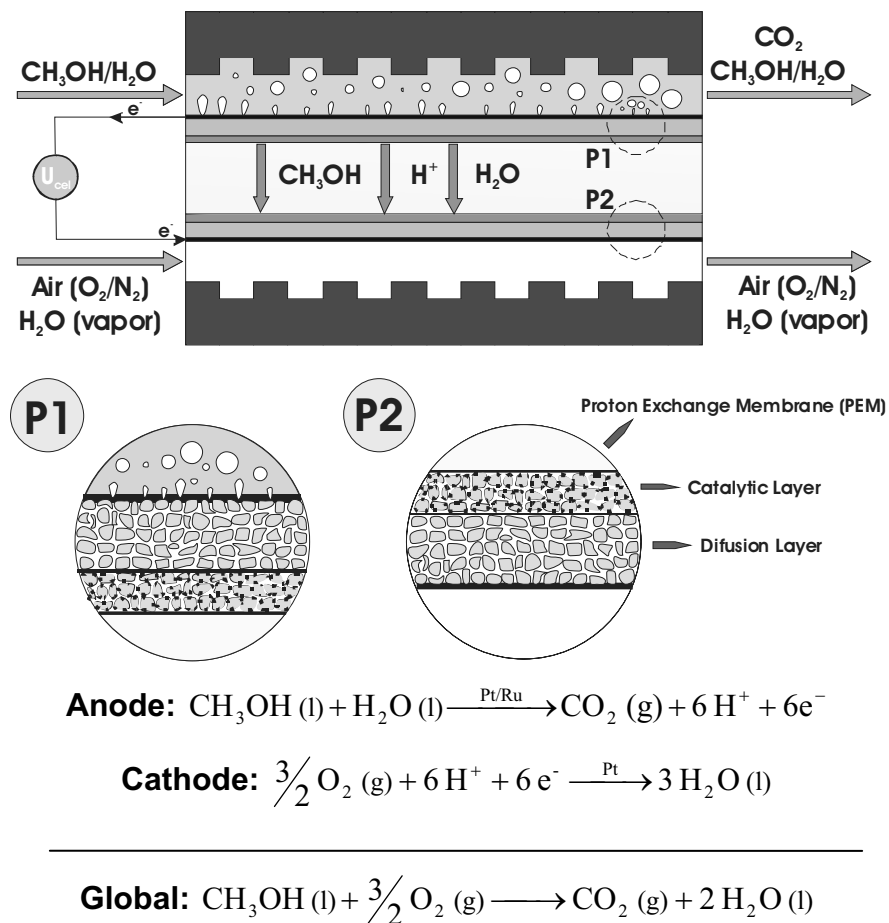


Fig. 9.1. Sketch of a DMFC: water, methanol and proton transport through the proton exchange membrane.

The lower cell performance of a DMFC is caused mainly by the poor kinetics of the anode electro-oxidation of methanol and by the crossover of methanol through the polymer electrolyte membrane (PEM) [3]. The slow oxidation kinetic of methanol to carbon dioxide is due to the formation of carbon monoxide as an intermediate which strongly adsorbs on the Pt catalyst surface [4]. Since the adduct Pt-CO is thermolabile, the catalytic electro-oxidation activity towards

methanol can be improved increasing the DMFC operation temperature to about 120 - 130°C, in order to drastically reduce or eliminate the catalyst poisoning [4, 5]. Apart from that, an increase in the operation temperature improves the oxygen reduction reaction at the cathode, the polymer electrolyte membrane proton conductivity and decreases the polarization effects [3, 5-8]. However, the methanol crossover is believed to increase with temperature and becomes the prevailing effect, at least, for the perfluorinated membranes [6].

In general, DMFCs operating at medium temperatures require membranes that are thermally stable, proton conductive for distinct hydration conditions (vapor feed) and present good barrier properties towards the DMFC species, mainly methanol. Nowadays, the commercially available membrane electrode assemblies (MEAs) use plain perfluorosulfonic membranes, such as Nafion<sup>®</sup>, that are thermally stable but not ideal for DMFC applications [3]. Apart from being costly, this type of membranes has high permeability towards methanol even at low temperatures, which drastically reduces the DMFC performance [9]. These limitations stimulated the development of alternative polymeric proton exchange membranes, such as sulfonated poly(ether ether ketone) (sPEEK) [10-13]. Recently, Li et al. reported better DMFC performances for sPEEK membranes with sulfonation degrees of 39% and 47% at 80°C compared to Nafion<sup>®</sup> 115 [14]. Similar results were obtained by us for a sPEEK membrane with SD = 42%. However, this membrane was not mechanically stable when operated for longer periods than 4 days at 110°C. It was observed that the membrane breaks and a strong leakage of gas from cathode to anode occurred.

Therefore, the present study aims to evaluate DMFC tests at low and medium temperatures (from 50°C up to 130°C) using non-fluorinated composite membranes prepared using sPEEK polymer as polymer matrix (SD = 42 and 68%), incorporating different amounts of  $\alpha$ -zirconium phosphate (ZrPh) pre-treated with *n*-propylamine and polybenzimidazole (PBI). In the present chapter it is also described a method for evaluation of the fuel cell efficiency.

## 9.2. Experimental

### 9.2.1. Materials and methods

sPEEK polymer with sulfonation degrees of 42 and 68% were obtained by sulfonation of poly(ether ether ketone) 450P, supplied as pellets by Victrex, following the procedure described elsewhere [15]. The sulfonation degree was determined by elemental analysis and by H-NMR as described by Nolte et al. [16].

### 9.2.2. Zirconium phosphate preparation

Layered  $\alpha$ -zirconium phosphate (ZrPh) was synthesised using the method described by Ruffmann et al. [17], where  $ZrOCl_2$  is used as precursor of  $ZrO_2$ . In order to promote the exfoliation of the zirconium phosphate layers, the ZrPh solution (6 wt.% in dimethylformamide, DMF) was treated adding *n*-propylamine solution (1M in DMF) using the weight ratio of 5.7g to 6.2g, respectively. After stirring for 3 days the dispersion of treated zirconium phosphate, at 60°C, 6.2 g of polybenzimidazole (PBI) solution (2.5 wt.% in DMF) was added and the dispersion further stirred for 6 days at the same temperature.

### 9.2.3. Membrane preparation

The sPEEK polymer was dissolved in dimethylsulfoxide (DMSO). Then the ZrPh/PBI dispersion solution was added and the final solution left to stir for 3 days at 60°C. After filtration, the solution was cast on a glass plate heated at 70°C. The glass plate was previously hydrophobized with octadecyl trichlorosilane. After casting, the membranes were stored in a vacuum oven for 24 hours at 90 °C. The final thickness of the composite membranes varied between 63 and 84 $\mu$ m [1]. It is expected that the membrane thickness should influence the measurements in the fuel cell giving a lower current for 35mV, higher OCV, higher impedance and lower methanol permeation for a thicker membrane. However, in the present study it is assumed that the influence of the inorganic composition of the membrane on the characterization and DMFC tests outputs is much higher than that of the membrane thickness. This is due essentially to the use of two sPEEK polymers with two distinct sulfonation degrees (SD = 42 and 68%) and high variation of the inorganic composition (0.0, 10.0 and 20.0wt.% ZrPh ; 0.0, 5.6 and 11.2wt.% PBI) of the prepared composite membranes.

### 9.2.4. Characterization methods

#### 9.2.4.1. Proton conductivity

The proton conductivity evaluation procedure is described in detail elsewhere [18]. The proton conductivity was measured using sulfuric acid (0.33M) as electrolyte, at 25°C, and determining the impedance modulus at null phase shift [18]. The spectrometer used was a HP 4284A, working in the frequency range between 100 and 10<sup>5</sup> Hz. As pretreatment, samples were

immersed in water at room temperature during 3 days to ensure total leaching. One hour before initiating the measurement, the samples were immersed in the electrolyte solution.

#### 9.2.4.2. Swelling in aqueous methanol

Swelling studies were carried out by drying the samples in a vacuum oven at 90 °C for 5 hours. After drying, four samples of each membrane were weighed and immersed in 20wt.% aqueous methanol solution and equilibrated for 2 days at 70°C. The weights of the swollen membranes were measured after removing carefully the solution from both surfaces. Membrane swelling (wt.%) was evaluated calculating the ratio between the difference of the wet and dry weight and the dry weight.

#### 9.2.4.3. Pervaporation measurements

The methanol permeability coefficient was evaluated through pervaporation measurements as described in [15]. The measurements were performed at 55°C with a 20wt.% aqueous methanol solution as feed. Prior to all measurements, samples were immersed in the feed solution for 1 hour.

### 9.2.5. DMFC operation

The membrane electrode assemblies (MEAs) were prepared by hot pressing the membrane samples between two Etek<sup>®</sup> ELAT electrodes. Supported PtRu (1 mg/cm<sup>2</sup> 30wt.% PtRu(1:1 a/o) on carbon with 0.7 mg/cm<sup>2</sup> Nafion<sup>®</sup> on single sided hydrophobic carbon cloth) and Pt (0.4 mg/cm<sup>2</sup> 20wt.% Pt on carbon with 0.7 mg/cm<sup>2</sup> Nafion<sup>®</sup> on single sided hydrophobic carbon cloth) were used as anode and cathode electrodes, respectively. The DMFC experimental set-up is described elsewhere [19]. The MEAs (electrode area: 25 cm<sup>2</sup>) were fed with an aqueous 1.5M methanol solution (4 ml/min, 2.5 bar) on the anode side and humidified air (10 sccm/s, 3 bar, 100% relative humidity) on the cathode side.

The following characteristics of direct methanol fuel cells using the prepared MEAs' have been experimentally determined:

- current-voltage polarization curves;
- constant voltage current at 35mV (CV, 35mV);
- open circuit voltage (OCV).

For the last two parameters mentioned above, the cell impedance (null phase angle impedance, NPAI) and CO<sub>2</sub> concentration at the cathode exhaust were also measured. The NPAI was monitored for evaluating the MEA ohmic resistance during DMFC operation [19]. The cell temperature was varied from 50°C to 130°C in order to obtain the Arrhenius plots for the studied variables (50, 70, 90, 100, 110, 130°C). The studied membranes were not previously conditioned before DMFC tests.

### 9.2.6. Efficiency of the DMFC

The DMFC efficiency depends strongly on the two main limiting factors of the fuel cell performance: i) poor electro-catalytic kinetics of the methanol oxidation at the anode and ii) high permeability of the proton exchange membranes towards methanol. The first limitation leads to considerable high anodic overpotentials, lowering the cell voltage significantly below the theoretically expected values. On the other hand, the high methanol permeation from the anode to the cathode through the proton exchange membrane promotes the methanol oxidation in the cathode leading to a loss of potential due to the methanol/oxidation mixed potential. Apart from that, it leads also to a loss of reactant and therefore lower DMFC efficiency. The reacted methanol in the cathode catalyst can be estimated using a CO<sub>2</sub> sensor at the cathode outlet. However, one must also quantify the CO<sub>2</sub> fraction that permeates through the membrane from the anode to the cathode during fuel cell operation.

Therefore, the carbon dioxide molar flow rate due to the parasitic methanol oxidation at the cathode,  $N_{CO_2}^{MeOH}$ , was evaluated using the following equation:

$$N_{CO_2}^{MeOH} = N_{CO_2}^{Out} - N_{CO_2}^{Memb} \quad (9.1)$$

where  $N_{CO_2}^{Memb}$  is the CO<sub>2</sub> flow rate from the anode to the cathode through the proton exchange membrane and  $N_{CO_2}^{Out}$  the CO<sub>2</sub> flow rate at the cathode outlet, measured during DMFC operation.

The CO<sub>2</sub> flow rate at the cathode outlet can be evaluated as:

$$N_{CO_2}^{Out} = \%CO_2 (N_{N_2}^{Out} + N_{O_2}^{Out} + N_{H_2O}^{Out} + N_{CO_2}^{Out}) \quad (9.2)$$

where %CO<sub>2</sub> refers to the carbon dioxide mole fraction at the cathode outlet (measured on-line during DMFC experiments) and  $N_i^{Out}$  to the outlet molar flow rate of species  $i$ . This evaluation assumes that the crossover methanol is fully converted to carbon dioxide in the catalyst layer at the cathode and therefore  $N_{MeOH}^{Out} = 0$ .

The O<sub>2</sub>, N<sub>2</sub> and H<sub>2</sub>O flow rates at the cathode outlet are evaluated using the following equations:

$$N_{O_2}^{Out} = N_{O_2}^{In} - N_{O_2}^{H^+} - N_{O_2}^{MeOH} - N_{O_2}^{Memb} \quad (9.3)$$

$$N_{N_2}^{Out} = N_{N_2}^{In} - N_{N_2}^{Memb} \quad (9.4)$$

$$N_{H_2O}^{Out} = N_{H_2O}^{In} + N_{H_2O}^{MeOH} + N_{H_2O}^{O_2} + N_{H_2O}^{Memb} \quad (9.5)$$

where  $N_i^{In}$  is the inlet molar flux of specie  $i$ ,  $N_{O_2}^{H^+}$  the reacted oxygen in the cathode catalyst layer with H<sup>+</sup>,  $N_{O_2}^{MeOH}$  the reacted oxygen with the crossover methanol,  $N_{H_2O}^{MeOH}$  the formed water by the reaction between O<sub>2</sub> and the crossover methanol,  $N_{H_2O}^{O_2}$  the formed water due to the reduction of O<sub>2</sub> and  $N_i^{Memb}$  the permeated component  $i$  from the anode to the cathode through the membrane.

The mass transport of the DMFC species through the membrane is described by the following equations. For water and carbon dioxide, it is assumed that the permeation is caused by diffusion and convection. In the diffusion term it is assumed that the molar flow is proportional to the concentration gradient between the cathode and anode:

$$N_{H_2O}^{Memb} = -P_{H_2O}^{Memb} \frac{C_{H_2O}^{cath} - C_{H_2O}^{anod}}{d_{Memb}} + n_{drag} \frac{q}{F} \quad (9.6)$$

$$N_{CO_2}^{Memb} = -P_{CO_2}^{Memb} \frac{C_{CO_2}^{cath} - C_{CO_2}^{anod}}{d_{Memb}} + n_{drag} P_{CO_2}^{anod} H(T) \frac{M_{H_2O}}{V_{H_2O}^M} \frac{q}{F} \quad (9.7)$$

where  $q$  is the fuel cell output current,  $C_i^j$  the concentration of species  $i$  in the compartment  $j$  (anode or cathode),  $n_{drag}$  the drag coefficient (number of entrained molecules per proton),  $d_{Memb}$  the membrane thickness,  $H(T)$  the Henry's law constant,  $P_{CO_2}^{anod}$  the partial pressure of CO<sub>2</sub> in the anode,  $M_{H_2O}$  the molecular weight of water (18 g/mol),  $V_{H_2O}^M$  the molar volume of water,  $F$  the Faraday constant (96485 C/mol) and, finally  $P_i$  refers to the permeability coefficients evaluated through the characterizations methods (H<sub>2</sub>O and CH<sub>3</sub>OH: pervaporation experiments; O<sub>2</sub>, N<sub>2</sub> and CO<sub>2</sub>: gas permeation experiments) [1].

The Henry's law constant for the solubility of carbon dioxide in water (low concentration aqueous methanol solution) is determined using the following equation [20]:

$$H(T) = 1.668656 - 5.9802 \times 10^{-3} T + 1.155184 \times 10^{-3} T^2 - 1.118743 \times 10^{-5} T^3 + 4.208352 \times 10^{-8} T^4 \quad (9.8)$$

in which  $T$  is the fuel cell operation temperature.

As mentioned before, it is assumed that methanol is completely converted to carbon dioxide in the cathode catalyst layer and thus the methanol molar flux through the membrane is equal to the carbon dioxide molar flow rate due to the crossover methanol oxidation at the cathode:

$$N_{MeOH}^{Memb} = N_{CO_2}^{MeOH} \quad (9.9)$$

On the other hand, for nitrogen and oxygen it is assumed that only the diffusion mass transfer term is required:

$$N_{N_2}^{Memb} = -P_{N_2}^{Memb} \frac{C_{N_2}^{cath} - C_{N_2}^{anod}}{d_{Memb}} \quad (9.10)$$

$$N_{O_2}^{Memb} = -P_{O_2}^{Memb} \frac{C_{O_2}^{cath} - C_{O_2}^{anod}}{d_{Memb}} \quad (9.11)$$

The use of permeability coefficients evaluated by standard characterization methods to simulate the permeation of species through the membrane is a rough estimate because real values for DMFC operation depend on the operation conditions in the entire MEA. In real DMFC operation, the concentration of species in the anode and cathode changes with the applied load and, therefore, different mass transport conditions exist compared to standard characterization methods as pervaporation and gas permeation [18]. As an example, at high load (CV experiments at 35mV), the methanol concentration in the anode is strongly reduced, the water concentration in the anode is somewhat reduced and the CO<sub>2</sub> concentration in the anode is increased as compared to a pervaporation experiment. On the other hand, the methanol concentration at the cathode is lower than in a standard pervaporation experiment because methanol is mostly consumed by the anode reaction. Also, due to the electro-osmotic drag, the water and methanol permeation from the anode to the cathode would increase with increased current density.

However, the use of parameters obtained through easily implementable characterization methods enables the successful connection between results obtained by membrane and fuel cell developers. In fact, recently published results showed qualitatively good agreement between DMFC results and the output of standard characterization methods [21].

According to the stoichiometry of the oxidation and reduction reactions (Fig. 9.1) one obtains:

$$N_{H_2O}^{MeOH} = 2N_{CO_2}^{MeOH} \quad (9.12)$$

$$N_{O_2}^{MeOH} = 1.5N_{CO_2}^{MeOH} \quad (9.13)$$

$$N_{O_2}^{H^+} = \frac{1.5 q}{6 F} \quad (9.14)$$

$$N_{H_2O}^{O_2} = \frac{3 q}{6 F} \quad (9.15)$$

Inserting the above equations into Eq. (9.2) yields the following expression for the carbon dioxide molar flow rate due to the methanol oxidation in the cathode:

$$N_{CO_2}^{MeOH} = \frac{\%CO_2 (N_T^{In} + \frac{1.5 q}{6 F} - N_T^{Memb}) - N_{CO_2}^{Memb}}{1 + 1.5 \times \%CO_2} \quad (9.16)$$

where  $N_T^{In}$  is the total molar flow rate in the cathode inlet and  $N_T^{Memb}$  is the total molar flow rate through the membrane. This last variable is defined as:

$$N_T^{Memb} = N_{H_2O}^{Memb} + N_{CO_2}^{Memb} + N_{N_2}^{Memb} + N_{O_2}^{Memb} \quad (9.17)$$

Assuming the Faraday law for the methanol oxidation in the cathode, the current density loss due to methanol crossover,  $I_{MeOH}$ , can be evaluated through the following equation:

$$I_{MeOH} = \frac{N_{CO_2}^{MeOH} 6 F}{A_{cell}} \quad (9.18)$$

where  $A_{cell}$  is the DMFC effective area.

Once one only knows the  $\%CO_2$  for the open circuit voltage and constant voltage (35mV), the current density loss due to methanol crossover is only evaluated for these two situations, i.e.  $I_{OCV,MeOH}$  and  $I_{35mV,MeOH}$ , respectively. Therefore, it is assumed that the current density loss due to methanol crossover varies linearly between the estimated methanol loss current density at open circuit,  $(I_{OCV})_{MeOH}$ , and constant voltage (35mV),  $(I_{35mV})_{MeOH}$  (Fig. 9.2) [22]. Thus, in order to evaluate  $I_{i,MeOH}$  for the intermediate current densities the following equation was applied:

$$I_{i,MeOH} = I_{OCV,MeOH} - \frac{I_{OCV,MeOH} - I_{35mV,MeOH}}{I_{35mV}} I_{i,cell} \quad (9.19)$$

The potential efficiency,  $\eta_E$ , is evaluated from:

$$\eta_E = \frac{E_{i,cell}}{E_{rev}} \quad (9.20)$$

where  $E_{i,cell}$  is the measured cell voltage during the polarization curve evaluation and  $E_{rev}$  is the reversible voltage of the DMFC (1.21V).

On the other hand, the Faraday efficiency,  $\eta_F$ , is evaluated from:

$$\eta_F = \frac{I_{i,cell}}{I_{i,cell} + I_{i,MeOH}} \quad (9.21)$$

Finally, the overall DMFC efficiency,  $\eta_{DMFC}$ , is evaluated using the following equation:

$$\eta_{DMFC} = \eta_E \eta_F \quad (9.22)$$

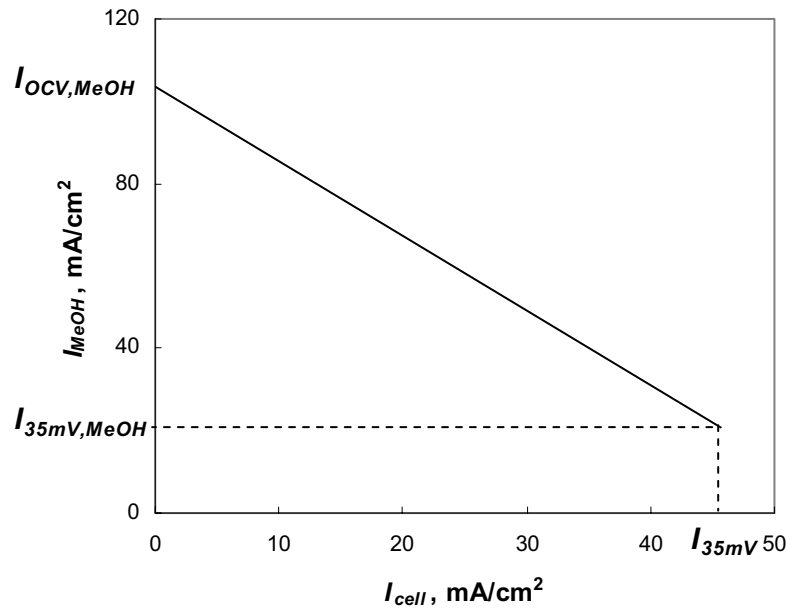


Fig. 9.2. Current density loss due to methanol crossover as a function of the DMFC current density (linear approximation).

### 9.3. Results and discussion

#### 9.3.1. Characterization results

The prepared composite membranes were previously characterized in terms of the following properties: proton conductivity, swelling in water and aqueous methanol, permeability coefficients towards DMFC species (water, methanol, oxygen, carbon dioxide and nitrogen) and morphology [1]. In the present chapter, some of previous data was selected in order to better understand the results obtained in the DMFC tests using the prepared composite membranes. The selected properties of the membrane characterization study were: proton conductivity, aqueous methanol swelling and permeability towards methanol.

In general, the main goal in the development of membranes for DMFC application is to achieve the best balance between proton conductivity and methanol sorption/permeation. The proton exchange membrane should have sufficient proton conductivity and low methanol sorption/permeation. Fig. 9.3 shows the effect on these properties after incorporation of zirconium phosphate, pretreated with *n*-propylamine/PBI, in the SPEEK polymer. As can be seen, the sample's proton conductivity (25°C, impedance spectroscopy) decreases with the amount of inorganic incorporation. This fact can be assumed as a disadvantage for the DMFC performance due to the

increase of the proton transport resistance in the membrane (higher ohmic losses). On the other hand, it can be also observed that the inorganic incorporation also decreases the samples swelling in methanol (70°C, batch experiments) and permeability towards methanol (55°C, pervaporation experiments). These two results can be assumed as advantages because detrimental methanol crossover is reduced due to the improved properties in terms of lower methanol solubility and diffusivity.

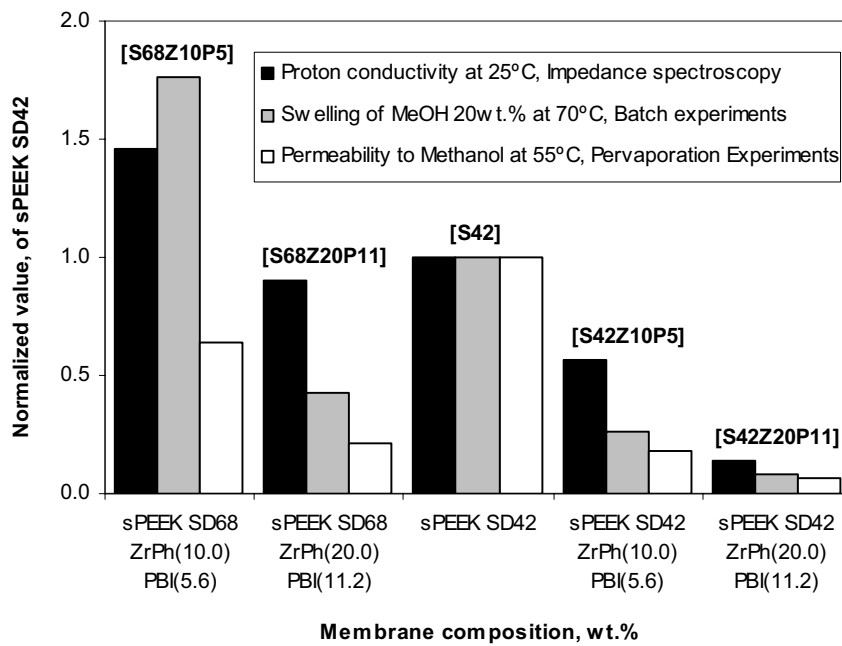


Fig. 9.3. Proton conductivity, aqueous methanol swelling and methanol permeability coefficients of the sPEEK composite membranes, using the data of sPEEK SD42 membrane as reference.

Taking the unmodified membrane sPEEK SD=42%, S42, as reference material (Fig. 9.3), it can be verified that the composite membrane prepared with sPEEK SD=68% and inorganic composition of 20.0wt.%ZrPh and 11.2wt.%PBI, S68Z20P11, provides a similar proton conductivity, but reduced swelling in aqueous methanol and permeability. It can be also seen that the composite membrane S68Z10P5 has higher proton conductivity than that of S42, although its swelling in methanol can be considered as excessive compared to others. The composite membranes prepared with sPEEK SD=42% as base polymer, show low proton conductivity, and also low swelling of aqueous methanol and permeability towards methanol.

### 9.3.2. DMFC temperature study

The open circuit voltage obtained for the investigated MEAs is shown in Fig. 9.4a as a function of temperature (*Arrhenius* plots). It can be observed that the composite membrane S68Z20P11 presents the highest values for OCV in the studied range of temperatures. As mentioned before, it is believed that this membrane presents improved properties in terms of good proton conductivity and low methanol permeation (reduced potential loss). However, it can be seen that for this membrane the OCV *Arrhenius* plot flats as temperature increases. For the other composite membranes, it can be observed that the OCV increase with temperature is more pronounced. The membrane S42Z10P5 is believed to have the lowest OCV for all temperatures due to its high ohmic resistance (low proton conductivity, Fig. 9.3) with simultaneous considerable methanol permeability. On the other hand, in the particular case of the unmodified membrane (SD42), it can be seen that OCV has a maximum value at intermediate temperature (Fig. 9.4a). This result may indicate that this membrane could present low chemical stability for DMFC use at medium temperatures (excessive methanol swelling). From Fig. 9.4a it can also be verified that, for both sPEEK polymers, the composite membranes with higher amount of inorganic incorporation (20.0wt.%ZrPh and 11.2wt.%PBI) provide higher open circuit voltage values, in agreement with the trends shown in Fig. 9.3 regarding proton conductivity and methanol sorption/permeation.

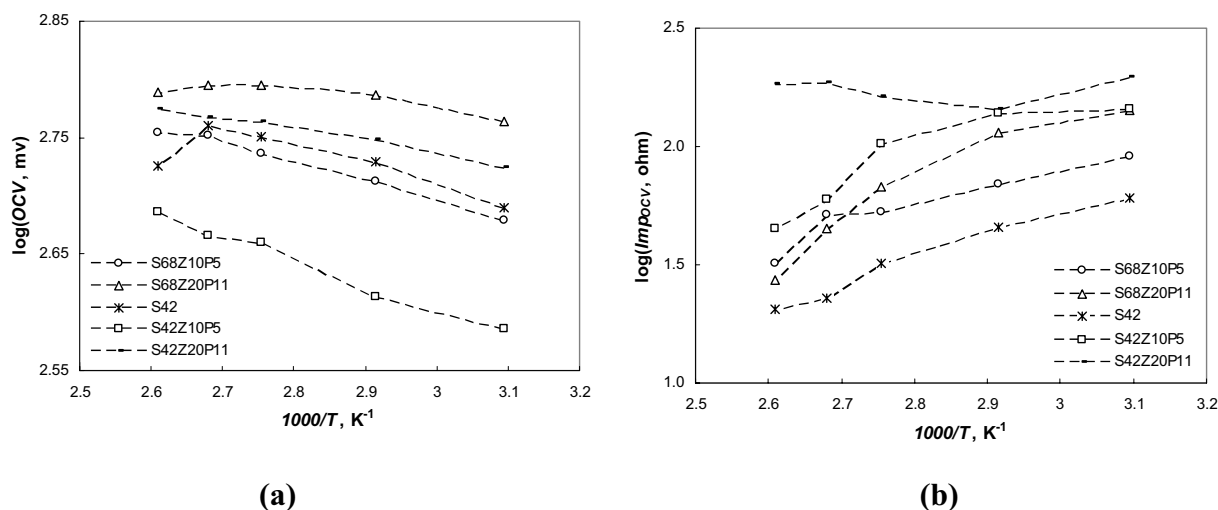


Fig. 9.4. Open circuit voltage experiments: a) Open circuit voltage and b) Null phase angle impedance as a function of temperature for the DMFC using sPEEK composite membranes.

With respect to the null phase angle impedance variation with temperature, from Fig. 9.4b it can be observed that it decreases with temperature for all membranes, as expected, except for

S42Z20P11. It is believed that this membrane presents the highest NPAI value (higher ohmic resistance) due to its lower sulfonation degree (SD42%) and highest amount of inorganic incorporation (lower proton conductivity and swelling). For higher temperatures, it is possible that for this membrane the NPAI increase is due to less favorable membrane humidification conditions (vapor feed and temperatures above the water boiling point) [1]. On the other hand, for the DMFC with the unmodified S42 membrane, it can be observed that although having an intermediate open circuit voltage value (Fig. 9.4a), it presents the lowest ohmic resistance for OCV experiments (Fig. 9.4b). It can be also observed that for both sPEEK matrix polymers (SD=42 and 68%), the ohmic resistance associated with the composite membranes increases with the amount of inorganic modification (lower proton conductivity, Fig. 9.3).

Table 9.1. Carbon dioxide concentration (vol.%) at the cathode outlet for open circuit experiments as a function of the DMFC operation temperature.

<i>Membrane</i>	Cell temperature, °C				
	50	70	90	100	110
	CO <sub>2</sub> cathode outlet, vol.%				
S68Z10P5	0.1	0.1	0.2	0.2	0.4
S68Z20P11	0.1	0.1	0.1	0.2	0.8
S42	0.2	0.2	0.4	1.1	1.4
S42Z10P5	0.0	0.1	0.1	0.3	1.3
S42Z20P11	0.1	0.2	0.5	0.7	1.2

In Table 9.1, the carbon dioxide concentration (vol.%) at the cathode outlet for OCV experiments is presented as a function of temperature. It can be observed that the unmodified sPEEK membrane (S42) has the highest CO<sub>2</sub> concentrations and this fact may explain its moderate OCV value (Fig. 9.4a). This result seems to be also in agreement with the high methanol permeability obtained through pervaporation experiments for this membrane (Fig. 9.3). In contrast, the inorganic incorporation of ZrPh and PBI in both sPEEK polymers (mainly SD=68%) produced membranes that when tested in the DMFC produced low CO<sub>2</sub> emissions for temperatures up to 100°C. For 110°C, the CO<sub>2</sub> concentration at the cathode outlet increases more strongly for the composite membranes, although to lower levels than those obtained for the unmodified membrane (S42).

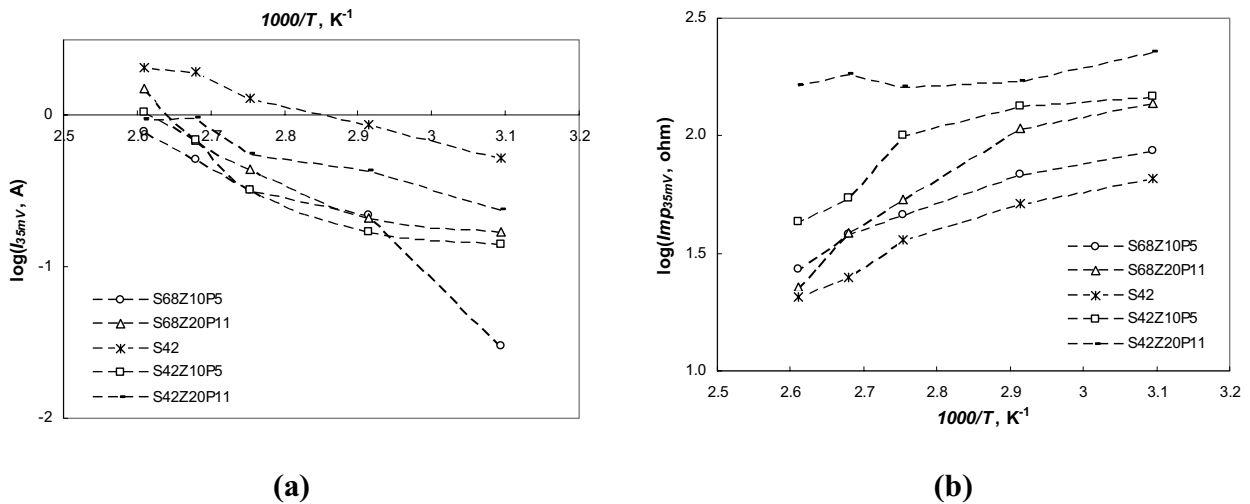


Fig. 9.5. Constant voltage experiments, 35mV: a) Current density and b) Null phase angle impedance as a function of temperature for the DMFC using sPEEK composite membranes.

In Fig. 9.5a is plotted the membranes current density at 35mV as a function of the DMFC operation temperature. It can be observed that the unmodified membrane presents the best performance in terms of production of electric energy. Moreover, it can be seen that for this membrane the logarithm of the current density increases almost linearly with the reciprocal value of the temperature. In contrast, for the composite membranes S68Z10P5, S68Z20P11 and S42Z10P5, higher temperatures seem to have a more pronounced effect on the fuel cell current.

Fig. 9.5b shows the NPAI of the studied membranes tested for constant voltage experiments (35mV). In contrast with the open circuit results obtained for the unmodified membrane, S42, i.e. lower NPAI values does not mean higher OCV values (Figs. 9.4a and b, mainly related with methanol crossover), from Fig. 9.5b it can be observed that NPAI is in agreement with the current density plots presented in Fig. 9.5a. This membrane presents the lowest ohmic resistance and the highest current density during DMFC tests at constant voltage. As it was obtained for the OCV experiments, the highest value for NPAI is obtained for the composite membrane prepared with the sPEEK of lower sulfonation degree (SD=42%) and higher amount of inorganic modification (20.0wt.% ZrPh and 11.2wt.% PBI), which exhibits lower proton conductivity. Also, the results for this membrane shows a more flat NPAI variation with temperature than that observed for other tested membranes.

In terms of the  $CO_2$  concentration at the cathode outlet for CV experiments (Table 9.2), it can be noticed that lower values are usually recorded compared to OCV experiments (Table 9.1). It is believed that this fact is due to the lower methanol crossover at higher current densities (lower concentration of methanol in the anode, thus lowering the mass transfer driving force). On the other

hand, it can be observed from Table 9.2 that, although with the best performance in terms of energy production (Fig. 9.5a), the unmodified membrane, S42, presents the highest CO<sub>2</sub> concentration at the cathode outlet (higher methanol crossover). For the highest tested temperature (110°C), the composite membrane S68Z20P11 presents a much lower CO<sub>2</sub> concentration, 0.1vol.%, and a current density near the one obtained for the unmodified membrane (Fig. 9.5a).

Table 9.2. Carbon dioxide concentration (vol.%) at the cathode outlet for constant voltage experiments (35mV) as a function of the DMFC operation temperature.

Membrane	Cell temperature, °C				
	50	70	90	100	110
	CO <sub>2</sub> cathode outlet, vol.%				
S68Z10P5	0.0	0.0	0.1	0.1	0.1
S68Z20P11	0.0	0.0	0.0	0.1	0.1
S42	0.1	0.2	0.3	0.8	1.8
S42Z10P5	0.0	0.0	0.0	0.2	0.4
S42Z20P11	0.0	0.1	0.1	0.2	1.1

Therefore, it should be interesting to plot the Faraday efficiency for CV experiments at 35mV for each membrane evaluated through equation (9.21) (Fig. 9.6). In the present work, for the Faraday and global DMFC efficiency evaluation it was assumed that  $N_{H_2O}^{Out} = 0$  due to the fact that water is removed from the cathode outlet before the stream reaches the CO<sub>2</sub> sensor [19]. From this figure it can be observed that, although with higher current density, the S42 membrane presents always a lower Faraday efficiency than S68Z20P11, which has efficiencies of 100% at the lower temperatures tested – null CO<sub>2</sub> concentration at the cathode outlet (Table 9.2). Apart from that, it can also be observed that for S42, S42Z10P5 and S42Z20P11, the Faraday efficiency tends to decrease with increasing temperatures, due to the increase in CO<sub>2</sub> concentration at the cathode outlet (higher methanol crossover). Finally, from Fig. 9.6, it can also be observed that the composite membrane prepared with sPEEK polymer SD=68% and inorganic composition 20.0wt.% ZrPh and 11.2wt.% PBI presented always the highest Faraday efficiency for the studied temperature range. This fact shows that for this membrane, the parasitic current density due to the methanol oxidation at the cathode is the lowest in comparison with the other membranes.

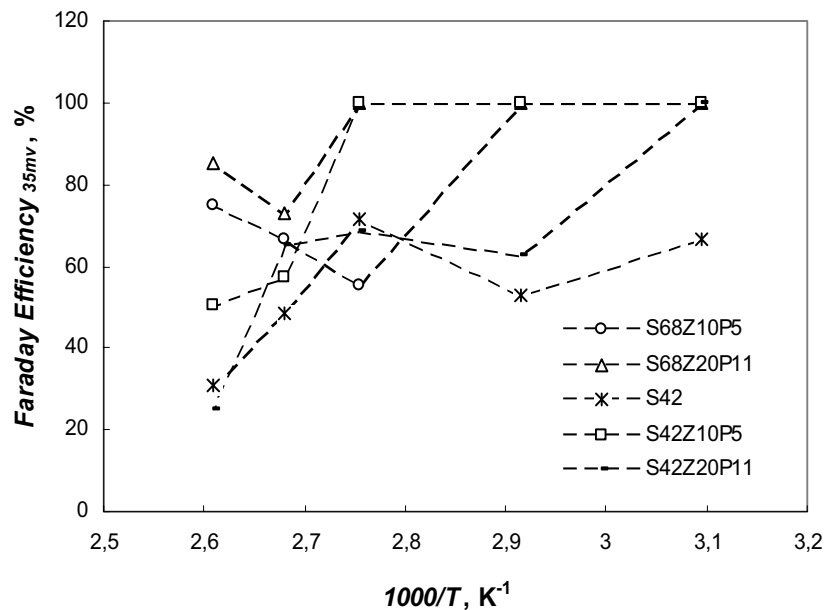


Fig. 9.6. Faraday efficiency (constant voltage experiments, 35mV) as a function of temperature for the DMFC using sPEEK composite membranes.

### 9.3.3. Polarization curves and global efficiency

The current density-potential and current density-fuel cell efficiency plots obtained for the DMFC using the MEAs made from sPEEK composite membranes at 110°C are shown in Fig. 9.7. For the tested operation conditions, it was only possible to obtain the polarization curves for the following membranes: S42, S42Z10P5 and S68Z20P11, which are those that exhibited the highest current densities at this temperature (see Fig. 9.5a). For the other prepared membranes one can assume lower polarization curves than the plotted for S42Z10P5 membrane. The plotted polarization curves differ from the shown data in [1] due to distinct conditioning conditions during the DMFC tests. From data shown in Fig. 9.7 one can conclude that the unmodified membrane presents the best DMFC performance in terms of energy production among all the studied MEAs, achieving a maximum power density output of 10.4mW/cm<sup>2</sup> for a current density of 51.8mA/cm<sup>2</sup> (Table 9.3).

In comparison, the composite membrane S68Z20P11 achieves an output value of 8.6mW/cm<sup>2</sup> at 34.3 mA/cm<sup>2</sup>. Although with lower energy output, the application of the composite membrane S68Z20P11 in the DMFC resulted in much lower concentrations of CO<sub>2</sub> at the cathode outlet compared to the S42 membrane (0.1 and 1.8vol.% at 35mV, respectively, Table 9.2). Therefore, plotting the global DMFC efficiency as a function of the current density (Fig. 9.7), evidences that the composite membrane S68Z20P11 achieves a fuel cell efficiency peak of almost

12%. It can also be observed that the unmodified membrane, S42, has a maximum global efficiency that is even lower than the composite membrane S42Z10P5.

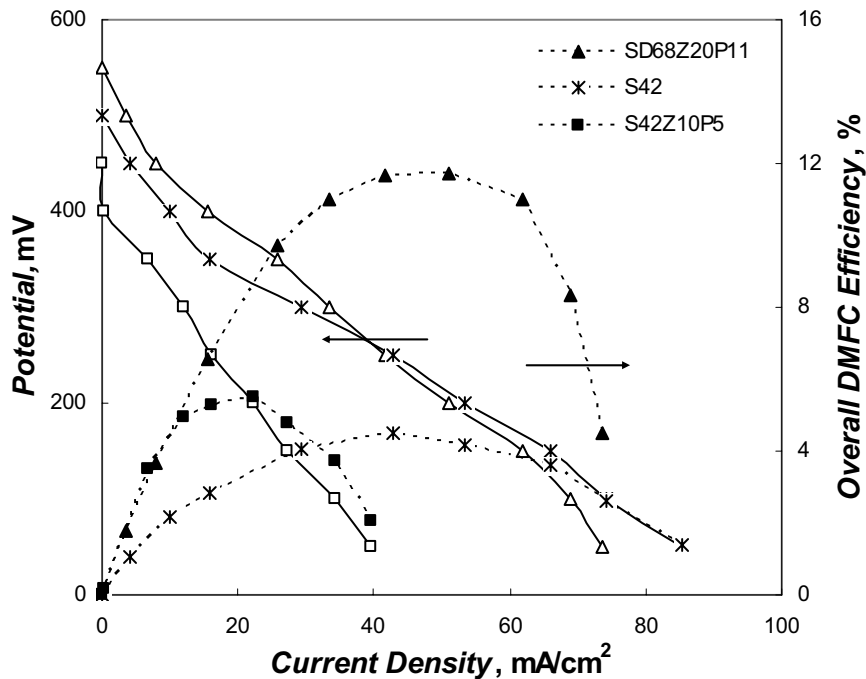


Fig. 9.7. Polarization curves and estimated efficiency of the DMFC using sPEEK composite membranes at 110°C.

Table 9.3. Peak power density and corresponding potential evaluated for DMFC using sPEEK composite membranes at 110°C.

<i>Membrane</i>	Peak Power Density mW/cm <sup>2</sup>	Potential mV
S68Z20P11	8.6	250
S42	10.4	200
S42Z10P5	4.8	200

Once the S68Z20P11 membrane achieved the best performance in terms of efficiency and similar energy production as that of the unmodified membrane, S42, the previously studied MEA using that membrane was further tested in the DMFC, at higher temperatures - up to 130°C (Fig. 9.8). The membrane was also tested using pure oxygen as feed in the cathode inlet. From Fig. 9.8 it can be observed that the membrane performance, in terms of energy production, increased in

comparison to the previous study, for the same temperature of 110°C (Fig. 9.7). It is believed that this increase of the DMFC performance in terms of energy production is essentially due to the distinct conditioning conditions before the DMFC test. From this plot it can be observed that the DMFC performance in terms of energy production increases with temperature (Table 9.4), although having the maximum of the overall DMFC efficiency at 110°C. It is believed that this is due to fact that apart from improving the membrane proton conductivity and methanol oxidation kinetics at the anode, the increase of the DMFC temperature also increases the methanol crossover. When using pure oxygen in the cathode feed instead of air, at 130°C, Fig. 9.8 shows that the DMFC performance increases in terms of both energy production and efficiency. The DMFC using this membrane achieves a power output of 49.5 mW/cm<sup>2</sup> at 198.0 mA/cm<sup>2</sup> in comparison with 31.2mW/cm<sup>2</sup> at 124.9mA/cm<sup>2</sup> for air feed (Table 9.4). The explanation of these results is the increased stoichiometry of oxygen in the cathode electro-reduction reaction. However, in terms of fuel cell efficiency, it can be observed that the maximum global efficiency is obtained for the temperature of 110°C (Fig. 9.8). It is believed that this result is due to the higher effect of the methanol crossover for higher temperatures (120 and 130°C). Finally, it is worth noting that during the DMFC tests at 130°C, the membrane remained stable and no bubbles were detected at the anode exhaust. This fact shows the improved properties of the prepared composite membrane in terms of stability for DMFC applications at low/medium operation temperatures.

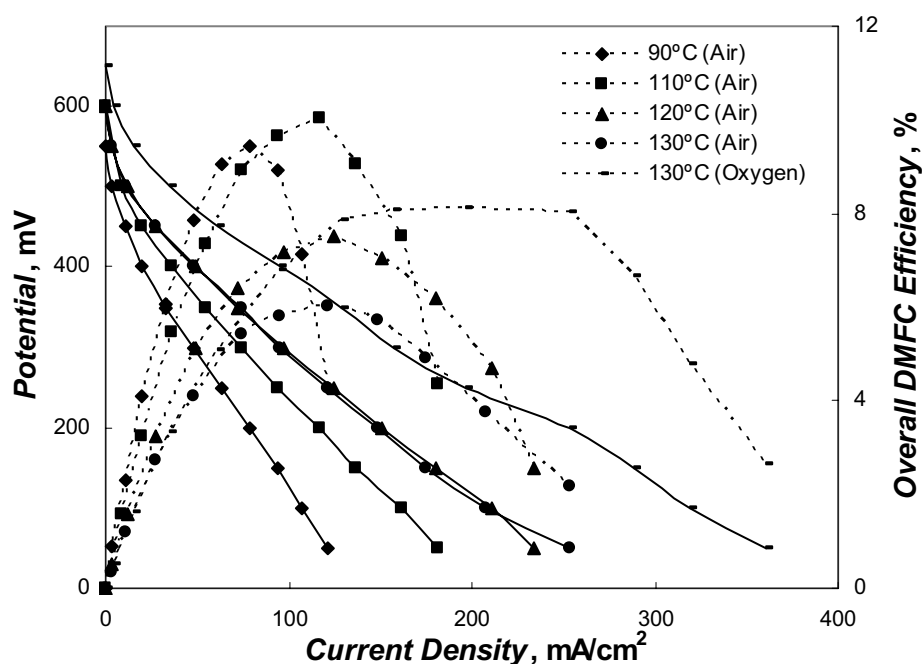


Fig. 9.8. Polarization curves and estimated efficiency of the DMFC, for several temperatures, using the composite membrane sPEEK SD=68% 20.0wt% ZrPh 11.2wt.%PBI.

Table 9.4. Peak power density at 250mV evaluated for the DMFC, at several temperatures, using the sPEEK composite membrane SD=68% 20.0wt% ZrPh 11.2wt.%PBI.

<i>Temperature</i>	Peak Power Density @ 250mV
<i>°C</i>	mW/cm <sup>2</sup>
90 (Air)	15.8
110 (Air)	23.5
120 (Air)	30.0
130 (Air)	31.2
130 (O <sub>2</sub> )	49.5

## 9.4. Conclusions

The characterization results showed that the inorganic incorporation of pretreated zirconium phosphate decreases the membrane proton conductivity, aqueous methanol swelling and permeability towards methanol. However, the incorporation of pretreated ZrPh enabled the preparation of membranes with improved relationship between proton conductivity and permeability towards methanol (sorption and diffusion). Although with lower production of current density, the composite membranes S68Z20P11 and S42Z10P5 achieved a higher global efficiency than the unmodified sPEEK membrane, S42. Moreover, for temperatures up to 110°C, the membrane S68Z20P11 achieved a similar current density as S42, but with significantly reduced CO<sub>2</sub> production in the cathode (lower methanol crossover). This membrane proved to be stable for temperatures up to 130°C.

In general, the present work shows that the incorporation of zirconium phosphate pretreated with *n*-propylamine and polybenzimidazole allows the preparation of sPEEK composite membranes with improved properties in terms of chemical stability and DMFC efficiency. These composite membranes proved to be promising for DMFC application at low/medium temperatures (up to 130°C).

## Acknowledgements

Financial support by the HGF-Venetzungsfonds is gratefully acknowledged. The work of Vasco Silva was supported by FCT (Grant SFRH/BD/6818/2001). Vasco Silva would like to acknowledge both FCT and GKSS for the assigned grant for his stay at GKSS Forschungszentrum

GmbH. The present work was in part supported by FCT/FEDER projects POCTI/EQU/38075/2001 and POCTI/EQU/45225/2002.

### List of symbols

$A_{cell}$	Reaction area (fuel cell active area), $m^2$ .
$C_i$	Molar concentration of species $i$ , $mol\ m^{-3}$ .
$d$	Membrane thickness, m.
$F$	Faraday constant, $C\ mol^{-1}$ .
$H$	Henry's law constant, $cm^3_{CO_2} g_{H_2O}^{-1} Pa^{-1}$ .
$I$	Current density, $A\ m^{-2}$ .
$M_i$	Molar mass of species $i$ , $g\ mol^{-1}$ .
$N_i$	Molar flow rate of species $i$ , $mol\ s^{-1}$ .
$n_{drag}$	Transport number (electro-osmotic drag).
$p_i$	Partial pressure of species $i$ , Pa.
$P_i$	Permeability towards species $i$ , $m^3\ m\ s^{-1}$ .
$q$	Current, A.
$T$	Temperature, K.
$V_i^M$	Molar volume of species $i$ , $m^3\ mol^{-1}$ .

### Greek letters

$\eta_F$	Faraday efficiency.
$\eta_P$	Potential efficiency.
$\eta_{DMFC}$	Overall DMFC efficiency.

### Subscripts

35mV	Constant voltage, 35mV.
<i>Cell</i>	<i>DMFC cell</i> .
<i>i</i>	Species <i>i</i> .
<i>j</i>	Species <i>j</i> .
Memb	Membrane.

MeOH	Methanol (cathode related, crossover).
OCV	Open circuit voltage.
T	Total.

### Superscripts

anod	Anode.
cath	Cathode.
In	Cathode inlet.
Memb	Membrane.
MeOH	Methanol (cathode related, crossover).
Out	Cathode outlet.

### References

- [1] V.S. Silva, B. Ruffmann, S. Vetter, A. Mendes, L.M. Madeira and S.P. Nunes, Characterization and application of composite membranes in DMFC, *Catalysis Today*, (in press, 2005).
- [2] A.S. Aricò, P. Cretí, P.C. Antonucci and V. Antonucci, Comparison of ethanol and methanol oxidation in a liquid-feed solid polymer electrolyte fuel cell at high temperature, *Electrochem. Solid State Lett.* 1 (1998) 66.
- [3] M. Baldauf and W. Preidel, Status of the development of a direct methanol fuel cell, *J. Power Sources* 84 (1999) 161.
- [4] R. Parsons and T. VanderNoot, The oxidation of small organic molecules: A survey of recent fuel cell related research, *J. Electroanal. Chem.* 257 (1988) 9.
- [5] G. Alberti, M. Casciola, L. Massinelli and B. Bauer, Polymeric proton conducting membranes for medium temperature fuel cells (110-160°C), *J. Membr. Sci.* 185 (2001) 73.
- [6] B. Gurau and E.S. Smotkin, Methanol crossover in direct methanol fuel cells: a link between power and energy density, *J. Power Sources* 112 (2002) 339.
- [7] Z. Qi and A. Kaufman, Open circuit voltage and methanol crossover in DMFCs, *J. Power Sources* 110 (2002) 117.
- [8] A. Heinzl and V.M. Barragán, A review of the state-of-the-art of the methanol crossover in direct methanol fuel cells, *J. Power Sources* 84 (1999) 70.
- [9] J. Cruickshank and K. Scott, The degree and effect of methanol crossover in the direct methanol fuel cell, *J. Power Sources* 70 (1998) 40.

- [10] S.M.J. Zaidi, S.D. Mikailenko, G.P. Robertson, M.D. Guiver and S. Kaliaguine, Proton conducting composite membranes for polyether ether ketone and heteropolyacids for fuel cell applications, *J. Membr. Sci.* 173 (2000) 17.
- [11] S.D. Mikhailenko, S.M.J. Zaidi and S. Kaliaguine, Sulfonated polyether ether ketone composite polymer electrolyte membranes, *Catal. Today* 67 (2001) 225.
- [12] K.A. Kreuer, On the development of proton conducting polymer membranes for hydrogen and methanol fuel cells, *J. Membr. Sci.* 185 (2001) 3.
- [13] L. Jörissen, V. Gogel, J. Kerres and J. Garche, New membranes for direct methanol fuel cells, *J. Power Sources* 105 (2002) 267.
- [14] L. Li, J. Zhang and Y. Wang, Sulfonated poly(ether ether ketone) membranes for direct methanol fuel cell, *J. Membr. Sci.* 226 (2003) 159.
- [15] S.P. Nunes, B. Ruffmann, E. Rikowsky, S. Vetter and K. Richau, Inorganic modification of proton conductive polymer membranes for direct methanol fuel cells, *J. Membr. Sci.* 203 (2002) 215.
- [16] R. Nolte, K. Ledjeff, M. Bauer and R. Mulhaupt, Partially sulfonated poly(arylene ether sulfone) – a versatile proton conducting membrane material for modern energy conversion technologies, *J. Membr. Sci.* 83 (1993) 211.
- [17] B. Ruffmann, H. Silva, B. Schulte and S. Nunes, Organic/inorganic composite membranes for application in DMFC, *Solid State Ionics*, 162-163 (2003) 269.
- [18] V.S. Silva, B. Ruffmann, H. Silva, Y. A.-Gallego, A. Mendes, L. M. Madeira and S.P. Nunes, Proton electrolyte membrane properties and direct methanol fuel cell performance: Part I. Characterization of hybrid sulfonated poly(ether ether ketone)/zirconium oxide membranes, *J. Power Sources* 140 (2005) 34.
- [19] E. Gulzow, T. Kaz, R. Reissner, H. Sander, L. Schilling and M. V. Bradke, Study of membrane electrode assemblies for direct methanol fuel cells, *J. Power Sources* 105 (2002) 261.
- [20] K.-H. Hellwege and A. M. Hellwege (ed.), *Landolt-Börnstein: Zahlenwerte und Funktionen aus Physik*, Springer-Verl., Berlin, 1962.
- [21] V.S. Silva, J. Schirmer, R. Reissner, B. Ruffmann, H. Silva, A. Mendes, L.M. Madeira and S.P. Nunes, Proton electrolyte membrane properties and direct methanol fuel cell performance: Part II. Fuel cell performance and membrane properties effects, *J. Power Sources* 40 (2005) 41.
- [22] H. Dohle and K. Wippermann, Experimental evaluation and semi-empirical modeling of U/I characteristics and methanol permeation of a direct methanol fuel cell, *J. Power Sources* 135 (2004) 152.

## Conclusions and suggestions for future work

The present work aimed the development and study of novel proton exchange membranes (PEM) for direct methanol fuel cell (DMFC) applications. The used matrix polymer was the sulfonated poly(ether ether ketone) (sPEEK) and the inorganic modifications were performed using stand alone zirconium oxide ( $\text{ZrO}_2$ ) or zirconium phosphate (ZrPh) pretreated with *n*-propylamine and polybenzimidazole (PBI). Nafion<sup>®</sup> from Dupont was used as reference. Apart from this, it was aimed to perform a fundamental research work concerning the membrane preparation, characterization, application and modeling, in order to improve the PEM research strategy concerning the key characteristics that control the DMFC performance.

From the characterization results obtained for the plain sPEEK polymer it was observed that the proton conductivity and the permeability coefficients of water, methanol, oxygen and carbon dioxide increase with its sulfonation degree (SD). In contrast, the SD seems to not affect the nitrogen permeability coefficient. In terms of selectivity, it was observed that the selectivity towards carbon dioxide/oxygen increases with the sPEEK SD. In contrast, the selectivity towards nitrogen/oxygen decreases. In terms of barrier properties for preventing the DMFC reactants loss, the PEMs based on the sPEEK polymer with SD lower or equal to 71%, although having slightly lower proton conductivity, presented much better characteristics for fuel cell applications compared to the well known Nafion<sup>®</sup> 112. From the DMFC tests at low temperature (50°C) it was observed that the fuel cell performance increases with the sulfonation degree. The sPEEK membrane with SD = 71% showed to have similar performance, or even better, to that of Nafion<sup>®</sup> 112. However, the highest DMFC overall efficiency was achieved using sPEEK membrane with SD = 52% (lower sulfonation degrees). In summary, based on the criterion of minimization of the reactants loss, chemical stability along with enough proton conductivity, the sPEEK membrane proved to be a potential material for DMFC applications. Depending on the polymer sulfonation degree, the sPEEK membrane exhibits characteristics that can improve the DMFC performance and the global efficiency when compared to Nafion<sup>®</sup> 112.

On the other hand, regarding the  $\text{ZrO}_2$  modification of the sPEEK polymer with two distinct sulfonation degrees, the characterization results obtained show that the inorganic oxide network decreases the membrane's proton conductivity and water swelling. It was found that it leads also to a decrease of the water, methanol, carbon dioxide and oxygen permeability coefficients, an increase of the water/methanol selectivity and a decrease of the carbon dioxide/nitrogen and oxygen/nitrogen selectivities. In terms of morphology, it was found that *in situ* zirconium alkoxide hydrolysis

enables the preparation of homogeneous membranes that present a good adhesion between inorganic domains and the polymer matrix. The results obtained from the application of these membranes in the DMFC showed that increasing the zirconium oxide content in the sPEEK composite membranes leads to a decrease in the DMFC current density at 35mV, CO<sub>2</sub> concentration at the cathode exhaust and, finally, maximum power density output. The opposite trend was verified in terms of the ohmic resistance of the cell (null phase angle impedance). A maximal open circuit voltage was obtained for the sPEEK composite membrane with intermediate ZrO<sub>2</sub> content (7.5wt.%) due to improved ratio between methanol crossover and ohmic resistance in comparison with the other studied membranes.

With respect to the validation of the characterization methods, the results obtained for sPEEK membranes with increased amounts of ZrO<sub>2</sub> (distinct properties) showed a co-current variation between proton conductivity, evaluated by impedance spectroscopy (acid electrolyte and water vapor cells), and DMFC output current density. The same behavior was observed regarding the proton transport resistance, evaluated using the cells referred above, and the DMFC null phase angle impedance at 35mV. On the other hand, an almost linear variation was detected between the water uptake and the DMFC output current density at 35mV. The fuel cell ohmic resistance seems to increase strongly for membranes with low water uptake, while it is almost independent for higher values of this property. Finally, our results showed a good agreement between the membranes' methanol permeability coefficients obtained by pervaporation experiments and the CO<sub>2</sub> concentration at the cathode outlet. In summary, the obtained results show that characterization results obtained by impedance spectroscopy, water uptake and pervaporation experiments can be used as critical parameters for the selection of proton electrolyte membranes for DMFC application purposes.

Additionally, the DMFC simulations using the developed mathematical model based on the sPEEK membranes with increased amounts of ZrO<sub>2</sub> (wide range of physical/chemical properties) showed a good agreement with the experimental results for different temperatures and membrane properties. The model predicts correctly the DMFC performance, accounting the distinct membrane properties evaluated by standard characterization methods (pervaporation, impedance spectroscopy, pressure rise and water swelling). The simulator proved that it can be useful for membrane research and development.

On the other hand, from the study regarding the PEM electrolyte and barrier properties influence on the DMFC overall performance, the developed model showed, as expected, that both PEM proton conductivity and methanol permeability play an important role on the DMFC overall performance. The proton conductivity seems to influence mainly the DMFC current and power

density production and the cell efficiency regarding fuel conversion (Faraday efficiency). Apart from this, very low proton conductivity seems to have very high influence in the DMFC performance due to limiting characteristics concerning the cell ohmic losses, even for low current densities. On the other hand, the permeability towards methanol was found to influence all the studied parameters as it is directly related to the fuel loss and parasitic reaction of methanol at the cathode catalyst layer (potential and Faraday efficiencies). As expected, the simulations show that the optimal PEM properties for DMFC applications are high proton conductivity to reduce the ohmic losses and low methanol permeability in order to prevent the crossover of methanol from the anode to the cathode. This model will be used in order to improve our PEM development strategy and, consequently, to reduce the applied efforts to find the material with the optimal characteristics for DMFC application.

Finally, from the characterization results obtained using sPEEK polymer modified with zirconium phosphate pretreated with *n*-propylamine and polybenzimidazole, it was seen that increasing the inorganic incorporation leads to a decrease of the proton conductivity. In terms of the membranes swelling in water or methanol aqueous solution, batch experiments showed that the ZrPh/PBI content decreased the swelling of the composite sPEEK membranes. All the composite membranes showed improved thermal and chemical stability in the methanol aqueous solution in comparison with the plain polymer. Pervaporation (H<sub>2</sub>O, CH<sub>3</sub>OH) and pressure rise (N<sub>2</sub>, O<sub>2</sub>, CO<sub>2</sub>) experiments showed that the incorporation of ZrPh/PBI in the sPEEK polymer organic matrix decreased the DMFC species permeability coefficients. Micrographs obtained by scanning electron microscopy showed a good adhesion between inorganic particles domains and the polymer matrix. In the DMFC tests, for temperatures up to 110°C, the composite membrane with SD=68% and 20.0wt.% of ZrPh and 11.2wt.% of PBI achieved a similar current density as the plain polymer with SD=42%, but with significantly reduced CO<sub>2</sub> production at the cathode (lower methanol crossover). This membrane proved to be stable for temperatures up to 130°C and was found to be the most favorable for future application in DMFC systems working at temperature up to 130°C (medium/low temperatures).

We believe that the direct methanol fuel cell will be the next generation power source that will revolutionize the performance and easy-of-use of electronic portable equipments. From the experimental results obtained in the present work, we believed that the sulfonated poly(ether ether ketone) can be considered to have very promising properties for DMFC applications (as plain or matrix polymer). Furthermore, the modification with zirconium phosphate pre-treated with *n*-

propylamine and polybenzimidazole resulted to improve the membranes characteristics for medium temperature DMFC applications (up to 130°C), mainly in terms of barrier properties and chemical/thermal stability. Therefore, future work should explore these features, performing long-term stability tests, studying and optimizing the membrane inorganic composition, in order to effectively develop membranes that can be considered as alternatives to Nafion<sup>®</sup> for DMFC applications. In addition, future work should also focus on the development and test of new inorganic materials for composite membranes, alternative to the tested ones.

Apart from this, it should be also interesting to expand the fundamental research regarding the characterization methods validation. Future studies should aim the improvement of the standard characterization methods conditions (pervaporation, impedance, liquid and vapor sorption, gas permeation), in order to improve the qualitative prediction of the DMFC performance. Experiments at several temperatures and accounting, as much as possible, to the operation conditions of real fuel cell systems should be performed. If necessary, new experimental set-ups should be designed in order to improve the usefulness of the characterization methods. However, the simplicity of the characterization methods should be always kept in mind, in order to facilitate and quicken the development process of proton exchange membranes.

Additionally, it should be interesting to perform DMFC experimental tests using a mass spectrometer at both anode and cathode outlet, in order to have an effective on-line study of the concentration variation of all species. In fact, this experimental procedure can be extremely useful for model validation and evaluation of the DMFC performance. Also, it should be very interesting to investigate the DMFC performance using distinct PEMs by impedance spectroscopy, in order to infer about the membrane properties influence on the DMFC performance. Membrane conductivity, sorbed water, methanol crossover and cathode flooding effects should be studied through impedance spectra modeling, developing equivalent electrical circuits.

Other important subject is to improve the accuracy of the model's parameters using more materials, with distinct properties. Thus, the model error should become significantly smaller, increasing its usefulness and improving its capabilities to predict the DMFC performance for novel materials. The aim should be to develop a model that could be commercialized and contribute to the improvement of the PEM research capabilities for DMFC applications.

Finally, several improvements can be performed regarding the developed mathematical model: a) assume a two phase system in both cathode and anode (liquid and gas); b) take into account a detailed electrochemical reaction mechanism of the methanol electro-oxidation; c) application of more general mass transport equations, such as Stefan-Maxwell; d) take into account the cathode flooding effects; e) relax the assumptions concerning the mass and charge transport

equations for the gas diffusion and catalyst layers; f) consider a two or three dimensional mathematical model and g) consider an unsteady state formulation.



***This is not the end.***

***It is not even the beginning of the end.***

***But it is, perhaps, the end of the beginning.***

*Sir Winston Churchill*